Investigation on Supramolecular Arrangement and On-Resin Modification of Small Peptides

A Dissertation Submitted to the

Indian Institute of Technology Guwahati

As Partial Fulfillment for the Degree of

Doctor of Philosophy in Chemistry

Submitted by

Rajat Subhra Giri

Roll No. 146122015

Department of Chemistry
Indian Institute of Technology Guwahati
Guwahati-781039, Assam, India

November-2019

Dedicated

To

My Parents

INDIAN INSTITUTE OF TECHNOLOGY GUWAHATI

Department of Chemistry

STATEMENT

I do hereby declare that the matter embodied in this thesis entitled "**Investigation on Supramolecular Arrangement and On-Resin Modification of Small Peptides**" is the result of experiments carried out by me in the Department of Chemistry, Indian Institute of Technology Guwahati, India, under the supervision of Prof. Bhubaneswar Mandal.

In keeping with the general practice of reporting scientific observations, due acknowledgements have been made wherever the work described is based on the findings of other investigators.

Date: 22.11.2019
Place: IIT Guwahati

Rajat Subhra Giri

Indian Institute of Technology Guwahati
Department of Chemistry
North Guwahati, Guwahati-781039, India
Phone: +91 (361) 258 2319 (O); Fax: +91 (361) 258 2349
e-mail: **bmandal@iitg.ac.in**

CERTIFICATE

This is to certify that **Mr. Rajat Subhra Giri** (Roll No. 146122015) has been working under my supervision since July 2014 as a regular registered Ph.D. student. I am forwarding his thesis entitled "**Investigation on Supramolecular Arrangement and On-Resin Modification of Small Peptides**" to be submitted for the Ph.D. (Science) Degree of this Institute. I certify that he has fulfilled all the requirements according to the rules of this institute regarding the investigations embodied in his thesis and this work has not been submitted elsewhere for a degree.

Date: 22.11.2019
Place: IIT Guwahati

Prof. Bhubaneswar Mandal
Thesis Supervisor
Department of Chemistry

Acknowledgements

The journey of the Ph.D. is not always a smooth one. However, along the way, I have encountered persons who helped to make this journey a pleasurable. I would like to express sincere gratitude to them who directly or indirectly helped me throughout the Ph.D. journey and motivated me on the path to success.

First and foremost, I would like to express my sincere gratitude and thanks to my thesis supervisor Prof. Bhubaneswar Mandal for his invaluable guidance, encouragement, and inspiration throughout my Ph.D. program, which helped me to enhance my knowledge and inspired me to take right decisions at crucial moments. I am also thankful to him for giving me the freedom to pursue my interests in his lab, and I find myself privileged to have worked under his kind guidance.

I would like to acknowledge my sincere gratitude to all my doctoral committee members, Prof. Tharmalingam Punniyamurthy, Dr. Lal Mohan Kundu, and Dr. A. S. Achalkumar for their valuable suggestions and pieces of advice during my doctoral studies. I want to thank Prof. Sandip Paul for the theoretical studies, Dr. Debapratim Das, for providing me the facility of lyophilizer and Dr. Sunanda Chatterjee for giving me the facility of HPLC.

I am grateful to the Ministry of Human Resource and Development (MHRD), India, for financial support and IIT Guwahati for all the facilities that were made available to me. I want to thank the department of chemistry and the Central Instrument Facility (CIF), IIT Guwahati, for providing the instrumental facilities. I am highly thankful to the CIF for allowing me to operate the NMR (600 MHz) instrument as an authorized operator for four years during my Ph.D. tenure. I would also like to thank the Advanced Materials Research Centre (AMRC), IIT Mandi, for SC-XRD experimental facility.

Further, I would like to thank all my past and present group members for their friendship and assistance. I especially want to thank Dr. Ashim Paul for his assistance and for always being willing to discuss problems and ideas with me. I also especially thank my two juniors, Gobinda and Sayanta, for their help during the Ph.D. tenure. I thank the other labmates, Dr. Dharam Dev, Dr. Srinivasa Rao Manne (Srinu da), Tanmay da, Sourav, Tapasi, Sujan, Sandip, Altaf and Sukesh for their co-operation in my research work, without which it would not be easy to complete the Ph.D. thesis. It was great to work and spend time with these lovely human beings, and I will always carry the memories of their jokes, laughter, and humor throughout my life. It was a great joyful memory during lab picnics and tours like Pobitora Wildlife Sanctuary (Guwahati), Barapani (Shillong), Bhutan, and Sikkim. I am lucky to get such type of research environment and labmates.

My heartful special thanks to M.Sc. cum Ph.D. best friend Dr. Utsab for his endless help, love, and friendship. Another heartiest thanks to my lovely friend Dr. Bapan for his encouragement, support, love, and help. I am also express my sincere thanks to my lovely friends, Dr. Ayan, Dr. Nilotpal, Dr. Mostakim, Dr. Ganesh, Dr. Arup, Dr. Rana, Sourav, Pinaki, Gourab, Gopal, Dipankar, Santanu, Surajit and Krishnangsu for their support, love, encouragement, and help. Still, many names are missing whose contribution and help is worth mentioning. Most of these people have a positive approach to life, and I wish them success in every aspect of their life.

I thank all of my Ph.D. batchmates (July 2014), the other research scholars in the chemistry department, and all my IITG friends who have shared their thoughts and views with me. I also thank my all M.Sc. and Ph.D. friends at IIT Guwahati with whom I spent time and shared many joyful moments during festivals and picnics.

I also would like to thank my school and college friends, Santu, Abhijit, Atanu, Bidit, Arjun, Don, Supriya, Alok, Animesh, Harekrishna, Manas, Rakesh, Mrinal, Bodhi, Sumanata, Surya, Bidhan, Sumitava, Tapas, Dr. Subhankar and other close friends for their support and help.

I express my sincere gratitude to all my teachers who always encourage, motivate and guide me since my childhood, especially, Mr. Swapan Kar, Mr. Prasanta Das, Mr. Asis Kumar Nandi, Mr. Ajay Senapati, Mr. Sanjay Nandi, and Dr. Tridip Tripathy for their teaching, inspiration, invaluable motivation, suggestions and advice for academic as well as for progress of life.

Finally, I want to thank all of my family members. Without their love, care, support, and encouragement, it would not have been possible. They have been nothing short of incredible. I wish to express my sincere gratitude to my parents, brothers, sisters, uncle, aunt, brother-in-law, sister-in-law, my wife, and my little nephew and niece for their endless moral support and motivation, especially at difficult times. My Ph.D. endeavors would not have been completed without their blessings. They are the main soul and inspiration for every step that I achieve in my life. I would especially like to recognize my brother (vai) Pallab Kishor Giri, who has been a source of encouragement and inspiration throughout my life. I wish him success in every aspect of his life. Besides, no words would suffice to express my feelings for beloved Soumyashree, my wife, whose love and care have so luxuriously continued to enrich my life. I wish to express my hearty thanks to her. I would like to thank all others who are associated with my work directly or indirectly at IIT Guwahati for their help.

Rajat Subhra Giri

List of abbreviations

Aβ	Amyloid beta
Ac_2O	Acetic anhydride
AD	Alzheimer's disease
AFM	Atomic force microscopy
AU	Arbitrary unit
Aib	2-aminoisobutyric acid
Ant	Anthranilic acid
Boc	*tert*-Butyloxycarbonyl
BOP	Benzotriazol-1-yloxy-tris(dimethylamino) phosphoniumhexafluorophosphate
BHA	Benzhydrylamine
Bzl	Benzyl
Cbz	Benzyloxycarbonyl
CD	Circular dichroism
croEM	Cryogenic electron microscopy
COSY	Correlation Spectroscopy
DBU	1,8-Diazabicyclo[5.4.0]undec-7-ene
DCM	Dichloromethane
Dmb	2,4-dimethoxybenzyl
Dmab	4-{N-[1-(4,4-dimethyl-2,6-dioxocyclohexylidene)-3 methylbutyl]amino}benzyl
DIPEA	*N*,*N*-Diisopropylethyl amine
deg	degree
3D	Three dimensional

DMF	*N*,*N*-Dimethylformamide
DNA	Deoxyribonucleic Acid
ESI-MS	Electrospray Ionization Mass Spectrometry
EtOAc	Ethyl Acetate
Et	Ethyl
Equiv	Equivalent
Fmoc	9-Fluorenylmethoxycarbonyl
FT-IR	Fourier Transformation Infra-red Spectroscopy
FE-SEM	Field Emission Scanning Electron Microscopy
Gbn	Gababutin
Gpn	Gabapentin
HF	Hydrofluoric acid
KBr	Potassium bromide
HPLC	High performance Liquid Chromatography
MALDI	Matrix-assisted laser desorption/ionization
MeOH	Methanol
MeCN	Acetonitrile
Me	Methyl
mL	Milli Liter
MW	Microwave
mM	milli mol
μM	micro mol
m-ABA	*meta* amino benzoic acid
MS	Mass spectra
nm	Nanometre

NMI	*N*-Methyl imidazole
NOESY	Nuclear Overhauser Effect Spectroscopy
NMR	Nuclear Magnetic Resonance
ORTEP	Oak Ridge Thermal Ellipsoid Plot
o-NosylOXY	Ethyl 2-cyano-2-(2-nitrophenylsulfonyloxyimino)
Oxyma	Ethyl 2-cyano-2-(hydroxyimino)acetate
o-NBS	*Othro*-nitrobenzene sulfonyl
Pbf	2,2,4,6,7-Pentamethyldihydrobenzofuran-5-sulfonyl
PBS	Phosphate buffer solution
Phg	Phenylglycine
PTMs	Post-translational modifications
PXRD	Powder X-Ray Diffraction
RB	Round bottom flask
RP	Reverse Phase
RNA	Ribonucleic Acid
SC-XRD	Single Crystal X-Ray Diffraction
ssNMR	Solid-State Nuclear Magnetic Resonance
SPPS	Solid Phase Peptide Synthesis
tBu	*tert*-Butyl
TEM	Transmission electron microscopy
TFA	Trifluoroacetic Acid
TGA	Thermogravimetric Analysis
ThT	Thioflavin T
THF	Tetrahydrofuran
TLC	Thin-layer chromatography

TOCSY	Total Correlation Spectroscopy
Tos	Tosyl
Trt	Trityl
t_R	Retention time
UV	Ultraviolet
XRD	X-Ray Diffraction

Abbreviations for intensities of ^{1}H-NMR signals

s	singlet	m	multiplet
d	doublet	brs	broad signal
dd	doublet of doublet	br	broad
t	triplet	Hz	Hertz
q	quartet	MHz	Mega-Hertz

Abstract

The contents of the thesis entitled, **"Investigation on Supramolecular Arrangement and On-Resin Modification of Small Peptides,"** are divided into seven chapters based on the results of the experimental work performed during the complete course of the doctoral studies.

Chapter 1: Contains the general introduction of supramolecular self-association of peptides.

Chapter 2: We demonstrate the investigation of supramolecular self-assembly of two dipeptides: $A\beta_{39\text{-}40}$ and $A\beta_{41\text{-}42}$.

Chapter 3: We describe the investigation of various nanostructures from alternating L/L and D/L amino acid-containing dipeptides.

Chapter 4: We discuss the supramolecular helical self-association of two designed tripeptides.

Chapter 5: We demonstrate the formation of supramolecular single helical and double helical architecture from alternating D/L amino acid containing designed tripeptides.

Chapter 6: We focus on the on-resin side chain modification of aspartic acid and glutamic acid-containing peptides.

Chapter 7: We describe the $FeCl_3$-mediated Boc deprotection and peptide synthesis in solution and SPPS.

The chapter-wise summaries of the mentioned research works are described below.

Chapter 1: Introduction

The self-assembly of small peptides is highly important for biological, chemical, and material sciences. The building blocks undergo self-association to form various supramolecular structures through non-covalent interactions, e.g., hydrogen bonding, electrostatic interactions, π−π stacking, and hydrophobic interactions. Various functional nanostructures such as nanofibrils, nanowires, and nanotubes have been fabricated by self-assembly of small di- or tripeptides.

On the other hand, due to distinctive polyamide structure conformation and function, peptides and their derivatives are used for drug design, disease diagnosis, and molecular imaging. Emil Fischer first synthesized a dipeptide using the acyl chloride method in 1903. Then, peptide chemists developed various protecting groups for *N*- and *C*- termini of amino acids and relevant coupling reagents for solution-phase peptide synthesis. However, the synthesis of long-chain peptides and its purification were strenuous. All these problems were solved by R. B. Merrifield (Nobel Prize 1984) by the invention of the solid phase peptide synthesis (SPPS), which is a milestone of peptide synthesis history. He synthesized a tetrapeptide using a solid support, called Merrifield resin, consisting of the cross-linked chloromethylated styrene-divinylbenzene copolymer. At present, two protocols exist for SPPS based on either Boc/Bzl or Fmoc/^{t}Bu based orthogonal protection strategy.

Chapter 2: Investigation of Supramolecular Self-Assembly of Two Dipeptides: $A\beta_{39-40}$ and $A\beta_{41-42}$.

Alzheimer's disease (AD) is a neurodegenerative disease that causes dementia. The cause of Alzheimer's disease is not fully understood to date. It is believed that AD involves majorly by the accumulation of amyloid β (Aβ) peptides. Moreover, the structure of Aβ peptide is not fully understood. The NMR, XRD, and cryoEM studies suggested that Aβ aggregated to form a cross-β-sheet structure. But, the crystal structures of the full-length Aβ peptide is yet to be reported. Few crystal structures of Aβ fragments are reported.

With this inspiration, we designed and synthesized two dipeptides, Boc-Val-Val-OMe (**2A**) and Boc-Ile-Ala-OMe (**2B**), bearing sequence homogeneity with the *C*-terminus of Alzheimer's $A\beta_{39-40}$ and $A\beta_{41-42}$, respectively. Both two peptides adopted a parallel β-sheet structure in the crystalline state. Peptide **2B** further self-assembled to form a supramolecular cross-β-sheet structure in higher-order packing. The formation of β-sheet structures of both peptides was also confirmed by FT-IR, CD and PXRD experiments. Furthermore, peptide **2A** and **2B** self-associated to form a highly organized straight unbranched several μm long two ended spear-like and a hexagonal hollow tube-like structure, respectively, in methanol-water (2:1) solution incubated at 37 °C for ten days. Interestingly, these self-associated peptides were found to bind with the amyloid binding dyes ThT and Congo red.

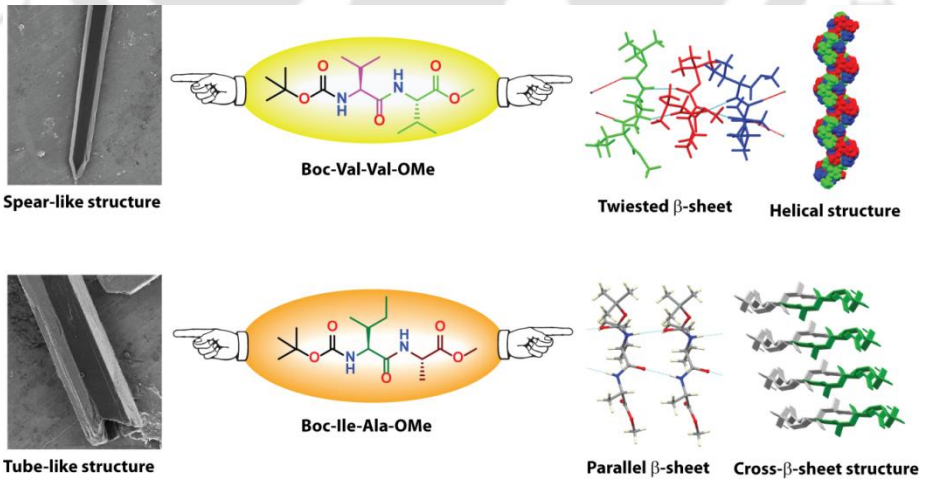

Figure.1. The self-assembled structures of $A\beta_{39-40}$ and $A\beta_{41-42}$

Chapter 3: Investigation of Various Nanostructures from Alternating L/L and D/L Amino Acid Containing Dipeptides

The self-association of peptides to generate various micro- or nano-level structures such as nanofibrils, nanotubes, nanorods, and nanospheres have numerous applications in medicinal chemistry and biotechnology. Nanostructures of the peptide are important as their biocompatibility and biodegradability, self-association ability, capability for specific molecular recognition, and chemical variety. There are several peptide-based nanotubes reported, but most of them are obtained from alternating L/L amino acids. Alternating D/L or unnatural amino acid containing peptide-based nanotubes is not explored enough. However, in the presence of unnatural or alternating D/L amino acid in a peptide sequence increases the proteolytic stability of the nanotube.

To explore the alternating L/L and D/L amino acid containing peptide-based nanostructures, we designed and synthesized both *N*-and *C*- protected four dipeptides, Boc-L-Val-L-Ile-OMe (**3A**), Boc-D-Val-L-Ile-OMe (**3B**), Boc-L-Ile-L-Val-OMe (**3C**), and Boc-L-Ile-D-Val-OMe (**3D**). Peptide **3A** and **3C** self-assembled to build highly organized straight net rods whereas peptide **3B** and **3D** self-assembled to form a hexagonal hollow tube-like architecture in the acetonitrile-water medium. Peptide **3A** and **3B** adopted the twisted β-sheet structure in the crystalline state. They further self-assembled to form helical architecture in higher-order packing. Moreover, each molecule of **3B** inter-connected through two H-bonds to generate a hexagonal cylinder-like architecture around the six-fold screw axis. The obtained nanostructures showed significant thermal stability on dry heating. Interestingly, all those self-associated peptides found to bind with Congo red and ThT dyes.

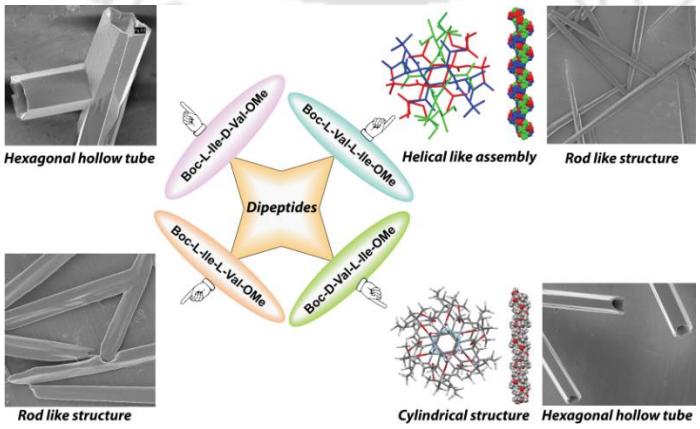

Figure.2. Formation of various nanostructures from alternating L/L and D/L amino acid containing peptide

Chapter 4: The Supramolecular Helical Self-Association of Two Designed Tripeptides

The naturally occurring helical structures, e.g., α-helix of protein, single-stranded helical RNA, double-stranded helices of DNA, and triple-stranded collagen helix, plays an essential role in the biological system. Moreover, the reported peptide-based helical structures are generated by the incorporation of pre-organized kink forming moieties such as proline or Aib. Therefore, the construction of helical structures from without pre-organized kink moieties has attributed an attraction.

To develop the *de novo* designed helical peptides, we synthesized both *N*- and *C*-protected two tripeptides, Boc-Gly-Phe-Phe-OMe (**4A**) and it's analog Boc-Gly-Phg-Phe-OMe (**4B**). Interestingly, **4A** adopted distorted type II β-turn structure (N···O = 3.24 Å and O···HN = 2.58 Å), but no intramolecular (4 → 1) H-bond was observed between *i* (Boc-CO) and *i* + *3* (NH of Phe 2) to form a 10-member cycle in the crystalline state. Such type of structure is known as an open turn structure. Most interestingly, the structure of **4A** is unique, and to the best of our knowledge, this is the first report on a designed open turn tripeptide without having a kink-forming element. Further, it self-associated to form a supramolecular herringbone-like helical architecture in higher-order packing through intermolecular C–H···O interaction. On the other hand, peptide **4B** adopted a parallel β-sheet structure, which further self-organized to form a helical structure through intermolecular C–H···O and C–H···π interactions in higher-order packing in the crystalline state. The conformations of these peptides were also checked by solvent dependent NMR titration, 2D NOESY, and CD spectroscopic experiments in solution.

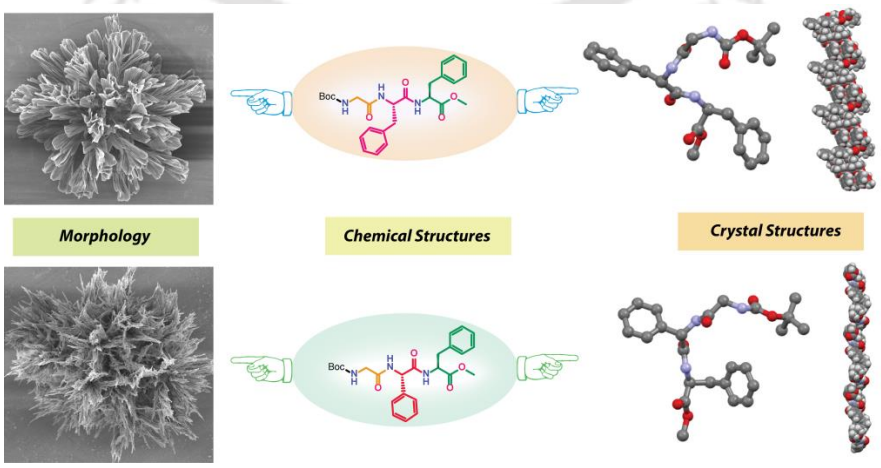

Figure 3. The crystal structures and morphology of the above two peptides.

Chapter 5: Formation of Supramolecular Single Helical and Double Helical Architecture from Alternating D/L Amino Acid Containing Designed Tripeptides

The naturally occurring double-stranded helical structure is rare. DNA adopts a double-stranded helix, plays an essential role in the biological system, e.g., information storage and transcription. The development of the peptide-based double-stranded helix is a challenging task. Few double helices of small peptides are reported, but most of them are generated from the installation of preorganized kink moieties.

To explore the alternating D/L amino acids containing peptide-based helical and double helical structures, we designed and synthesized both *N*- and *C*- protected two tripeptides, Boc-Gly-L-Phg-D-Phe-OMe (**5A**) and Boc-Gly-L-Phg-D-Phg-OMe (**5B**). Both peptide **5A** and **5B** adopted an anti-parallel β-sheet structure in the crystalline state, but they further self-organized to form a supramolecular single helix and double helix-like architectures, respectively, by various non-covalent interactions. To the best of our knowledge, this is the first crystallographic report for the formation of a double helix-like structure from alternating D/L unnatural amino acid containing small tripeptide. The conformations of these peptides were further investigated by solvent dependent NMR titration, 2D NOESY, and CD spectroscopic experiments in solution. The self-assembled peptides **5A** and **5B** exhibited a bunch of flower-petal-like and flower-like architectures, respectively, in an acetonitrile-water solution.

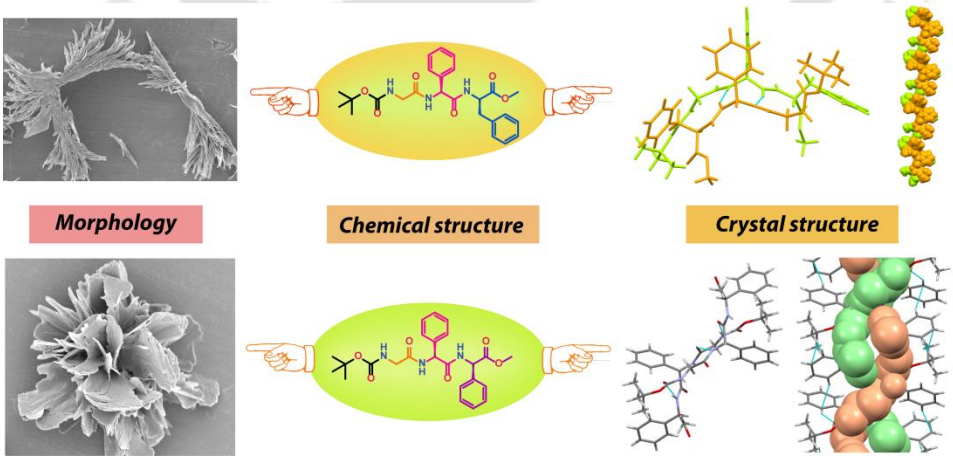

Figure 4. The morphology and crystal structure of self-assembled alternating D/L amino acid-containing peptides

Chapter 6: On-resin Side Chain Modification of Aspartic Acid and Glutamic Acid Containing Peptides

To understand the molecular mechanisms and biomedical applications, chemical modification of peptides or proteins is important. The artificial chemical modifications refer to the incorporation of various fluorophores for bioimaging and PEGylation for increasing *in vivo* stability and solubility or reduce immunogenicity and glycosylation for preparation of vaccine and drug. Normally, the tert-butyl ester protected side-chain of Fmoc-Asp/Glu is used to synthesis of peptides in SPPS. This tert-butyl ester group can be removed by various protic acids and Lewis acids in solution. However, they suffer from some problems, e.g., high acidic conditions, corrosive, and handling problems. To the best of our knowledge, the above methods were used on tert-butyl ester cleavage in solution only. Therefore, a mild, efficient, convenient, and environmentally friendly method is needed for tert-butyl ester cleavage of the side-chain of Asp/Glu containing peptide on-resin.

Herein, we developed a Lewis acid, $FeCl_3$-based method for removal of tert-butyl group from the side-chain of Asp/Glu during SPPS. This method is mild, cost-effective, and Fmoc chemistry compatible. The tert-butyl group on the side-chain of Asp/Glu was easily removed by using $FeCl_3$ (5 equiv) in DCM within 1.5 h without cleavage of resin, and the excess $FeCl_3$ was removed from the resin by washing with DMF. Then the esterification, thioesterification, and amidation were performed on that desired carboxylic acid of the side chain of Asp/Glu by using coupling reagent, base, and corresponding nucleophiles, e.g., alcohols, thiols, and amines. The isolated yields were found to be moderate to good. We were also able to attach a fluorophore on the side chain of Asp on-resin.

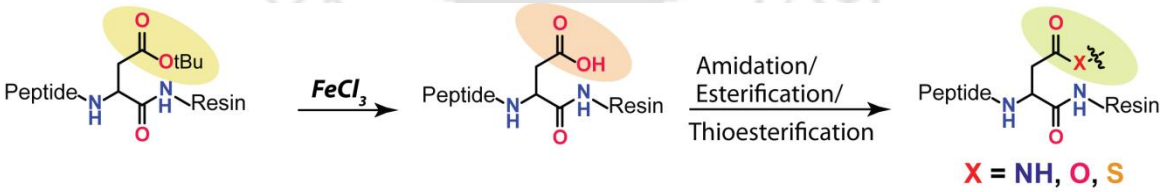

Figure 5. Side-chain modification of Asp/Glu on-resin

Chapter 7: $FeCl_3$-Mediated Boc Deprotection and Peptide Synthesis in Solution and SPPS

Generally, peptides are synthesized by standard coupling methods in solution. The Boc protected amino acids are frequently used for peptide synthesis in solution and Boc/Bzl SPPS. Each step of Boc deprotection of *N*-terminal amino acid is carried out by TFA. But, the TFA is non-environmentally friendly, cost-effective, and corrosive. The Boc group is also removed by strong acids, or by Lewis acids. To the best of our knowledge, the reported Lewis acid-based methods were applied for Boc deprotection of only amine or amino acids but were not explored further for peptide synthesis.

Herein, we developed a mild, effective, and greener $FeCl_3$ based method for deprotection of the Boc group from the *N*-terminus of amino acid containing peptide and peptide sequence could be elongated by using coupling reagent and base both in solution and SPPS. In this way, we synthesized a library of di-, tri- and tetra-peptides in solution with moderate to good yield. Interestingly, this protocol could be applied for peptide synthesis by using Boc protected amino acid on the acid-sensitive Rink amide resin, which is usually used for Fmoc chemistry. We synthesized some biologically active small peptides, e.g., LVFFA-NH_2 (17-21) of $A\beta_{1\text{-}42}$, NFGAIL-NH_2 (22-27) of Amylin (1-37), YGGFL-NH_2 of Leu-enkephalin, and YaGFM-NH_2 of [D-Ala^2, Met^5]-enkephalinamide by using this protocol. Most interestingly, we performed both Fomc chemistry and Boc chemistry on the same resin (Rink amide), and in this way, we synthesized a model *N*-terminally branched peptide and a model side-chain to side-chain cyclic peptide.

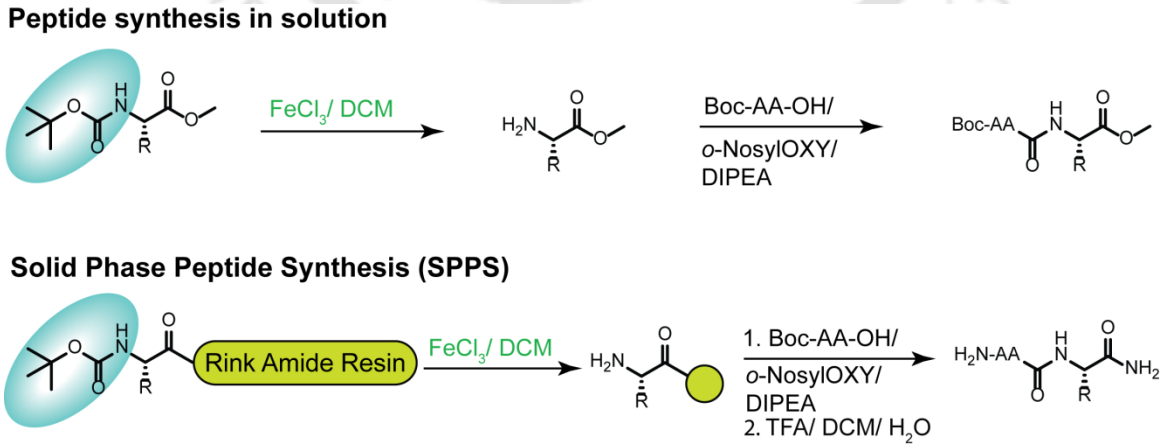

Figure 6. A schematic representation of peptide synthesis in solution and SPPS

Table of contents

Statement		i
Certificate		ii
Acknowledgements		iii
List of Abbreviations		v
Abstract		ix
Contents		xvii

Chapter 1. Introduction and objectives

1.1.	Introduction	1
1.2.	Amino acids	1
1.3.	Peptides and proteins	3
	1.3.1. Torsion angles and Ramachandran plot	3
	1.3.2. Structure of proteins	5
1.4.	Supramolecular assemblies	10
1.5.	Alzheimer's disease	11
	1.5.1 Amyloid β (Aβ) peptide	11
	1.5.2 The structural feature of Aβ peptide	11
1.6.	Nanostructures of small peptides	12
1.7.	Helical and double-helical assemblies of small peptides	14
	1.7.1 Single helical structures	14
	1.7.2 Double-helical structures	15
1.8.	Peptide modifications	15
	1.8.1. Existing methods for modification of peptides	17
1.9.	Peptide synthesis	19
	1.9.1. Peptide synthesis in solution	19

1.9.2. Solid phase peptide synthesis 20

1.10. Drawbacks of the existing methods 21

1.11. Objectives of the thesis 22

1.12. References 23

Chapter 2. Investigation of Supramolecular Self-assembly of Two Dipeptides: $A\beta_{39-40}$ and $A\beta_{41-42}$

2.1. Background 33

2.2. Design of peptides 33

2.3. Synthesis and characterization of the designed peptides 34

2.4. Investigation of secondary structure by FT-IR 34

2.5. Investigation of self-assembly process by SC-XRD 35

2.6. Conformation analysis by CD experiment in solution 38

2.7. Investigation of the secondary structure of 10-day incubated samples by FT-IR 39

2.8. Monitoring the self-association of 2A and 2B in solution by FE-SEM 39

2.9. Investigation of dye binding affinity of this self-aggregated peptide by fluorescence microscope 40

2.10. Investigation of self-assembly process by PXRD 41

2.11. Investigation of thermal stability by TGA 42

2.12. Conclusion 43

2.13. Experimental section 44

2.13.1. Materials and instrumentations 44

2.13.2. General procedure for the synthesis of dipeptides 44

2.13.3. Sample preparation 44

2.14. Characterization data 45

2.15. References 46

2.16. Selected spectra 47

2.16.1. Spectra of peptide 2A 47

2.16.2. Spectra of peptide 2B 49

2.17. Crystallographic data 51

Chapter 3: Investigation of Various Nanostructures from Alternating L/L and D/L Amino Acid Containing Dipeptides

3.1. Background 53

3.2. Design of peptides 53

3.3 Synthesis and characterization of the designed peptides 54

3.4. Investigation of nanostructures by various microscopes 54

3.5. Investigation of self-assembly process by SC-XRD 57

3.6. Investigation of self-assembly process by PXRD 60

3.7. Investigation of secondary structure by FT-IR 61

3.8. Conformation analysis by CD experiment in solution 62

3.9. Investigation of dye binding affinity of these self-aggregated peptides by fluorescence microscope 63

3.10. Monitoring the thermal stabilities of the nanostructures 64

3.11. Conclusion 65

3.12. Experimental section 66

3.12.1. Materials and instrumentations 66

3.12.2. General procedure for the synthesis of dipeptides 66

3.12.1. Sample preparation 66

3.13. Characterization data 66

3.14. References 68

3.15. Selected spectra 69

3.15.1. Spectra of peptide 3A 69

3.15.2. Spectra of peptide 3B 71

3.15.1. Spectra of peptide 3C 73

3.15.1. Spectra of peptide 3D 75

3.16. Crystallographic data 77

Chapter 4: The Supramolecular Helical Self-Association of Two Designed Tripeptides

4.1. Background 79

4.2. Design of peptides 79

4.3. Synthesis and characterization of the designed peptides 79

4.4 Investigation of self-assembly process by SC-XRD 80

4.5. Comparison between type II β-turn and open turn . 83

4.6. Comparison of the molecular structure of peptide 4A and 4B 86

4.7. Investigation of intra- or intermolecular H-bond in solution 87

4.8. Characterization of conformation of 4A and 4B by NOE interactions in solution 89

4.9. Conformation analysis by CD experiment in solution 90

4.10. Monitoring the self-association of 4A and 4B in solution by various microscopic experiment 91

4.11. Conclusion 92

4.12. Experimental section 93

4.12.1. Materials and instrumentations 93

4.12.2. General procedure for the synthesis of tripeptides 93

4.12.3. Sample preparation 93

4.13. Characterization data 94

4.14. References 95

4.15. Selected spectra 96

4.15.1. Spectra of peptide 4A 96

4.15.2. Spectra of peptide 4B 99

4.16. Crystallographic data 103

Chapter 5: Formation of Supramolecular Single Helical and Double Helical Architectures from Alternating D/L Amino Acid Containing Designed Tripeptides

5.1. Background 105

5.2. Design of peptides 105

5.3. Synthesis and characterization of the designed peptides 106

5.4. Investigation of self-assembly process by SC-XRD 106

5.5. Comparison of the molecular structure of peptide 5A and 5B 110

5.6. Investigation of intra- or intermolecular H-bond in solution . 112

5.7. Characterization of conformation of 5A and 5B by NOE interactions in solution 114

5.8. Conformation analysis by CD experiment in solution 115

5.9. Monitoring the self-association of 5A and 5B in solution by various microscopic experiment 116

5.10. Conclusion 117

5.11. Experimental section 117

5.11.1. Materials and instrumentations 117

5.11.2. General procedure for the synthesis of tripeptides 117

5.11.3. Sample preparation 118

5.12. Characterization data 118

5.13. References 119

5.14. Selected spectra 120

5.14.1. Spectra of peptide 5A 120

5.14.2. Spectra of peptide 5B 122

5.15. Crystallographic data 124

Chapter 6: On-resin Side Chain Modification of AsparticAcid- and Glutamic acid-Containing Peptides

6.1. Background 127

6.2. The existing method for removal of tert-butyl group 127

6.3. Our approach 127

6.4. Optimization of the tert-butyl cleavage condition 128

6.5. Compatibility with some frequently used protecting groups in solution 130

6.6. Racemization study 132

6.7. Formation of C-N/C-O/C-S bond after removal of tBu in SPPS 132

6.8. Sustainability of the Rink amide resin during $FeCl_3$ treatment 134
6.9. Compatibility with some frequently used protecting groups in solid phase 135
6.10. Multi-functionalization of the side-chain of Asp/Glu on solid-support 136
6.11. Fluorophore attachment 137
6.12. Plausible mechanism 137
6.13. Conclusion 138
6.14. Experimental section 138
6.14.1. Materials and instrumentation 138
6.14.2. General procedure for the removal of tert-butyl ester 138
6.14.3. Monitoring of removal of tert-butyl ester (I) by HPLC 138
6.14.4. General procedure for peptide syntheses in SPPS 139
6.15. Characterization data 141
6.16. References 146
6.17. Selected spectra 148

Chapter 7: $FeCl_3$-Mediated Boc Deprotection and Peptide Synthesis in Solution and SPPS

7.1. Background 153
7.2. Existing method for removal of Boc group 153
7.3. Our approach 153
7.4. A time-dependent HPLC study to monitor the Boc cleavage 154
7.5. Isolation of Boc-deprotected product 155
7.6. Substrates scope for the synthesis of peptides in solution 155
7.7. Crystallographic evidence of the formation of the dipeptides 158
7.8. Racemization study 158
7.9. Wide scope for SPPS on acid-sensitive Rink amide resin 159
7.10. Monitoring of peptide synthesis by HPLC 160
7.11. Synthesis of some biologically important peptides 160

7.12. Peptide synthesis by both Fmoc and Boc chemistry on Rink amide resin 161

7.12.1. Application of the protocol for peptide branching 161

7.12.2. Application of the protocol for cyclic peptide synthesis 162

7.13. Drawbacks and advantages of this protocol 163

7.14. Plausible mechanism 163

7.15. Conclusion 164

7.16. Experimental section 165

7.16.1. Materials and instrumentation 165

7.16.2. General procedure for Boc-deprotection in solution 165

7.16.3. Monitoring of Boc-cleavage by HPLC 165

7.16.4. General procedure for dipeptide synthesis in solution 165

7.16.5. General procedure for tri-/tetra-peptide synthesis in solution 166

7.16.6. General procedure for peptide synthesis in the solid phase (SPPS) 166

7.17. Characterization data 168

7.18. References 177

7.19. Selected spectra 178

7.19.1. HPLC profile of deprotection of Boc-Phe-OMe (A) to H_2N-Phe-OMe (B) using 1.5 equiv of $FeCl_3$ in DCM with time 178

7.19.2. Spectra of synthesized peptides from solution 181

7.19.3. Racemization study 183

7.19.4. Spectra of synthesized peptides from SPPS 184

7.20. Crystallographic data 190

Chapter 8: Materials and Instrumentations

8.1. Materials 191

8.2. Instrumentation 191

8.2.1. Chromatographic technique 191

8.2.2. High-performance liquid chromatography (HPLC) 191

8.2.3. Solvent evaporation technique 192
8.2.4. Mass spectrometry 192
8.2.5. Nuclear magnetic resonance (NMR) spectroscopy 192
8.2.6. Single crystal X-ray diffraction (SC-XRD) 192
8.2.7. Fourier-transform infrared (FT-IR) spectroscopy 192
8.2.8. Melting point 193
8.2.9. Circular dichroism (CD) 193
8.2.10. Powder X-ray diffraction (PXRD) 193
8.2.11. Thermogravimetric analysis (TGA) 193
8.2.12. Optical microscopic images 193
8.2.13. Field emission scanning electron microscopy (FE-SEM) 193
8.2.14. Transmission electron microscope (TEM) 193
8.2.15. Atomic force microscopy (AFM) 194
8.2.16. Congo red and ThT dye interacting image 194
Conclusion and future directions 195
Research Outcome 197
Curriculum vitae 201

Chapter 1

Introduction and Objectives

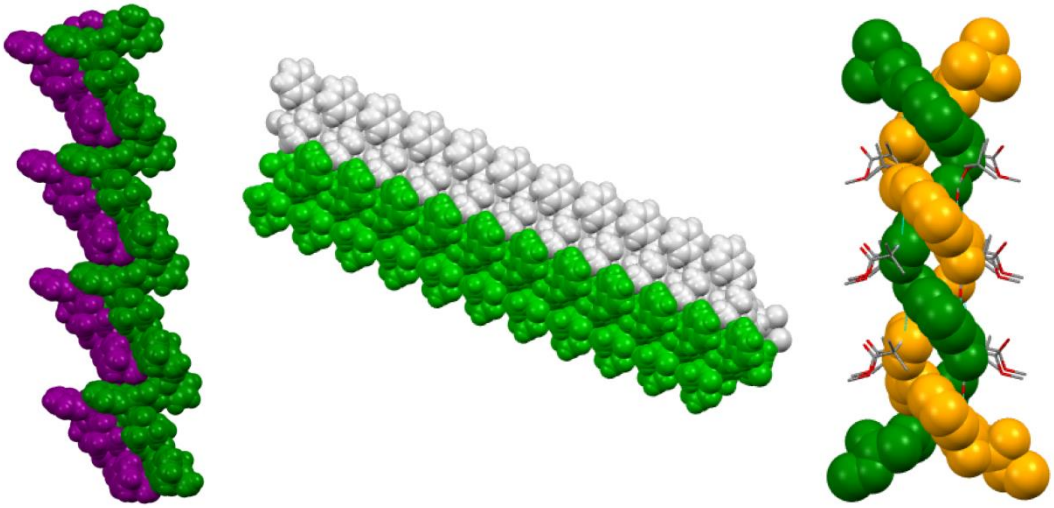

1.1. Introduction

We describe the supramolecular self-assembly, conformation, and morphology of small peptides, as well as the development of new strategies for peptide synthesis and modification in solution and on solid support in this thesis. In this introductory chapter, we describe different features related to self-association and existing methods for peptide synthesis and modifications.

1.2. Amino acids

Amino acids are building blocks of peptides and proteins. There are 22 naturally occurring α-amino acids, which are involved in protein construction. These α-amino acids exist in two optically isomeric forms, i.e., L and D isomers, but only L-isomers are present in the proteins; therefore, these amino acids (L) are known as proteinogenic or coded amino acids. It has a central chiral carbon, connected with a carboxylic acid group (-COOH), amino group (-NH_2), hydrogen (H), and a side chain R group (Figure 1.1a). The R group bears the functional groups, e.g., hydrogen, alkyl, aromatic, -COOH,-NH_2, -$CONH_2$, -OH, -SH, *etc.* The chemical and physical properties of amino acids depend on the side chain. They exist in a zwitterionic form (Figure 1.1b) at biological pH (7.4).

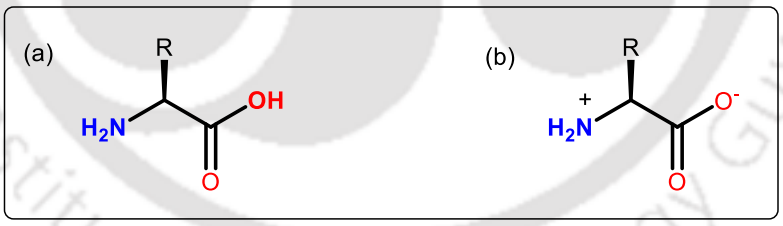

Figure 1.1. *(a) Neutral structure of an α-amino acid and (b) its zwitterionic structure*

Besides the standard amino acids, there are many unnatural amino acids present in the biological system, e.g., Phenylglycine (Phg), 2-aminoisobutyric acid (Aib), ornithine, β-alanine, and D-amino acids, which increases the proteolytic stability of a peptide whereas the standard amino acids fail to do so. The natural amino acids are categorized into five classes depending on the properties of the side-chain R group. All amino acids are listed in Table 1.1.

Table 1.1. The classification of 22 natural amino acids

R group	*Amino acids*	*Abbreviation*	
		Three letter code	*One letter code*
Non-polar	Glycine	Gly	G
	Alanine	Ala	A
	Proline	Pro	P
	Valine	Val	V
	Leucine	Leu	L
	Isoleucine	Ile	I
	Methionine	Met	M
	Selenocysteine	Sec	U
Aromatic	Phenylalanine	Phe	F
	Tyrosine	Tyr	Y
	Tryptophan	Trp	W
Polar, uncharged	Serine	Ser	S
	Threonine	Thr	T
	Cysteine	Cys	C
	Asparagine	Asn	N
	Glutamine	Gln	Q
Positively charged	Lysine	Lys	K
	Arginine	Arg	R
	Histidine	His	H
	Pyrrolysine	Pyl	O
Negatively charged	Aspartic acid	Asp	D
	Glutamic acid	Glu	E

1.3. Peptides and proteins

Proteins are an important class of bio-macromolecules, consisting of one or more long-chain polypeptides in the living system. The polypeptide chain contains more than 50 amino acid residues to build a protein, and the molecular weights of most proteins vary from 10 to 100 kilo Daltons (kDa). Proteins act as enzymes, neurotransmitters, hormones, cytokines, growth factors, and receptors.[1-3]

Figure 1.2. *Schematic representation of the formation of protein*

A peptide bond is formed by condensation of the carboxylic acid group of one amino acid and the amino group of another amino acid. The amide or peptide bonds (C-N) are planer and unable to rotate as they contain partial double bond character by delocalization of electron from the lone pair of nitrogen between amino and carbonyl group (Figure 1.3a). Due to the presence of the double bond character of the C-N bond, it generates two geometrical isomers, i.e., *cis* and *trans* (Figure 1.3b).

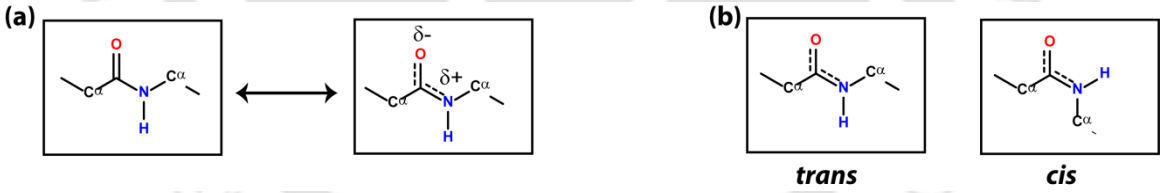

Figure 1.3. *(a) Resonance stabilized the structure and (b) geometrical isomers of peptide bond*

1.3.1. Torsion angles and Ramachandran plot

In peptide, the peptide bond (C-N) is planer and restricted for free rotation, but the other two Cα-C and N-Cα bonds can be rotated.[4] The rotation around the N-Cα bond and Cα-C is called as phi (ϕ) angle and psi (ψ) angle, respectively (Figure 1.4). The value of ϕ and ψ can vary between -180^{o} to +180^{o}. Due to the double bond character of the omega (ω) bond (C-N), the value of ω angle always closed to 180^{o}.

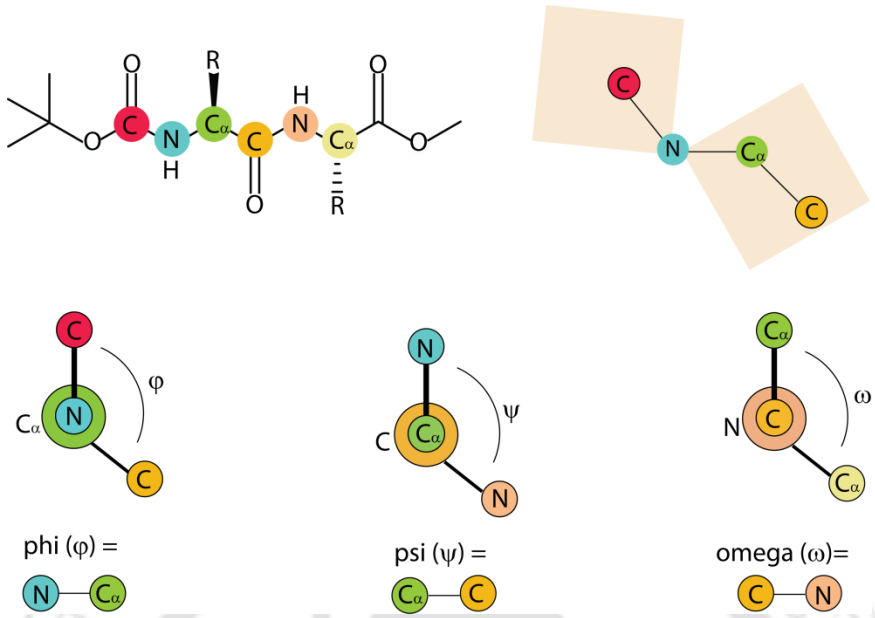

Figure 1.4. *Schematic representation of various torsion angles of both N- and C- protected dipeptide*

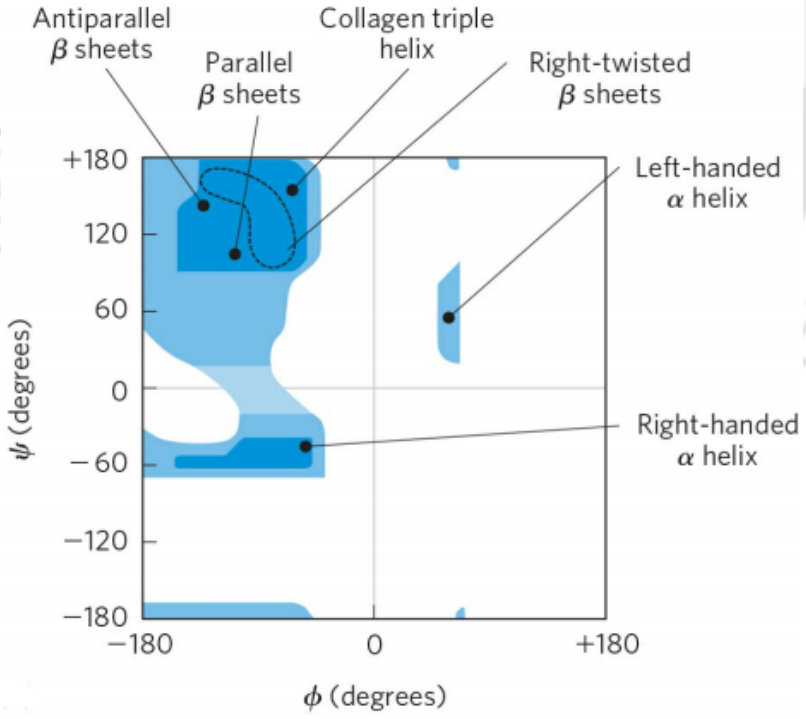

Figure 1.5*. A graphical representation of Ramachandran plot (Courtesy: image taken from Nelson, D. L. and Cox, M. M. Lehninger principles of biochemistry, seventh edition)*

The conformation of a peptide is described by two torsion angles ϕ and ψ, which was first proposed by Ramachandran.[5] Based on these two torsion angles, he plotted a graph called Ramachandran plot where all allowed, sterically less hindered, and the stable conformational region was indicated (Figure 1.5). From this plot, we can easily predict the secondary structure of a peptide or protein.

1.3.2. Structure of proteins

The structure of proteins is described by in levels, i.e., primary, secondary, tertiary and quaternary structures.[4,6]

Primary structure

The sequence of amino acid residues (basically peptide bonds and disulfide bonds) in a polypeptide chain gives the primary structure of a protein.

Secondary structure

Secondary structure refers to the backbone orientation, which is stabilized by mainly hydrogen bonding interactions between NH and CO of the peptide bond. The observed most common secondary structures are: α-helix, β-sheet, and β-turn.[7]

α-helix

It is a coiled structure of a polypeptide or protein, where the backbone carbonyl group (C=O) of residue *i* interacts with the amide NH of (*i*+4) through intramolecular H-bond. The backbone is grown around an imaginary axis (passing through the middle of the helix), where all side-chain groups are located outside of the backbone (Figure 1.6). The distance between the helical turn is 5.4 Å, and the distance between two amino acid residues along the helical axis is 1.5 Å. There are 3.6 amino acid residues present per turn and the consecutive amino acid residues from angles of 100^o around the helical axis.[8] The backbone torsion angles of an α-helix are ϕ=-57^o and ψ=-47^o. The naturally occurring right-handed α-helixes (constructed by amino acids of L-configuration) are more stable

than left-handed α-helixes (constructed by amino acids of D-configuration) which are rare in nature (Figure 1.6c).

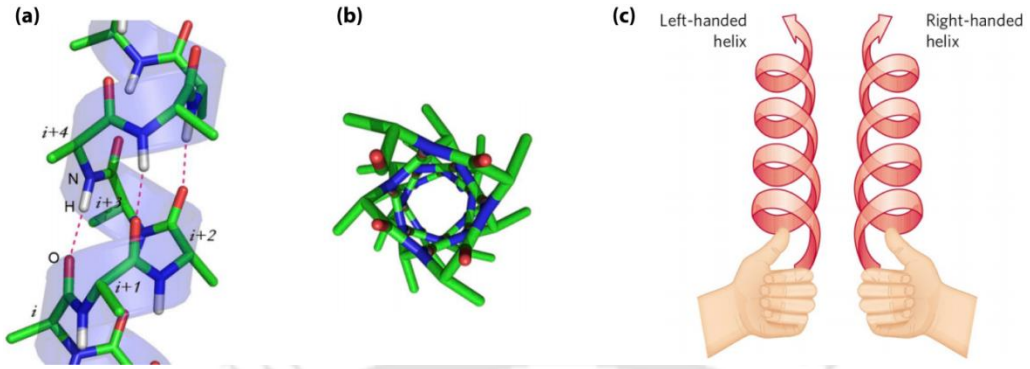

Figure 1.6. *(a) The side view and (b) top view of α-helix (Courtesy: image taken from Vieira-Pires, R. S.; Morais-Cabral, J. H. J. Gen. Physiol.* ***2010****, 136, 585-592). (c) The left-handed and right-handed α-helix (Courtesy: image taken from Nelson, D. L. and Cox, M. M. Lehninger principles of biochemistry, seventh edition).*

3_{10}-helix

3_{10}-helix is also a similar type of α-helix, but the backbone carbonyl group of amino acid residue *i* interconnect with the amide NH of *i*+3 through intramolecular H-bond (Figure 1.7). The helical pitch is 5.8-6 Å, and the distance between two amino acid residues along the helical axis is 1.93-2.0 Å.

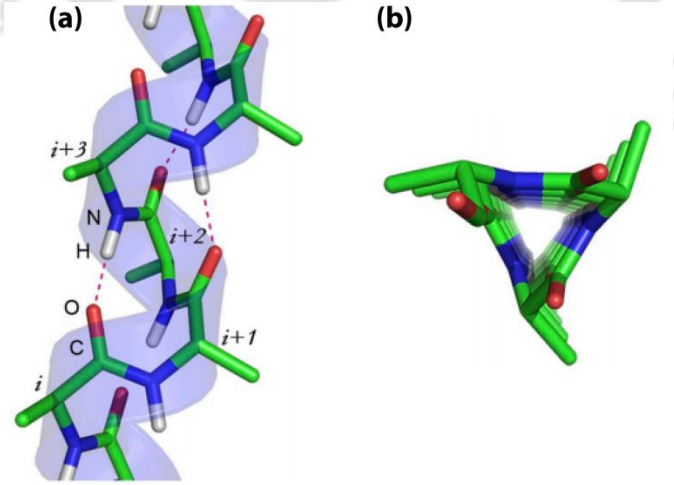

Figure 1.7. *(a) The side view and (b) top view of a 3_{10}-helix (Courtesy: image taken from Vieira-Pires, R. S.; Morais-Cabral, J. H. J. Gen. Physiol.* ***2010****, 136, 585-592).*

It contains 3 amino acid residues per turn and the consecutive amino acid residues from angles of 120^o around the helical axis.[8] The backbone torsion angles (ϕ, ψ) of a 3_{10}-helix is around (-49^o, -26^o). It is longer, thinner, and tightly wound than an α-helix. Such helix is first proposed by Max Perutz.

β-sheet

It is a backbone extended structure of polypeptide chains, and the structure is stabilized by intermolecular H-bond between carbonyl group (C=O) of one strand and the amide NH group of the adjacent strand to form an H-bonding network.[9] When a series of polypeptide strands are connected through H-bond is called *beta-pleated sheet*. There are two types of β-sheet structure: parallel β-sheet (adjacent strands can run in the same direction, Figure 1.8a), and anti-parallel β-sheet (adjacent strands can run in the opposite direction, Figure 1.8a). The distance between the Cα of *i* residue and Cα of *i*+2 residue in a parallel strand (6.5 Å) is shorter than the anti-parallel strand (7.0 Å). The anti-parallel β-sheets are more stable than parallel β-sheet as the intermolecular H-bond of anti-parallel β-sheet is lying in-line between two adjacent strands whereas, in parallel β-sheet, the intermolecular H-bonds are distorted or not lying in-line. The torsion angles (ϕ, ψ) of the parallel and ant-parallel β-sheets are (-119^o, 113^o) and (-139^o, 135^o).

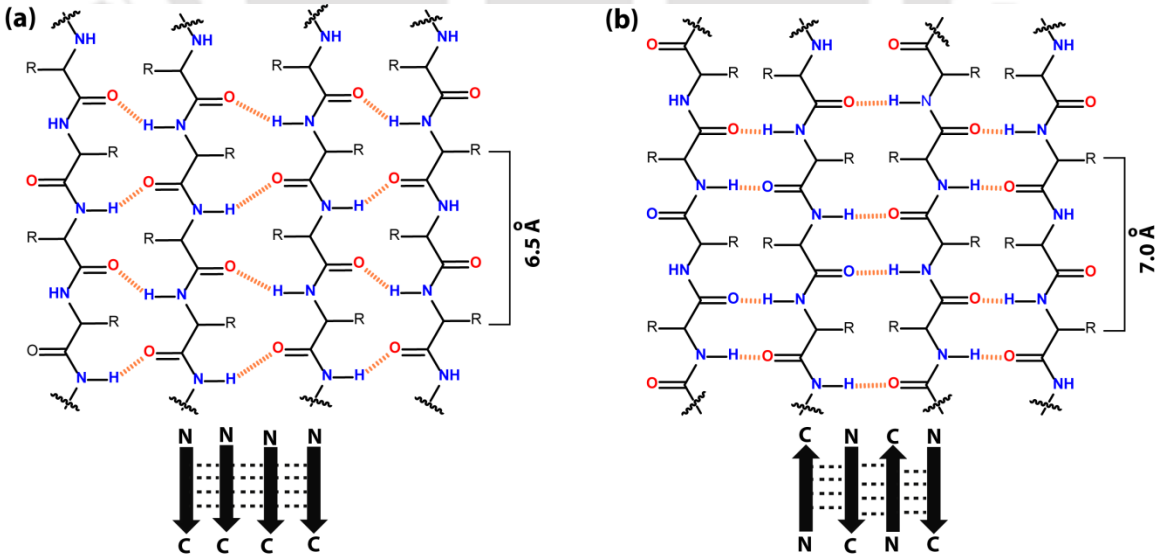

Figure 1.8. *The secondary structure of (a) parallel and (b) anti-parallel β-sheet*

β-turn

It is another type of secondary structure of protein where the backbone carbonyl group (C=O) of residue *i* and the amide NH of *i*+3 are interconnected through an intramolecular H-bond to form a 180^{o} turn, and the direction of the polypeptide chain is reversed. Such type of structure is called *β*-turn or reverse turn (Figure 1.9). There are nine types of β-turn structures, which are classified based on the backbone torsion angles. The torsion angles of all types of *β*-turn are listed in a tabular form (Table 1.2). In 1968, Venkatachalam first determined the possible types of β-turn.[10]

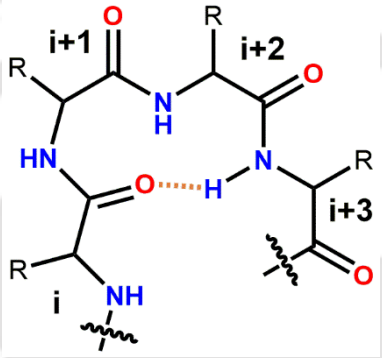

Figure 1.9. *β-turn structure*

Table 1.2. A list of torsion angles (deg) of all possible *β*-turn structures[10,11]

β-turn type	***i+1***		***i+2***	
	ϕ	***ψ***	***ϕ***	***ψ***
Type I	-60	-30	-90	0
Type I'	60	30	90	0
Type II	-60	120	80	0
Type II'	60	-120	-80	0
Type VIII	-60	-30	-120	120
Type VIa1	-60	120	-90	0
Type VIa2	-120	120	-60	0
Type VIb	-135	135	-75	160
Type IV	-61	10	-53	17

Table 1.3. List of torsion angles of common secondary structures of polypeptide or protein

Structure	***Torsion angles (deg)***	
	ϕ	***ψ***
α-helix	-57	-47
3_{10}-helix	-49	-26
Parallel β-sheet	-119	113
Anti-parallel β-sheet	-139	135
Type I β-turn:i+1 residue	-60	-30
i+2 residue	-90	0
Type II β-turn:i+1 residue	-60	120
i+2 residue	80	0

Tertiary structure

It is the 3D folded structure of a polypeptide (Figure 1.10). The folding may happen by supramolecular non-covalent interactions, e.g., salt-bridge interaction, H-bonding interaction, hydrophobic interaction, and van der Waals interaction of the side chains of amino acid residues in a polypeptide. The two major 3D shapes of proteins occur naturally: fibrous and globular. For example, myoglobin is a globular protein that consists of eight helical segments.

Quaternary structure

The subunits of many proteins are interconnected together through non-covalent interactions, and the formation of such type of arrangement is called the quaternary structure of a protein (Figure 1.10).

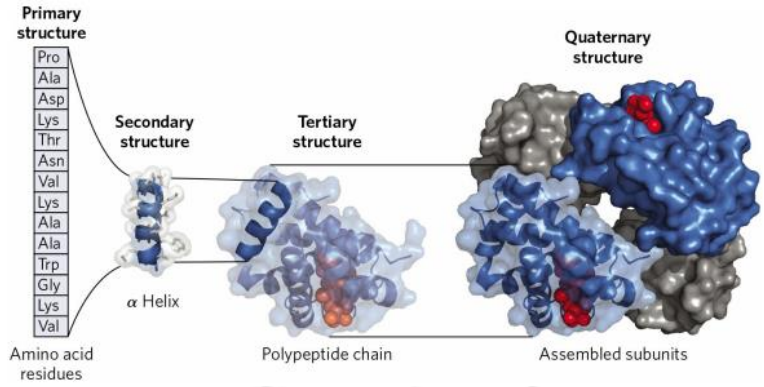

Figure 1.10. *Overview of the all four-level structures of a protein (Courtesy: image taken from Nelson, D. L. and Cox, M. M. Lehninger principles of biochemistry, seventh edition)*

1.4. Supramolecular assemblies

The term 'supramolecular chemistry' indicates 'chemistry beyond the molecule,' i.e., the molecules assembled through noncovalent interactions. Thus, this chemistry is slightly different from molecular chemistry, where the covalent bond formation is the main feature.

The supramolecular assemblies are generated by the noncovalent interactions between molecules. The noncovalent interactions are:

- Electrostatic interactions
- Van der Waals interactions
- Hydrophobic interactions
- Hydrogen bonding interactions
- π-π stacking interactions

1.5. Alzheimer's disease

German psychiatrist Dr. Alois Alzheimer first noted this disease in his women patient, Auguste Deter, in 1906. It causes progressive attrition of cognition, speech, mood, behavior, and memory.[12] The cause of Alzheimer's disease (AD) is not fully understood to date. It is believed that AD involves majorly two types of protein aggregation:

1. Intracellular aggregation of the microtubule-associated tau protein (called neurofibrillary tangles- NFTs).

2. Extracellular peptide aggregation is known as senile plaques, due to the accumulation of amyloid β (Aβ) peptides.[13]

1.5.1. Amyloid β (Aβ) peptide

The origin of Aβ peptide is obtained from the proteolytic cleavage of a membrane protein called Amyloid precursor protein (APP).[14] Aβ peptide is generated from the cleavage of APP protein by the enzyme β-secretase and γ-secretase.[15] The sequence of $A\beta_{1-42}$ is shown in Figure 1.11.

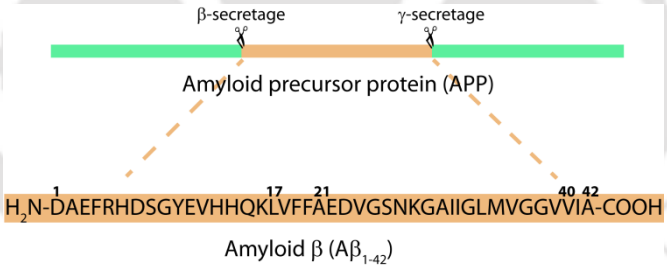

Figure 1.11. *A schematic diagram of the formation of Aβ peptide from APP*

The growing evidence suggests that the native form of Aβ is a random coil, but in the disease condition, it first aggregate to form soluble oligomer then converts to insoluble β-sheet rich fibrillar aggregates.[16,17]

1.5.2. The structural feature of Aβ peptide

The NMR, XRD, and cryoEM studies revealed that Aβ aggregate to form cross-β-sheet structure.[18-23] Lansbury *et al.* demonstrated the antiparallel β-sheet structure of $A\beta_{34-42}$ peptide by using ssNMR.[24,25] Tycko and coworkers described an antiparallel β-sheet

structure of a model $A\beta_{16–22}$ peptides by ssNMR spectroscopy.[26] Further, they also observed that $A\beta_{1–40}$ aggregated to form a U-shaped structure wherein the first 10 residues are structurally disordered but 12–24 and 30–40 amino acid residues formed two parallel β-strand through intramolecular H-bonding and the U-turn region residues 25-29 are present, and this turn is stabilized by salt-bridge interaction between the side chain carboxylic acid group of Asp (Asp-23) and the amine group of Lys (Lys-28) based on ssNMR investigation.[27] It is believed that the formation of the fibril of Aβ is more crucial at the central hydrophobic core region (17-21, LVFFA) than that of the *C*-terminal hydrophobic region (29-42).[28-30] The mechanism of aggregation of Aβ to form fibril is not fully understood until now. Scientists are trying to understand the structure of the full length of Aβ or the small fragments of Aβ peptide by SC-XRD. Banerjee *et al.* developed the crystal structure of $A\beta_{40–42,}$ which adopted the anti-parallel β-sheet structure and also exhibited an amyloidogenic nature.[31] They also reported the amyloidogenic nature of $A\beta_{9–11}$ and it adopted a β-sheet structure in crystalline state.[32] Haldar *et al.* reported the crystal structure of both *N*- and *C*- protected dipeptide bearing sequence homogeneity with $A\beta_{18–19}$ exhibited a cross-β-sheet structure.[33] Görbitz *et al.* described the crystal structure of Boc-VV-OMe which showed a twisted parallel β-sheet structure.[34]

1.6. Nanostructures of small peptides

Molecular self-assembly deals with a unique way for the construction of novel supramolecular structures. The development of such types of structures was inspired by nature as the biological system forms various complex structures from nucleic acids, lipids, and amino acids. Nanostructures of the peptide are important as their biocompatibility and biodegradability, self-association ability, capability for specific molecular recognition, and chemical variety.[35-38] The self-assembly of peptides, e.g., cyclic peptides,[39,40] aromatic or aliphatic dipeptides,[41-43] surfactant-like peptides[44] or amphiphile peptides[45] constructed the defined supramolecular assemblies such as nanofibrils, nanoribbons, nanotubes, nanorods, nanospheres, nanotapes, nanobelts, and gels. have numerous applications in medicinal chemistry and biotechnology such as tissue engineering,[37,46] drug-delivery,[47,48] glucose transporters,[49] ion channels,[50] nano-electronics,[51] and sensors.[52]

Ghadiri *et al.* first developed the peptide-based nanotube from the self-assembly of alternating D/L amino acids containing cyclic octapeptide peptide, *cyclo*[-(D-Ala-Glu-D-Ala-Gln)$_2$-].[53] This is the milestone of peptide nanotube chemistry. Later, Lorenzi *et al.* reported the crystal structures of alternating D/L or L/D amino acid-containing dipeptides, which self-assembled to form a hexagonal cylinder-like structure.[54] Zhang *et al.* reported the open-ended nanotube network from the self-assembly of liner surfactant-like hepta- or octapeptides.[55]

Görbitz first demonstrated the peptide-based nanotube structure from the small dipeptides based on the SC-XRD experiment. He reported a library of crystal structures of small dipeptides, e.g., Phe-Leu, Leu-Phe, Leu-Leu, Phe-Phe (Figure 1.12), *etc.* [56-58] Ripmeester *et al.* also observed the tubular assembly of various hydrophobic dipeptides.[59]

A new era of the peptide-based nanotubes has been started when Gazit *et al.* described the application of the nanotube of diphenylalanine. The diphenylalanine is the core hydrophobic recognition sequence of the Alzheimer's amyloid β. The nanotubes of diphenylalanine are formed from the 1,1,1,3,3,3 hexafluoro-2-propanol solvent, and they act as a template for silver nanowire formation.[41] These nanotubes are applied for electrochemical biosensing,[60-62] template for magnetic nanoparticles,[62] nanoforests,[63] and low molecular-mass organo gel.[64,65]

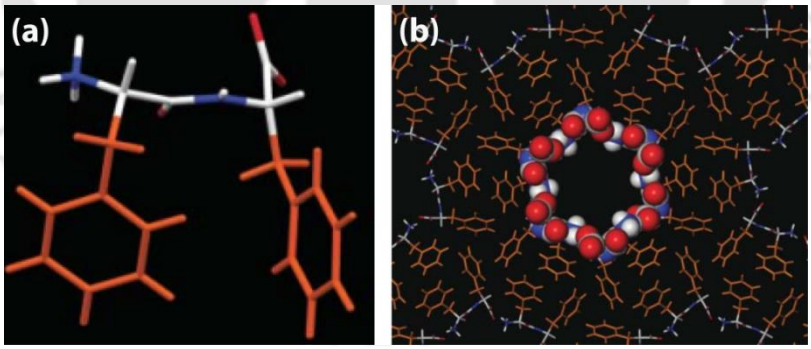

Figure 1.12. *The crystal structure (a) and nanotube structure (b) of Phe-Phe (Courtesy: image taken from* C. H. Görbitz, *Chem. Commun.* **2006**, 2332-2334*)*

Shelnutt *et al.* reported the nanotubes of D-Phe-D-Phe dipeptide, which can form a novel peptide-nanotube platinum-nanoparticle composites.[66] Chauhan and co-workers reported a proteolytically and pH stable dipeptide nanotube (confirmed by both crystal structure and microscopic images) of conformationally restricted dehydrophenylalanine (Phe-ΔPhe, ΔPhe = α, β- dehydro phenylalanine).[67] They also demonstrated the crystal structure, and

morphology of βPhe-ΔPhe and βPhe-Phe dipeptides, which exhibited a rectangular channel-like structure in the crystalline state and tubular structure in solution, respectively.[68] Banerjee *et al.* established a thermally, proteolytically, and pH stable dipeptide nanotube from *N*-terminally located ω–amino acid-containing dipeptides.[69] They also reported dipeptide nanotube of β-alanine and α-amino acid (β-Ala-L-Xaa, Xaa =Val/Ile/Phe), and their application of fabricating the gold nanoparticle.[70] Pramanik and co-workers reported nanotube from single amino acid-based molecule and fabrication of silver nanoparticles.[71] Moretto *et al.* observed that the dipeptide, Boc-Cys(Me)-Leu-OMe self-assembled to form a hollow rod in both crystalline state and solution.[72] Nagaraj and co-workers demonstrated the structural changes of terminally protected hydrophobic dipeptides with solvent.[73] Recently, Haldar *et al.* reported the crystal structures of terminally protected hydrophobic dipeptide self-assembled to form a tube-like structure in the crystalline state.[74]

1.7. Helical and double-helical assemblies of small peptides

In nature, the molecular self-assembly process is involved in various biological systems, e.g., spider silks,[75] tobacco mosaic virus (TMV),[76] single-stranded helical RNA,[77] DNA double helix[78] and collagen triple helix.[79] The development of various supramolecular self-assembled helical and β-sheet structures of small peptides attracted attention in the current research for their significance in various neurodegenerative diseases, e.g., Parkinson disease, Huntington's disease, Alzheimer's disease, and prion disease.[80,81] Moreover, the self-association of small peptides to generate various micro- or nano-level structures has essential applications in materials science, nanotechnology, medicinal chemistry, and biological chemistry.[82-84]

1.7.1. Single helical structures

Banerjee *et al.* reported a library of helical assemblies of tri- and tetrapeptides using the unnatural amino acid Aib or both Aib and β-Ala in a peptide sequence.[85-89] They also reported the supramolecular helical nanofibers by using pseudo peptides bis(*N*-α-amido-L-valine methyl ester) malonate (S), the enantiomer bis(*N*-α-amido-D-valine methyl ester) malonate (R), and a bis-valine derivative of 1,1-cyclopropane dicarboxamide.[90,91]

Pramanik and co-workers demonstrated the helical structures of terminally protected tetra- or hexapeptides which contained non-proteinogenic amino acids Aib or both Aib and mABA with natural amino acids in the peptide sequence.[92-94] Haldar *et al.* reported a dipeptide-based helical structure of Phe and aromatic β/γ/δ amino acid-containing peptide.[95] Dutta Konar *et al.* also described the helical structures of model Aib, mABA or mono-fluorinated phenylalanine, and Aib containing tripeptides.[96,97] Sanjayan *et al.* demonstrated the right and left-handed helical structures of sulfonamide and carboxamide of $(Pro\text{-}Ant\text{-}Aib)_n$ oligomers, respectively.[98] Huc and co-workers described the formation of a herringbone helix from aromatic-aliphatic δ-peptides.[99] Gopi and co-workers reported α/γ^4-hybrid peptide helical assembly with 12-membered H-bond pseudo cycles.[100] Das *et al.* described the supramolecular helical structure of unnatural amino acids gabapentin (Gpn) or gababutin (Gbn) or Aib containing tetrapeptides.[101,102] Recently, Gazit *et al.* reported a rigid helical-like sheet structure of most aggregation-prone tripeptide, Pro-Phe-Phe.[103]

1.7.2. Double-helical structures

Banerjee *et al.* described the formation of a double-helical structure from *N*-terminal β-alanine containing dipeptides.[104] Haldar and co-workers developed the double-helical assemblies from Tyr and central Aib containing tripeptides.[105] They also described the formation of a double-helical structure from Boc and *N,N′*-dicyclohexylurea capped γ-peptides.[106] Dutt Konar *et al.* discussed the double-helical assembly of Aib containing tripeptides, substituted phenylalanine and Aib containing tripeptide, and pyridine carboxamide containing tyrosine analog pseudo peptides.[107-109] Görbitz demonstrated a series of dipeptide based double-helix.[42] The dipeptides belong to a Val-Ala class. Gopi and co-workers developed the β double-helical structures from achiral γ-peptides.[110]

1.8. Peptide modifications

Post-translational modifications (PTMs) play crucial tasks in eukaryotic proteins as well as in all parts of cellular life. These modifications belong to phosphorylation of serine, threonine, and tyrosine; sulfation of tyrosine; acetylation, glycosylation, methylation,

hydroxylation, and ubiquitination lysine; methylation of arginine; lipidation of cysteine, *etc.*[111] PTMs regulate signal transduction, metabolic intersections, gene expression, and the cellular location of the protein. Most of the PTMs are reversible in a biological cell and precisely regulated. However, understanding the molecular mechanisms and biomedical applications, chemical modification of peptides or proteins is important.[112] These artificial chemical modifications refer to the incorporation of various fluorophore for bioimaging[113] and PEGylation for increasing *in vivo* stability and solubility or reduce immunogenicity[114] and glycosylation for preparation of vaccine and drug.[115]

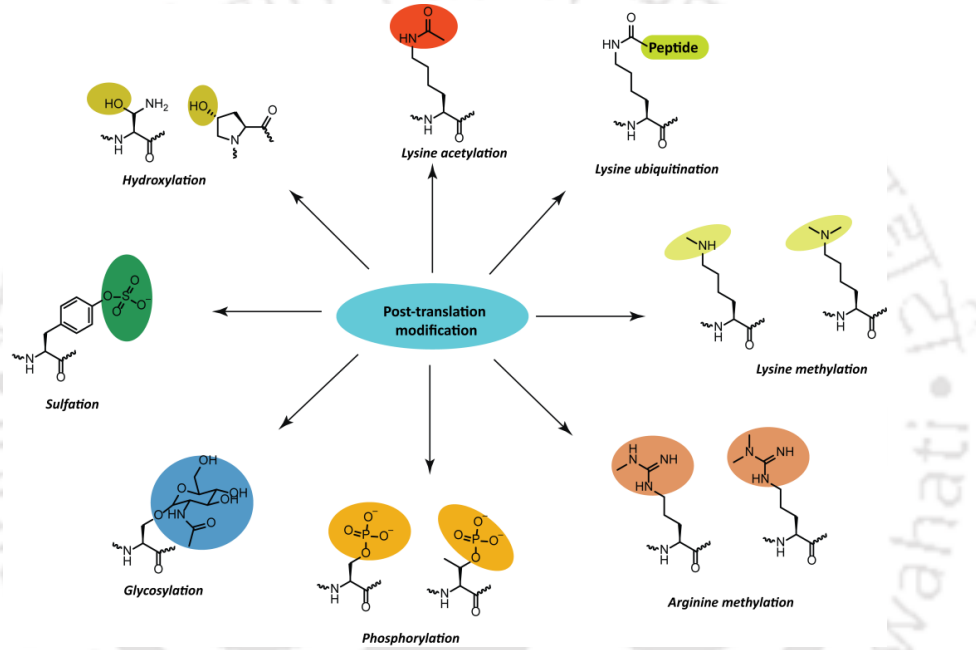

Figure 1.13. *Post-translation modification on proteins*

This strategy is most applicable for bioactive compounds, e.g., peptides, as they have recognized site, unique conformation, and functional features. This chemical derivatization can be possible by the installation of the bioactive group at the side chain (mainly in polar amino acids, e.g., Lys, Asp, Glu, Ser, Cys, *etc.*), *N*-terminus or *C*-terminus of amino acids during solution phase or SPPS. Numerous methods for introduction of electrophilic groups on nucleophilic substances, e.g., lysine and cysteine were reported.[116]

1.8.1. Existing methods for modification of peptides

De Luca *et al.* reported an alkylation reaction on the thiol group of cysteine in a peptide selectively.[117] They performed the reaction with molecular sieves and alkyl bromide in DMF under an Ar atmosphere (Scheme 1.1).

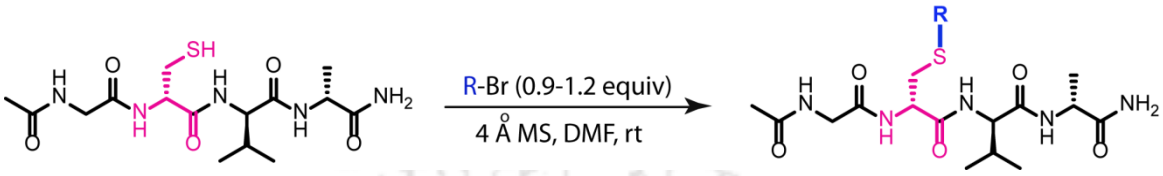

Scheme 1.1. *S-alkylation on the side-chain of Cys*

Pentelute *et al.* disclosed an approach for the selective addition of nucleophiles to the isocyanates of the peptide backbone, generated by Curtius rearrangement (Scheme 1.2).[118]

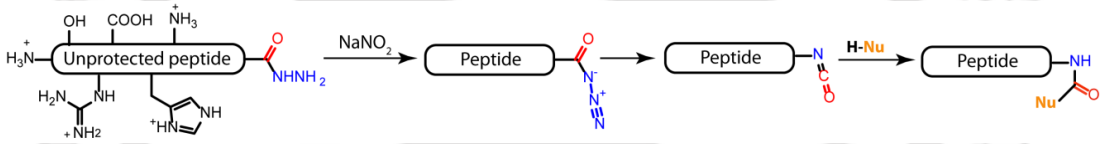

Scheme 1.2. *In situ generation of peptide isocyanate via Curtius rearrangements*

The same group also developed a macrocyclization reaction of unprotected peptide isocyanates. The cyclization happened through isocyanates of two side chain glutamic acid residue and dihydrazide units (Scheme 1.3).[119]

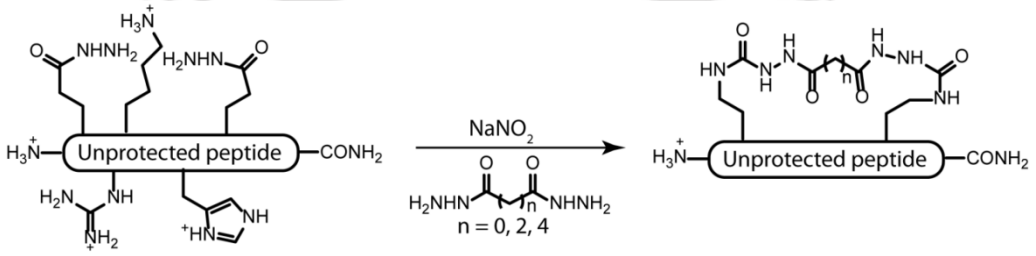

Scheme 1.3. *Side-chain macrocyclization of a peptide*

Raj *et al.* established a site-specific peptide bond hydrolysis method at glutamic acid residue in a peptide through the formation of pyroglutamyl imide moiety under neutral aqueous conditions (Scheme 1.4).[120]

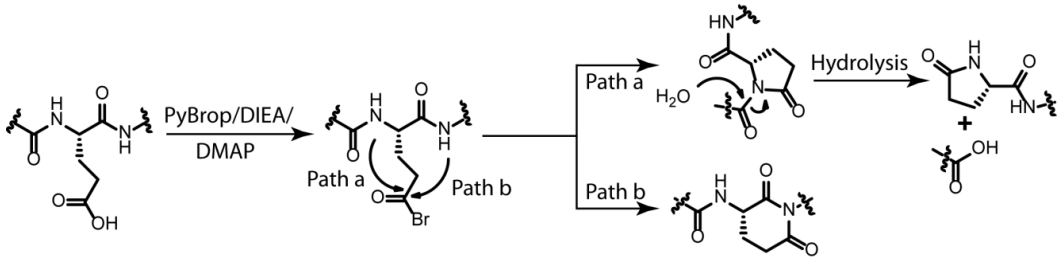

Scheme 1.4. *Hydrolysis of peptide bond through the activation of backbone amide*

Kanai *et al.* reported asparagine-selective peptide bond cleavage through Hofmann rearrangement.[121] They performed the reaction by using diacetoxyiodobenzene (DIB) and a phosphate buffer solution (0.1 M, pH 7.4) of a peptide (1 mM) at 37°C for 72h (Scheme 1.5).

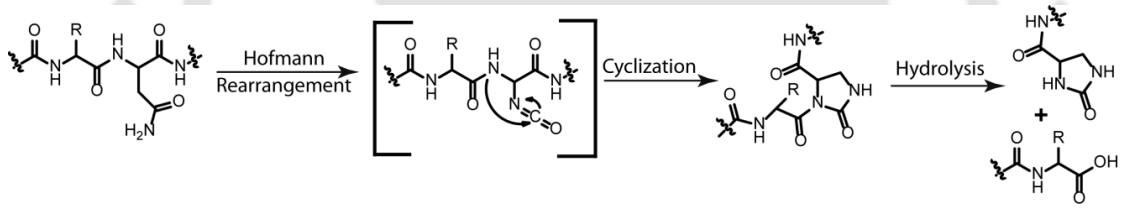

Scheme 1.5. *PhI(OAc)$_2$ mediated peptide bond cleavage in the aqueous medium*

Mashima *et al.* developed a method for amide bond cleavage using Zn(OTf)$_2$ as a catalyst and esterification of beta-hydroxyethylamides (Scheme 1.6). [122]

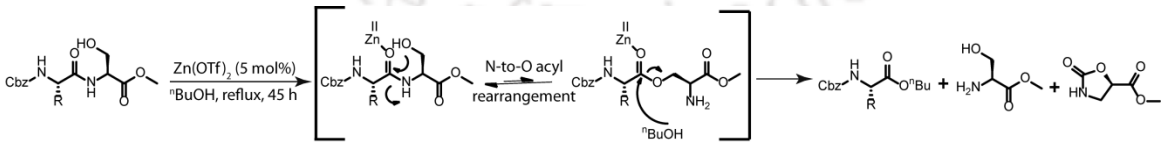

Scheme 1.6. *Zinc-catalyzed Ser-selective peptide cleavage*

Lavilla and co-workers established a Pd-catalyzed C-H arylation of the side chain of the Trp residue in a peptide by using aryl iodides (Scheme 1.7).[123] This reaction is highly selective for Trp in the presence of other residues, e.g., His, Phe, Tyr, *etc.*

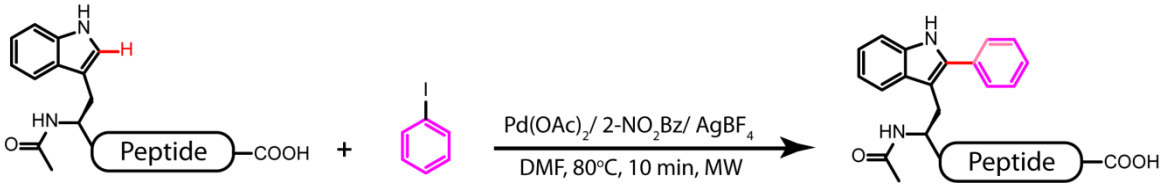

Scheme 1.7. *Pd-catalyzed direct arylation on Trp residue in aqueous media*

1.9. Peptide synthesis

Peptides are synthesized by two standard protocols: peptide synthesis in solution and solid phase peptide synthesis (SPPS). We discussed each method below.

1.9.1. Peptide synthesis in solution

The first peptide synthesis was shown by Theodor Curtius (1882) and Emil Fisher (1903).[124] They synthesized a peptide derivative of benzoylglycylglycine and a free dipeptide of glycylglycine, respectively. A new era of peptide synthesis was started when Bergmann invented the benzyloxycarboxyl (z) group for the protection of the amine group on amino acids[125] in 1932. Up to here, peptides were synthesized without using a coupling reagent. In 1952, Anderson *et al*. introduced tetraethyl pyrophosphate as a coupling reagent,[126] followed by dicyclohexylcarbodiimide (DCC),[127] which increased the impact of peptide bond formation by Sheehan and Hess. Now, peptides are frequently synthesized by using Boc protected amino acids, coupling reagents, and base (Scheme 1.8). Despite, the development of the *N*-protecting groups, the *C*-protecting active ester group of amino acids, coupling reagents for long-chain peptide synthesis, and its purification were very strenuous in solution phase.

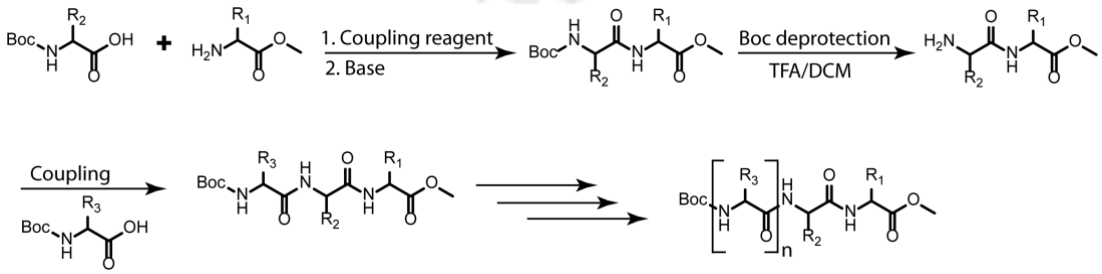

Scheme 1.8. *A schematic diagram of peptide synthesis in solution*

1.9.2. Solid phase peptide synthesis

All the above problems associated with solution phase peptide synthesis were solved by R. B. Merrifield (Nobel Prize 1984) by the invention of solid phase peptide synthesis,[128,] which is a milestone of peptide synthesis history. He synthesized a tetrapeptide (L-leucyl-L-alanyl-glycyl-L-valine) from a solid support, called Merrifield resin, which consisted of the cross-linked chloromethylated styrene-divinylbenezene copolymer. The advantage of solid phase peptide synthesis in comparison to solution phase is that it offers long and branched-chain peptide formation with a faster coupling reaction. The excess unreacted reagents are removed by washing. At present, two suitable strategies are present for SPPS technique: Boc/Bzl and Fmoc/tBu strategy (Scheme 1.9).[129,130]

The Boc/Bzl strategy has several advantages, e.g., synthesis of 'difficult' sequences;[131,132] thioesters based native chemical ligation,[133] long-chain polypeptides, and cyclic peptides[134] formation. But the final cleavage of the peptide from the resin using HF is problematic as it is extremely corrosive, aggressive, and hazards. On the other hand, Fmoc/tBu strategy[135] developed by Carpino in 1970, offers milder conditions for solid phase peptide synthesis.

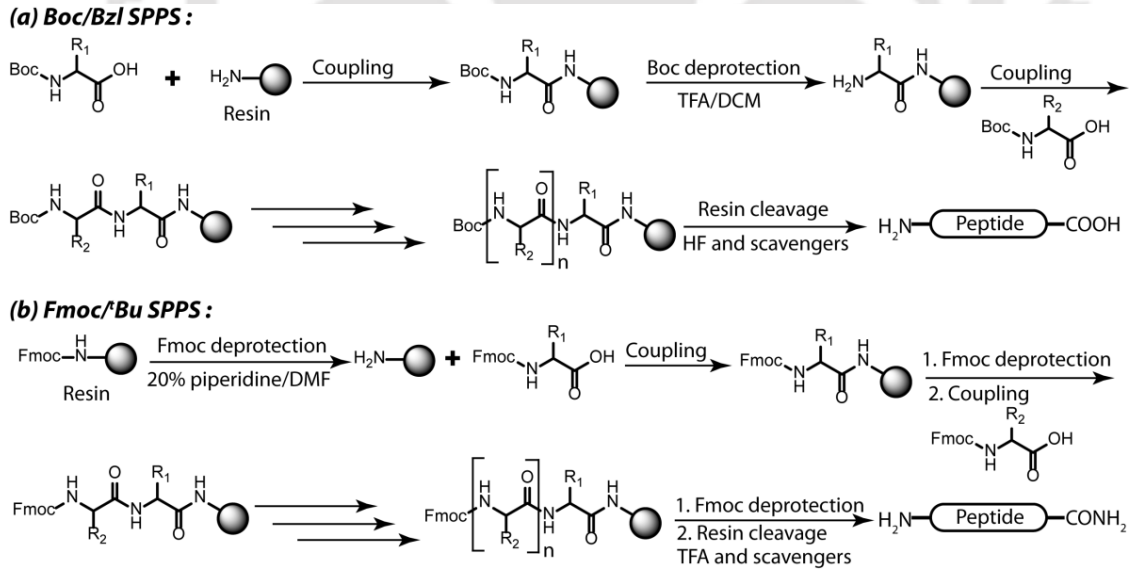

Scheme 1.9. *(a) Boc based and (b) Fmoc based SPPS*

1.10. Drawbacks of the existing methods

The literature reports revealed that the structure of Aβ peptide is not fully understood. The NMR, XRD and cryoEM studies suggested that Aβ aggregated to form cross-β-sheet structure.[18-23] The crystal structures of the full-length Aβ peptide is yet to be reported.

Next, most of the reported peptide-based nanotubes are obtained from alternating L/L amino acids. Alternating D/L or unnatural amino acid containing peptide-based nanotubes is not explored enough. But in the presence of unnatural or alternating D/L amino acid in a peptide sequence increases the proteolytic stability of the nanotube.

Next, most of the reported peptide-based supramolecular helical or double helical assemblies are obtained from the installation of pre-organized natural or unnatural kink moieties, e.g., Pro, Aib, Ant, mABA, Gpn, and Gbn in the peptide sequence.

Therefore, the design and development of peptide-based supramolecular helical and double helical structures without pre-organized kink moieties are challenging tasks.

Next, the reported methods for tert-butly ester cleavage suffer from some problems such as high acidic conditions, corrosive, handling problems, unsatisfactory yields, *etc*. Moreover, to the best of our knowledge, the above methods were used on only solution-phase tert-butyl ester hydrolysis. Therefore, an environmentally friendly method is needed.

Moreover, the popular peptide synthesis in solution is carried out by using Boc protected amino acids as its urethane moiety helps to reduce the epimerization in its activated ester form, and this protecting group is removed by TFA. However, it is non-environmentally friendly, cost-effective, and corrosive. Therefore, an alternate method is necessary.

1.11. Objectives of the thesis

Based on the above observations, we proposed the following investigations to overcome the mentioned problems.

1. Investigation of supramolecular self-assembly of both *N*- and *C*-protected dipeptides, bearing sequence homogeneity with the *C*-terminus of Alzheimer's $A\beta_{39-40}$ and $A\beta_{41-42}$, respectively.
2. Development of various nanostructures from alternatingly L/L and D/L amino acids containing dipeptides.
3. *De novo* design and development of helical structures from tripeptides without having pre-organized kink moieties in the peptide sequence.
4. Constructions of supramolecular helical and double helical structures from alternating D/L amino acids containing tripeptides.
5. The side-chain modification of Asp/Glu containing peptides on-resin.
6. Greener $FeCl_3$-mediated Boc chemistry in solution and solid-phase peptide synthesis.

1.12. References

1. Clamp, M.; Fry, B.; Kamal, M.; Xie, X.; Cuff, J.; Lin, M. F.; Kellis, M.; Lindblad-Toh, K.; Lander, E. S. Distinguishing protein-coding and noncoding genes in the human genome. *Proc. Natl. Acad. Sci. U.S.A.* **2007**,*104*, 19428-19433.
2. Berg, J.; Tymoczko, J.; Stryer, L. *Biochemistry*, 5th ed.; W H Freeman: New York, 2002.
3. Priller, C.; Bauer, T.; Mitteregger, G.; Krebs, B.; Kretzschmar, H. A.; Herms, J. Synapse formation and function is modulated by the amyloid precursor protein. *J. Neurosci.* **2006**, *26*, 7212-7221.
4. Nelson, D. L; Cox, M. M. *Lehninger's Principles of Biochemistry*, 7th ed.*;* W. H. Freeman and Company: New York, 2017.
5. Ramachandran, G. N. Protein structure and crystallography. *Science* **1963**, *141*, 288-291.
6. Petsko, G.; Ringe, D. *Protein structure and function.* 1st ed.; New Age Press: London, 2004.
7. Pauling, L.; Corey, R. B.; Branson, H. R. The structure of proteins: Two hydrogen-bonded helical configuration of the polypeptide chain. *Proc. Nat. Acad. Sci. U.S.A.* **1951**, *37*, 205-211.
8. Vieira-Pires, R. S.; Morais-Cabral, J. H. 3_{10} helices in channels and other membrane proteins. *J. Gen. Physiol.* **2010**, *136*, 585-592.
9. Pauling, L.; Corey, R. B. The pleated sheet, A new layer configuration of polypeptide chains. *Proc. Nat. Acad. Sci. U.S.A.* **1951**, *37*, 251-256.
10. Venkatachalam, C. M. Stereochemical criteria for polypeptides and proteins. V. Conformation of a system of three linked peptide units. *Biopolymers*, **1968**, *6*, 1425-1436.
11. (a) Hutchinson, E. G.; Thornton J. M. A revised set of potentials for beta-turn formation in proteins. *Protein Sci.*, **1994**, *3*, 2207-2216; (b) de Brevern, A. G. Extension of the classical classification of β-turns. *Sci Rep* **2016**, *6***,** 33191; (c) Shapovalov, M.; Vucetic, S.; Dunbrack, R. L., Jr. A new clustering and nomenclature for beta turns derived from high-resolution protein structures. *PLoS Comput.Biol.* **2019**, *15(3)*: e 1006844.
12. Hamley, I. W. The amyloid beta peptide: a chemist's perspective. Role in and Alzheimer's fibrillization. *Chem. Rev*., **2012**, *112*, 5147-5192.
13. Knowles, T. P. J.; Vendruscolo, M.; Dobson, C. M., The amyloid state and its association with protein misfolding diseases. *Nat. Rev. Mol. Cell Biol*., **2014**, *15*, 384-396.
14. Muller, U. C.; Zheng, H. Physiological functions of APP family proteins. *Cold Spring Harbor Perspect. Med*., **2012**, *2*, a006288.
15. Zheng, H.; Koo, E. H. Biology and pathophysiology of the amyloid precursor protein. *Mol. Neurodegener*, **2011**, *6***,** 27.
16. Sharoar, M. G.; Thapa, A.; Shahnawaz, M.; Ramasamy, V. S.; Woo, E. R.; Shin, S. Y.; Park, I. S. Keampferol-3-O-rhamnoside abrogates amyloid beta toxicity by modulating monomers and remodeling oligomers and fibrils to non-toxic aggregates. *J. Biomed. Sci.*, **2012**, *19*, 104.

17. Harper, J. D.; Lansbury, P. T., Jr. Models of amyloid seeding in Alzheimer's disease and scrapie: Mechanistic truths and physiological consequences of the time-dependent solubility of amyloid proteins. *Annu. Rev. Biochem.*, **1997**, *66*, 385-407.
18. Makin, O. S.; Serpell, L. C. Structures for amyloid fibrils. *FEBS Journal*, **2005**, *272*, 5950-5961.
19. Tycko, R.; Wickner, R. B. Molecular structures of amyloid and prion fibrils: Consensus versus controversy. *Acc. Chem. Res.* **2013**, *46*, 1487-1496.
20. Squires, A. M.; Devlin, G. L.; Gras, S. L.; Tickler, A. K.; MacPhee C. E.; Dobson, C. M. X-ray scattering study of the effect of hydration on the cross-β structure of amyloid fibrils. *J. Am. Chem. Soc.*, **2006**, *128*, 11738-11739.
21. Schmidt, M.; Sachse, C.; Richter, W.; Xu, C.; Fandrich, M.; Grigorieff, N. Comparison of Alzheimer Aβ (1–40) and Aβ (1–42) amyloid fibrils reveals similar protofilament structures. *Proc. Natl. Acad. Sci. U. S. A.*, **2009**, *106*, 19813-19818.
22. Zhang, R.; Hu, X.; Khant, H.; Ludtke, S. J.; Chiu, W.; Schmid, M. F.; Frieden C.; Lee, J.-M. Interprotofilament interactions between Alzheimer's Aβ_{1-42} peptides in amyloid fibrils revealed by cryoEM. *Proc. Natl. Acad. Sci. U. S. A.*, **2009**, *106*, 4653-4658.
23. Miller, Y.; Ma, B.; Tsai C.-J.; Nussinov, R. Hollow core of Alzheimer's Aβ_{42} amyloid observed by cryoEM is relevant at physiological pH. *Proc. Natl. Acad. Sci. U. S. A.*, **2010**, *107*, 14128-14133.
24. Lansbury, P.; Costa, P. R.; Griffiths, J. M.; Simon, E. J.; Auger, M.; Halverson, K. J.; Kocisko, D. A.; Hendsch, Z. S.; Ashburn, T. T.; Spencer, R. G. S.; Tidor, B.; Griffin, R. G. Structural model for the β-amyloid fibril based on interstrand alignment of an antiparallel-sheet comprising a C-terminal peptide. *Nat. Struct. Biol.*, **1995**, *2*, 990-998.
25. Griffiths, J. M.; Ashburn, T. T.; Lansbury, P. T.; Auger, M.; Costa P. R.; Griffin, R. G. Rotational resonance solid-state NMR elucidates a structural model of pancreatic amyloid. *J. Am. Chem. Soc.*, **1995**, *117*, 3539-3546.
26. Balbach, J. J.; Ishii, Y.; Antzutkin, O. N.; Leapman, R. D.; Rizzo, N. W.; Dyda, F.; Reed J.; Tycko, R. Amyloid fibril formation by Aβ_{16-22}, a seven-residue fragment of the Alzheimer's β-amyloid peptide, and structural characterization by solid state NMR. *Biochemistry*, **2000**, *39*, 13748-13759.
27. Petkova, A. T.; Ishii, Y.; Balbach, J. J.; Antzutkin, O. N.; Leapman, R. D.; Delaglio F.; Tycko, R. A structural model for Alzheimer's β-amyloid fibrils based on experimental constraints from solid state NMR. *Proc. Natl. Acad. Sci. U. S. A.*, **2002**, *99*, 16742-16747.
28. Tjernberg, L. O.; Naslund, J.; Lindqvist, F.; Johansson, J.; Karlstromi, A. R.; Thyberg, J.; Terenius, L.; Nordstedt, C. Arrest of β-amyloid fibril formation by a pentapeptide ligand. *The J. Biol. Chem.* **1996**, *271*, 8545-8548.
29. Tartaglia, G. G.; Cavalli, A.; Pellarin, R.; Caflisch, A. The role of aromaticity, exposed surface, and dipole moment in determining protein aggregation rates. *Protein Science*, **2004**, *13*, 1939-1941.
30. Doran, T. M.; Kamens, A. J.; Byrnes, N. K.; Nilsson, B. L. Role of amino acid hydrophobicity, aromaticity, and molecular volume on IAPP (20–29) amyloid self-assembly. *Proteins*, **2012**, *80*, 1053-1065.

31. Ray, S.; Das, A. K.; Drew M. G. B.; Banerjee, A. A short water-soluble self-assembling peptide forms amyloid-like fibrils. *Chem. Commun.*, **2006**, 4230-4232.
32. Naskar, J.; Drew, M. G. B.; Deb, I.; Das S.; Banerjee, A. Water-Soluble tripeptide Aβ (9-11) forms amyloid-like fibrils and exhibits neurotoxicity. *Org. Lett.*, **2008**, *10*, 2625-2628.
33. Maity, S.; Kumar P.; Haldar, D. An amyloid-like fibril-forming supramolecular cross-β-structure of a model peptide: a crystallographic insight. *Org. Biomol. Chem.*, **2011**, *9*, 3787-3791.
34. Jacobsen, Ø.; Gebreslasie, H. G.; Klaveness, J.; Rongved P.; Görbitz, C. H. N-(tert-Butoxycarbonyl)-L-valyl-L-valine methyl ester: a twisted parallel β-sheet in the crystal structure of a protected dipeptide. *Acta Crystallogr., Sect. C: Cryst. Struct. Commun.*, **2011**, *67*, 278-282.
35. Gazit, E. Self-assembled peptide nanostructures: the design of molecular building blocks and their technological utilization. *Chem. Soc. Rev.* **2007**, *36*, 1263-1269.
36. Ulijn, R. V.; Smith, A. M. Designing peptide based nanomaterials. *Chem. Soc. Rev.* **2008**, *37*, 664-675.
37. Yang, Y.; Khoe, U.; Wang, X.; Horii, A.; Yokoi, H.; Zhang, S. Designer self-assembling peptide nanomaterials. *Nano Today* **2009**, *4*, 193-210.
38. Valery, C.; Artzner, F.; Paternostre, M. Peptide nanotubes: molecular organisations, self-assembly mechanisms and applications. *Soft Matter*, **2011**, *7*, 9583-9594.
39. Bong, D. T.; Clark, T. D.; Granja, J. R.; Ghadiri, M. R. Self-assembling organic nanotubes. *Angew. Chem. Int. Ed.* **2001**, *40*, 988-1011.
40. Brea, R. J.; Reiriz, C.; Granja, J. R. Towards functional bionanomaterials based on self-assembling cyclic peptide nanotubes. *Chem. Soc. Rev.*, **2010**, *39*, 1448-1456.
41. Reches, M.; Gazit, E. Casting metal nanowires within discrete self-assembled peptide nanotubes. *Science* **2003**, *300*, 625-627.
42. Görbitz, C. H. Microporous organic materials from hydrophobic dipeptides. *Chem. Eur. J.* **2007**, *13*, 1022-1031.
43. Yan, X.; Zhua, P.; Li, J. Self-assembly and application of diphenylalanine-based nanostructures. *Chem. Soc. Rev.* **2010**, *39*, 1877-1890.
44. Vauthey, S.; Santoso, S.; Gong, H.; Watson, N.; Zhang, S. Molecular self-assembly of surfactant-like peptides to form nanotubes and nanovesicles. *Proc Natl Acad Sci U. S. A.* **2002**, *99*, 5355-5360.
45. Cavalli, S.; Albericio, F.; Kros, A. Amphiphilic peptides and their cross-disciplinary role as building blocks for nanoscience. *Chem. Soc. Rev.* **2010**, *39*, 241-263.
46. Zhang, S. Designer Self-assembling peptide nanofiber scaffolds for study of 3-D cell biology and beyond. *Adv. Cancer Res.* **2008**, *99*, 335-362.
47. Maji, S. K.; Schubert, D.; Rivier, C.; Lee, S.; Rivier, J. E.; Riek, R. Amyloid as a depot for the formulation of long-acting drugs. *PLoS Biol.* **2008**, *6*, e17.
48. Zhao, F.; Ma, M. L.; Xu, B. Molecular hydrogels of therapeutic agents. *Chem. Soc. Rev.* **2009**, *38*, 883-891.
49. Granja, J. R.; Ghadiri, M. R. Channel-mediated transport of glucose across lipid bilayers. *J. Am. Chem. Soc.* **1994**, *116*, 10785-10786.

50. Sanchez-Quesada, J.; Isler, M. P.; Ghadiri, M. R. Modulating ion channel properties of transmembrane peptide nanotubes through heteromeric supramolecular assemblies. *J. Am. Chem. Soc.* **2002,** *124*, 10004-10005.
51. Ashkenasy, N.; Horne, W. S.; Ghadiri, M. R. Design of self-assembling peptide nanotubes with delocalized electronic states. *Small* **2006**, *2*, 99-102.
52. Kiyonaka, S.; Sada, K.; Yoshimura, I.; Shibkai, S.; Kato, N.; Hamachi, I. Semi-wet peptide/protein array using supramolecular hydrogel. *Nat Mater* **2004**, *3*, 58-64.
53. Ghadiri, M. R.; Granja, J. R.; Milligan, R. A.; McRee, D. E.; Khazanovich, N. Self-assembling organic nanotubes based on a cyclic peptide architecture. *Nature* **1993**, *366*, 324-327.
54. Blasio, B. D.; Saviano, M.; Duca, V. D.; Simone, G. D.; Rossi, F.; Pedone, C.; Benedetti, E.; Lorenzi, G. P. Conformational studies of heterochiral peptides with diastereoisomeric residues: Crystal and molecular structures of linear dipeptides derived from leucine, isoleucine, and allo-isoleucine. *Biopolymers* **1995**, *36*, 401-408.
55. Vauthey, S.; Santoso, S.; Gong, H.; Watson, N.; Zhang, S. Molecular self-assembly of surfactant-like peptides to form nanotubes and nanovesicles *Proc. Natl. Acad. Sci. U.S.A.* **2002**, *99*, 5355-5360.
56. Görbitz, C. H. Nanotube formation by hydrophobic dipeptides. *Chem.-Eur. J.*, **2001**, *7*, 5153-5159.
57. Görbitz, C. H. Nanotubes from hydrophobic dipeptides: pore size regulation through side chain substitution. *New J. Chem.* **2003**, *27*, 1789-1893.
58. Görbitz, C. H. The structure of nanotubes formed by diphenylalanine, the core recognition motif of Alzheimer's β-amyloid polypeptide. *Chem. Commun.* **2006**, 2332-2334.
59. Soldatov, D. V.; Moudrakovski, I. L.; Grachev, E. V.; Ripmeester, J. A. Micropores in Crystalline dipeptides as seen from the crystal structure, He pycnometry, and ^{129}Xe NMR spectroscopy. *J. Am. Chem. Soc.* **2006**, *128*, 6737-6744.
60. Carny, O.; Shalev, D. E.; Gazit, E. Fabrication of coaxial metal nanocables using a self-assembled peptide nanotube scaffold. *Nano Lett.* **2006**, *6*, 1594-1597.
61. Gan, Z.; Wu, X.; Zhu, X.; Shen, J. Light-Induced ferroelectricity in bioinspired self-assembled diphenylalanine nanotubes/microtubes. *Angew. Chem. Int. Ed.* **2013**, *52*, 2055-2059.
62. Yemini, M.; Reches, M.; Rishpon, J.; Gazit, E. Novel electrochemical biosensing platform using self-assembled peptide nanotubes. *Nano Lett.* **2005**, *5*, 183-186.
63. Reches, M.; Gazit, E. Controlled patterning of aligned self-assembled peptide nanotubes. *Nat. Nanotechnol.* **2006**, *1*, 195-200.
64. Smith, A. M.; Williams, R. J.; Tang, C.; Coppo, P.; Collins, R. F.; Turner, M. L.; Saiani, A.; Ulijn, R. V. Fmoc-Diphenylalanine self assembles to a hydrogel via a novel architecture based on π–π interlocked β-sheets. *Adv. Mater.* **2008**, *20*, 37-41
65. Yan, X. H.; Cui, Y.; He, Q.; Wang, K. W.; Li, J. B. Organogels based on self-assembly of diphenylalanine peptide and their application to immobilize quantum dots. *Chem. Mater.* **2008**, *20*, 1522-1526.

66. Song, Y; Challa, S. R.; Medforth, C. J.; Qiu, Y.; Watt, R. K.; Peña, D.; Miller, J. E.; Swolab, F. V.; Shelnutt, J. A. Synthesis of peptide-nanotube platinum-nanoparticle composites. *Chem. Commun.* **2004**, 1044-1045.

67. Gupta, M.; Bagaria, A.; Mishra, A.; Mathur, P.; Basu, A.; Ramakumar, S.; Chauhan, V. S. Self-Assembly of a dipeptide-containing conformationally restricted dehydrophenylalanine residue to form ordered nanotubes. *Adv. Mater.* **2007**, *19*, 858-861.

68. Parween, S.; Misra, A.; Ramakumarb, S.; Chauhan, V. S. Self-assembled dipeptide nanotubes constituted by flexible β-phenylalanine and conformationally constrained α,β-dehydrophenylalanine residues as drug delivery system. *J. Mater. Chem. B*, **2014**, *2*, 3096-3106.

69. Guha, S.; Drew, M. G. B.; Banerjee, A. Dipeptide nanotubes, with N-terminally located ω-amino acid residues, that are stable proteolytically, thermally, and over a wide range of pH. *Chem. Mater.* **2008**, *20*, 2282-2290.

70. Guha, S.; Banerjee, A. Self-assembled robust dipeptide nanotubes and fabrication of dipeptide-capped gold nanoparticles on the surface of these nanotubes. *Adv. Funct. Mater.* **2009**, *19*, 1949-1961.

71. Koley, P.; Pramanik, A. Nanostructures from single amino acid-based molecules: stability, fibrillation, encapsulation, and fabrication of silver nanoparticles. *Adv. Funct. Mater.* **2011**, *21*, 4126-4136.

72. Mazzier, D.; Carraro, F.; Crisma, M.; Rancan, M.; Toniolo C.; Moretto, A. A terminally protected dipeptide: from crystal structure and self-assembly, through co-assembly with carbon-based materials, to a ternary catalyst for reduction chemistry in water. *Soft Matter* **2016**, *12*, 238-245.

73. Subbalakshmi, C.; Basak, P.; Nagaraj, R. Self-assembly of t-butyloxycarbonyl protected dipeptide methyl esters composed of leucine, isoleucine, and valine into highly organized structures from alcohol and aqueous alcohol mixtures. *Biopolymers* **2017**; *108*, 1-14.

74. Maji, K.; Saha, S.; Dey, R.; Ghosh, N.; Haldar, D. Mueller matrix fluorescence spectroscopy for probing self-assembled peptide-based hybrid supramolecular structure and orientation. *J. Phys. Chem. C* **2017**, *121*, 19519-19529.

75. Vincent J. F.; Currey, J. D. *The mechanical properties of biological materials; eds*; Cambridge University Press: Cambridge, **1980**.

76. Franklin, R. E. Structure of Tobacco mosaic virus: location of the ribonucleic acid in the tobacco mosaic virus particle. *Nature* **1956**, *177*, 928-930.

77. Eichhorn, C. D.; Al-Hashimi, H. M. Structural dynamics of a single-stranded RNA-helix junction using NMR. *RNA* **2014**, *20*, 782–791.

78. Wittung, P.; Nielsen, P. E.; Buchardt, O.; Egholm, M.; Nordén, B. DNA-like double helix formed by peptide nucleic acid. *Nature* **1994**, *368*, 561–563.

79. Eyre, D. R. Collagen: molecular diversity in the body's protein scaffold. *Science* **1980**, *207*, 1315–1322.

80. Selkoe, D. J. Folding proteins in fatal ways. *Nature*, **2003**, *426*, 900-904.

81. Aguzzi, A.; O'Connor, T. Protein aggregation diseases: pathogenicity and therapeutic perspectives. *Nat. Rev. Drug Discovery*, **2010**, *9*, 237-248.
82. Moreira, I. P.; Piskorz, T. K.; Van Esch, J. H.; Tuttle, T.; Ulijn, R. V. Biocatalytic self-assembly of tripeptide gels and emulsions. *Langmuir*, **2017**, *33*, 4986-4995.
83. Li, Y.; Wang, Y.; Huang, G.; Gao, J. Cooperativity principles in self-assembled nanomedicine. *Chem. Rev.*, **2018**, *118*, 5359-5391.
84. Habibi, N.; Kamaly, N.; Memic, A.; Shafiee, H. Self-assembled peptide-based nanostructures: Smart nanomaterials toward targeted drug delivery. *Nano Today* **2016**, *11*, 41-60.
85. Haldar, D.; Maji, S. K.; Drew, M. G. B.; Banerjee, A.; Banerjee, A. Self-assembly of a short peptide monomer into a continuous hydrogen bonded supramolecular helix: the crystallographic signature. *Tetrahedron Letters* **2002**, *43*, 5465-5468.
86. Das, A. K.; Banerjee, A.; Drew, M. G. B.; Ray, S.; Haldar, H.; Banerjee, A. Can a consecutive double turn conformation be considered as a peptide based molecular scaffold for supramolecular helix in the solid state? *Tetrahedron* **2005**, *61*, 5027-5036.
87. Haldar, D.; Maji, S. K.; Sheldrick, W. S.; Banerjee, A. First crystallographic signature of the highly ordered supramolecular helical assemblage from a tripeptide containing a non-coded amino acid. *Tetrahedron Letters* **2002**, *43*, 2653-2656.
88. Maji, S. K.; Banerjee, A.; Drew, M. G. B.; Haldar, D.; Banerjee, A. Self-assembly of a tetrapeptide in which a unique supramolecular helical structure is formed via intermolecular hydrogen bonding in the solid state. *Tetrahedron Letters* **2002**, *43*, 6759-6762.
89. Banerjee, A.; Maji, S. K.; Drew, M. G. B.; Haldar, D.; Banerjee, A. Supramolecular peptide helix from a novel double turn forming peptide containing β-amino acid. *Tetrahedron Letters* **2003**, *44*, 699-702.
90. Guha, S; Drew, M. G. B.; Banerjee, A. Construction of helical nanofibers from self-assembling pseudopeptide building blocks: modulating the handedness and breaking the helicity. *small* **2008**, *4*, 1993-2005.
91. Guha, S; Drew, M. G. B.; Banerjee, A. Construction of supramolecular helices and breaking the helicity by forming supramolecular β-sheet structures using suitable self-assembling pseudopeptide building blocks. *Cryst. Growth Des.*, **2010**, *10*, 4716-4721.
92. Kar, S.; Dutta, A.; Drew, M. G. B.; Koley, P.; Pramanik, A. Overlapping double turn conformations adopted by tetrapeptides containing non-coded amino isobutyric acid (Aib) and formation of tape-like structures through supramolecular helix mediated self-assembly. *Protein & Peptide Letters*, **2009**, *16*, 1063-1073.
93. Dutta, A.; Drew, M. G. B.; Pramanik, A. Conformational and self-assembly studies of helix forming hexapeptides containing two a-amino isobutyric acids. *Tetrahedron* **2008**, *64*, 549-558.
94. Dutta, A.; Dutta, A.; Drew, M. G. B.; Pramanik, A. Supramolecular helix and β-sheet through self-assembly of two isomeric tetrapeptides in crystals and formation of filaments and ribbons in the solid state. *Supramolecular Chemistry*, **2008**, *20*, 625-633.

95. Maity, S.; Jana, P.; Maity, S. K.; Kumar, P.; Haldar, D. Conformational heterogeneity, self-assembly, and gas adsorption studies of isomeric hybrid peptides. *Cryst. Growth Des.*, **2012**, *12*, 422-428.
96. Dutt Konar, A. The unique crystallographic signature of a β-turn mimic nucleated by N-methylated phenylalanine and Aib as corner residue: conformational and self-assembly studies. *CrystEngComm* **2013**, *15*, 10569-10578.
97. Sharma, A.; Goswami, S.; Rajagopalan, R; Dutt Konar, A. Supramolecular heterogeneity in β-turn forming synthetic tripeptides nucleated by isomers of fluorinated phenylalanine and aib as corner residues. *Supramolecular Chemistry* **2015**, *27*, 669-678.
98. Ramesh, V. V. E.; Kale, S. S.; Kotmale, A. S.; Gawade, R. L.; Puranik, V. G.; Rajamohanan, P. R.; Sanjayan, G. J. Carboxamide versus sulfonamide in peptide backbone folding: a case study with a hetero foldamer. *Org. Lett.* **2013**, *15*, 1504-1507.
99. Jiang, H.; Leger, J. M.; Huc, I. Aromatic δ-peptides**.** *J. Am. Chem. Soc*. **2003**, *125*, 3448-3449.
100. Bandyopadhyay, A.; Jadhav, S. V.; Gopi, H. N. α/γ^4-Hybrid peptide helices: synthesis, crystal conformations and analogy with the α-helix. *Chem. Commun.* **2012**, *48*, 7170-7172.
101. Konda, M.; Kauffmann, B.; Rasalea, D. B.; Das, A. K. Structural and morphological diversity of self-assembled synthetic γ-amino acid containing peptides. *Org. Biomol. Chem.* **2016**, *14*, 4089-4102.
102. Konda, M.; Jadhav, R. G. Maiti, S.; Mobin, S. M.; Kauffmann, B.; Das, A. K. Understanding the conformational analysis of gababutin based hybrid peptides. *Org. Biomol. Chem.* **2018**, *16*, 1728-1735.
103. Bera, S.; Mondal, S.; Xue, B.; Shimon, L. J. W.; Cao. Y.; Gazit, E. Rigid helical-like assemblies from a self-aggregating tripeptide. *Nat. Mater*. **2019**, *18*, 503-509.
104. Guha, S; Drew, M. G. B.; Banerjee, A. A new molecular scaffold for the formation of supramolecular peptide double helices: the crystallographic insight. *Org. Lett*., **2007,** *9*, 1347-1350.
105. Jana, P.; Maity, S.; Maity, S. K.; Haldar, D. A new peptide motif in the formation of supramolecular double helices. *Chem. Commun.* **2011**, *47*, 2092-2094.
106. Maity, S. K.; Maity, S.; Jana, P.;Haldar, D. Supramolecular double helix from capped γ-peptide. *Chem. Commun.* **2012**, *48*, 711-713.
107. Sharma, A.; Tiwari, P.; Dutt Konar, A. The dominant role of side chains in supramolecular double helical organisation in synthetic tripeptides. *J. Mol. Struct.* **2018**, *1161*, 44-54.
108. Sharma Gangele, A.; Goswami, S.; Bera, A. K.; Tiwari, P.; Konar, S.; Dutt Konar, A. Can side chain interactions nucleate supramolecular heterogeneity in synthetic tripeptides? *Cryst. Growth Des.* **2016**, *16*, 2130-2139.
109. Tiwari, P.; Biswas, S.; Verma, R.; Sharma, A.; Dutt Konar, A. Porous biomaterials via side chain-side chain interactions of tyrosine analogue of pyridine carboxamides. *ChemistrySelect* **2018**, *3*, 262-272.
110. Misra, R.; Dey, S.; Reja, R. M.; Gopi, H. N. Artificial β-double helices from achiral γ-peptides. *Angew. Chem. Int. Ed.* **2018**, *57*, 1057-1061.

111. Wells, L.; Vosseller, K.; Hart, G. W. Glycosylation of nucleocytoplasmic proteins: signal transduction and O-GlcNAc. *Science* **2001**, *291*, 2376-2378.
112. Liu, W. R.; Wang, Y.-S.; Wan, W. Synthesis of proteins with defined posttranslational modifications using the genetic noncanonical amino acid incorporation approach. *Mol. BioSyst.***2011**, *7*, 38-47.
113. Carter, P. J. Introduction to current and future protein therapeutics: a protein engineering perspective. *Exp. Cell Res.* **2011**, *317*, 1261-1269.
114. Payne, R. J.; Wong, C. H. Advances in chemical ligation strategies for the synthesis of glycopeptides and glycoproteins. *Chem. Commun*. **2010**, *46*, 21-43.
115. Zhang, Y.; Xu, C.; Lam, H. Y.; Lee, C. L.; Li, X. Protein chemical synthesis by serine and threonine ligation. *Proc. Natl. Acad. Sci USA* **2013**, *110*, 6657-6662.
116. Wollack, J. W.; Zeliadt, N. A.; Mullen, D. G.; Amundson, G.; Geier, S.; Falkum, S.; Wattenberg, E. V.; Barany, G.; Distefano, M. D. Multifunctional prenylated peptides for live cell analysis. *J. Am. Chem. Soc.* **2009**, *131*, 7293-7303.
117. Calce, E.; Leone, M.; Monfregola, L.; De Luca, S. Chemical modifications of peptide sequences via S-alkylation reaction. *Org. Lett.* **2013**, *15*, 5354-5357.
118. Vinogradov, A. A.; Simon, M. D.; Pentelute, B. L. C-terminal modification of fully unprotected peptide hydrazides via in situ generation of isocyanates. *Org. Lett.* **2016**, *18*, 1222-1225.
119. Vinogradov, A. A.; Choo, Z.-N.; Totaro, K. A.; Pentelute, B. L. Macrocyclization of unprotected peptide isocyanates. *Org. Lett.* **2016**, *18*, 1226-1229.
120. Nalbone, J. M.; Lahankar, N.; Buissereth, L.; Raj, M. Glutamic acid selective chemical cleavage of peptide bonds. *Org. Lett.* **2016**, *18*, 1186-1189.
121. Tanabe, K.; Taniguchi, A.; Matsumoto, T.; Oisaki, K.; Sohma, Y.; Kanai, M. Asparagine-selective cleavage of peptide bonds through hypervalent iodine-mediated Hofmann rearrangement in neutral aqueous solution. *Chem. Sci*. **2014**, *5***,** 2747-2753.
122. Kita, Y.; Nishii, Y.; Higuchi, T.; Mashima, K. Zinc-catalyzed amide cleavage and esterification of β-hydroxyethylamide. *Angew. Chem. Int. Ed.* **2012**, *51*, 5723-5726.
123. Ruiz-Rodriguez, J.; Albericio, F.; Lavilla, R. Postsynthetic modification of peptides: chemoselective C-arylation of tryptophan residues. *Chem. Eur. J.* **2010**, *16***,** 1124-1127.
124. Fischer, E.; Otto, E. Synthese von derivaten einiger dipeptide. *Ber. Deutsch. Chem. Ges.* **1903**, *36*, 2106-2116.
125. Bergmann, M.; Zervas, L. Über ein allgemeines verfahren der peptid-synthese. *Ber. Deutsch. Chem. Ges.*, **1932**, *65*, 1192-1201.
126. Anderson, G. W.; Blodinger, J.; Welcher, A. D. Tetraethyl pyrophosphite as a reagent for peptide syntheses. *J. Am. Chem. Soc.* **1952**, *74*, 5309–5311.
127. Sheehan, J. C.; Hess, G. P. A new method of forming peptide bonds. *J. Am. Chem. Soc.* **1955**, ***77***, 1067-1068.
128. Merrifield, R. B. Solid phase peptide synthesis. I. The synthesis of a tetrapeptide. *J. Am. Chem. Soc.* **1963**, *85*, 2149-2154.

129. Muttenthaler, M.; Albericio, F.; Dawson, P. E. Methods, setup and safe handling for anhydrous hydrogen fluoride cleavage in Boc solid-phase peptide synthesis. *Nat. Protoc.*, **2015**, *10*, 1067-1083.
130. Coin, I.; Beyermann, M.; Bienert, M. Solid-phase peptide synthesis: from standard procedures to the synthesis of difficult sequences. *Nat. Protoc.*, **2007**, *2*, 3247-3256.
131. Schnölzer, M.; Alewood, P.; Jones, A.; Alewood, D.; Kent, S. B. H. In situ neutralization in Boc-chemistry solid phase peptide synthesis. *Int. J. Pept. Protein Res.* **1992**, *40*, 180-193.
132. Hyde, C.; Johnson, T.; Owen, D.; Quibell, M.; Sheppard, R. C. Some 'difficult sequences' made easy. A study of interchain association in solid-phase peptide synthesis. *Int. J. Pept. Protein Res.* **1994**, *43*, 431-440.
133. Dawson, P. E.; Muir, T. W.; Clark-Lewis, I.; Kent, S. B. Synthesis of proteins by native chemical ligation. *Science* **1994**, *266*, 776-779.
134. Tam, J. P.; Lu, Y.-A.; Yang, J.-L.; Chiu, K.-W. An unusual structural motif of antimicrobial peptides containing end-to-end macrocycle and cystine-knot disulfides. *Proc. Natl. Acad. Sci. USA* **1999**, *96*, 8913-8918.
135. Carpino, L. A. 9-Fluorenylmethoxycarbonyl function, a new base-sensitive amino-protecting group. *J. Am. Chem. Soc.* **1970**, *92*, 5748-5749.

Chapter 2

Investigation of Supramolecular Self-assembly of Two Dipeptides: $A\beta_{39-40}$ and $A\beta_{41-42}$

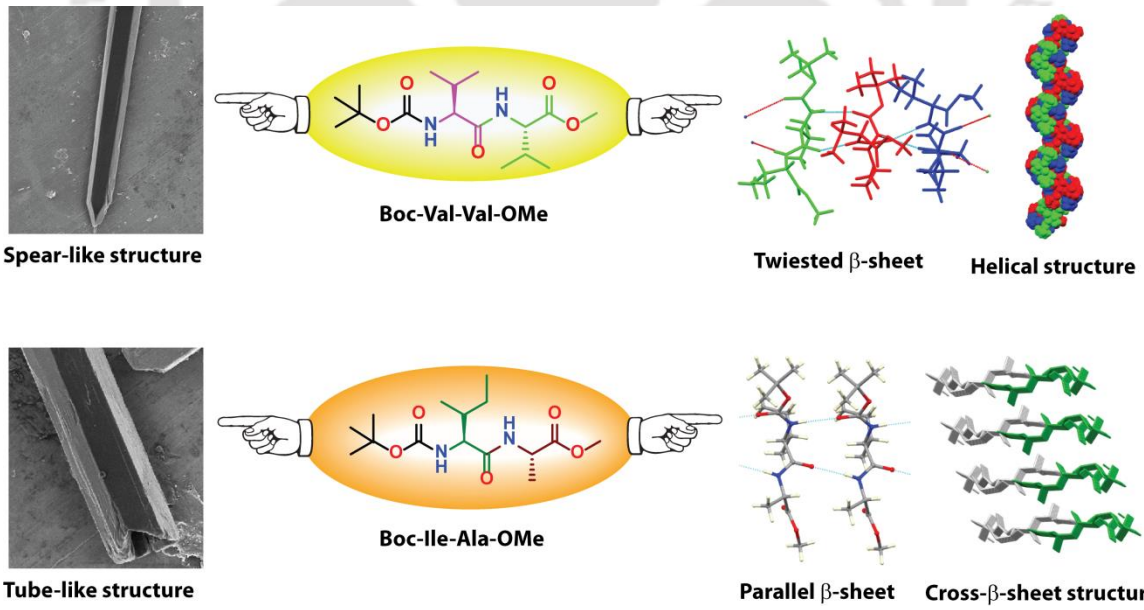

2.1. Background

Understanding of protein folding, misfolding, and aggregation mechanism is a real challenge at present for the scientists and researchers. The *in vivo* aggregation of protein to generate amyloid fibrils which causes several human degenerative diseases e.g. Alzheimer's disease (AD), Huntington's disease (HD), Parkinson's disease (PD), type II diabetes (T2D), *etc*.[1-3] We have discussed the cause of Alzheimer's disease, the origin of amyloid β ($A\beta_{1\text{-}40}$ or $A\beta_{1\text{-}42}$) peptide, and their aggregation and their structural features in Chapter 1, section 1.5.

2.2. Design of peptides

To understand the molecular structure, self-assembly, conformation and morphology of *C*-terminal hydrophobic sequence (VVIA) of amyloid β ($A\beta_{1\text{-}42}$), we have designed two dipeptides, Boc-Val-Val-OMe (**2A**) and Boc-Ile-Ala-OMe (**2B**), bearing sequence homogeneity with the *C*-terminus of Alzheimer's $A\beta_{39\text{–}40}$ and $A\beta_{41\text{–}42}$, respectively (Figure 2.1). Such type of structural analysis of Aβ peptide is important for amyloid research as, till now, no crystal structure of Aβ peptide is reported.

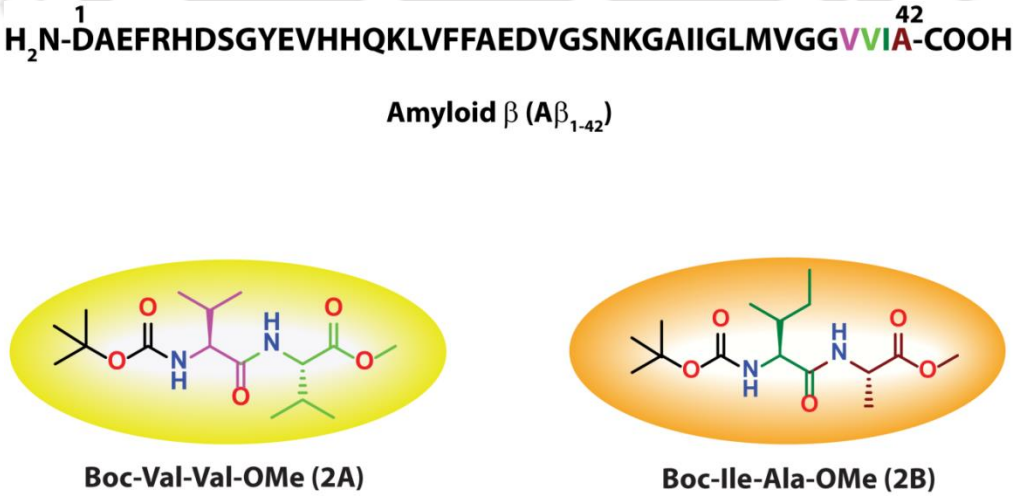

Figure 2.1. *The one-letter representation of the full-length amino acid sequence of the amyloid β ($A\beta_{1\text{–}42}$) peptide and the chemical structures of peptide* ***2A*** *and* ***2B****.*

2.3. Synthesis and characterization of the designed peptides

At first, we synthesized these dipeptides by using a standard conventional coupling method in solution. The detailed synthetic procedure is described in section 2.13.2. The synthetic scheme is represented in scheme 2.1. The designed peptides were purified by silica gel column chromatography, and the purity was checked by analytical HPLC. The purified peptides were characterized by mass spectrometry and 1D [^{1}H] and 2D [^{1}H, ^{1}H] NMR spectroscopy. The characterization data and spectra for the synthesized peptides are shown in section 2.14 and 2.16, respectively.

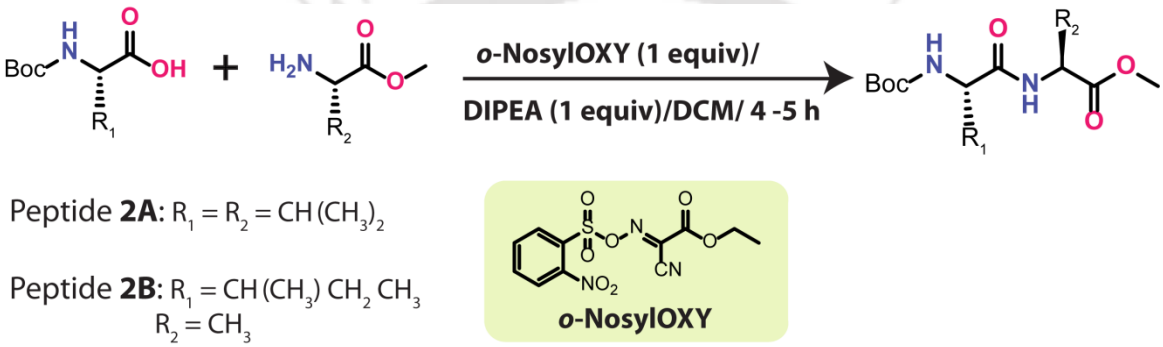

Scheme 2.1. *Schematic representation of peptide synthesis in solution.*

2.4. Investigation of secondary structure by FT-IR

To obtain the secondary structural information of both these peptides, we performed a solid-state FT-IR experiment. Generally, the asymmetric stretching frequencies of the amide I band (1600–1700 cm^{-1}), and N–H band (3200–3500 cm^{-1}) in the FT-IR profile reveals the secondary structure of a peptide.[4] Peptide **2A** and **2B** exhibited the NH band at 3318 cm^{-1}, 3273 cm$^{-1,}$ and 3327 cm^{-1}, respectively (Figure 2.2), indicating all NH's were involved in intermolecular H-bonding in solid-state. They also showed asymmetric stretching frequency of the amide I band (C=O stretching) at 1645 cm^{-1} and 1656 cm^{-1}, and the amide II band at 1529 cm^{-1} and 1525 cm^{-1}, urethane carbonyl stretching at 1686 cm^{-1} and 1689 cm^{-1} (Figure 2.2), suggested the formation of supramolecular β-sheet structure through intermolecular hydrogen bonding in the solid-state.

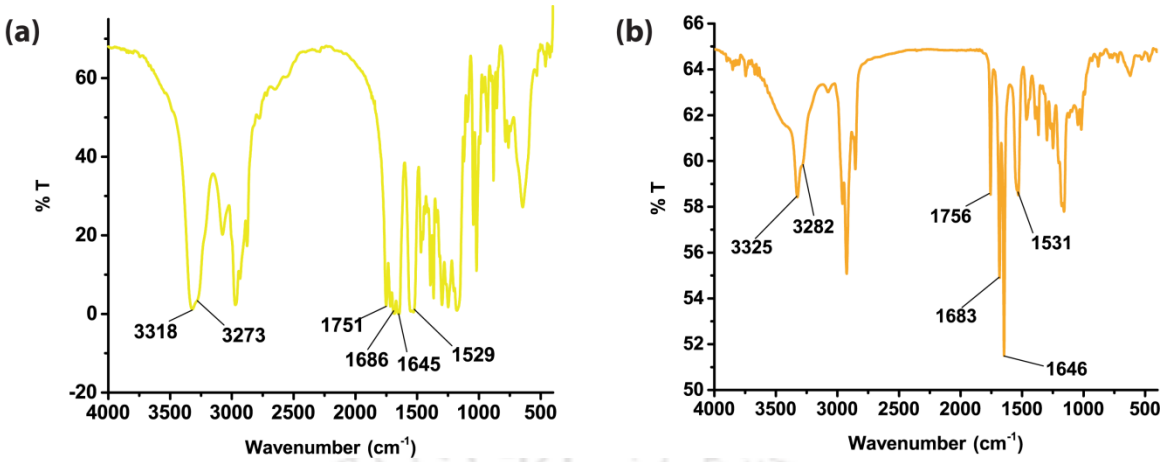

Figure 2.2. *FT-IR spectra of peptide(a)* ***2A*** *and (b)* ***2B****, in solid-state.*

2.5. Investigation of self-assembly process by SC-XRD

To obtain more detailed structural information of these peptides, we performed the SC-XRD experiment. Colorless block-shaped orthorhombic ($P2_12_12_1$) crystals (Figure 2.3) of peptide **2A** and **2B** were obtained from water-acetonitrile solution through slow evaporation at room temperature.

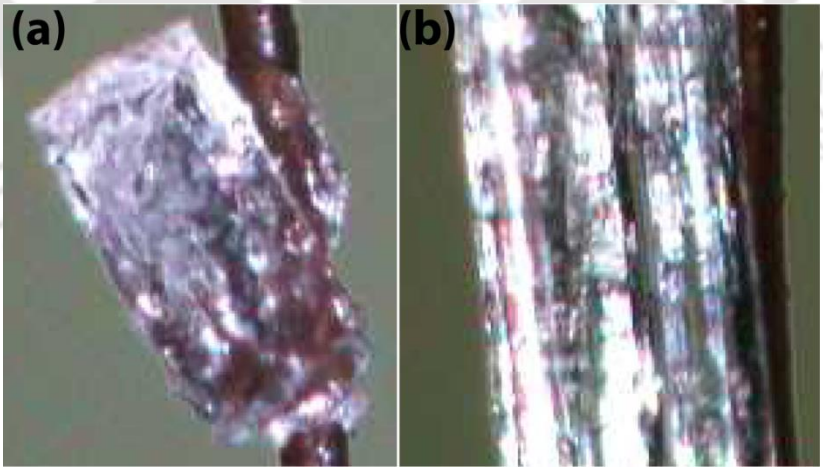

Figure 2.3. *The crystal images of dipeptides (a)* ***2A*** *and (b)* ***2B****.*

Peptide **2A** exhibited three molecules in an asymmetric unit (Figure 2.4), whereas **2B** exhibited one molecule in an asymmetric unit (Figure 2.5). The measured backbone torsion angles (Table 2.1) of these peptides fall in between the ideal parallel β-sheet region of the Ramachandran plot (Chapter 1, section 1.3.1).[5] In peptide **2A**, A, B, and C molecules exhibited 5 H-bonding (2 N–H···O donors, 2 N–H···O acceptors, 1 C–H···O

donor), 6 H-bonding (1 N–H···O donor, 1 N–H···O acceptor, 1 C–H···O donor, 3 C–H···O acceptor), and 9 H-bonding (2 N–H···O donor, 2 N–H···O acceptor, 3 C–H···O donor, 2 C–H···O acceptor) interaction in an asymmetric unit, respectively, suggesting a slightly twisted parallel β-sheet arrangement in crystalline state.

Table 2.1. The measured backbone torsion angles (deg) of **2A** and **2B**

Boc-Val-Val-OMe (**2A**)			Torsion angles (deg)	Boc-Ile-Ala-OMe (**2B**)
Molecule A	Molecule B	Molecule C		
C5–N1–C6–C10 = 117.5(4)	C21–N3–C22–C26 = 76.4(5)	C37–N5–C38–C42 = 87.6(5)	*φ1*	C5–N1–C6–C11 = −109.6(6)
C10–N2–C11–C15= 56.7(5)	C26–N4–C27–C31 = 58.4(5)	C42–N6–C43–C47 = 63.3(5)	*φ2*	C11–N2–C12–C14 = −71.4(7)
N1–C6–C10–N2 = −134.0(4)	N3–C22–C26–N4 = −129.5(4)	N5–C38–C42–N6= −126.6(4)	*ψ1*	N1–C6–C11–N2 = 104.2(5)
N2–C11–C15–O5 = −141.5(4)	N4–C27–C31–O10 = −145.7(4)	N6–C43–C47–O15 = −149.7(4)	*ψ2*	N2–C12–C14–O5 = 173.7(5)
O1–C5–N1–C6 = 174.5(3)	O6–C21–N3–C22 = −168.3(3)	O11–C37–N5–C38 = 177.4(4)	*ω1*	O1–C5–N1–C6 = 177.7(5)
C6–C10–N2–C11 = −177.4(3)	C22–C26–N4–C27 = 175.9(3)	C38–C42–N6–C43 = 176.0(4)	*ω2*	C6–C11–N2–C12 = 178.8(5)

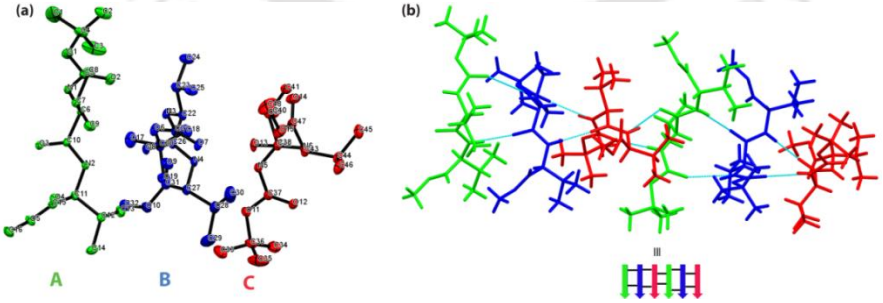

Figure 2.4. *(a) The ORTEP diagram with an ellipsoid of 30% probability of three molecules in an asymmetric unit, and (b) the supramolecular twisted parallel β-sheet structure, of peptide* ***2A.***

On the other hand, a total of 8 H-bonding interactions of which the 4 H-bond donors (2 N–H···O donors and 2 C–H···O donors) and 4-H-bond acceptor (2 N–H···O acceptors and 2 C–H···O acceptors) interactions were available in peptide **2B** in a single asymmetric unit (Figure 2.5c). Each sub-unit of this peptide formed a supramolecular parallel β-sheet through intermolecular H-bonding interaction (N1–H1···O2 of one sub-unit and N2–H2···O3 of another sub-unit) along the *b* direction of the crystallographic axis (Figure 2.5b; Table 2.4, section 2.17). The higher-order aggregation of peptide **2B** showed a supramolecular cross-β-sheet structure with a meridional distance of 5.0 Å along the *b* axis (Figure 2.5d). It also exhibited a flying hexagonal tube-like architecture along the *b* axis in higher-order packing. The obtained self-assembly structure of **2B** is interesting as it adopts a cross-β-sheet structure like Aβ peptide. The X-ray fiber diffraction study of Aβ suggested that it has a cross-β-sheet structure and has stabilized by hydrogen bonding interactions between β-strands aligned in parallel, perpendicular to the main fibril axis.[6] The crystallographic data are displayed in Table 2.5 (section 2.17).

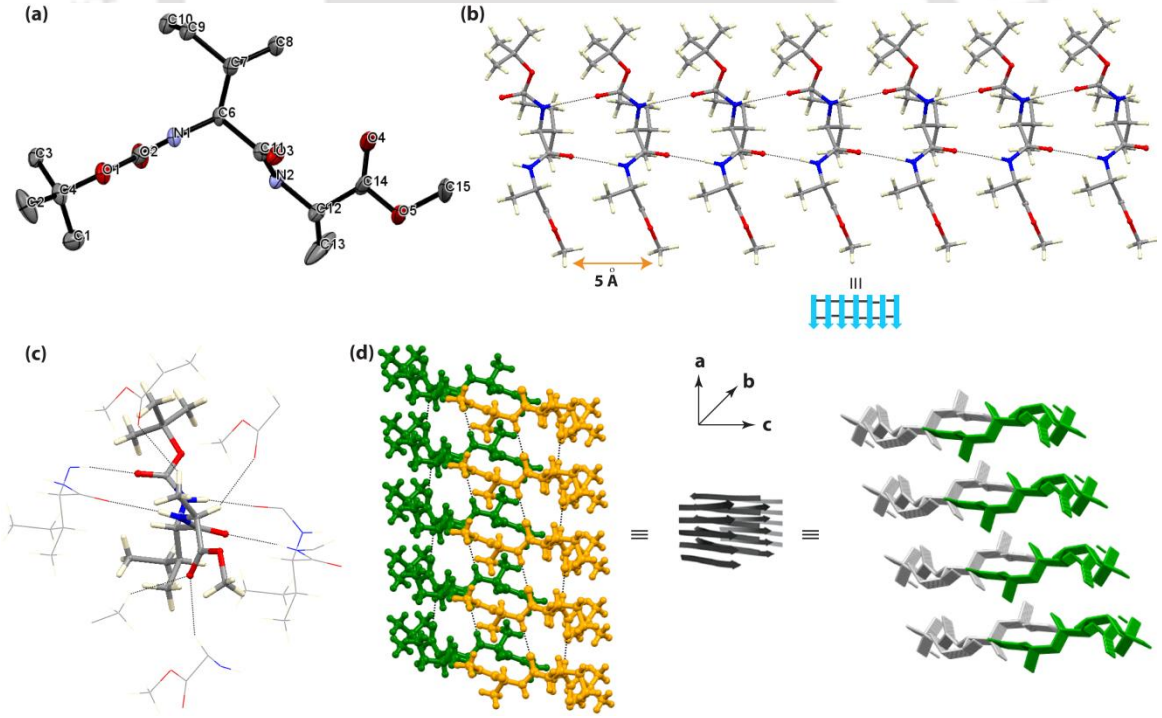

Figure 2.5. *(a) The ORTEP diagram with an ellipsoid of 30% probability, (b) the supramolecular parallel β-sheet structure, (c) intermolecular H-bonding interaction, and (d) the cross-β sheet structure along the b axis at higher-order assembly, of peptide* ***2B.***

2.6. Conformation analysis by CD experiment in solution

Next, we carried out the CD experiment to obtain the confirmation of these peptides in solution. For that, we prepared 1.58 mM of each peptide solution in methanol-water (2:1) medium incubated them at 37 ^{o}C for ten days (sample preparation was described in section 2.13.3). After ten days, these solutions were taken (400 µL) in a quartz cuvette, and CD was measured spanning the wavelength range between 190-260 nm (1 mm path length, and 1 nm bandwidth). The obtained curve of peptide **2A** (Figure 2.6, yellow curve) exhibited negative Cotton effects at 221 nm and a positive cotton effect at 196 nm, indicating the presence of a supramolecular β-sheet structure in that solution. However, peptide **2B** showed two negative cotton effects at 226 nm and 195 nm, indicating the presence of both unordered and β-sheet conformations (Figure 2.6, orange curve).

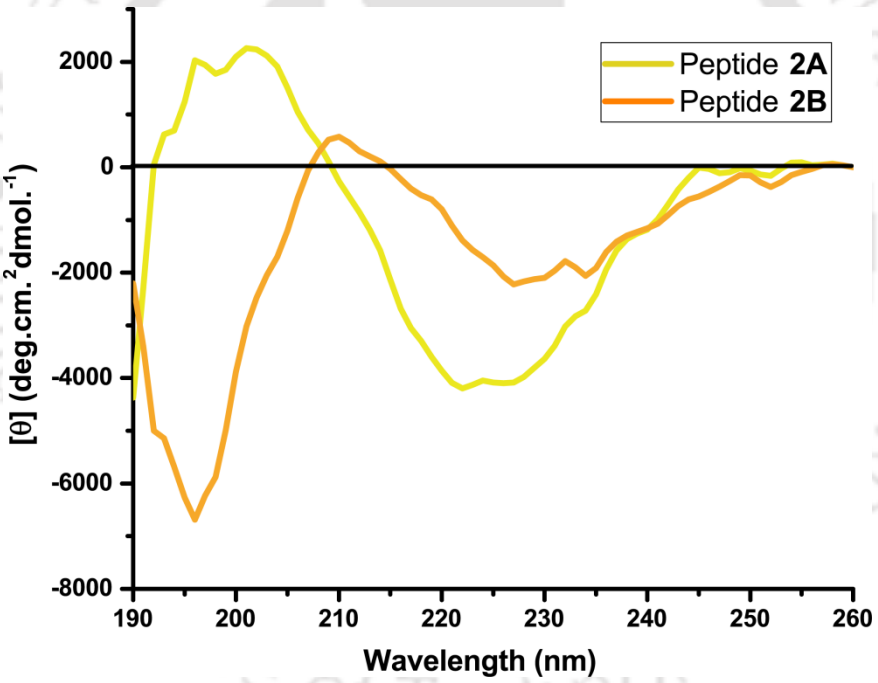

Figure 2.6. *CD profile of peptide* ***2A*** *(yellow curve) and* ***2B*** *(orange curve) in methanol-water (2:1) medium using a concentration of 1.58 mM.*

2.7. Investigation of the secondary structure of 10-day incubated samples by FT-IR

Next, we performed an FT-IR study of the 10-day old samples of the peptide incubated in methanol-water (2:1) solution at 37 ^{o}C to obtain information on their conformation in solution. The obtained spectra exhibited the stretching frequency of the N–H band at 3325 cm^{-1}, 3282 cm^{-1}, 3311 cm^{-1} and 3258 cm^{-1}, the amide I band at 1646 cm^{-1} and 1652 cm^{-1}, and the amide II band at 1531 cm^{-1} and 1528 cm^{-1}, urethane carbonyl stretching at 1683 cm^{-1} and 1680 cm^{-1}, respectively (Figure 2.7), indicated that the peptides self-assembled in a β-sheet structure in solution in a similar fashion to that in the solid-state (section 2.4).

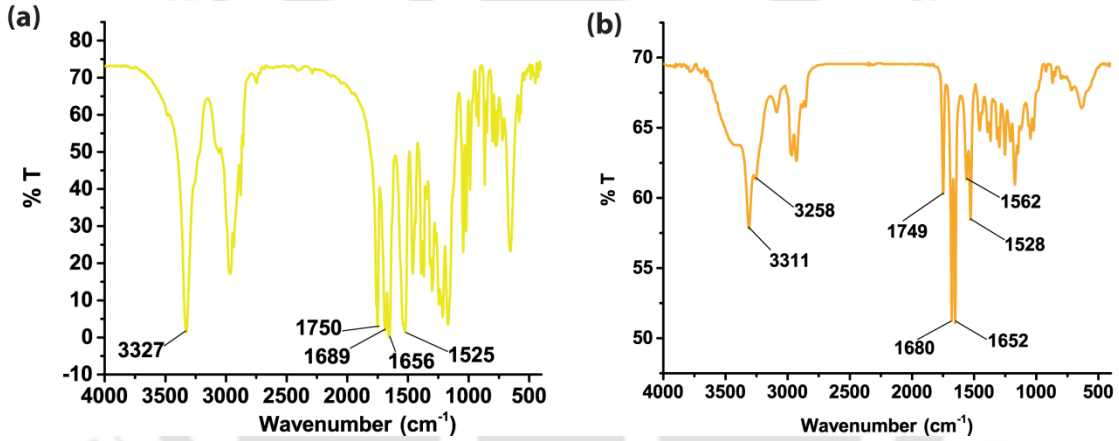

Figure 2.7. *FT-IR spectra of peptide(a)* ***2A*** *and (b)* ***2B****, in the 10-day aged solution in methanol-water.*

2.8. Monitoring the self-association of 2A and 2B in solution by FE-SEM

Then we checked the morphology of these peptides to understand their self-aggregation behavior. The morphology of these self-associated peptides was analyzed under a FE-SEM. For that, the 10-day incubated samples were drop-cast on an Al-foil and dried overnight inside a desiccator. The obtained FESEM images of **2A** indicated that it self-associated to form highly organized straight unbranched several μm long two ended spear-like structures (Figure 2.8a) whereas **2B** self-associated to build a hexagonal hollow tube-like structure (Figure 2.8b). Herein, we noted that these two both side protected dipeptides, the partial sequences of the *C*-terminal Aβ peptide, generated two different types of morphology (two ended spear-like for **2A** and hexagonal hollow tube-like structure for **2B**) which were different from Aβ aggregated peptide. Generally, Aβ

peptide aggregated to form several micrometers long bend fibrillar structures.[7] Moreover, the cryoEM suggested a unique fibril structure of Aβ with a tubular shape and a hollow core.[6]

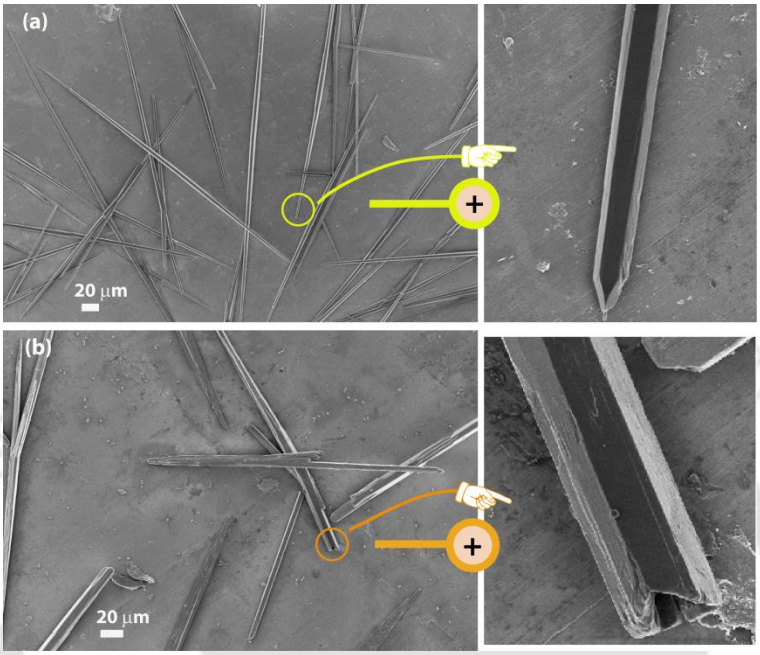

Figure 2.8. *FE-SEM images of self-aggregated dipeptides (a)* ***2A*** *and (b)* ***2B****, in MeOH–H_2O (2:1) solution using a concentration of 1.58 mM.*

2.9. Investigation of dye binding affinity of this self-aggregated peptide by fluorescence microscope

Dyes are generally used to visualize the structures in the cell, such as mitochondria, amyloid fibrils,[8] and hydrogels.[9] For that, we prepared 1 mM ThT solution[10,11] in 50 μM PBS buffer at pH 7.4 and then, from it, 5 μL solutions was added to the 5 μL of peptide **2A** and **2B** solutions which were incubated 10 days in MeOH-H_2O (2:1) medium at 37 ^oC and these solutions were dropped cast on microscopic slide. Similarly, 5 μL of each peptide solution was mixed with 5 μL of Congo red solution[10,11] (saturated solution in ethanol) separately and then dropped cast on a microscopic slide. Next, the dye stained microscopic slides are allowed to capture the bright field and corresponding fluorescence images under a fluorescence microscope. The excitation wavelength 465-495 nm and the emission wavelength 512-558 nm are used on the ThT stained slide, and the excitation wavelength 510-560 nm and the emission wavelength 580 nm were used for Congo red-

stained slides. The obtained images indicated that peptide **2A** and **2B** self-assembled to form a supramolecular parallel β-sheet structure that binds to ThT and Congo red.

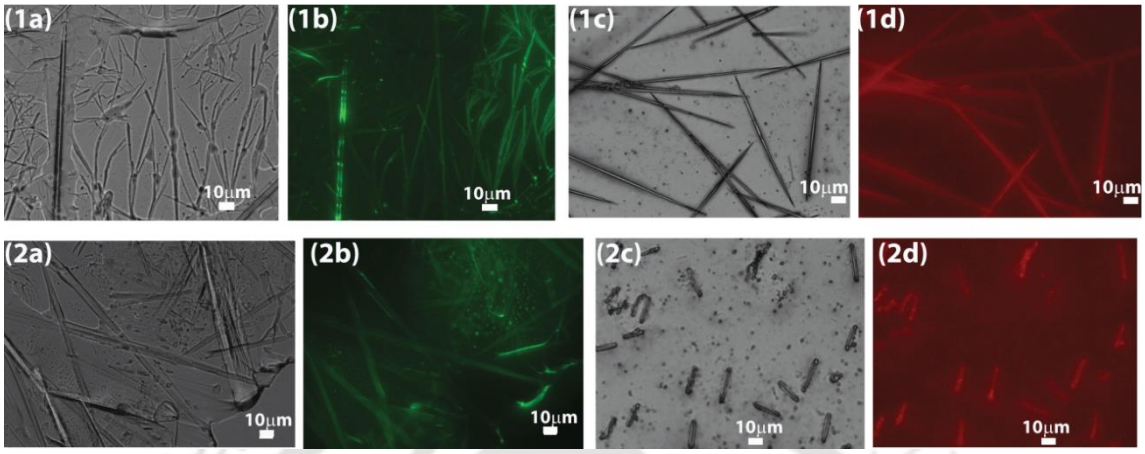

Figure 2.9. *Bright-field and the corresponding fluorescence images of peptide* ***2A*** *(1a–1d) and peptide* ***2B*** *(2a–2d) stained with ThT and Congo red, respectively.*

2.10. Investigation of self-assembly process by PXRD

Next, we performed the powder X-ray pattern analysis of these self-aggregated peptides. After 10 days of incubation of these peptides at 37 ^{o}C in MeOH: H_2O (2:1), they were freeze-dried and were allowed to XRD pattern analysis from 3–50^{o} of the 2θ range.

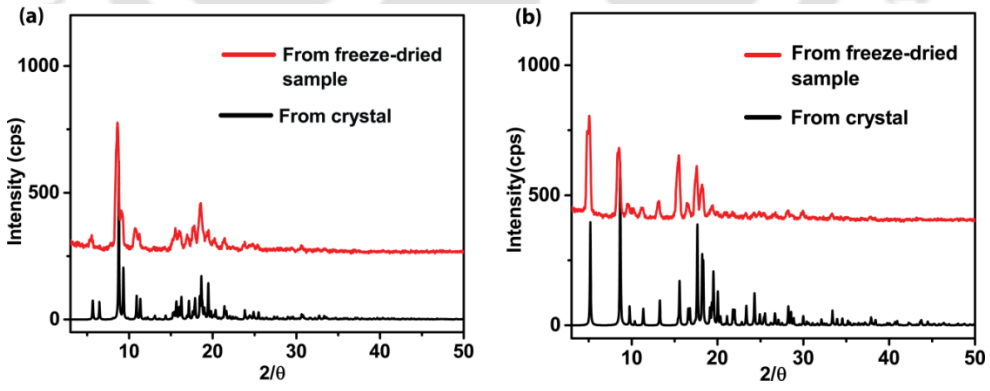

Figure 2.10. *PXRD patterns of peptides (a)* ***2A*** *and (b)* ***2B****, shows a self-assembled form (red) similar to the pattern (black) obtained from single-crystal X-ray analyses, respectively.*

We notated that the obtained PXRD patterns from these freeze-dried peptides were similar to the XRD patterns derived from the single-crystal analyses (Figure 2.10). Thus,

the peptides in the crystal state and the aged freeze-dried solid-state exhibited similar β-sheet based supramolecular structures.

2.11. Investigation of thermal stability by TGA

Next, we performed the TGA analysis to investigate the thermal stability of **2A** and **2B** in the solid-state. Generally, mass loss is observed from two thermal stages in a TGA plot of a peptide. While the mass loss due to the release of the adsorbed water molecules is observed in the temperature region between 25-200 ^{o}C, the mass loss due to the peptide bond breaking is observed between 200-500 ^{o}C. Peptide **2A** and **2B** showed a mass loss at 221 ^{o}C (mp 163 ^{o}C) and 219 ^{o}C (mp 144 ^{o}C), respectively, indicating significant thermal stability due to their supramolecular β-sheet arrangement (Figure 2.11). No mass loss was noted between 25-200 ^{o}C, confirming the absence of adsorbed water or solvent molecules for both peptides.

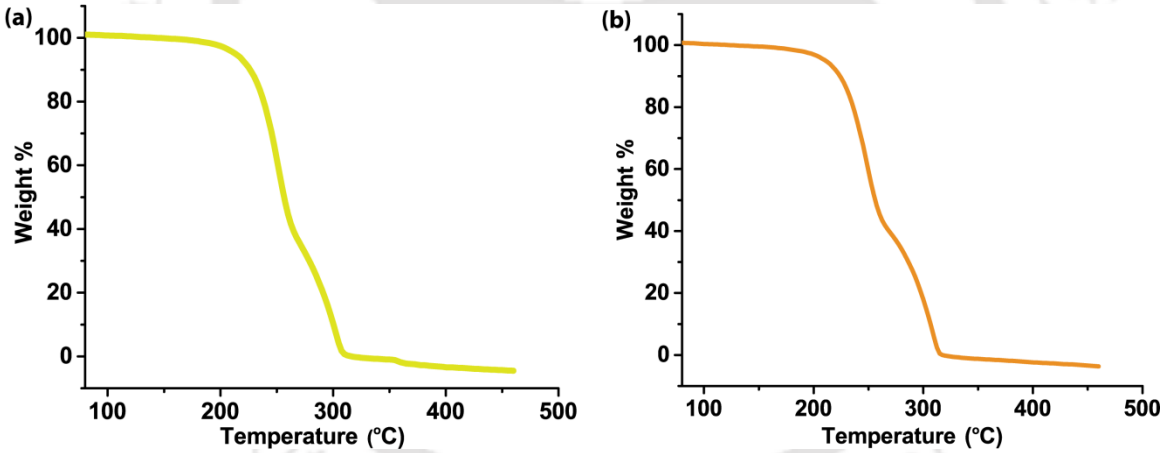

Figure 2.11. *TGA plot of peptides (a)* ***2A*** *and (b)* ***2B****.*

2.12. Conclusion

In conclusion, we demonstrated the self-assembly, conformation, and morphology of two small dipeptides, **2A** and **2B**, bearing sequence homogeneity with the *C*-terminus of Alzheimer's $A\beta_{39–40}$ and $A\beta_{41–42}$, respectively. The SC-XRD revealed that peptide **2A** self-assembled to form supramolecular twisted β-sheet structure, whereas peptide **2B** self-assembled to form a parallel β-sheet structure in the crystalline state. It is further self-assembled to form a cross-β-sheet structure in higher-order packing along the crystallographic *b* axis. The formation of β-sheet structures of both peptides was also confirmed by FT-IR, CD and PXRD experiments. Further, they self-associate to form highly organized straight unbranched two-ended spear-like and tube-like structures, respectively, in methanol-water (2:1) medium. Interestingly, these self-associated peptides were found to bind with the amyloid binding dyes ThT and Congo red. Such comparative analyses may help in understanding the amyloidogenesis of the *C*-terminal hydrophobic patch of the Alzheimer's Aβ peptide.

2.13. Experimental section

2.13.1. Materials and instrumentations

As described in chapter 8

2.13.2. General procedure for the synthesis of dipeptides

Boc protected amino acid (1 equiv), coupling reagent, *o*-NosylOXY (1 equiv), Hünig's base DIPEA (1 equiv) in DCM were taken in a 50 mL RB. and the reaction mixture was kept 5 min for preactivation.[12] In another beaker, the methyl ester of the next amino acid (1.2 equiv) with DIPEA (1.2 equiv) in DCM was taken for neutralization. Then, this solution was added dropwise to the above reaction vessel and kept stirring for 4-5 h at room temperature. After completion of the reaction, the reaction mixture was diluted with DCM and washed with a 10% citric acid solution followed by the saturated $NaHCO_3$ solution three times in each case. Then, the organic layer was dried over anhydrous Na_2SO_4, and the decanted solvent was evaporated to get solid both *N*- and *C*- protected dipeptide. The desired product was purified by silica gel column chromatography using ethyl acetate-hexane solvent system.

2.13.3. Sample preparation

3.03 mM peptide **2A** and 3.16 mM peptide **2B** solutions were prepared in two different Eppendorf vials (2 mL) by adding 1 mL MeOH-H_2O (2:1) solution. Then, we prepared a 1 mL (1.58 mM) solution (stock solution) from the above solutions for each peptide. These peptide stock solutions were incubated for 10 days at 37 ^oC.

2.14. Characterization data

Boc-Val-Val-OMe 2A.

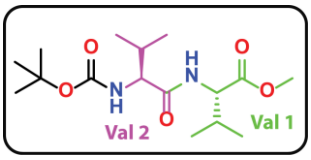

White solid; (256 mg, 84%), mp 161-163°C; ^{1}H NMR (DMSO-d_6, 600 MHz) δ 0.89-0.81 (12H, m); 1.37 (9H, s); 1.92-1.88 (1H, m); 2.06-2.00 (1H, m); 3.34 (3H, s); 3.87-3.84 (1H, t, *J*= 7.8 Hz); 4.18-4.16 (1H, t, *J* = 7.2 Hz); 6.69-6.67 (1H, d, *J* = 9 Hz); 7.98-7.97 (1H, d, *J* = 7.8 Hz). ^{13}C NMR (DMSO-d_6; 100 MHz) δ 18.2, 19.1, 28.1, 29.8, 30.3, 51.5, 57.2, 59.5, 77.9, 155.3, 171.8, 172.8. ESI-MS: calculated $[M+H]^+$ 331.2155, found m/z 331.2265. HPLC: retention time (t_R) = 8.97 min.

Boc-Ile-Ala-OMe 2B.

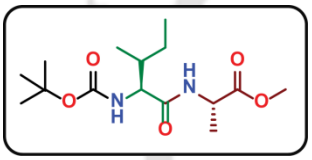

White solid; (238mg, 87%), mp 142-144°C; ^{1}H NMR (DMSO-d_6, 600 MHz) δ 0.84-0.79 (6H, m); 1.10-1.03 (1H, m); 1.27-1.26 (3H, d, *J* = 7.2 Hz); 1.37 (9H, s); 1.66-1.64 (1H, m); 3.33 (3H, s); 3.85-3.83 (1H, t, *J* = 7.8 Hz); 4.28-4.23 (1H, m); 6.61-6.59 (1H, d, *J* = 9 Hz); 8.27-8.26 (1H, d, *J* = 6.6 Hz). ^{13}C NMR (DMSO-d_6; 100 MHz) δ 10.9, 15.1, 16.8, 24.2, 28.1, 36.7, 47.4, 51.7, 58.2, 77.9, 155.2, 171.1, 172.9. ESI-MS: calculated $[M+H]^+$ 317.1998, found m/z 317.2110. HPLC: retention time (t_R) = 8.57 min.

2.15. References

1. Selkoe, D. J. Folding proteins in fatal ways. *Nature*, **2003**, *426*, 900-904.
2. Aguzzi, A.; O'Connor, T. Protein aggregation diseases: pathogenicity and therapeutic perspectives. *Nat. Rev. Drug Discovery*, **2010**, *9*, 237-248.
3. DeToma, A. S.; Salamekh, S.; Ramamoorthy A.; Lim, M. H. Misfolded proteins in Alzheimer's disease and type II diabetes. *Chem. Soc. Rev.*, **2012**, *41*, 608-621.
4. Nilsson, M. R. Techniques to study amyloid fibril formation in vitro. *Methods*, **2004**, *34*, 151-160.
5. Loughlin, W. A.; Tyndall, J. D. A.; Glenn, M. P.; Hill T. A.; Fairlie, D. P. Update 1 of: Beta-strand mimetics. *Chem. Rev.*, **2010**, *110*, PR32-PR69.
6. Miller, Y.; Ma, B.; Tsai C.-J.; Nussinov, R. Hollow core of Alzheimer's Aβ_{42} amyloid observed by cryoEM is relevant at physiological pH. *Proc. Natl. Acad. Sci. U. S. A.*, **2010**, *107*, 14128-14133.
7. Takai, E.; Ohashi, G.; Ueki, R.; Yamada, Y.; Fujita J. I.; Shiraki, K. Scanning electron microscope imaging of amyloid fibrils. *Am. J. Biochem. Biotechnol*., **2014**, *10*, 31-39.
8. Khurana, R.; Uversky, V. N.; Nielsen, L.; Fink, A. L. Is Congo red an amyloid-specific dye? *J Biol Chem* **2001**, *276*, 22715-22721.
9. Liang, G.; Xu, K.; Li, L.; Wang, L.; Kuang, Y.; Yang, Z.; Xu, B. Using Congo red to report intracellular hydrogelation resulted from self-assembly of small molecules. *Chem Commun* **2007**, 4096-4098.
10. Nadimpally, K. C.; Paul, A.; Mandal, B. Reversal of aggregation using β-breaker dipeptide containing peptides: application to Aβ(1−40) self-assembly and its inhibition. *ACS Chem. Neurosci.* **2014**, *5*, 400-408.
11. Paul, A.; Nadimpally, K. C.; Mondal, T.; Thalluri, K.; Mandal, B. Inhibition of Alzheimer's amyloid-β peptide aggregation and its disruption by a conformationally restricted α/β hybrid peptide. *Chem. Commun.* **2015**, *51*, 2245-2248.
12. Dev, D.; Palakurthy, N. B.; Thalluri, K.; Chandra, J.; Mandal, B. Ethyl 2-cyano-2-(2-nitrobenzene sulfonyloxyimino)acetate (*o*-NosylOXY): A recyclable coupling reagent for racemization free synthesis of peptide, amide, hydroxamate and ester. *J. Org. Chem*. **2014**, *79*, 5420-5431.

2.16. Selected spectra

2.16.1. Spectra of peptide 2A

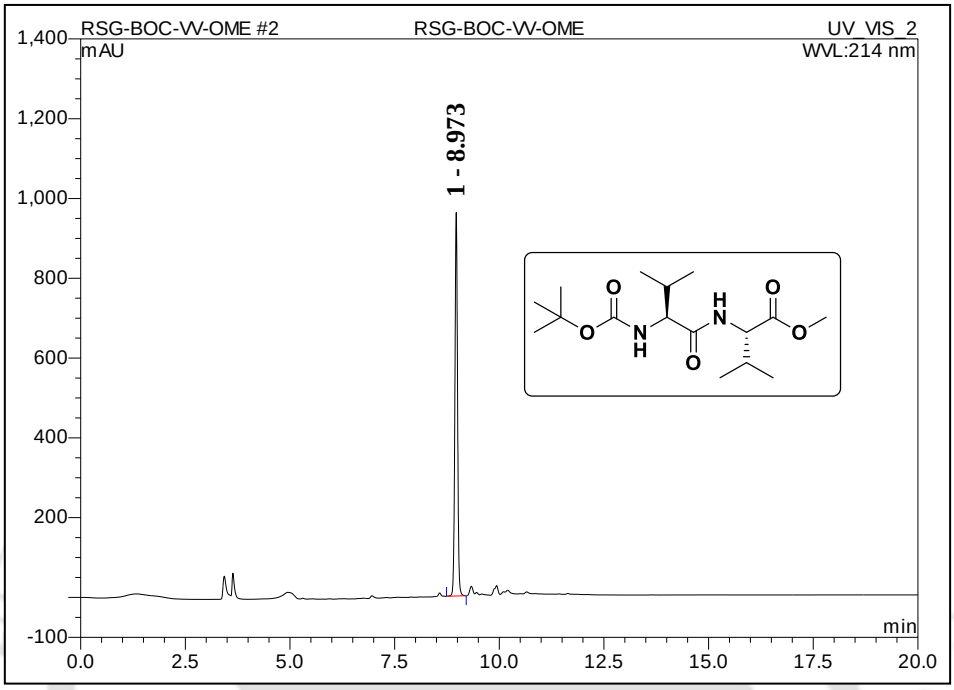

Figure 2.12. *HPLC profile picture of purified peptide* ***2A*** *(A linear gradient was used from 5 to 100% CH_3CN till 8 min, and a total run time of 20 min, flow rate 1mLmin^{-1})*

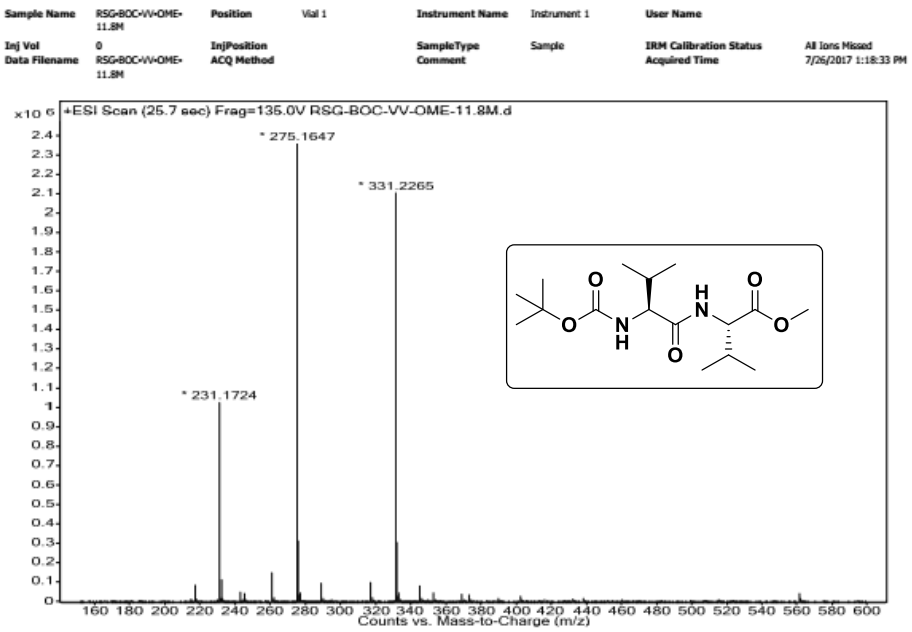

Figure 2.13. *MS spectra of peptide* ***2A***

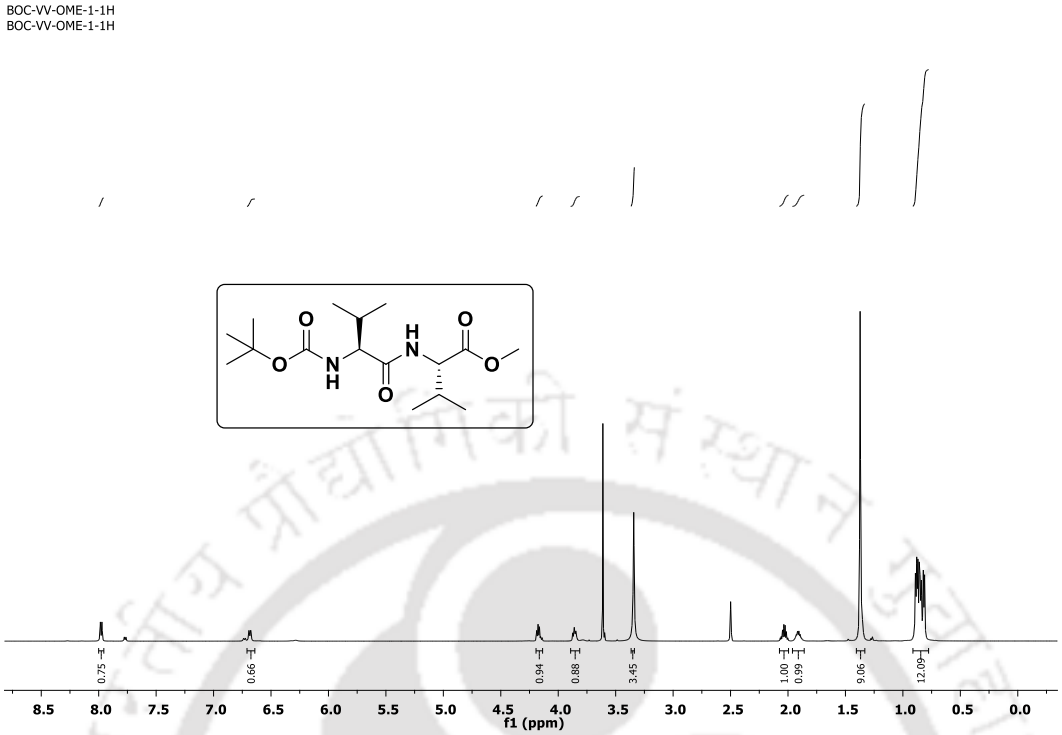

Figure 2.14. *^{1}H NMR spectra of peptide* ***2A***

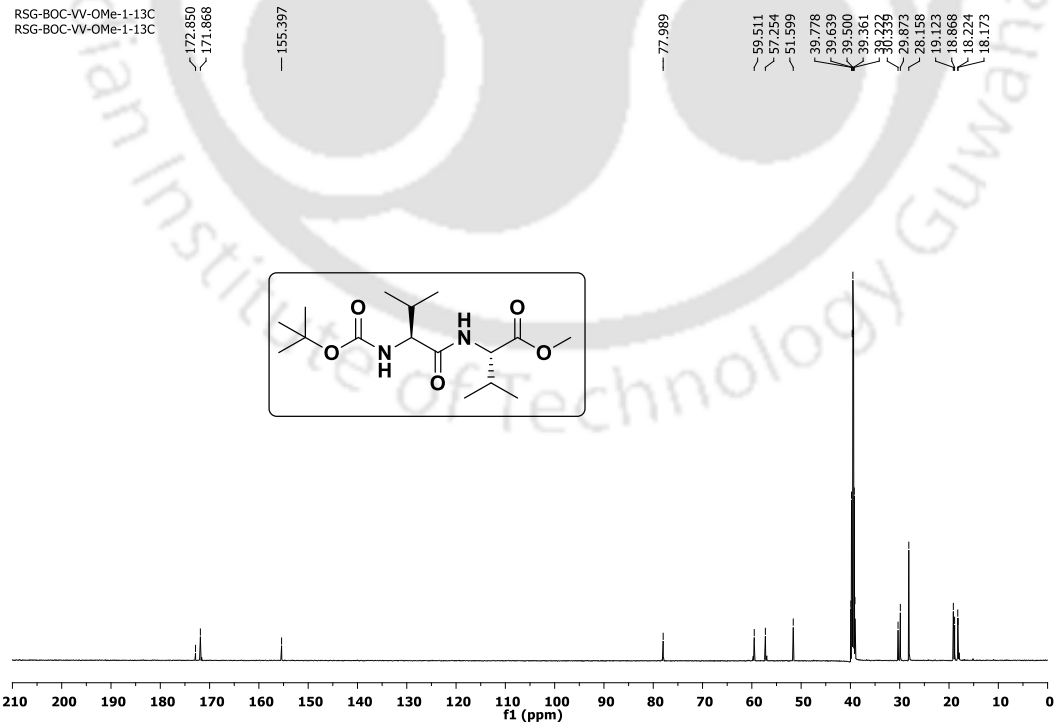

Figure 2.15. *^{13}C NMR spectra of peptide* ***2A***

2.15.2. Spectra of peptide 2B

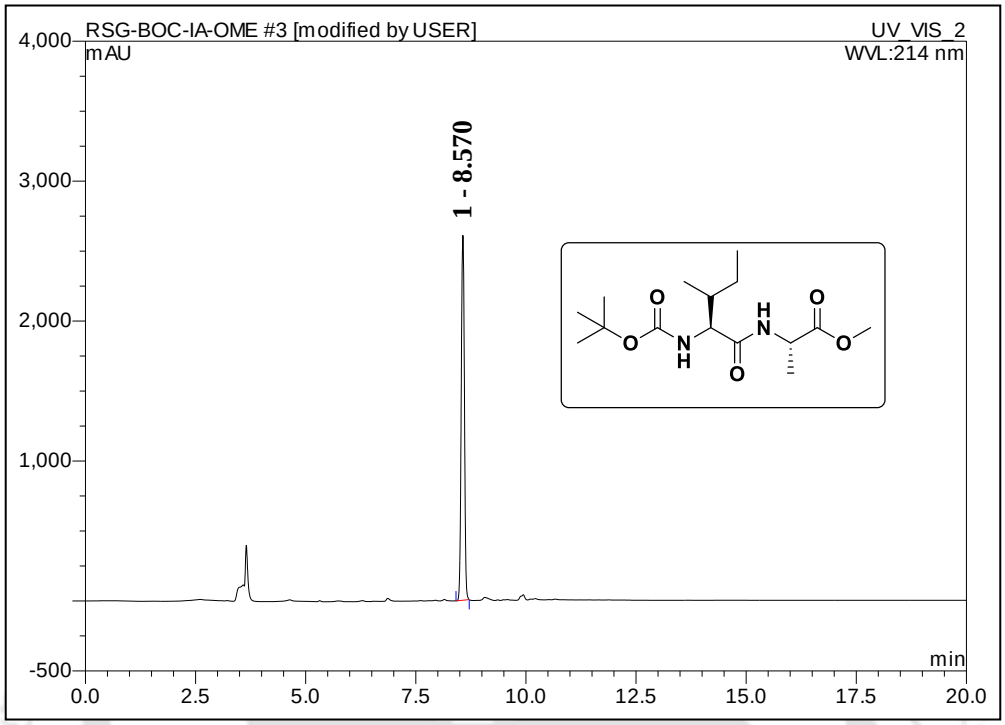

Figure 2.16. *HPLC profile picture of purified peptide* ***2B*** *(A linear gradient was used from 5 to 100% CH_3CN till 8 min, and a total run time of 20 min, flow rate 1mLmin^{-1})*

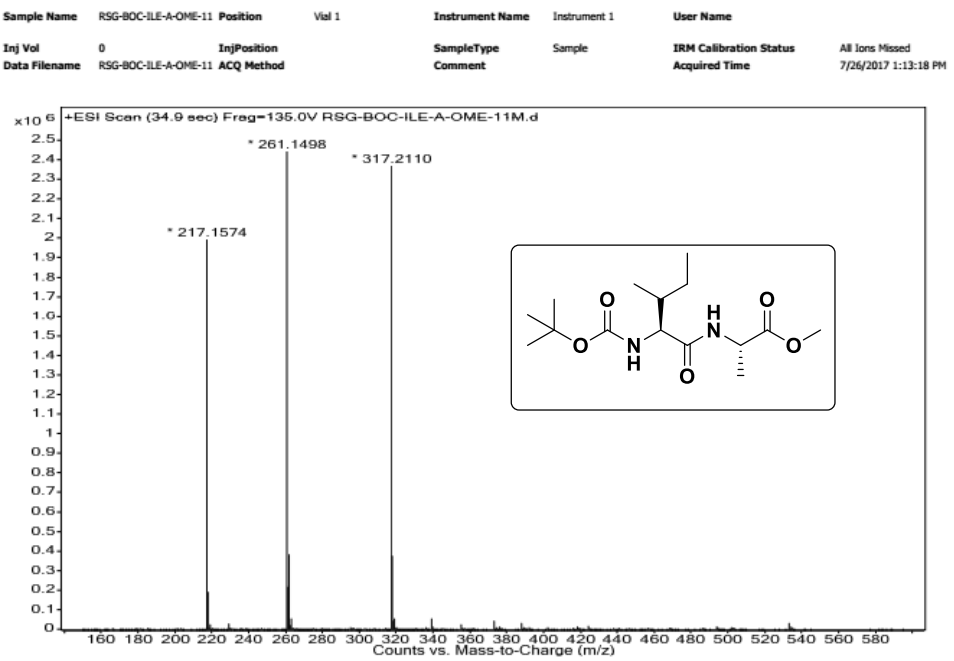

Figure 2.17. *MS spectra of peptide* ***2B***

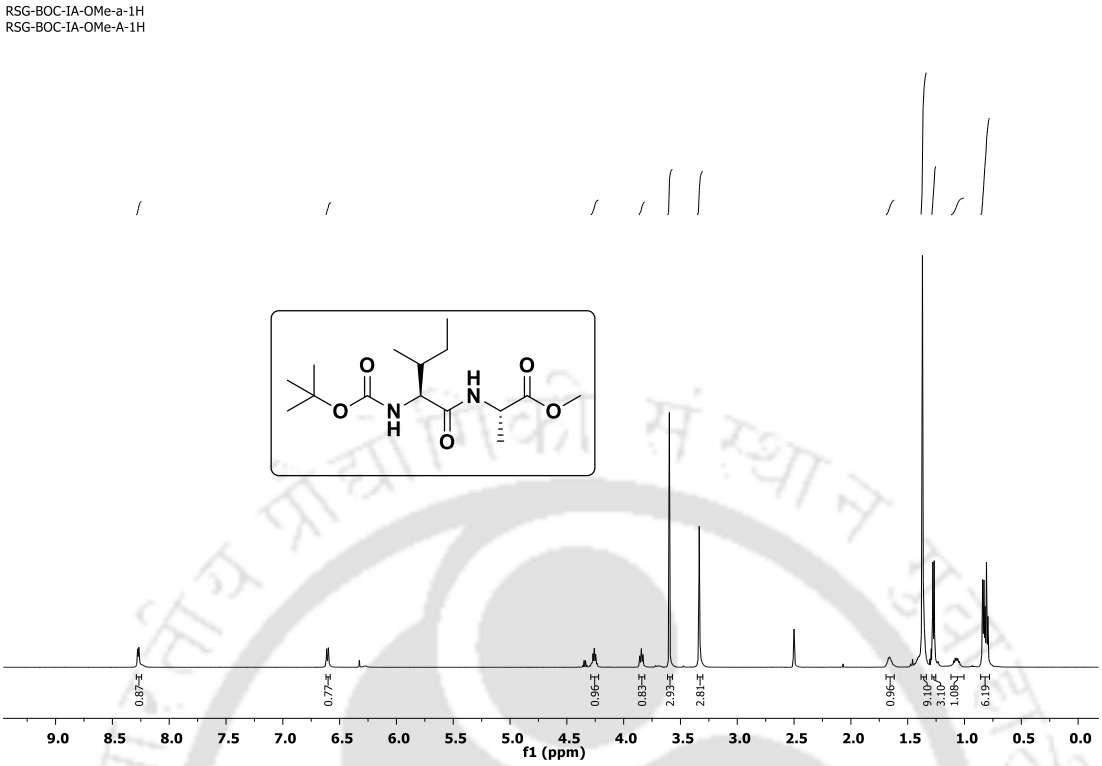

Figure 2.18. *^{1}H NMR spectra of peptide* ***2B***

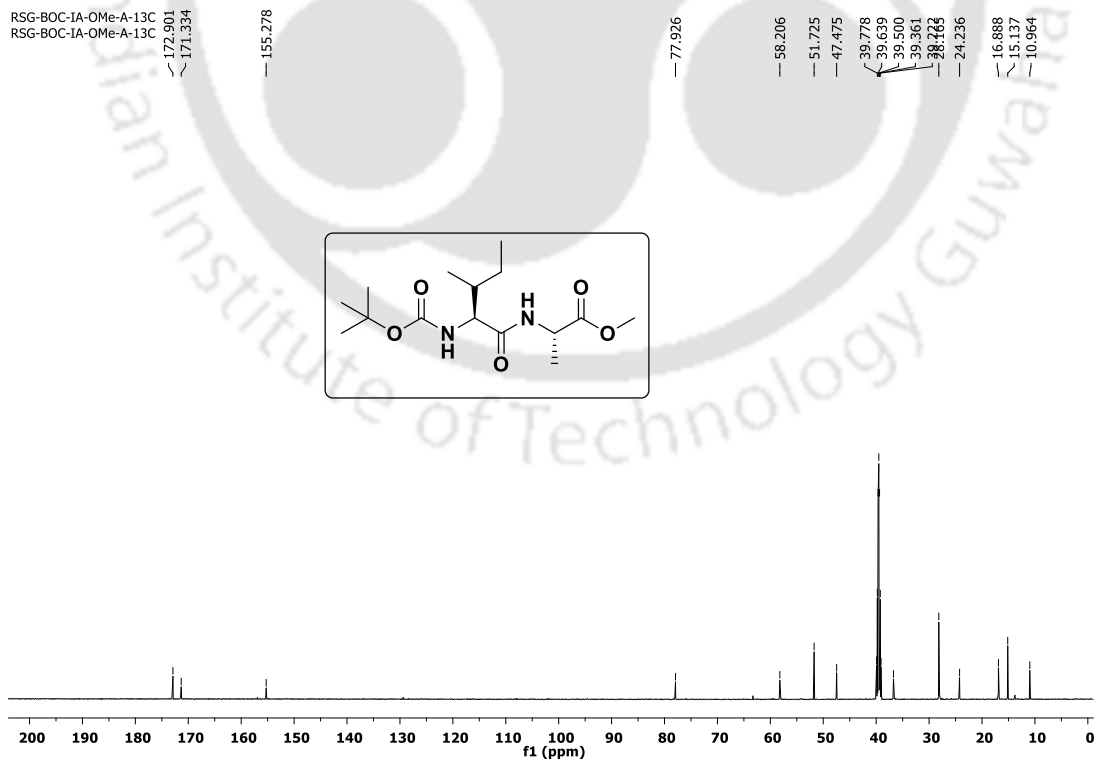

Figure 2.19. *^{13}C NMR spectra of peptide* ***2B***

2.17. Crystallographic data

Table 2.4. Hydrogen bonding distances (Å) and Bond angles (deg) of peptide **2A** and **2B**

molecule	***D−H···A***	***d(D···H) /Å***	***d(H···A)/Å***	***d(D···A)/Å***	***<D−H···A/°***
Boc-VV-OMe (**2A**)	N1-H1N···O12	0.86	2.23	2.956(5)	142
	N2-H2N···O8	0.86	1.96	2.810(5)	172
	N3-H3N···O2	0.86	2.14	2.963(5)	160
	N4-H4N···O13	0.86	1.92	2.782(5)	178
	N5-H5N···O7	0.86	2.07	2.921(5)	169
	N6-H6N···O3	0.86	2.05	2.882(5)	164
Boc-IA-OMe (**2B**)	N1-H1N···O2	0.86	2.11	2.957(6)	168
	N2-H2N···O3	0.86	2.14	2.996(6)	172
	C12-H12···O4	0.98	2.37	3.293(10)	156
	C13-H13A···O4	0.96	2.44	3.240(17)	141

Table 2.5. Crystal parameters and refinement data of **2A** and **2B**

Parameters	***Boc-Val-Val-OMe (2A)***	***Boc-Ile-Ala-OMe (2B)***
Formula	$C_{16}H_{30}N_2O_5$	$C_{15}H_{28}N_2O_5$
Fw	330.42	316.39
Crystal system	orthorhombic	orthorhombic
Space group	*P 21 21 21*	*P 21 21 21*
a/Å	11.7141(3)	5.0771(6)
b/Å	18.6463(5)	10.3940(19)
c/Å	27.0913(7)	33.371(7)
α/°	90.00	90.00
β/°	90.00	90.00
γ/°	90.00	90.00
V/Å^3	5917.4(3)	1761.0(5)
Z	12	4
D_c/g cm^{-3}	1.113	1.193
μ Mo K_α/mm^{-1}	0.082	0.734
F000	2160.0	688.0
T/K	150.00(10)	150.00(10)
θ max.	27.6420	66.8190
Total no. of reflections	13225	3375
Independent reflections	11053	2468
Observed reflections	8345	1958
Parameters refined	646	206
R_1, $I > 2\sigma(I)$	0.0590	0.0806
wR_2, $I > 2\sigma(I)$	0.1475	0.2175
GOF (F^2)	1.080	1.067
Flack parameter	0.3(6)	-0.2(4)
CCDC No.	1589438	1589439

Chapter 3

Investigation of Various Nanostructures from Alternating L/L and D/L Amino Acid Containing Dipeptides

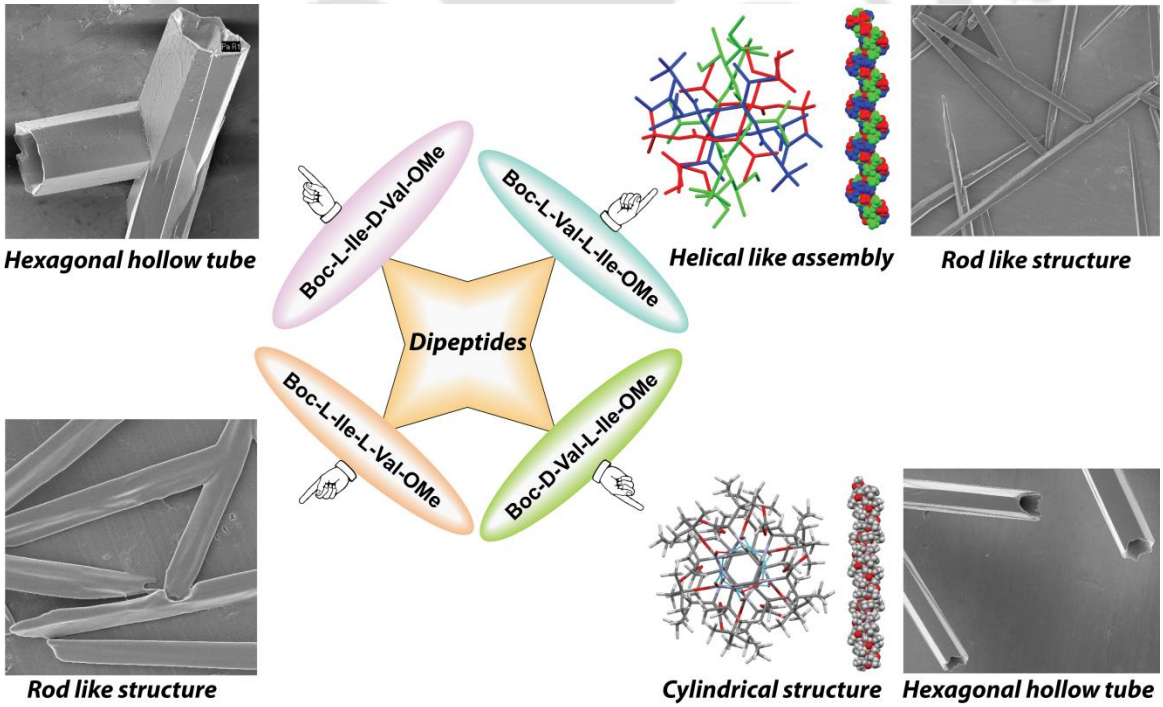

3.1. Background

The self-assembly of peptide generated various supramolecular structures such as nanofibrils, nanotubes, nanorods, nanospheres, *etc.* have numerous applications in medicinal chemistry and biotechnology.[1-4] Some nanotubes of small dipeptides are reported, discussed in Chapter 1, section 1.6. Mostly, the reported nanotubes are generated from alternating L/L amino acid containing peptide. Alternating D/L amino acid containing peptide-based nanotubes is not explored enough. But in the presence of alternating D/L amino acid in a peptide sequence increases the proteolytic stability of the nanotube. By this inspiration, we designed alternating L/L and D/L amino acid-containing dipeptides and checked their self-association.

3.2. Design of peptides

In chapter 2, we discussed the self-assembly, conformation, and morphology of two dipeptides, bearing sequence homogeneity with the *C*-terminus of Alzheimer's $A\beta_{39–40}$ and $A\beta_{41–42}$, respectively. Herein, we first designed a dipeptide, Boc-L-Val-L-Ile-OMe (**3A**), which is also identical to the *C*-terminus of Alzheimer's $A\beta_{40-41}$. Next, we designed another three peptides by interchanging the chirality and position of Val and Ile in the peptide sequence, i.e., Boc-D-Val-L-Ile-OMe (**3B**), Boc-L-Ile-L-Val-OMe (**3C**), and Boc-L-Ile-D-Val-OMe (**3D**).

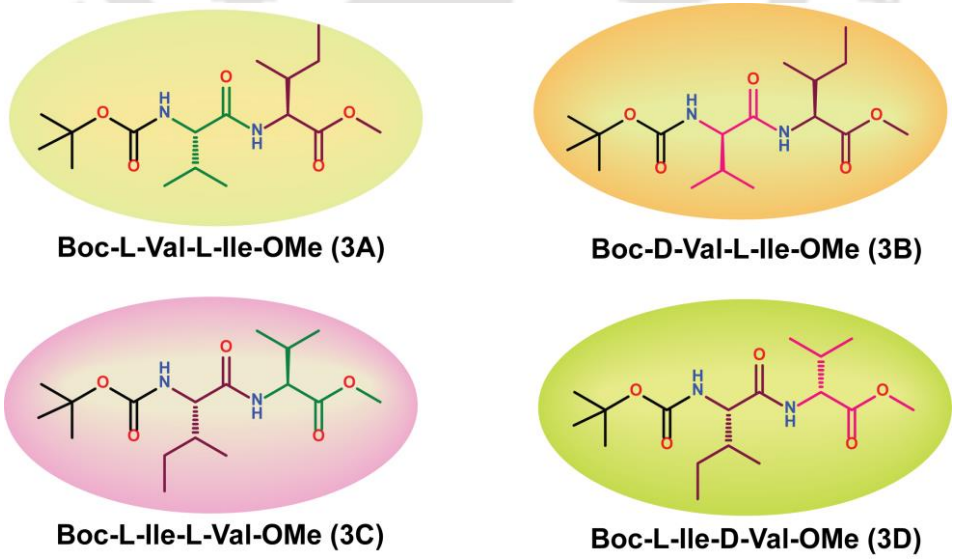

Figure 3.1. *The chemical structures of peptide* ***3A, 3B, 3C,*** *and* ***3D****.*

3.3. Synthesis and characterization of the designed peptides

At first, we synthesized these dipeptides by using a standard conventional coupling method in solution. The detailed synthetic procedure is described in Chapter 1, section 2.13.2. The synthetic scheme is also represented in Chapter 1, scheme 2.1. The designed peptides were purified by silica gel column chromatography, and the purity was checked by analytical HPLC. The purified peptides were characterized by mass spectrometry and 1D [^{1}H] NMR spectroscopy. The characterization data and spectra for the synthesized peptides are shown in section 3.13 and 3.15, respectively.

3.4. Investigation of nanostructures by various microscopes

To understand the molecular structure of these peptides, we prepared a 1.5 mM of each dipeptide solution by using a 30% acetonitrile-water solution and incubated them at 37 ^{o}C for seven days. The specific sample preparation method is described in section 3.12.3. Next, the 7-day old solutions were drop cast (10 µL) on a microscopic slide for optical microscope study and were drop cast (10 µL) on Al-foil for FE-SEM experiment.

The obtained optical microscopic images indicated that peptide **3A** and **3C** self-associated to generate a highly organized net rod-like structure (Figure 3.2, 1a and 3a) but peptide **3B** and **3D** self-associated to form a hollow tube-like structure (Figure 3.2, 2a and 4a).

Similarly, the FE-SEM images clearly suggested that **3A** and **3C** self-associated to adopt highly organized straight several µm long neat rod-like (~3 µm diameter for **3A** and ~2 µm for **3C**) structure (Figure 3.2, 1b and 3b) however **3B** and **3D** self-assembled to form several µm long hexagonal hollow tube (~9 µm diameter for **3B** and ~14 µm diameter for **3D**) structure (Figure 3.2, 2b and 4b).

Moreover, to achieve more detail structural information, a TEM study was performed. The uranyl acetate stained self-assembled peptides **3A** and **3C** (100 µM) showed a net nanorod like (~3.8 µm long and ~350 nm diameter for **3A** and ~0.9 µm long and ~85 nm diameter for **3C)** structure (Figure 3.2, 1c and 3c). However, the stained self-assembled **3B** and **3D** (100 µM) exhibited a hollow nanotube like (~5 µm long and ~190 nm

diameter for **3B** and ~1 µm long and ~90 nm diameter for **3D)** structure (Figure 3.2, 2c and 4c).

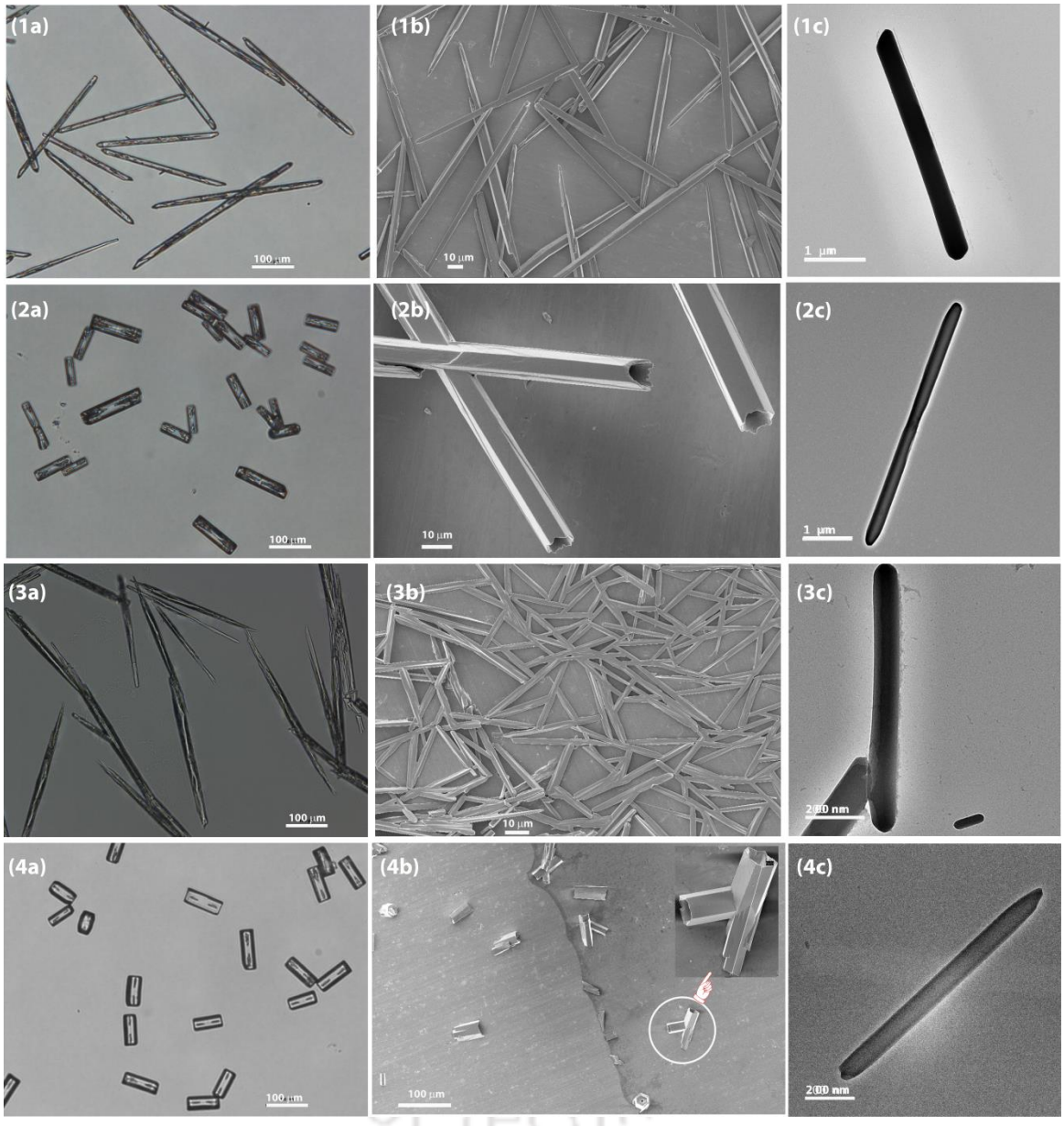

Figure 3.2. *Optical microscopic, FE-SEM and TEM images of self-associated dipeptides (1a), (1b) and (1c) of* ***3A****; (2a), (2b) and (2c) of* ***3B****; (3a), (3b) and (3c) of* ***3C****; and (4a), (4b) and (4c) of* ***3D****, respectively, in 30% acetonitrile-water medium. The self-associated* ***3A*** *and* ***3C*** *exhibited a nanorod structure, but* ***3B*** *and* ***3D*** *exhibited a nano tube-like structure, obtained from above three different types of microscope.*

Next, we performed the AFM experiment to obtain detail topographical information about the above nanostructures. For that, we prepared 30 µM of each peptide solution (diluted from 7 days old 1.5 mM solutions) and dropped cast on a silicon wafer and dried them and then allowed for capturing AFM images. The diameter of nanorod/tubes of peptide **3A, 3B, 3C,** and **3D** are around 0.8, 5.0, 1.2, and 6.0 µm, respectively, obtained from the cross-section area (height to distance profile plot) of AFM images (Figure 3.3).

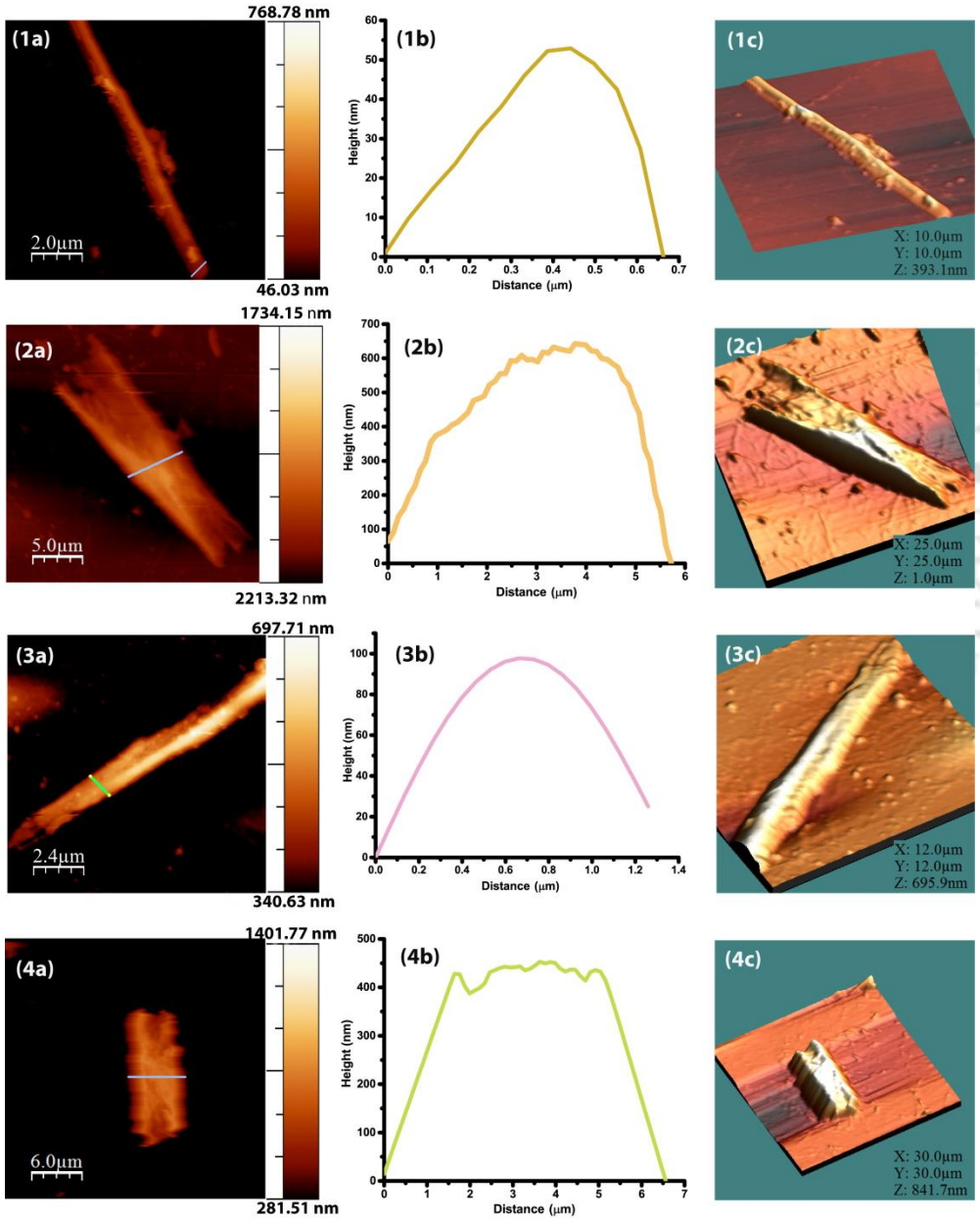

Figure 3.3*. 2D AFM images, height profile plots and 3D AFM images of self-assembled dipeptides (1a), (1b) and (1c) of* ***3A****; (2a), (2b) and (2c) of* ***3B****; (3a), (3b) and (3c) of* ***3C****; and (4a), (4b) and (4c) of* ***3D****, respectively, in 30% acetonitrile-water medium (30 µM)*

3.5. Investigation of self-assembly process by SC-XRD

To obtain more detailed structural information of these peptides, we performed the SC-XRD experiment. Colorless block-shaped crystals of peptide **3A** and **3B** were obtained from water–acetonitrile solution through slow evaporation at room temperature. The crystal structure of **3C** was reported by Jayakumar and co-workers.[5] Moreover, we got a crystal of **3D** but was not able to perform X-ray analysis as the quality of the crystal was not good enough.

Peptide **3A** crystallized in orthorhombic (*P 21 21 21*) space group and adopted three independent molecules (**A**, **B** and **C**) in an asymmetric unit whereas **3B** crystallized in hexagonal (*P 65*) space group and adopted one molecule in an asymmetric unit. The measured backbone torsion angles (Table 1.1) of these peptides suggested that both **3A** and **3B** adopted the twisted β-sheet structure in the crystalline state.

Table 1.1. The measured backbone torsion angles (deg) of **3A** and **3B**

Boc-L-Val-L-Ile-OMe (**3A**)			Torsion angles (deg)	Boc-D-Val-L-Ile-OMe (**3B**)
Molecule A	Molecule B	Molecule C		
C5-N1-C6-C10 = 111(1)	C22-N3-C23-C27 = 87(1)	C39-N5-C40-C44 = 94(1)	*φ1*	C5-N1-C6-C10 = -97(1)
C10-N2-C11-C12 = 65(1)	C27-N4-C28-C29 = 55(1)	C44-N6-C45-C46 = 60(2)	*φ2*	C10-N2-C11-C16 = 151(1)
N1-C6-C10-N2 = -134.7(9)	N3-C23-C27-N4 = -131.4(9)	N5-C40-C44-N6 = -127(1)	*ψ1*	N1-C6-C10-N2 = 125.8(9)
N2-C11-C12-O5 = -144(1)	N4-C28-C29-O10 = -141(1)	N6-C45-C46-O15 = -147(1)	*ψ2*	N2-C11-C16-O5 = 38(2)
O1-C5-N1-C6 = 173.7(9)	O6-C22-N3-C23 = -177.7(9)	O11-C39-N5-C40= 178.9(9)	*ω1*	O1-C5-N1-C6 = -179.7(9)
C6-C10-N2-C11 = -178.3(8)	C23-C27-N4-C28 = 177.2(9)	C40-C44-N6-C45 = 177(1)	*ω2*	C6-C10-N2-C11 = 178.8(9)

In peptide **3A**, the N1H group and O3 of Val (molecule **A**) was intermolecularly hydrogen-bonded to the O7 of urethane and N4H (molecule **B**), respectively. Next, molecule **B** was intermolecularly H-bonded with molecule **C** of **3A,** similarly. As a result, each molecule of **3A** inter-connected to next through two H-bonds and generated a helical assembly along the crystallographic *a*-axis (Figure 3.4b). It also exhibited a helical architecture along the crystallographic *c*-axis in higher-order packing (Figure 3.4c).

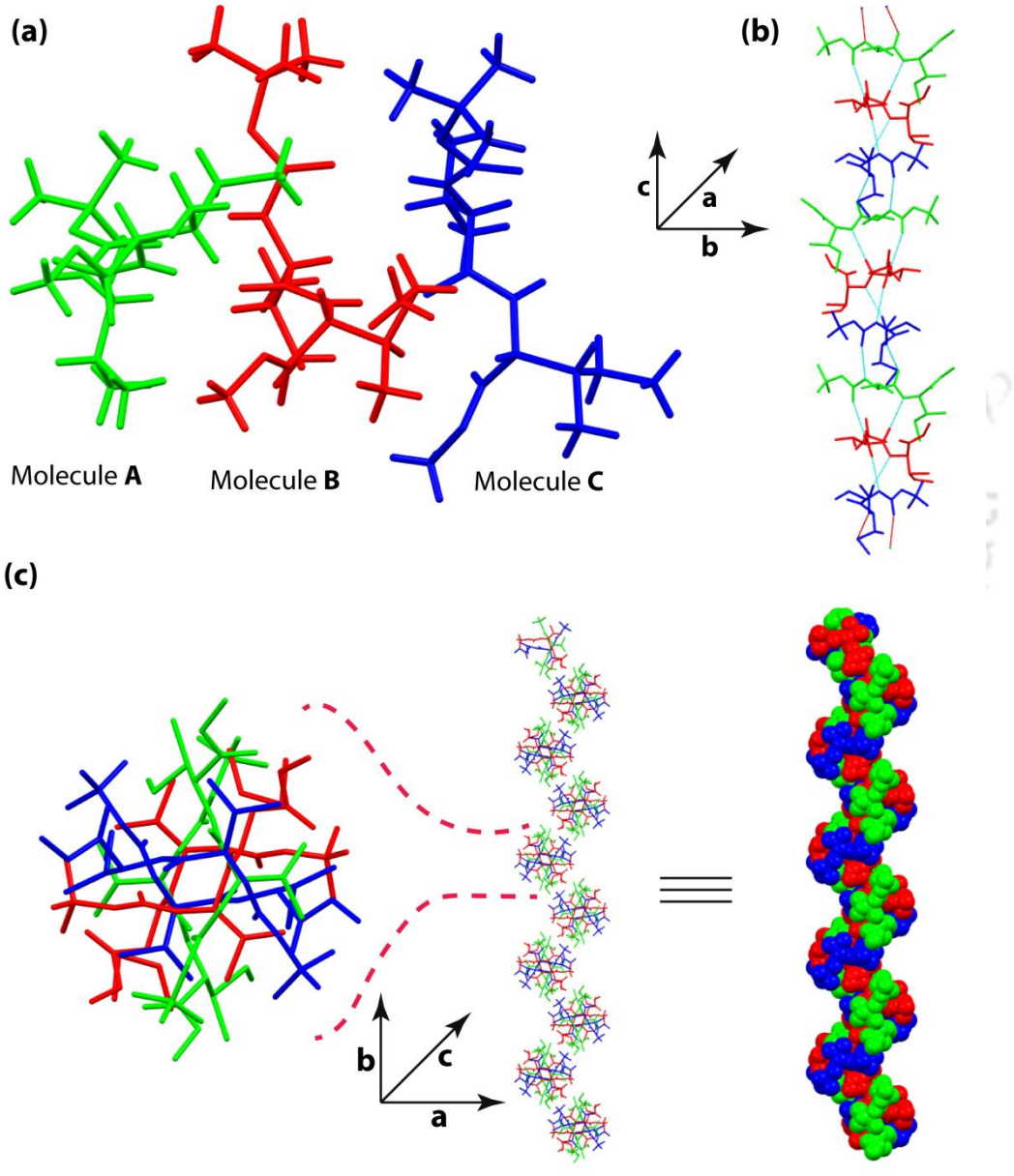

Figure 3.4. *The crystal structure of three molecules in an asymmetric unit (a), the supramolecular helical structure generated through intermolecular H-bond along a axis (b), and the helical structure in higher-order packing along c axis (c) of peptide* ***3A***

On the other hand, the N1H group of urethane and O3 of D-Val were intermolecularly hydrogen-bonded with the next O2 of urethane and N2H of Ile, respectively, in **3B**. A helical structure was produced through the H-bonding along the *a*-direction (Figure 3.5b). Moreover, each molecule of **3B** inter-connected through two H-bonds and generated a hexagonal cylinder-like architecture around the six-fold screw axis along *c*-direction (Figure 3.5c). The diameter of this hollow tube was around 2.5 Å. The reported crystal structure of **3C** also exhibited a helical structure in higher-order packing.[5]

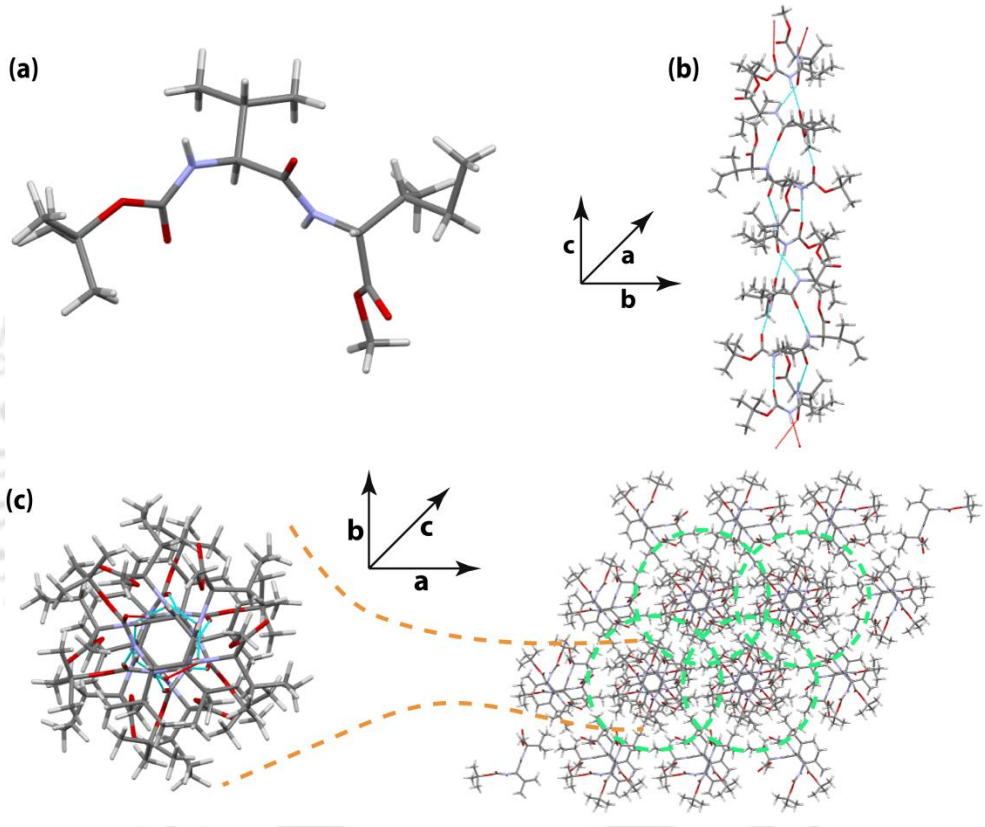

Figure 3.5. *The crystal structure of one molecule in an asymmetric unit (a), the supramolecular helical structure generated through intermolecular H-bond along a axis (b), and the hexagonal cylindrical structure in higher-order packing along c axis (c) of peptide **3B***

Generally, various types of nanostructures are formed from the supramolecular self-assembly of the molecules through various non-covalent interactions, e.g., H-bonding, hydrophobic, and Van der Waals interactions, *etc*. Here, although the self-assembly process of peptides **3A, 3B,** and **3C** are similar due to different packing patterns (Figure 3.4 and 3.5) of **3A** and **3C** from **3B**, their molecular structures are different (rod-like structure of **3A** and **3C** but the hollow tube-like structure of **3B,** Figure 3.2).

3.6. Investigation of self-assembly process by PXRD

Next, we performed a powder XRD experiment to obtain the XRD pattern of nanostructure of those peptides. The 7 days old incubated (37 ^{o}C) samples in 30% acetonitrile-water were freeze-dried and were allowed to XRD pattern analysis from 3-50^{o} of the 2θ range. We observed that the obtained powder XRD pattern from freeze-dried samples and the derived XRD pattern from SC-XRD were similar, which indicated that all peptides in the crystalline state and freeze-dried solid-state adopted similar supramolecular β-sheet structures (Figure 3.6).

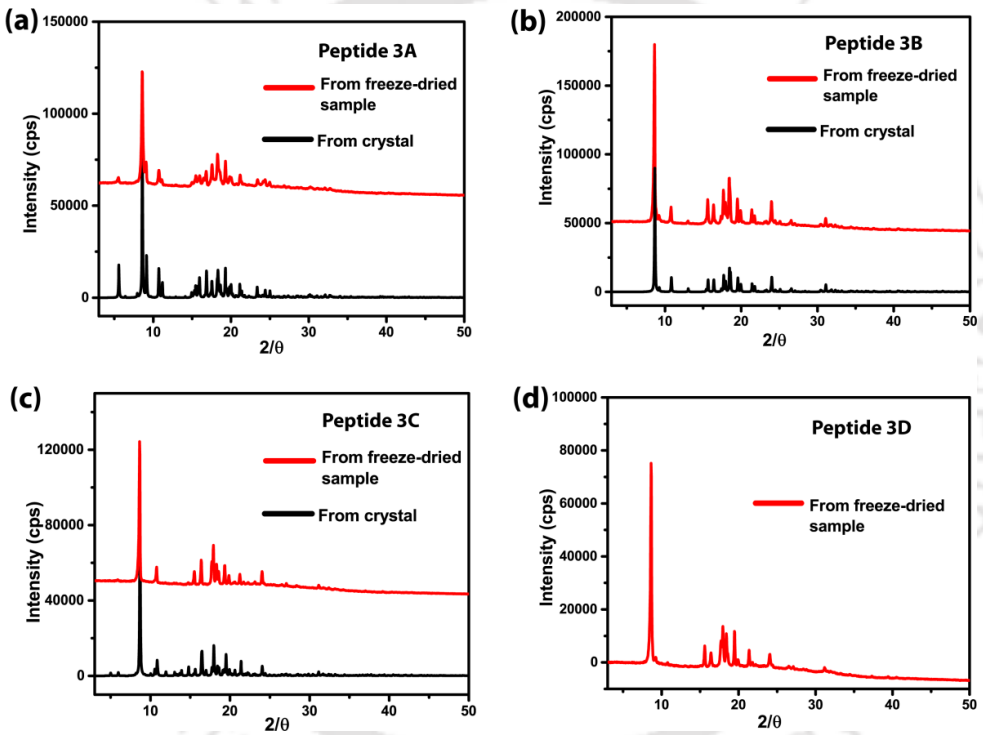

Figure 3.6. *Comparison of powder XRD pattern obtained from freeze-dried samples and SC-XRD of peptides (a)* ***3A****, (b)* ***3B,*** *and (c)* ***3C****. (d) Powder XRD pattern of peptide* ***3D****, obtained from the freeze-dried sample.*

The powder XRD pattern from SC-XRD of **3C** was obtained from reported crystal cif file, published by Jayakumar and coworkers.[5] Although, we were not able to compare the XRD pattern from SC-XRD (as we were not able to mount the crystal) and powder XRD pattern from the freeze-dried sample of **3D**, the obtained pattern indicated that it adopted β-sheet structure.

3.7. Investigation of secondary structure by FT-IR

Next, to investigate the secondary structure of these peptides, we performed the FT-IR experiment of 7 days incubated samples in 30% acetonitrile-water mixture at 37 ^{o}C The obtained asymmetric stretching frequency at 3440 cm$^{-1,}$ and 3337 cm^{-1} of **3A** indicated that all N-Hs were intermolecularly H-bonded. But, in the case of peptide **3B**, **3C,** and **3D,** some N-Hs were intermolecularly H-bonded (3327, 3329, and 3334 cm^{-1}, respectively), and others were not intermolecularly H-bonded (3430, 3432 and 3427 cm^{-1}, respectively). The obtained FT-IR profile exhibited the amide I band at 1649 cm^{-1} of **3A**, at 1645 cm^{-1} of **3B**, at 1648 cm^{-1} of **3C** and **3D,** which suggested that all peptides self-associated to form a β-sheet structure in solution (Figure 3.7).

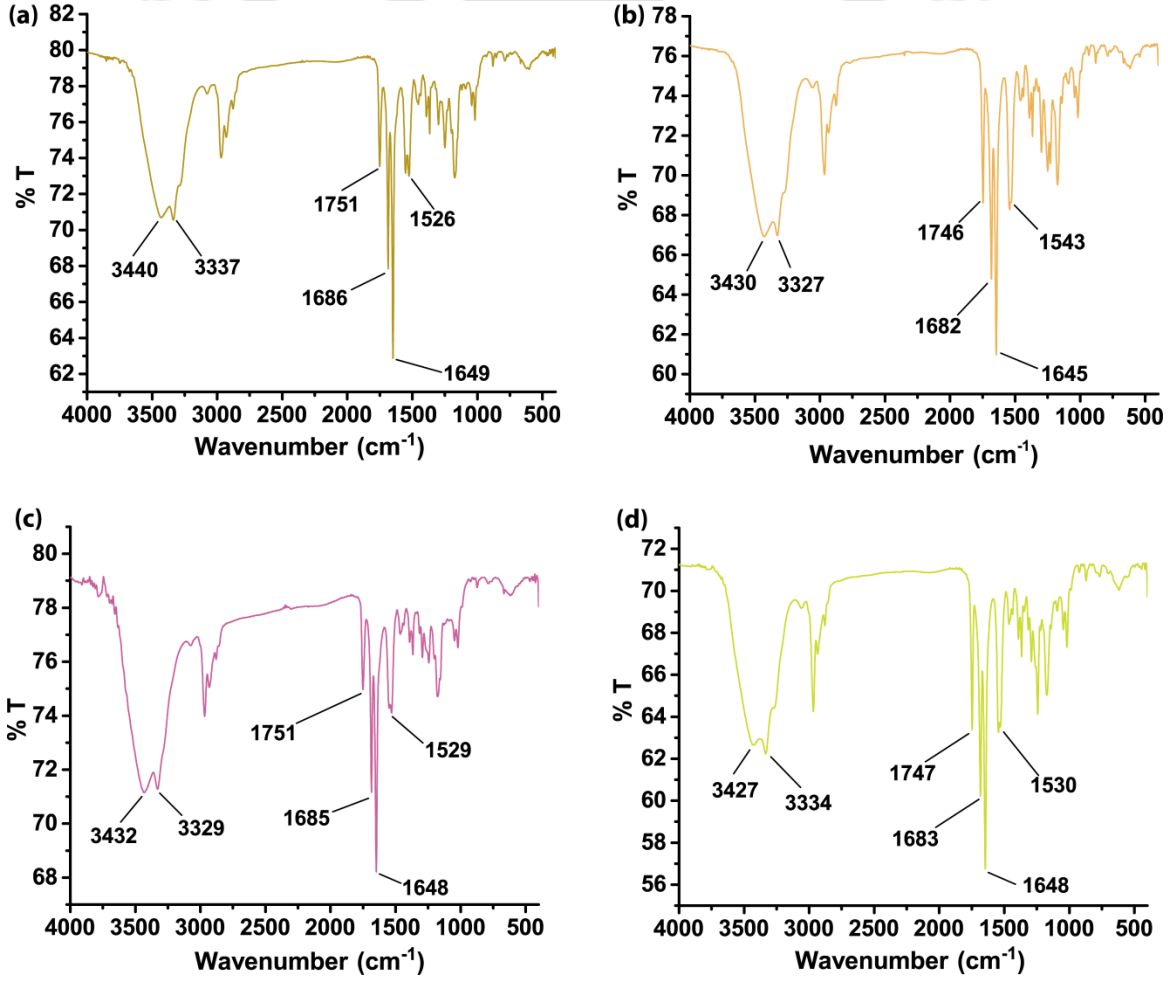

Figure 3.7. *FT-IR spectra of peptide (a)* ***3A****, (b)* ***3B****, (c)* ***3C****, and (d)* ***3D*** *respectively, at 7 days old solution in 30% acetonitrile-water medium*

3.8. Conformation analysis by CD experiment in solution

Next, we performed CD experiments to investigate the conformation of those chiral peptides. Peptide **3A** exhibited a negative Cotton effect at 226 nm and a positive Cotton effect at 204 nm (Figure 3.8, yellow curve), and peptide **3C** showed a negative Cotton effect at 222 nm and a positive Cotton effect at 202 nm (Figure 3.8, violet curve) in 30% acetonitrile-water medium, indicating the formation of supramolecular β-sheet structure. On the other hand, peptide **3B** showed a positive Cotton effect at 217 nm and a negative Cotton effect at 190 nm (Figure 3.8, orange curve), the reverse of peptide **3D** which exhibited a negative Cotton effect at 217 nm and a positive Cotton effect at 191 nm (Figure 3.8, green curve). This might be due to the presence of alternating reverse chirality D/L amino acid in a peptide sequence.[6]

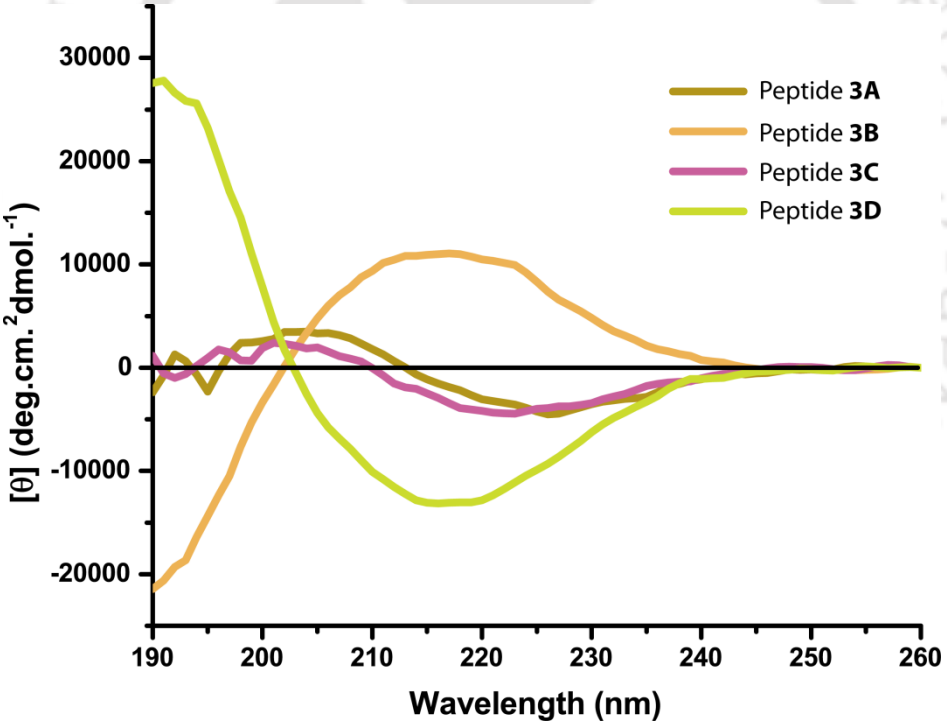

Figure 3.8. *CD spectra of peptide **3A** (yellow curve), **3B** (orange curve), **3C** (violet curve), and **3D** (green curve) in 30% acetonitrile-water medium using concentration of 1.5 mM*

3.9. Investigation of dye binding affinity of these self-aggregated peptides by fluorescence microscope

In chapter 2, we described the dye-binding affinity of both *N*- and *C*- protected two dipeptides, Boc-VV-OMe and Boc-IA-OMe, bearing sequence identity with Alzheimer's $A\beta_{39\text{-}40}$ and $A\beta_{41\text{-}42}$. Herein, we also investigated the binding propensity of Congo red and ThT with self-associated Boc-L-Val-L-Ile-OMe (**3A**) (Figure 3.9, 1a-1d, 1b: Congo red stain, and 1d: ThT stain), bearing sequence homogeneity with $A\beta_{40\text{-}41}$, D/L pair of Boc-D-Val-L-Ile-OMe (**3B**) (Figure 3.9, 2a-2d, 2b: Congo red stain, and 2d: ThT stain), L/L pair of Boc-L-Ile-L-Val-OMe (**3C**) (Figure 3.9, 3a-3d, 3b: Congo red stain, and 3d: ThT stain) and L/D pair of Boc-L-Ile-D-Val-OMe (**3D**) (Figure 3.9, 4a-4d, 4b: Congo red stain, and 4d: ThT stain).

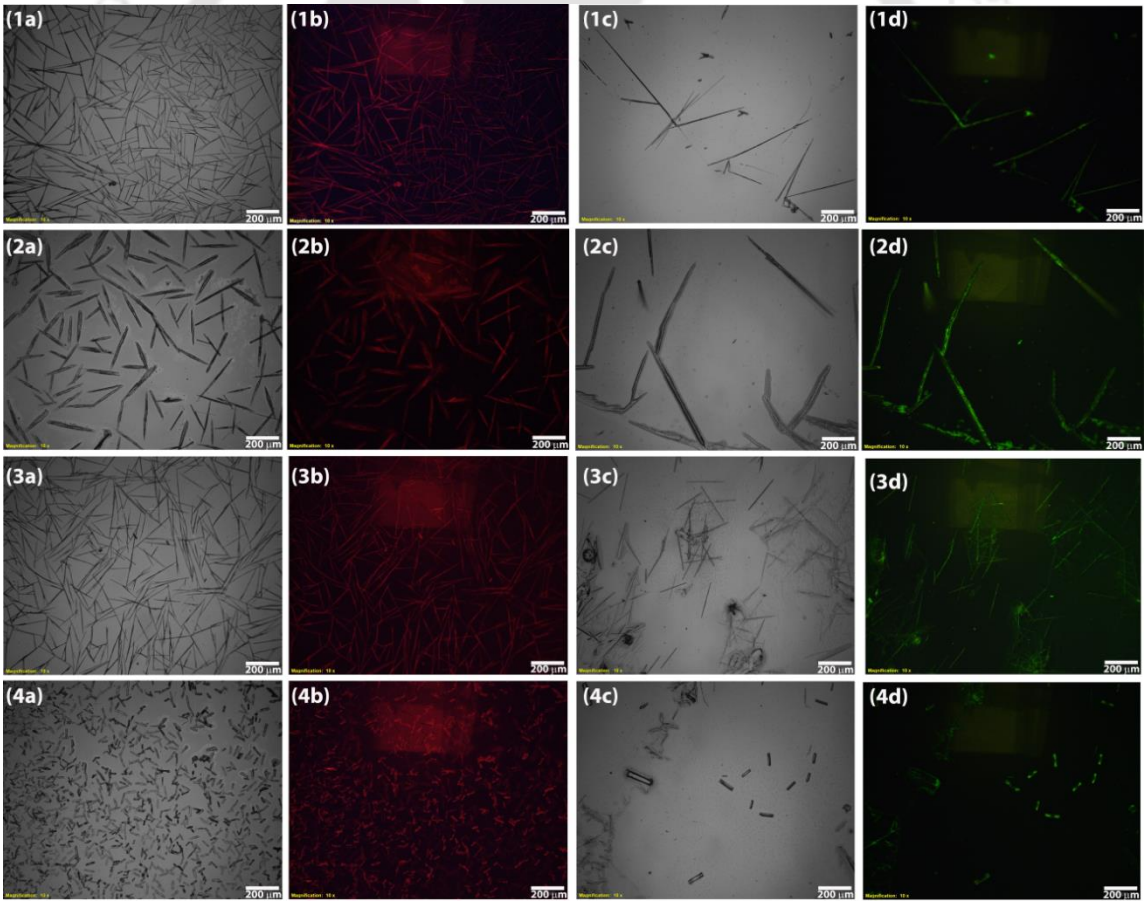

Figure 3.9. *Bright-field and the corresponding fluorescence microscopic images of peptide* ***3A*** *(1a-1d),* ***3B*** *(2a-2d),* ***3C*** *(3a-3d), and* ***3D*** *(4a-4d) stained with Congo red and ThT, respectively.*

The obtained fluorescence microscopic images indicated that all four peptides self-assembled to form a supramolecular parallel β-sheet structure that binds to ThT and Congo red.

3.10. Monitoring the thermal stabilities of the nanostructures

To check the thermal stability of the nanostructures of those peptides in dry conditions, we prepared a 1.5 mM of each peptide samples in 30% acetonitrile-water medium and incubated 7 days at 37 ^{o}C. Then the 7-day old solutions were drop cast (10 µL) on Al-foil separately and kept in a convection oven at a constant temperature of 60 ^{o}C and 100 ^{o}C for 1h. Next, these samples were allowed to capture images under FE-SEM. The obtained images suggested that all peptides nanostructures remained intact at 60 ^{o}C temperature (Figure 3.10). The nanorods of **3A** and **3C** remained similar to their initial structures at 100 ^{o}C (Figure 3.10, 1b and 3b) but nanotubes of **3B** and **3D** showed significance destruction of their structures (Figure 3.10, 2b and 4b) at that temperature, suggested that nanorods were found to be more stable than nanotubes.

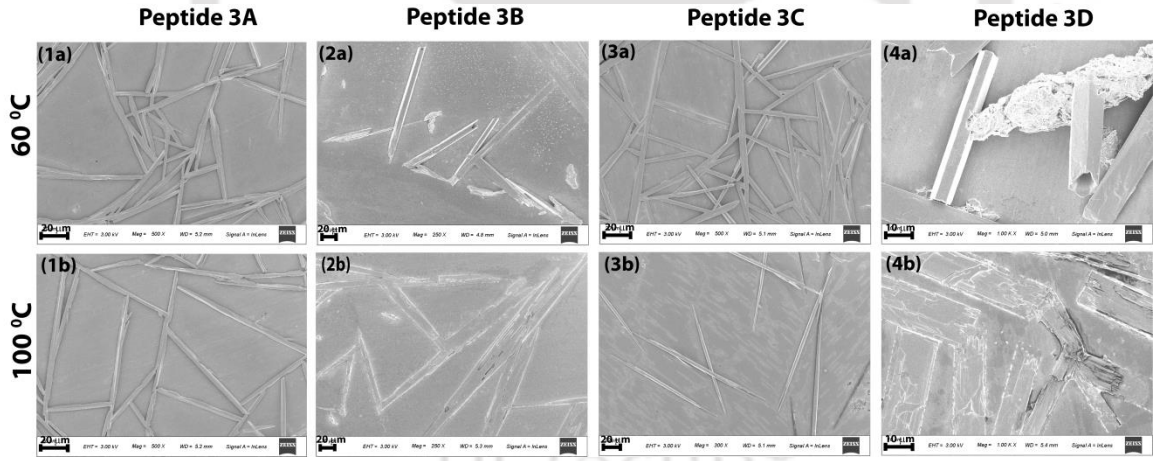

Figure 3.10. *Thermal stability of peptide* ***3A*** *(1a at 60 ^{o}C and 1b at 100 ^{o}C),* ***3B*** *(2a at 60 ^{o}C and 2b at 100 ^{o}C),* ***3C*** *(3a at 60 ^{o}C and 3b at 100 ^{o}C), and* ***3D*** *(4a at 60 ^{o}C and 4b at 100 ^{o}C), obtained from FE-SEM*

3.11. Conclusion

In conclusion, we demonstrated the self-assembly and morphology of both *N*- and *C*-protected alternating L/L or D/L amino acids containing four dipeptides. The obtained microscopic images suggested that they self-assemble to form two different nanostructures, i.e., nanorods and nanotubes. The SC-XRD experiment revealed that peptide **3A** and **3B** adopted twisted β-sheet structure, and each molecule was interconnected through intermolecular H-bond to form a helical assembly. Peptide **3B** also exhibited a hexagonal cylindrical structure in higher-order packing. The previously reported crystal structure of **3C** also showed a helical structure in higher-order packing. Moreover, we got the crystal of **3D** but could not able to X-ray analysis. The formation of different nanostructures may be due to their different higher-order packing association. The obtained nanostructures showed a significant thermal stability, although nanorods were found to be more stable than the nanotubes in dry heating. Interestingly, those nanorods and nanotubes were found to bind with Congo Red and thioflavin T (ThT) dyes[7,] which generally binds to amyloid fibrils.[8] Therefore, this alternating L/L or D/L amino acids containing dipeptides may open up an avenue for application in nanobiotechnology.

3.12. Experimental section

3.12.1. Materials and instrumentations

As described in chapter 8

3.12.2. General procedure for the synthesis of dipeptides

As described in chapter 2 section 2.13.2

3.12.3. Sample preparation

2.9 mM of peptides **3A, 3B, 3C,** and **3D** solutions were prepared in four different Eppendorf vials (2 mL) by adding 1 mL 30% acetonitrile-water solution followed by vortex to get a clear solution. Then, 1 mL (1.5 mM) stock solutions were prepared from the above solutions for each peptide. These stock solutions were incubated 7 days at 37 ^{o}C on a water bath. After 7 days, we prepared the FT-IR, CD, FE-SEM, TEM, AFM, and Microscopic slid samples.

3.13. Characterization data

Boc-L-Val-L-Ile-OMe 3A.

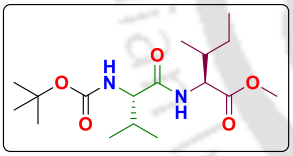

White solid, (270 mg, 85%), mp 141-144^{o}C, ^{1}H NMR ($CDCl_3$; 600 MHz) δ 0.92-0.87 (9H, m); 0.95-0.94 (3H, d, *J* = 6.6 Hz); 1.20-1.13 (1H, m); 1.42 (9H, s); 1.93-1.88 (2H, br); 2.10-2.09 (1H, br); 3.71 (3H, s); 3.91-3.88 (1H, t, *J* = 7.8 Hz); 4.57-4.55 (1H, dd, *J* = 5.4 Hz, *J* = 3 Hz), 5.08 (1H, brs); 6.45 (1H, brs). ^{13}C NMR ($CDCl_3$; 150 MHz) δ 11.6, 15.5, 18.0, 19.4, 25.2, 28.4, 30.8, 37.9, 52.2, 56.5, 60.2, 80.0, 156.0, 171.6, 172.3. HRMS (ESI): calculated $[M+H]^+$ 345.2391, found m/z . 345.2597, HPLC: retention time (t_R) = 5.55 min.

Boc-D-Val-L-Ile-OMe 3B.

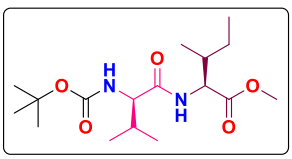

White solid, (267 mg, 84%) mp 103-106^{o}C, ^{1}H NMR ($CDCl_3$; 600 MHz) δ 0.92-0.90 (9H, m); 0.98-0.97 (3H, d, *J* = 6.6 Hz); 1.20-1.13 (1H, m); 1.44 (9H, s); 1.93-1.89 (1H, m); 2.22-2.17 (1H, m), 3.73 (3H, s); 4.00 (1H, br); 4.60-4.58 (1H, dd, *J* = 4.8 Hz, *J* = 3.6 Hz), 5.09 (1H, brs); 6.61 (1H, brs). ^{13}C NMR ($CDCl_3$; 150 MHz) δ 11.6, 15.6, 17.6,19.5, 25.2, 28.4,

30.8, 37.9, 52.3, 56.4, 60.0, 80.1, 155.9, 171.5, 172.4. HRMS (ESI): calculated $[M+H]^+$ 345.2391, found m/z . 345.2524, HPLC: retention time (t_R) = 5.55 min.

Boc-L-Ile-L-Val-OMe 3C.

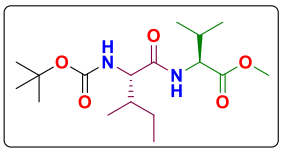

White solid, (241 mg, 81%) mp 165-167°C, ^{1}H NMR ($CDCl_3$; 600 MHz) δ 0.94-0.90 (12H, m); 1.19-1.12 (1H, m); 1.44 (9H, s); 1.87 (1H, br); 2.20-2.15 (1H, m); 3.73 (3H, s); 3.95-3.93 (1H, t, *J* = 7.8 Hz); 4.55-4.53 (1H, dd, *J* = 4.8 Hz, *J* = 3.6 Hz), 5.05-5.04 (1H, d, *J* = 8.4 Hz); 6.39-6.37 (1H, d, *J* = 7.2 Hz). ^{13}C NMR ($CDCl_3$; 150 MHz) δ 11.3, 15.4, 17.7, 18.9, 24.7, 28.2, 31.2, 36.9, 52.1, 57.0, 59.3, 79.9, 155.8, 171.6, 172.1. HRMS (ESI): calculated $[M+H]^+$ 345.2391, found m/z . 345.2392, HPLC: retention time (t_R) = 5.49 min.

Boc-L-Ile-D-Val-OMe 3D.

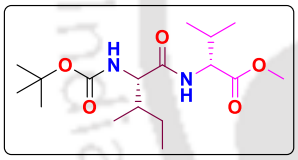

White solid, (238 mg, 80%), mp 122-124°C,^{1}H NMR ($CDCl_3$; 600 MHz) δ 0.96-0.89 (12H, m); 1.16-1.08 (1H, m); 1.45 (9H, s); 1.96-1.92 (1H, m); 2.21-2.16 (1H, m); 3.74 (3H, s); 4.03 (1H, brs); 4.57-4.54 (1H, dd, *J* = 4.8 Hz, *J* = 4.2 Hz), 5.02 (1H, brs); 6.52-6.50 (1H, d, *J* = 8.4 Hz). ^{13}C NMR ($CDCl_3$; 150 MHz) δ 11.4, 15.4, 17.5, 19.3, 25.0, 28.2, 30.7, 37.7, 52.1, 56.3, 59.8, 79.9, 155.8, 171.4, 172.3. HRMS (ESI): calculated $[M+H]^+$ 345.2391, found m/z . 345.2391, HPLC: retention time (t_R) = 5.56 min.

3.14. References

1. Zhang, S. Designer self-assembling peptide nanofiber scaffolds for study of 3-D cell biology and beyond. *Adv. Cancer Res.* **2008**, *99*, 335-362.
2. Maji, S. K.; Schubert, D.; Rivier, C.; Lee, S.; Rivier, J. E.; Riek, R. Amyloid as a depot for the formulation of long-acting drugs. *PLoS Biol.* **2008**, *6*, e17.
3. Zhao, F.; Ma, M. L.; Xu, B. Molecular hydrogels of therapeutic agents. *Chem. Soc. Rev.* **2009**, *38*, 883-891.
4. Granja, J. R.; Ghadiri, M. R. Channel-mediated transport of glucose across lipid bilayers. *J. Am. Chem. Soc.* **1994**, *116*, 10785-10786.
5. Sukumar, N.; Sony, S. M. M.; Ponnuswamy, M. N.; Jayakumar, R. Crystal Structure and Conformation of N-(tButoxycarbonyl)-L-Isoleucyl-L-Valine Methyl Ester (Boc-Ile-Val-OMe). *Mol. Cryst. Liq. Cryst.* **2005**, *428*, 77–85.
6. Marchesan, S.; Styan, K. E.; Easton, C. D.; Waddington, L.; Vargiu, A. V. Higher and lower supramolecular orders for the design of self-assembled heterochiral tripeptide hydrogel biomaterials. *J. Mater. Chem. B* **2015**, *3*, 8123-8132.
7. C. Subbalakshmi, P. Basak, and R. Nagaraj, Self-assembly of t-butyloxycarbonyl protected dipeptide methyl esters composed of leucine, isoleucine, and valine into highly organized structures from alcohol and aqueous alcohol mixtures. *Biopolymers 2017*; *108*, 1-14.
8. Paul, A. Nadimpally, K. C.; Mondal, T.; Thalluri, K.; Mandal, B. Inhibition of Alzheimer's amyloid-β peptide aggregation and its disruption by a conformationally restricted α/β hybrid peptide. *Chem. Commun*, **2015**, *51*, 2245–2248.

3.15. Selected spectra

3.15.1. Spectra of peptide 3A

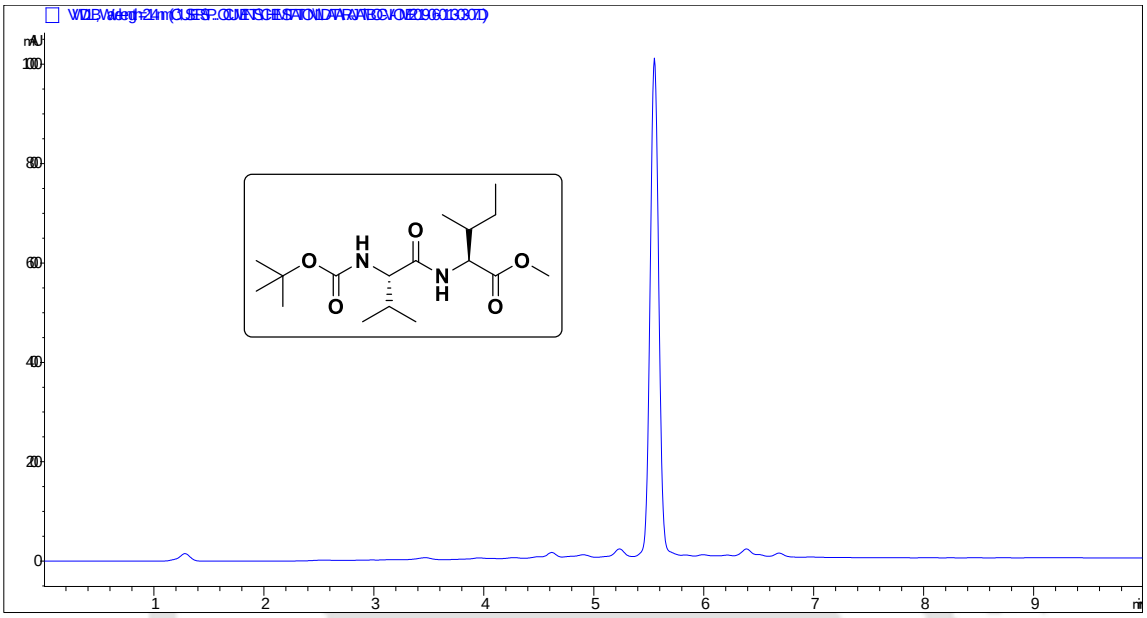

Figure 3.11. *HPLC profile picture of purified peptide* ***3A*** *(A linear gradient was used from 5-95% acetonitrile till 5 min and a total run time of 10 min with a flow rate 1 mLmin^{-1})*

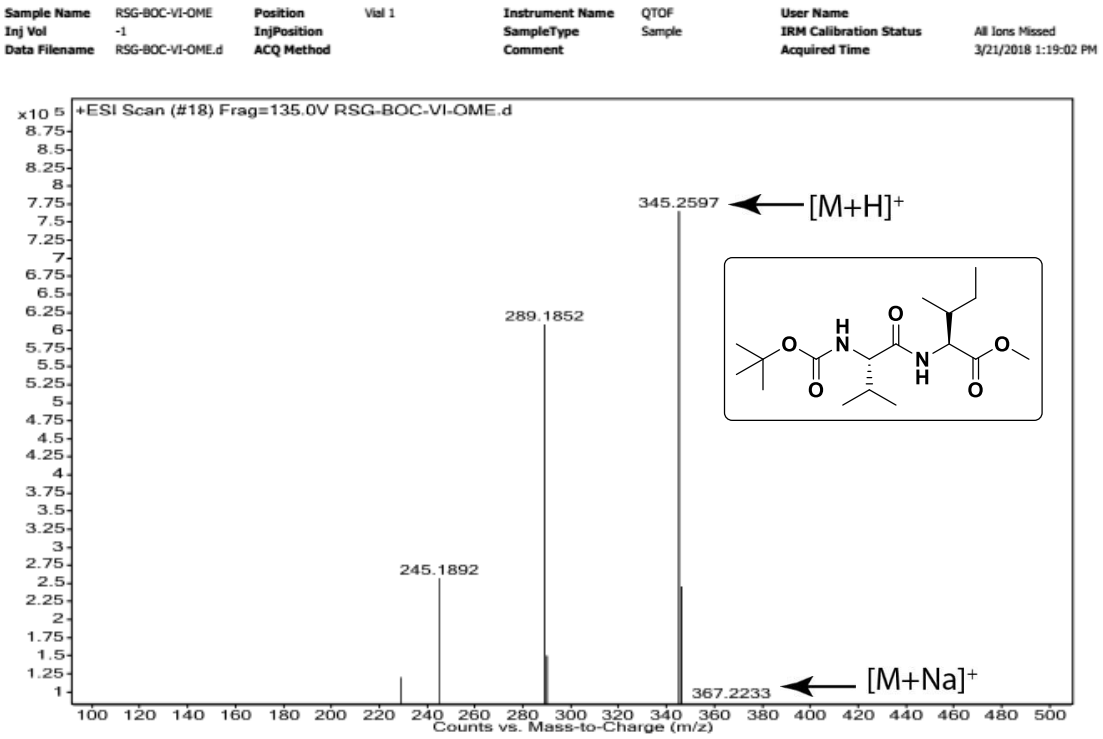

Figure 3.12. *MS spectra of peptide* ***3A***

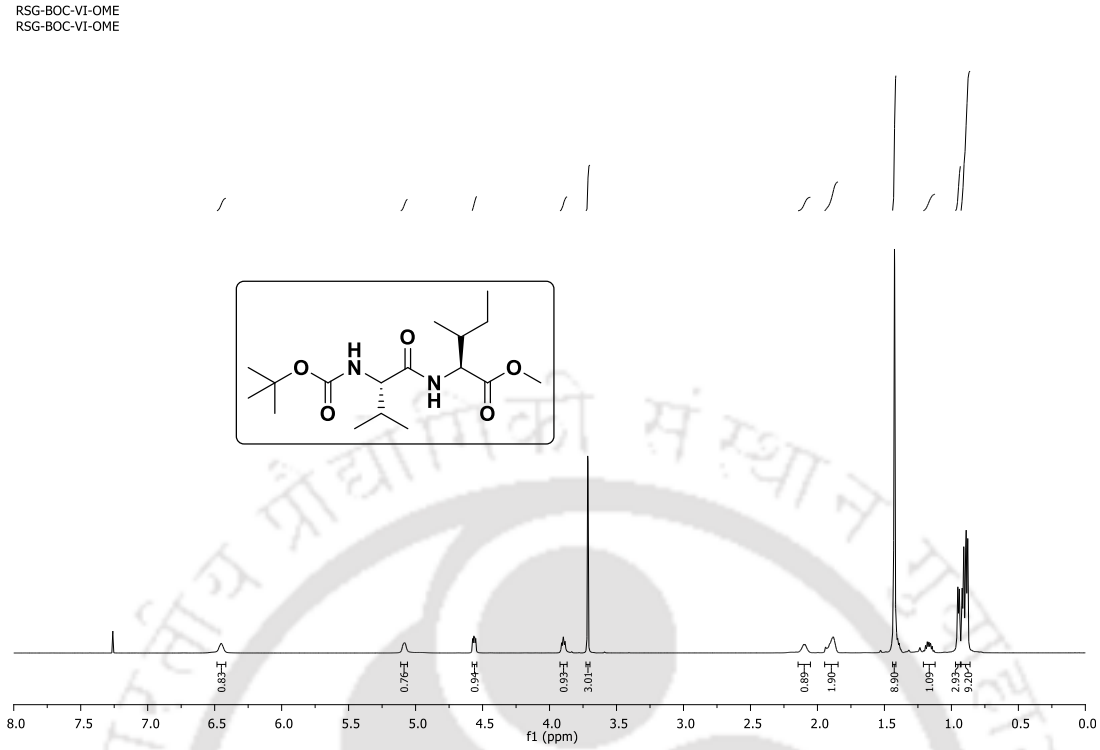

Figure 3.13. *^{1}H NMR spectra of peptide* ***3A***

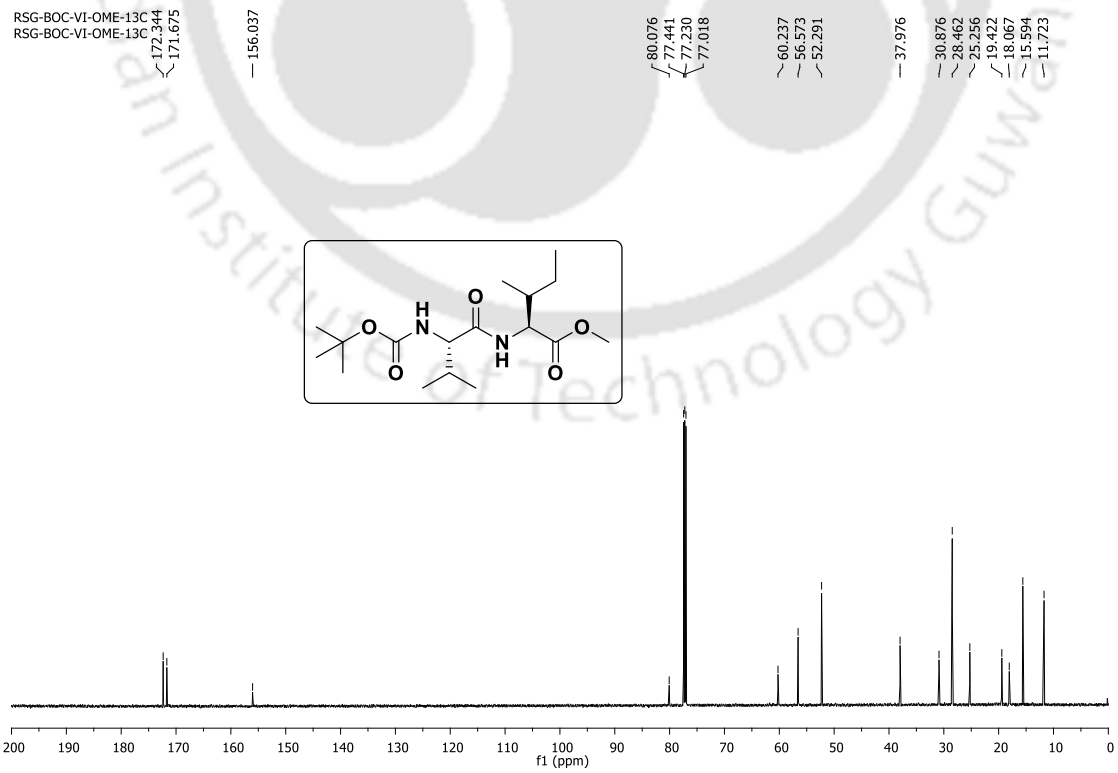

Figure 3.14. *^{13}C NMR spectra of peptide* ***3A***

3.15.2. Spectra of peptide 3B

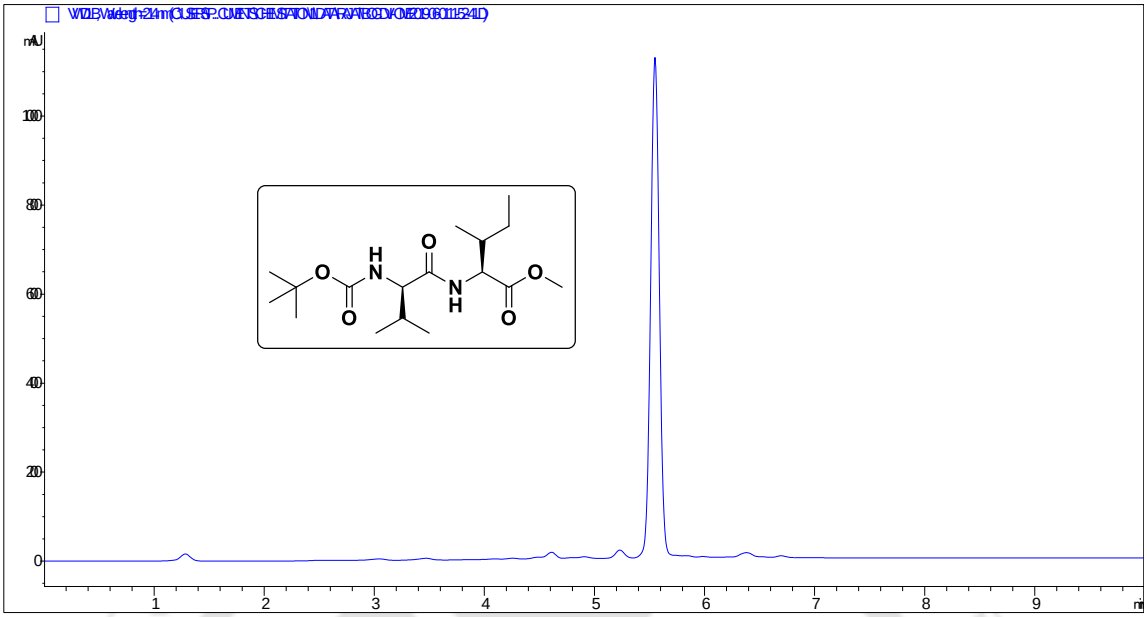

Figure 3.15. *HPLC profile picture of purified peptide* ***3B****(A linear gradient was used from 5-95% acetonitrile till 5 min and a total run time of 10 min with a flow rate 1 mLmin^{-1})*

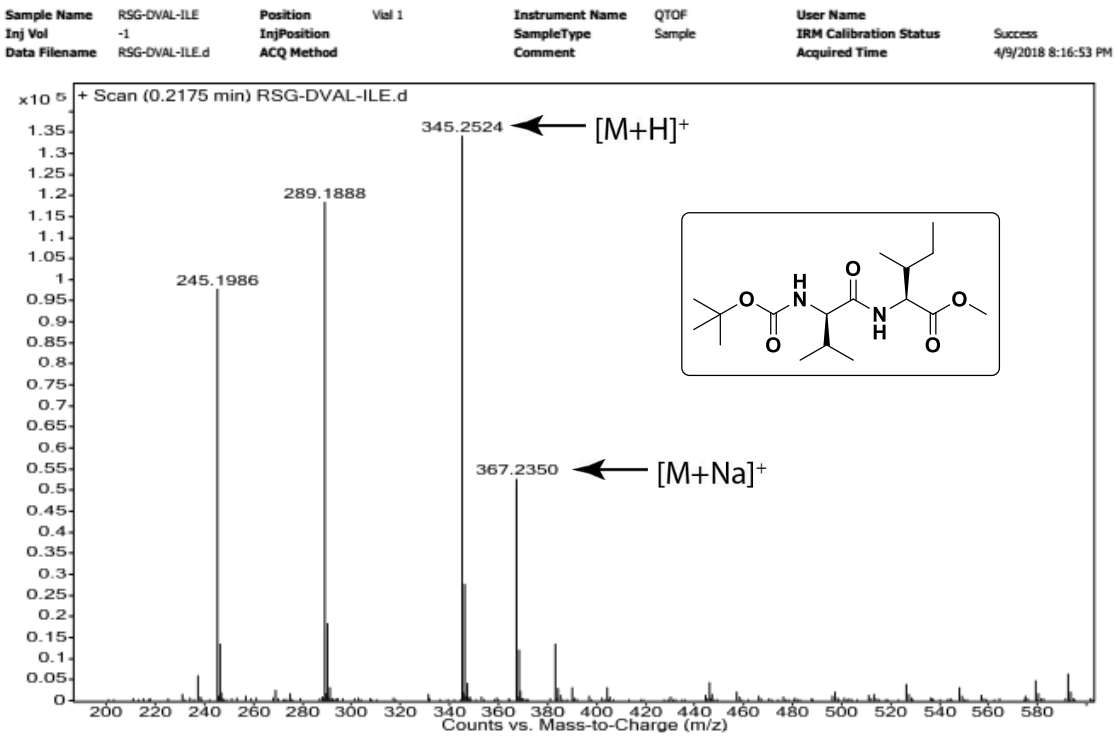

Figure 3.16. *MS spectra of peptide* ***3B***

RSG-BOC-DVAL-ILE-OME-1H
RSG-BOC-DVAL-ILE-OME-1H

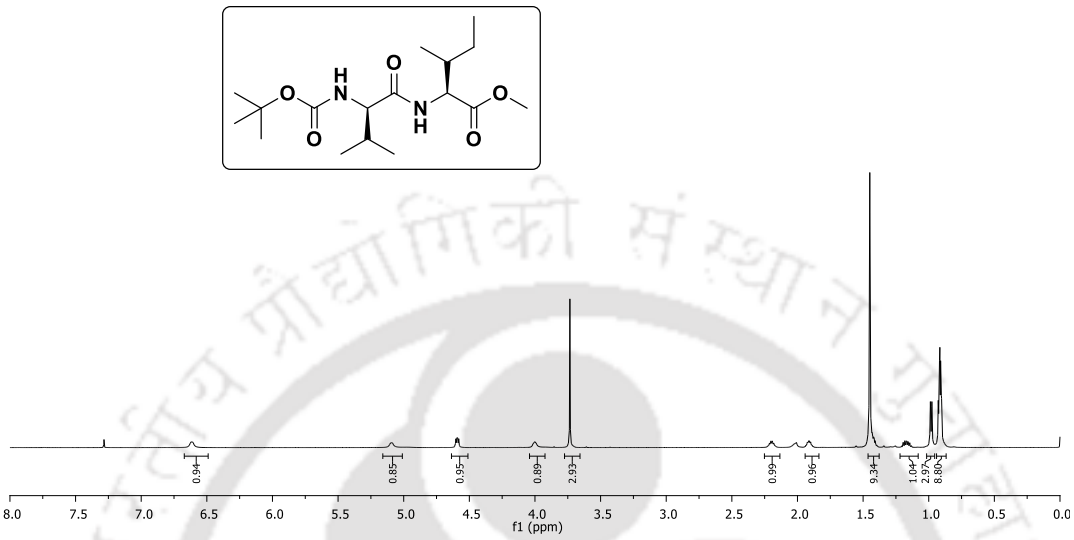

Figure 3.17. *^{1}H NMR spectra of peptide **3B***

RSG-BOC-DVAL-ILE-OME-13C
RSG-BOC-DVAL-ILE-OME-13C

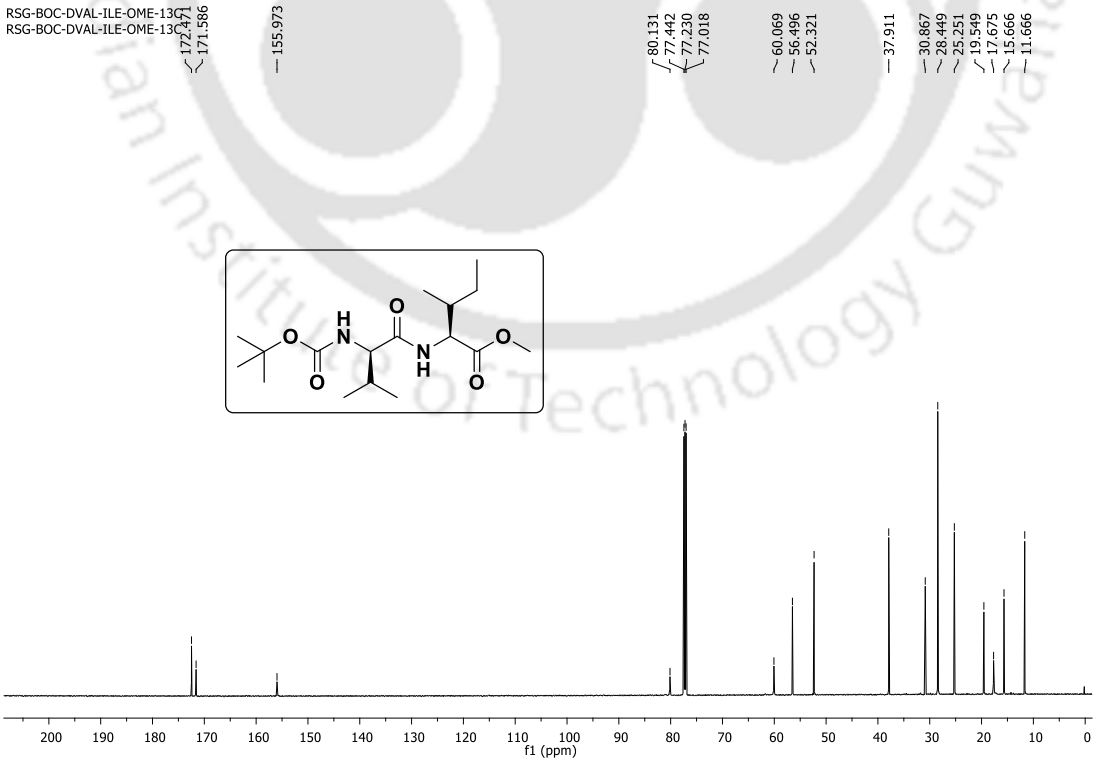

Figure 3.18. *^{13}C NMR spectra of peptide **3B***

3.15.3. Spectra of peptide 3C

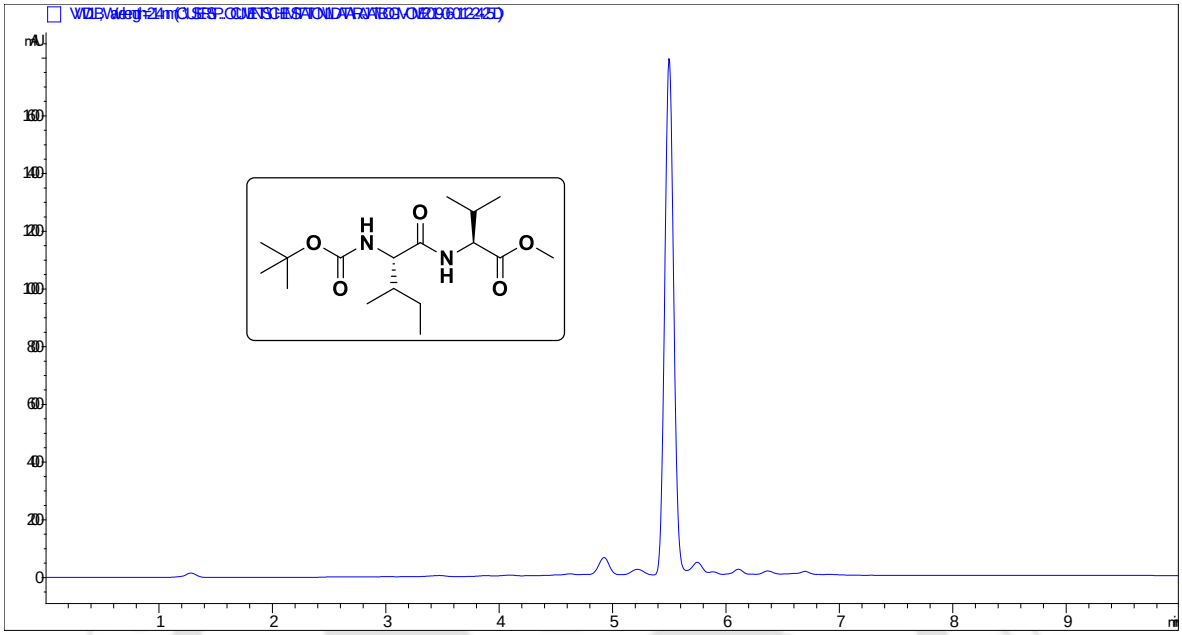

Figure 3.19. *HPLC profile picture of purified peptide* ***3C*** *(A linear gradient was used from 5-95% acetonitrile till 5 min and a total run time of 10 min with a flow rate 1 mLmin^{-1})*

Sample Name	SAMPLE 1	**Position**	P1-D1	**Instrument Name**	Instrument 1	**User Name**	
Inj Vol	20	**InjPosition**		**SampleType**	Sample	**IRM Calibration Status**	Success
Data Filename	RSG-IV-OME.d	**ACQ Method**	ESI ALS 100-500.m	**Comment**		**Acquired Time**	12/24/2018 5:19:34 PM

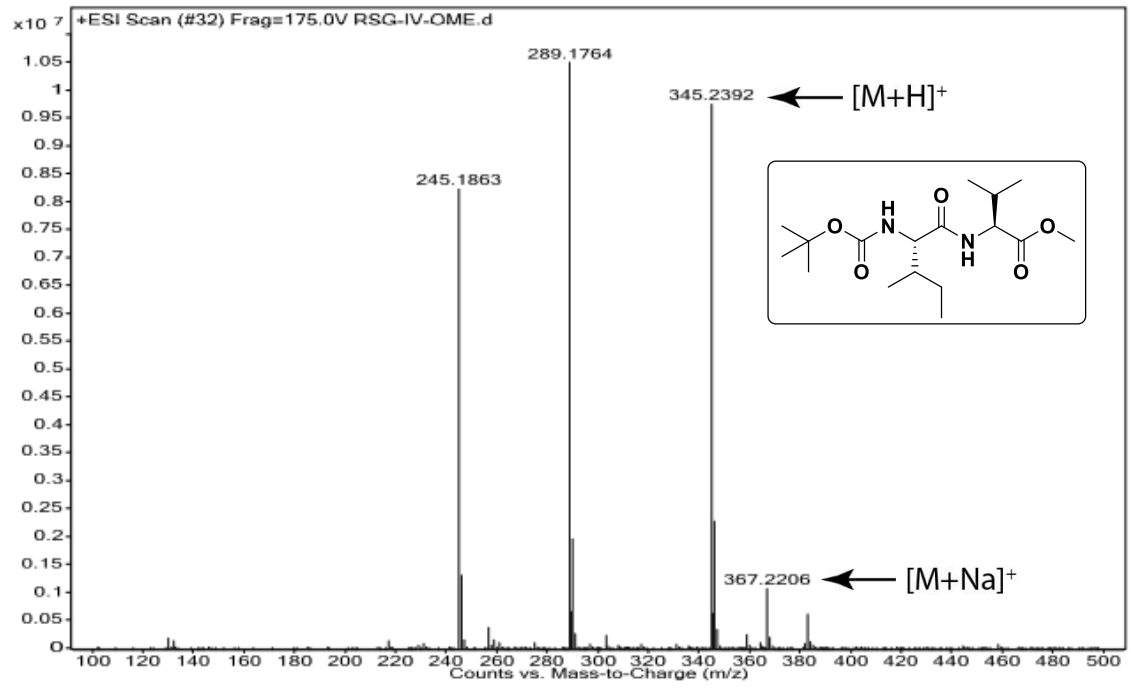

Figure 3.20. *MS spectra of peptide* ***3C***

RSG-BOC-IV-OME-1H
RSG-BOC-IV-OME-1H

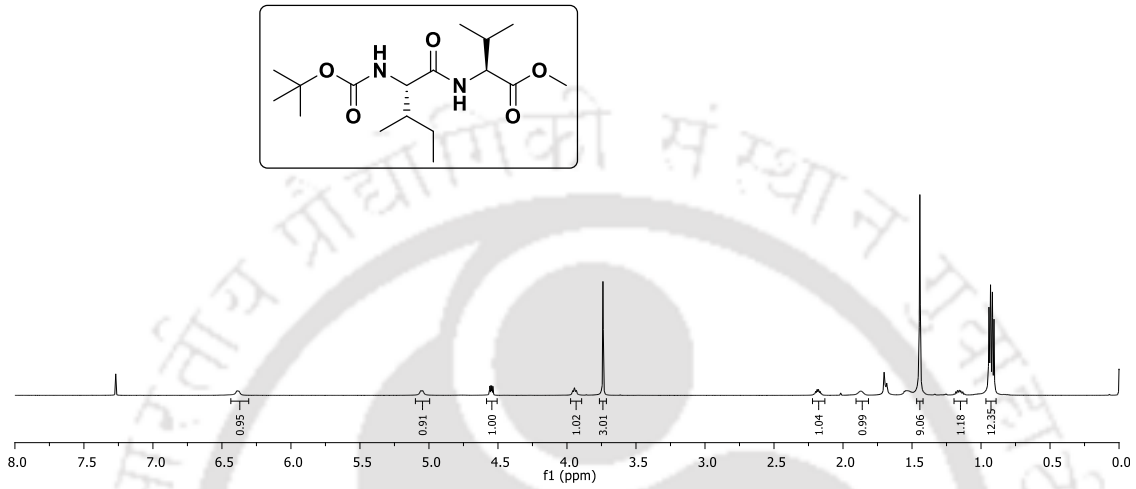

Figure 3.21. *^{1}H NMR spectra of peptide **3C***

RSG-BOC-ILE-VAL-OME-13C
RSG-BOC-ILE-VAL-OME-13C

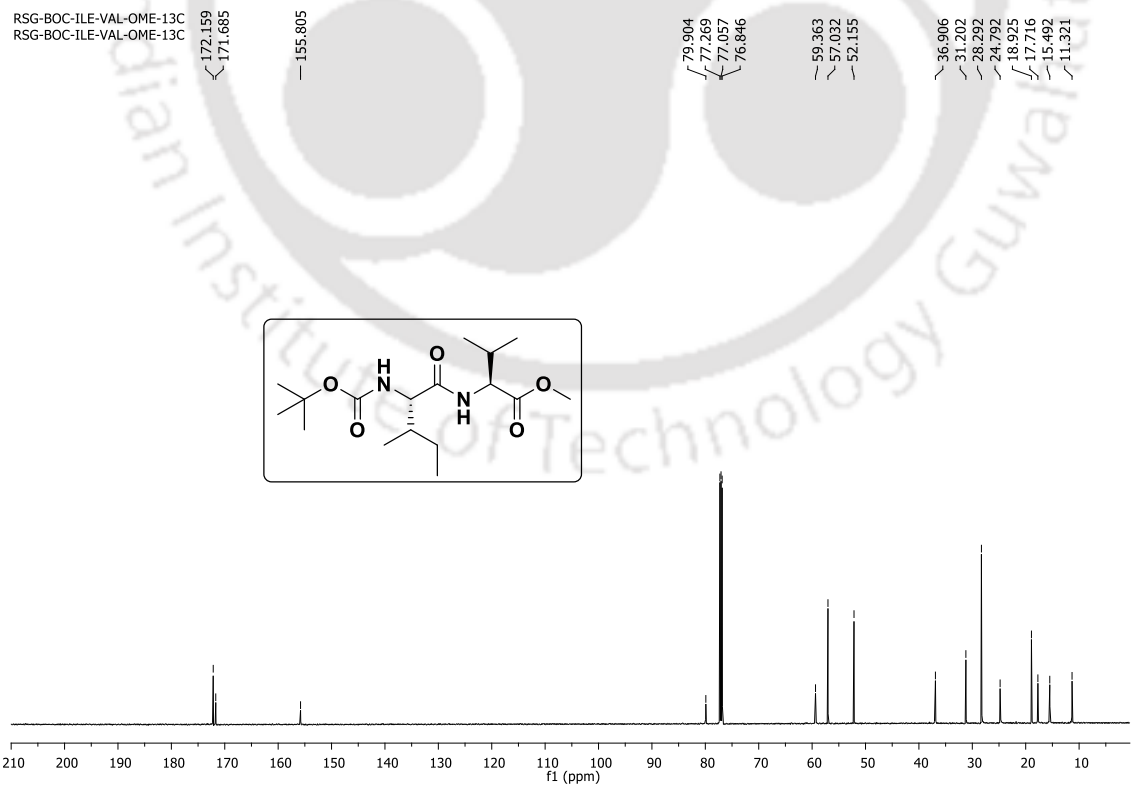

Figure 3.22. *^{13}C NMR spectra of peptide **3C***

3.15.4. Spectra of peptide 3D

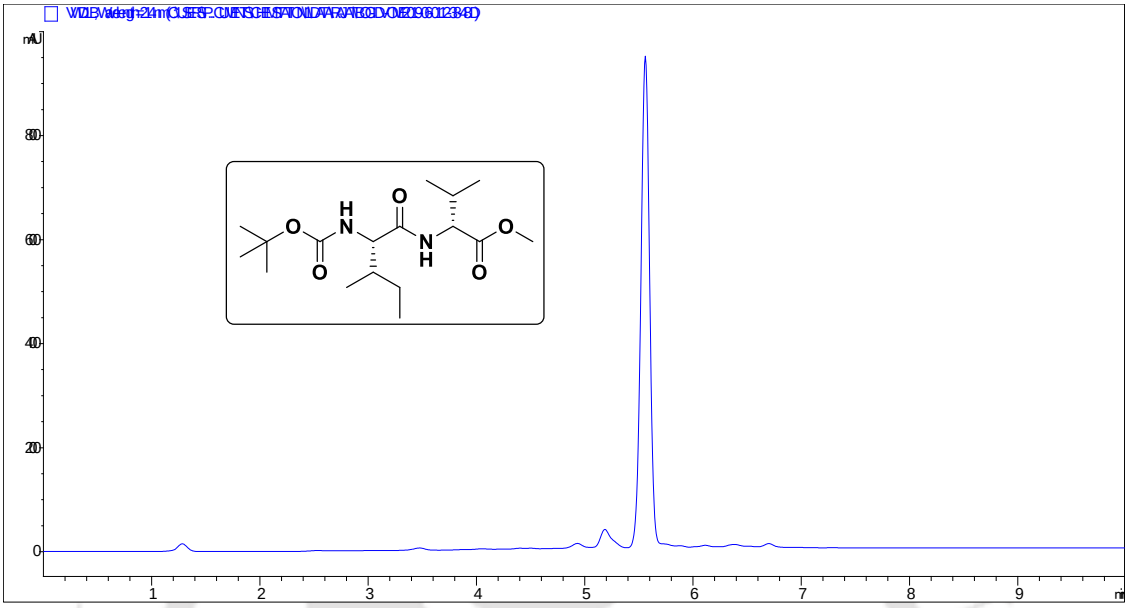

Figure 3.23. *HPLC profile picture of purified peptide* ***3D*** *(A linear gradient was used from 5-95% acetonitrile till 5 min and a total run time of 10 min with a flow rate 1 mLmin^{-1})*

Sample Name	SAMPLE 2	**Position**	P1-D2	**Instrument Name**	Instrument 1	**User Name**	
Inj Vol	20	**InjPosition**		**SampleType**	Sample	**IRM Calibration Status**	Success
Data Filename	RSG-IDV-OME.d	**ACQ Method**	ESI ALS 100-500.m	**Comment**		**Acquired Time**	12/24/2018 5:21:29 PM

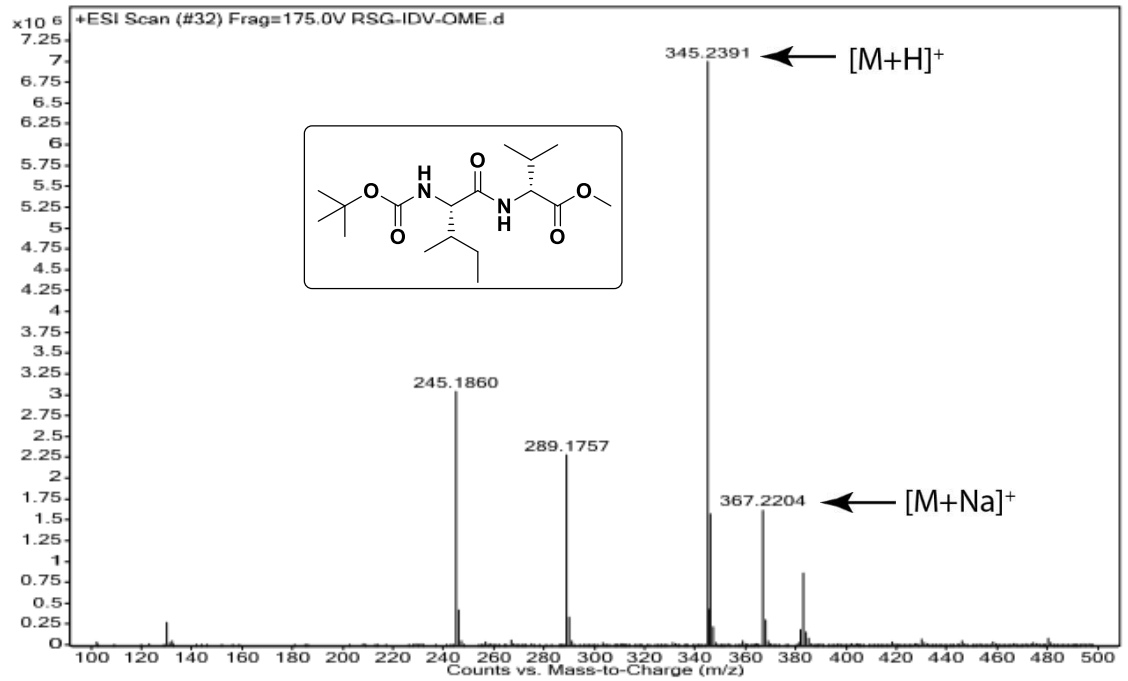

Figure 3.24. *MS spectra of peptide* ***3D***

RSG-BOC-IDV-OME-1H
RSG-BOC-IDV-OME-1H

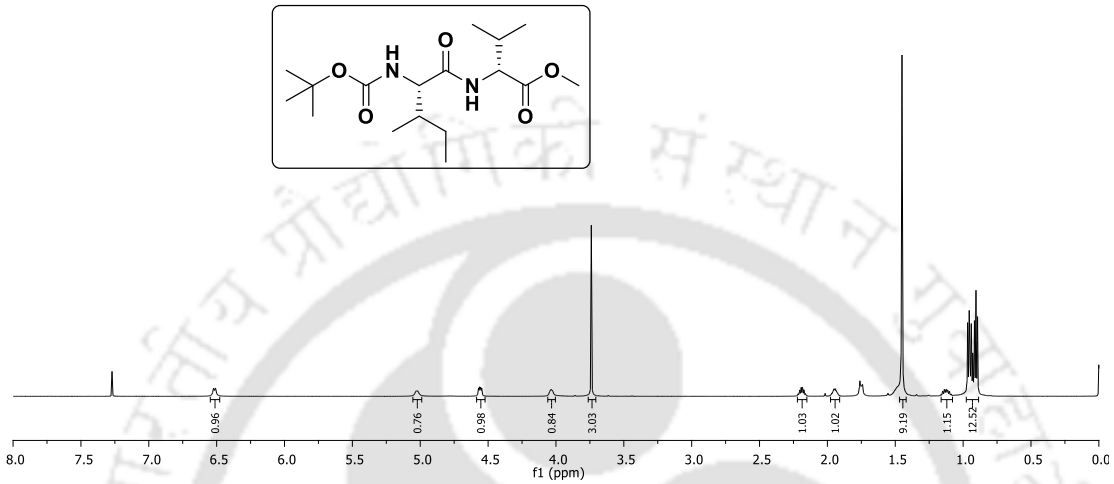

Figure 3.25. *^{1}H NMR spectra of peptide* ***3D***

RSG-BOC-ILE-DVAL-OME-13C
RSG-BOC-ILE-DVAL-OME-13C
172.306
171.426
155.808
79.955
77.274
77.062
76.850
59.895
56.327
52.147
37.732
30.710
28.279
25.081
19.376
17.503
15.494
11.488

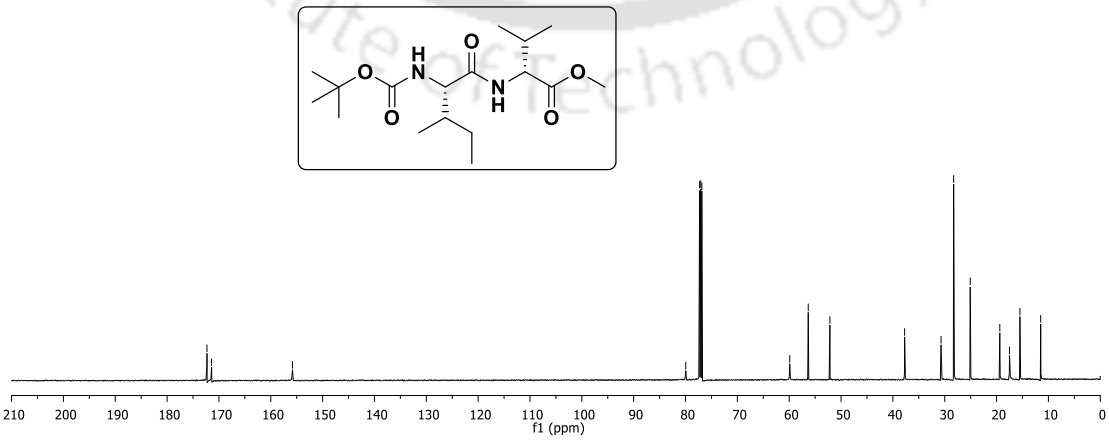

Figure 3.26. *^{13}C NMR spectra of peptide* ***3D***

3.16. Crystallographic data

Table 3.2. Hydrogen bonding distances (Å) and Bond angles (deg) of peptide **3A** and **3B**

Molecule	***D−H···A***	***d(D···H) /Å***	***d(H···A)/Å***	***d(D···A)/Å***	***<D−H···A/°***
Boc-L-Val-L-Ile-OMe (**3A**)	N1-H1N···O12	0.86	2.22	3.0151(6)	153
	N2-H2N···O8	0.86	1.99	2.8498(6)	174
	N3-H3N···O2	0.86	2.15	2.9901(6)	166
	N4-H4N···O13	0.86	1.99	2.8479(6)	174
	N5-H5N···O7	0.86	2.14	2.9860(6)	168
	N2-H2N···O8	0.86	2.07	2.9105(6)	167
	C40-H40···O3	0.98	2.55	3.3853(7)	143
Boc-D-Val-L-Ile-OMe (**3B**)	N1-H1···O2	0.86	2.08	2.9245(2)	169
	N2-H2···O3	0.86	2.07	2.8919(2)	161
	C6-H6···O3	0.98	2.48	3.3245(2)	144

Table 3.3. Crystal parameters and refinement data of **3A** and **3B**

Parameters	***Boc-L-Val-L-Ile-OMe(3A)***	***Boc-D-Val-L-Ile-OMe (3B)***
Formula	C_{17} H_{32} N_2 O_5	C_{17} H_{32} N_2 O_5
Fw	344.45	344.45
Crystal system	orthorhombic	hexagonal
Space group	*P 21 21 21*	*P 65*
a/Å	12.126(2)	11.7586(8)
b/Å	19.317(4)	11.7586(8)
c/Å	27.605(2)	27.2132(11)
α/°	90.00	90.00
β/°	90.00	90.00
γ/°	90.00	120.00
V/Å^3	6466.1(18)	3258.5(5)
Z	12	6
D_c/g cm^{-3}	1.061	1.053
μ Mo K_α/mm^{-1}	0.077	0.077
F000	2256.0	1128.0
T/K	293(2)	293(2)
θ max.	25.000	25.000
Total no. of reflections	18388	7384
Independent reflections	10758	3132
Observed reflections	3988	1907
Parameters refined	674	226
R_1, I > 2σ(I)	0.0947	0.0736
wR_2, I > 2σ(I)	0.1888	0.1834
GOF (F^2)	1.081	1.013
CCDC No.	1903663	1903664

Chapter 4

The Supramolecular Helical Self-Association of Two Designed Tripeptides

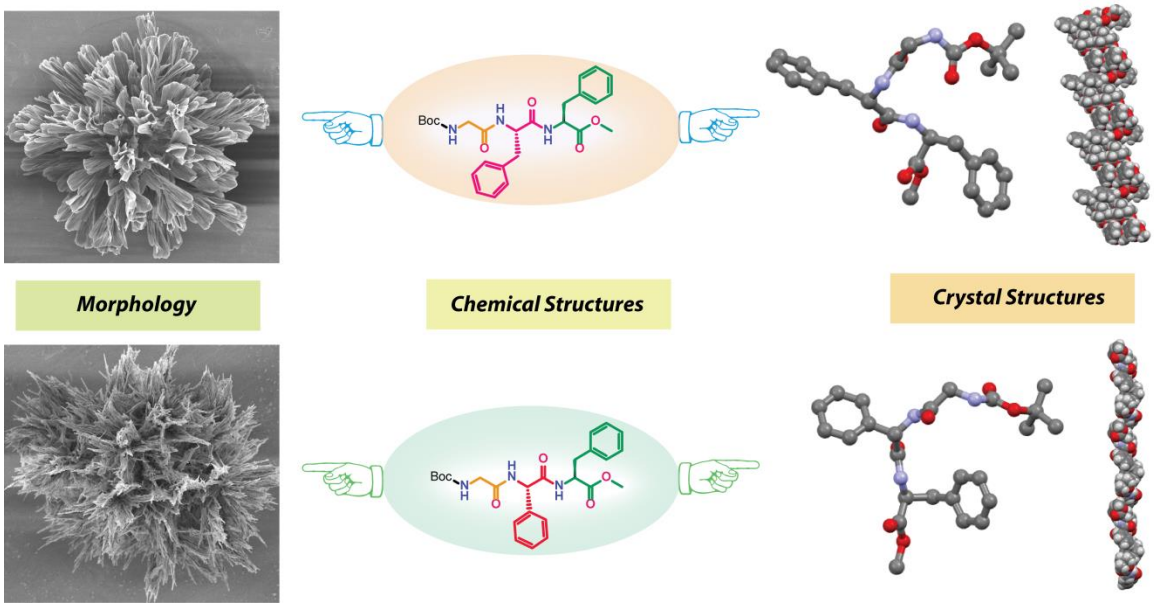

4.1. Background

Nature achieves a wide range of helical structures, e.g., α-helix of protein,[1] single-stranded helical RNA,[2] double-stranded helices of DNA,[3] and triple-stranded collagen helix[4]. They play an essential role in the biological system. Scientists are trying to mimic the peptide-based helical structures by incorporating various natural or unnatural amino acids in the peptide sequence. Mostly, the reported peptide-based helical assemblies are constructed by the incorporation of pre-organized kink forming moieties such as proline or Aib (Chapter 1, section 1.7). Therefore, the generation of helical structures from without pre-organized kink moieties is challenging.

4.2. Design of peptides

To develop the *de novo* designed helical peptides, we first designed both *N*- and *C*-protected tripeptides Boc-Gly-Phe-Phe-OMe (**4A**) and its analog Boc-Gly-Phg-Phe-OMe (**4B**, Figure 4. 1). In peptide **4B**, *N*-terminal Phe (phenylalanine) is replaced by Phg (phenylglycine), which is a non-proteinogenic amino acid, and it has one methylene group (–CH_2–) less in the side chain than that of Phe.

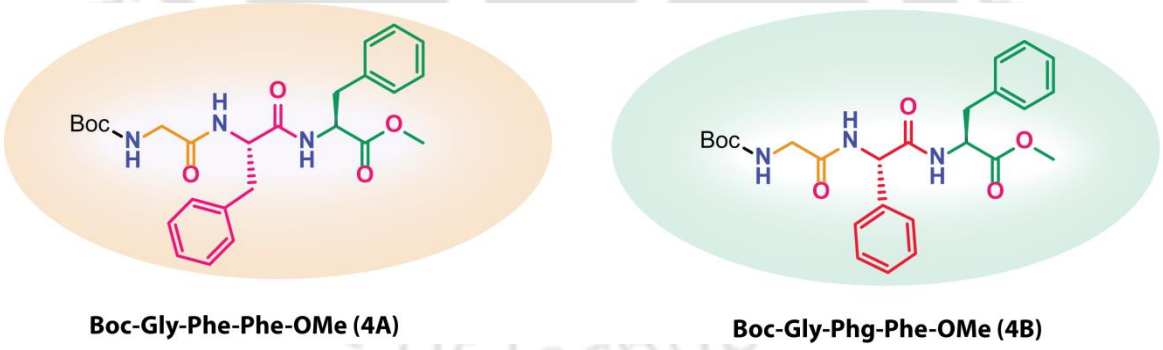

Figure 4.1. *The chemical structures of tripeptides* ***4A*** *and* ***4B****.*

4.3. Synthesis and characterization of the designed peptides

We have synthesized the mentioned peptides by using the standard conventional coupling method in solution. The detailed synthetic procedure is described in section 4.12.2. The synthetic scheme is depicted in scheme 4.1. The designed peptides were purified by silica

gel column chromatography, and purity was checked by analytical HPLC. The purified peptides were characterized by mass spectrometry and 1D [^{1}H] and 2D [^{1}H, ^{1}H] NMR spectroscopy. The characterization data and spectra for the synthesized peptides are shown in section 4.13 and 4.15, respectively.

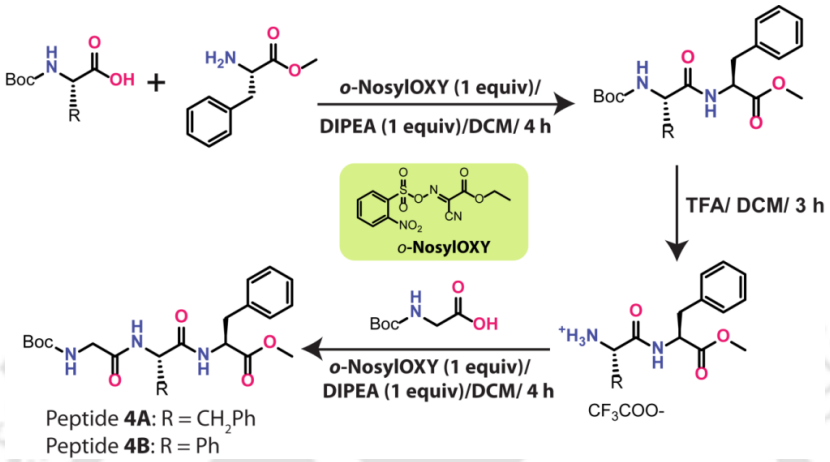

Scheme 4.1. *Schematic representation of peptide synthesis in solution.*

4.4. Investigation of self-assembly process by SC-XRD

To obtain detailed structural information of these peptides, we performed the SC-XRD experiment. Colorless block-shaped monoclinic ($P2_1$) crystals (Figure 4.2) of peptide **4A** and **4B** were grown from acetonitrile-water solution by slow evaporation at room temperature.

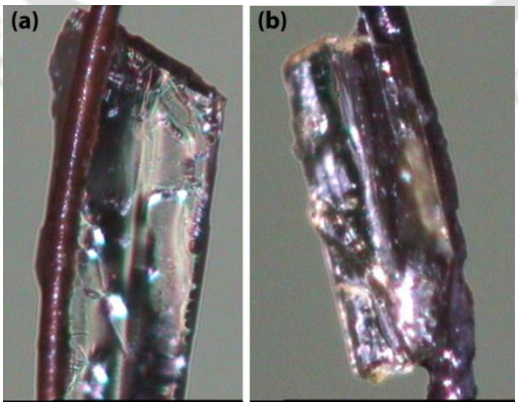

Figure 4.2. *The crystal structures of tripeptides (a)* ***4A*** *and (b)* ***4B****.*

The measured backbone torsion angles ($\varphi 1$ = −56.1, $\psi 1$ = 145.8 and $\varphi 2$ = 59.8, $\psi 2$ = 29.7, Table 4.1) indicated that **4A** adopts a conformation similar to the type II β-turn but slightly deviated from the ideal values ($\varphi 1$ = −60, $\psi 1$ = 120 and $\varphi 2$ = 80, $\psi 2$ = 0) of the type II β-turn. Although no intramolecular (4 → 1) H-bond between *i* (Boc-CO) and *i* + *3* (NH of Phe 2) was observed (Figure 4.3a), the distance between them, *i.e.*, N3···O2 and O2···H3N hydrogen bond distances, was 3.24 and 2.58 Å, respectively, which were close to the standard 10-membered intramolecular hydrogen-bonded type II β-turn tripeptide (N···O = 3.15 Å and O···HN = 2.35 Å). Most interestingly, such distorted type II β-turns without intramolecular H-bonding are known as open turn structure.

Table 4.1. The measured backbone torsion angles (deg) of **4A** and **4B**

Boc-Gly-Phe-Phe-OMe (**4A**)	Torsion angles (deg)	Boc-Gly-Phg-Phe-OMe (**4B**)
C5-N1-C6-C7 = -56.1(8)	$\varphi 1$	C5-N1-C6-C7 = 126.2(3)
C7-N2-C8-C16 = 59.8(7)	$\varphi 2$	C7-N2-C8-C15 = -127.6(3)
C16-N3-C17-C25 = -51.6(7)	$\varphi 3$	C15-N3-C16-C24 = -159.9(3)
N1-C6-C7-N2 = 145.8(5)	$\psi 1$	N1-C6-C7-N2 = -121.4(3)
N2-C8-C16-N3 = 29.7(8)	$\psi 2$	N2-C8-C15-N3 = 124.4(3)
N3-C17-C25-O6 = 136.4(5)	$\psi 3$	N3-C16-C24-O6 = -179.0(3)
O1-C5-N1-C6 = 175.2(5)	$\omega 1$	O1-C5-N1-C6 = -177.7(3)
C6-C7-N2-C8 = 178.1(5)	$\omega 2$	C6-C7-N2-C8 = 178.1(3)
C8-C16-N3-C17 = 172.0(5)	$\omega 3$	C8-C15-N3-C16 = -175.9(3)

There are four intermolecular H-bonds, *i.e.*, two N1–H1···O3 and two N2–H2···O4, in **4A** (Table 4.6, section 4.16). One β-turn subunit of **4A** is connected through N2–H2···O4 in a parallel manner and through N1–H1···O3 in an anti-parallel manner (Figure 4.3b) along

the *b*-axis. Next, it self-organized to form a supramolecular herringbone-like helical architecture in higher-order packing through intermolecular C–H···O interaction along the *c*-axis (Fig. 4.3c).

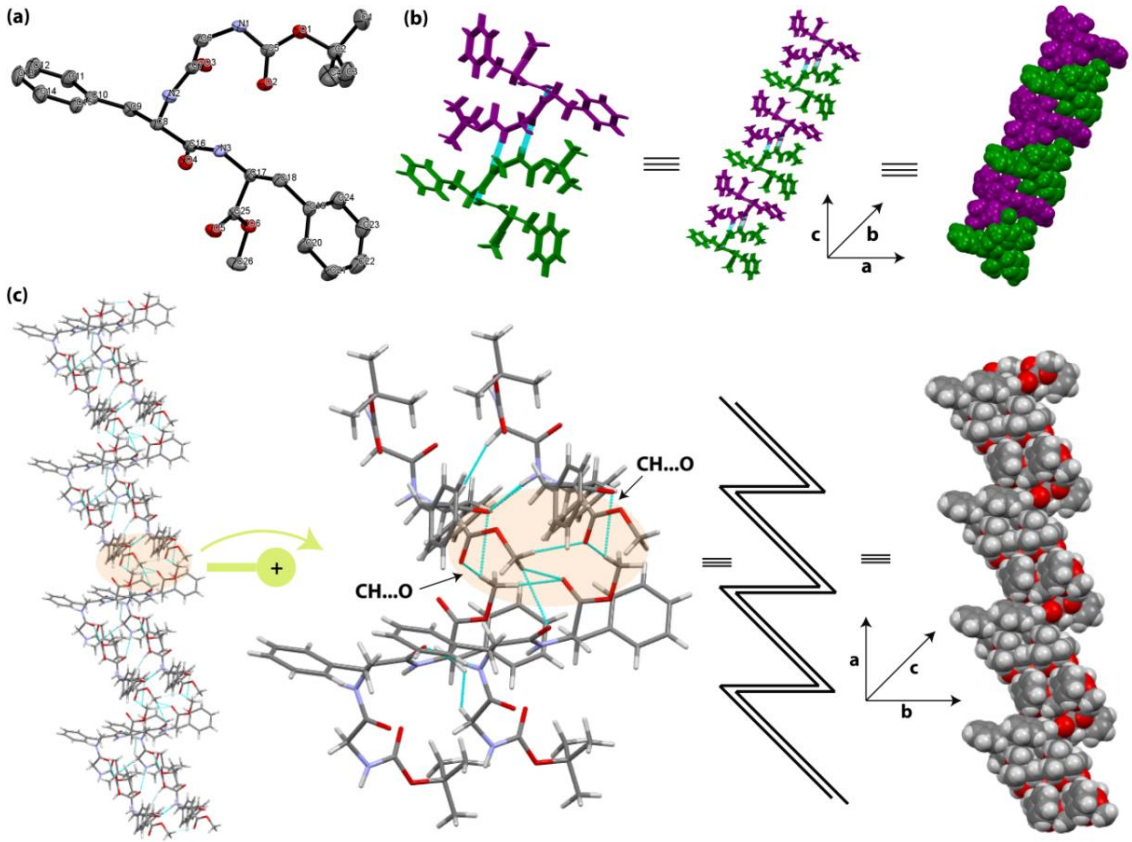

Figure 4.3. *(a) The ORTEP diagram with an ellipsoid of 30% probability, (b) intermolecular H-bonding structure along the b-axis, and (c) herringbone helical architecture in the higher-order assembly along the c-axis of peptide* ***4A.***

On the other hand, **4B** adopted a parallel β-sheet (Figure 4.4a) structure, confirmed by measured backbone torsion angles (Table 4.1) in the crystalline state. The presence of Phg instead of Phe in **4B** extended the backbone, unlike **4A**. It contained two N1–H1···O2 and two N2–H2···O3 intermolecular H-bonds (Table 4.6, section 4.16), and each subunit of **4B** is connected through those bonds to form a supramolecular β-sheet structure with a meridional distance of 4.97 Å along the *b*-axis (Figure 4.4b). They also further self-assembled to form a helical structure through intermolecular C–H···O and C–H···π interactions in higher-order packing (Figure 4.4c) along the crystallographic *c*-axis. The

bond distance of C–H···O and C–H···π was 2.62 Å and 2.88 Å, respectively. The crystallographic data are displayed in Table 4.7 (section 4.16).

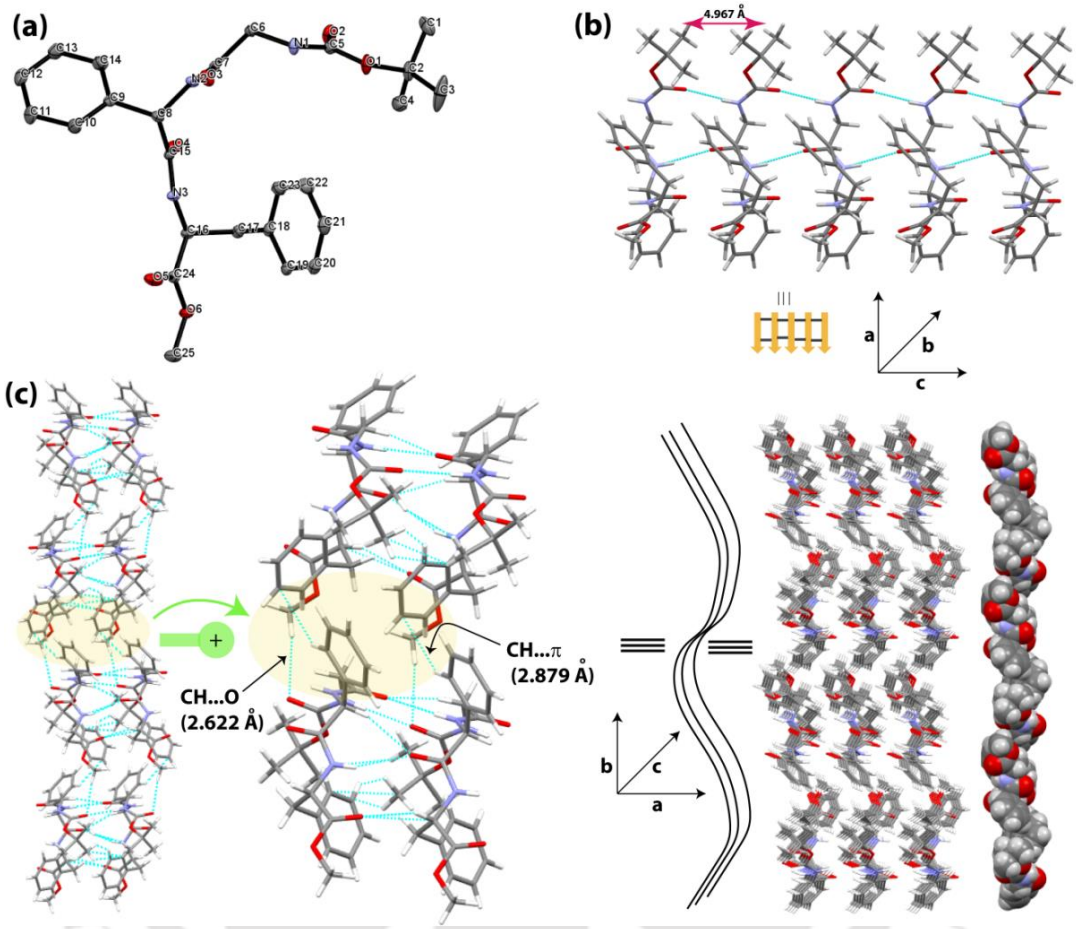

Figure 4.4. *(a) The ORTEP diagram with an ellipsoid of 30% probability, (b) parallel β-sheet along the b-axis, and (c) helical arrangement in the higher-order assembly along the c-axis of* ***4B****.*

4.5. Comparison between type II β-turn and open turn

Generally, an ideal type II β-turn exhibits an intramolecular (4 → 1) H-bond between CO of residue *i* and NH of residue *i* + *3*. Here, we have chosen a tripeptide, Boc-Phe-Aib-Leu-OMe, a representative example of type II β-turn. This peptide contained an intramolecular (4 → 1) H-bond between CO of Boc (*i*) and NH of Leu (*i*+*3*) and formed a 10-membered cyclic type II β-turn structure (N···O = 3.15 Å and O···HN = 2.35 Å). Interestingly, **4A** adopted distorted type II β-turn structure (N···O = 3.24 Å and O···HN =

2.58 Å), but no intramolecular (4 → 1) H-bond (Figure 4.5) was observed between *i* (Boc-CO) and *i + 3* (NH of Phe 2). Such type of structure is known as an open turn structure. There are very few reported open turn structures in literature, and they contain pre-organized kink inducing non-natural amino acids in their backbone. All those peptides are listed in Table 4.2.

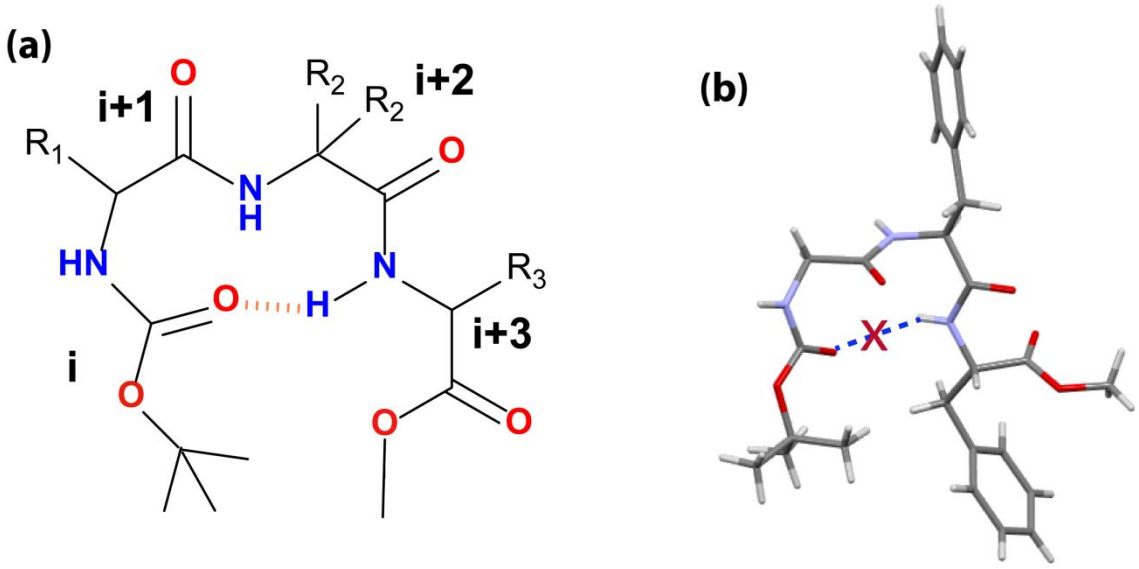

Figure 4.5. *A representative profile of (a) type II β-turn and (b) open turn structures of tripeptides*

Most interestingly, the structure of **4A** is unique as it forms an open turn without any help of turn inducing elements or pre-organized kink-forming moieties. Although it did not contain any intramolecular H-bond between *i* and *i + 3*, the observed torsion angles (φ and ψ) of the *i + 1* (Gly) and *i + 2* (Phe 1) amino acid residues fell close to the type II β-turn region in the Ramachandran plot. To the best of our knowledge, this is the first report on a designed open turn tripeptide without a kink-forming element.

Table 4.2. Comparison of type II β-turn peptides with their torsion angles (°), intramolecular H-bond distance (O···HN) and N···O distance (Å)

Entry	***Peptides***	***φ***	***ψ***	***φ***	***ψ***	***O···HN***	***N···O***	***Structure (Ref)***
1	Ideal type II β-turn	-60	120	80	0			type II β-turn (5)
2	Boc-Phe-Aib-Leu-OMe	-62.0	127.5	61.5	26.6	2.35	3.15	type II β-turn (6)
3	Boc-Ala-Dpg-Ala-OMe	-56.1	139.9	66.2	19.3	2.75	3.44	open turn (7)
4	Boc-Ala-Dbg-Ala-OMe	-61.5	143.3	66.5	21.1	2.78	3.63	open turn (7)
5	Boc-Leu-Aib-m-ABA-OMe	-71.9	142.4	55.8	33.3	3.27	3.89	open turn (8)
6	Boc-Phe-Aib-m-ABA-OMe	-61.6	142.0	63.6	22.6	3.07	3.87	open turn (8)
7	Boc-Gly-Phe-Phe-OMe	-56.1	145.8	59.8	29.7	3.24	2.58	open turn (This work)

4.6. Comparison of the molecular structure of peptide 4A and 4B

A comparison of molecular structures between **4A** and **4B** is described as the incorporation of Phg, *i.e.*, one carbon (–CH_2–) less in the side chain than that of Phe in **4B,** deviated the crystal structure from that of **4A** significantly. This is because the presence of the phenyl ring close to Cα (C8) of **4B**, a steric repulsion arises between the ortho protons of the phenyl ring and the Cα (C8) proton and NH of Phg (N2H) (Figure 4.6). Thus, the phenyl ring gets tilted, and the bond angle of N–Cα–C (τ) is reduced to 107.8(8)° (N2–C8–C15) (Figure 4.6). Therefore, the backbone was extended further, and the C=O of *i* (Boc) and N–H of *i* + *3* (Phe) were oriented in the opposite direction (Figure 4.6), favoring the formation of a β-sheet structure. On the other hand, due to the presence of an extra methylene group (–CH_2–) of Phe1 (Figure 4.6) attached to Cα, the sp3 carbon (C8) became more flexible, and therefore the backbone could arrange to a more stable orientation resulting in the open type II β-turn. The τ angle (N2–C8–C16) was 113.0(5)° and the C=O of *i* (Boc) and N–H of *i* + *3* (Phe 2) were oriented in the same direction (Figure 4.6) but could not form 4 → 1 intramolecular H-bonds probably due to the high *ψ1* (145.8) value compared to the intramolecular H-bonded β-turns (127.5).

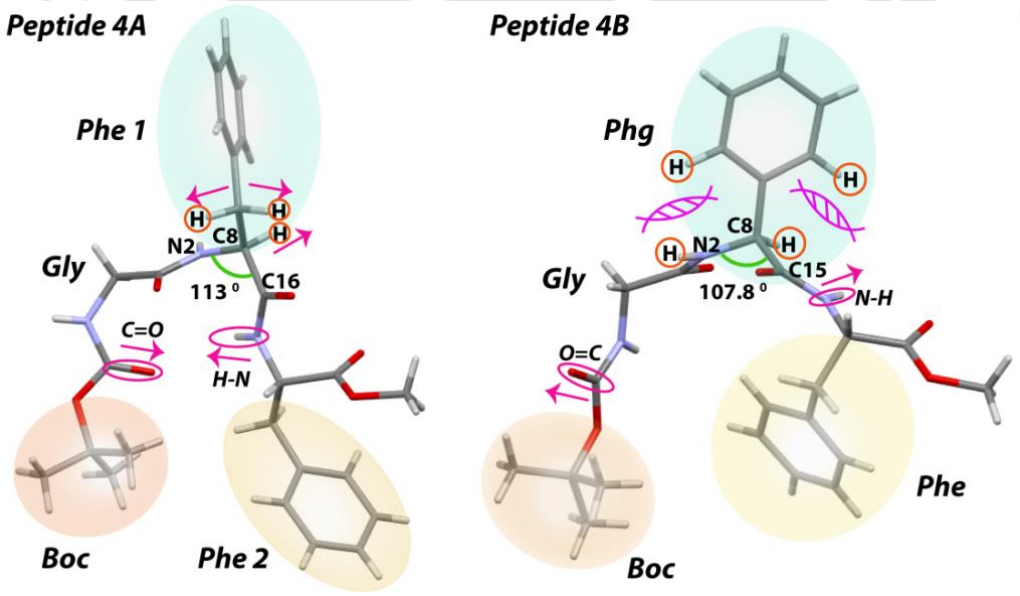

Figure 4.6. *Comparison of the molecular structures of* ***4A*** *and* ***4B.***

4.7. Investigation of intra- or intermolecular H-bond in solution

To understand whether the H-bonds are intra- or inter-molecular we performed a solvent titration NMR experiment. This study was carried out by adding d_6-DMSO to the $CDCl_3$ solution of these peptides. Generally, d_6-DMSO acts as a hydrogen bond accepting solvent, and therefore, when its concentration is increased, peptide NHs are shifted to the downfield region.

The results obtained from the NMR solvent titration illustrated that by increasing the concentration of d_6-DMSO in $CDCl_3$ (v/v) from 0 to 15% for **4A** and 0 to 20% for **4B** the deviation in chemical shift ($\Delta\delta$(NH)) increased by more than 0.2 ppm indicating that NHs were involved in intermolecular hydrogen bonding. All NMR solvent titration spectra and data are listed below (Figure 4.7 and Table 4.3 and 4.4).

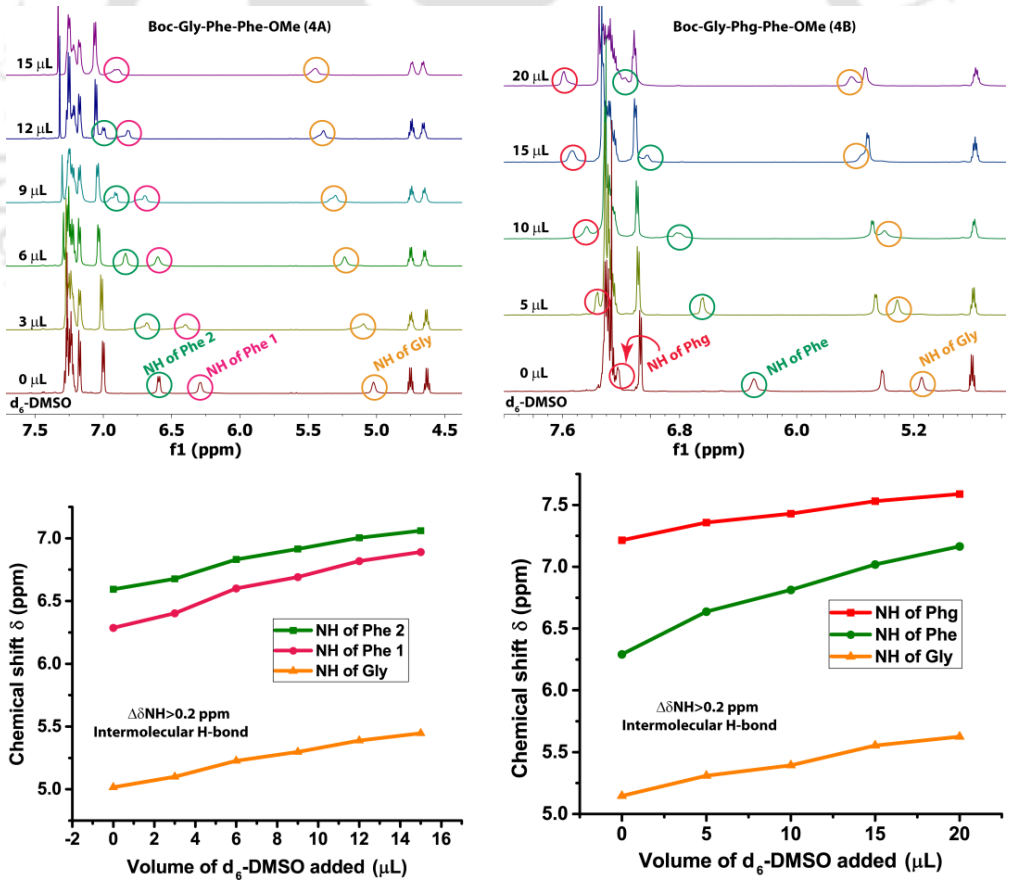

Figure 4.7. *NMR solvent titration spectra of the NH proton of* ***4A*** *and* ***4B.***

Table 4.3. NMR solvent titration data of peptide **4A** in $CDCl_3$ with d_6-DMSO

Sl. No.	*Volume of d_6-DMSO added (μL)*	*Chemical shifts δ (ppm)*					
		NH of Phe 2	*Δδ(NH) of Phe 2*	*NH of Phe 1*	*Δδ(NH) of Phe 1*	*NH of Gly*	*Δδ(NH) of Gly*
1	0	6.593		6.286		5.016	
2	3	6.677		6.402		5.099	
3	6	6.831		6.601		5.227	
4	9	6.914		6.691		5.298	
5	12	7.004		6.819		5.388	
6	15	7.061	0.468	6.890	0.604	5.446	0.430

Table 4.4. NMR solvent titration data of peptide **4B** in $CDCl_3$ with d_6-DMSO

Sl. No.	*Volume of d_6-DMSO added (μL)*	*Chemical shifts δ (ppm)*					
		NH of Phg	*Δδ(NH) of Phg*	*NH of Phe*	*Δδ(NH) of Phe*	*NH of Gly*	*Δδ(NH) of Gly*
1	0	7.215		6.292		5.146	
2	5	7.358		6.638		5.310	
3	10	7.429		6.813		5.394	
4	15	7.530		7.018		5.554	
5	20	7.588	0.373	7.165	0.873	5.626	0.48

4.8. Characterization of conformation of 4A and 4B by NOE interactions in solution

The conformation of these peptides was investigated by NOE interactions. At first, we performed 2D [^{1}H, ^{1}H] COSY (Figure 4.15 and 4.21, section 4.15) and [^{1}H, ^{1}H] TOCSY (Figure 4.16 and 4.22, section 4.15) NMR experiment for identification of the NH protons of each amino acid residue in the peptide sequence. Then, 2D [^{1}H, ^{1}H] NOESY experiment was performed to get intra- or inter-residual NOE interactions (Figure 4.8). Some selected important NOE interactions were listed in Table 4.5. The obtained NOE interactions in $CDCl_3$ indicated the formation of the turn-like structure of both peptides in solution.

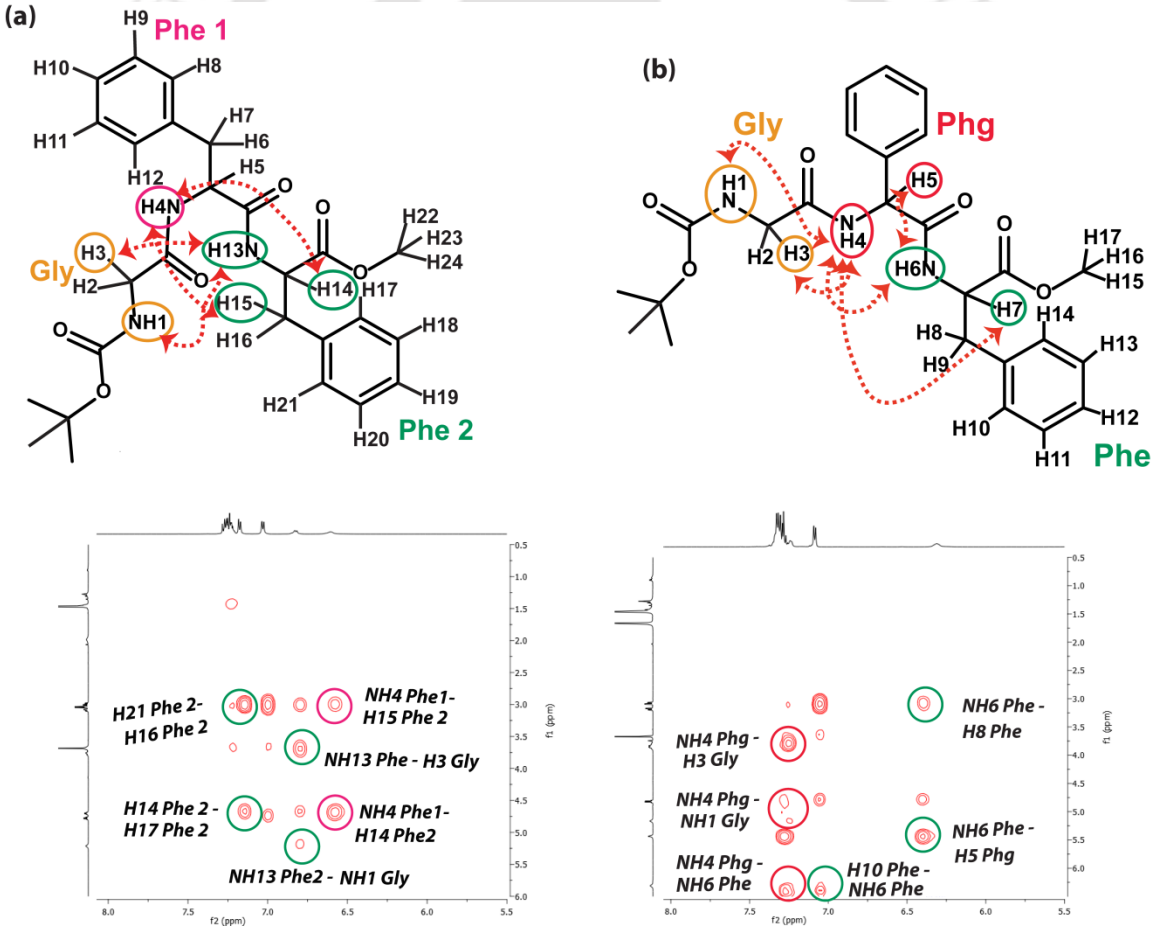

Figure 4.8. *NOE interactions of peptide (a)* ***4A*** *and (b)* ***4B****, obtained from 2D NOESY NMR experiment in* $CDCl_3$

Table 4.5. Selected NOEs of peptide **4A** and **4B** in $CDCl_3$

Peptide **4A**	Peptide **4B**
Gly Hα (H3) ↔ Phe 2 NH (H13N)	Gly Hα (H3) ↔ Phg NH (H4N)
Gly NH (H1N) ↔ Phe 2 NH (H13N)	Gly NH (H1N) ↔ Phg NH (H4N)
Phe 1 NH (H4N) ↔ Phe 2 Hα (H14)	Phg NH (H4N) ↔ Phe Hα (H7)
Phe 1 NH (H4N) ↔ Phe 2 Hβ (H15)	Phg NH (H4N) ↔ Phe NH (H6N)

4.9. Conformation analysis by CD experiment in solution

Next, we performed the CD experiment as it is an excellent biophysical tool to understand the conformation of peptides or proteins in solution. For this purpose, we prepared 1.5 mM each peptide solution in 30% acetonitrile-water medium and incubated them at 37 ^{o}C for seven days.

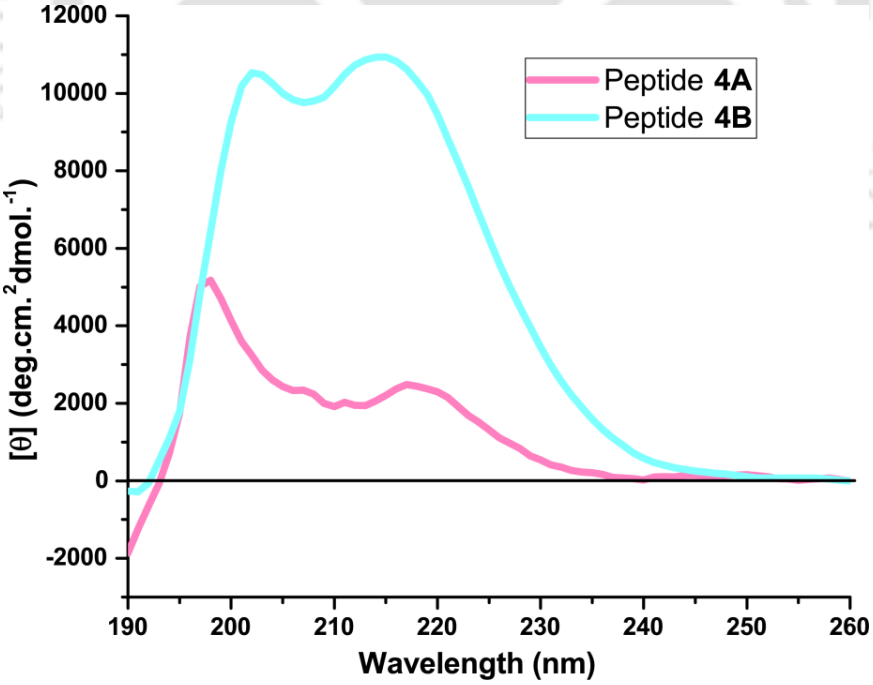

Figure 4.9. *CD profile of peptide **4A** (magenta curve) and **4B** (cyan curve)in 30% acetonitrile-water medium using a concentration of 1.5 mM.*

Then, these 7 days aged solutions were allowed to record the CD graph. The obtained curve of peptide **4A** (Figure 4.9, magenta curve) showed positive Cotton effects at 217 and 198 nm, whereas **4B** (Figure 4.9, cyan curve) exhibited positive Cotton effects at 215 and 202 nm indicating that both peptides contained a mixture of β-turn and β-sheet structure.

4.10. Monitoring the self-association of 4A and 4B in solution by various microscopic experiment

Then we checked the morphology of these peptides to understand their self-association behavior. The morphologies of these self-associated tripeptides were analyzed under an optical microscope, a FE-SEM, and a TEM.

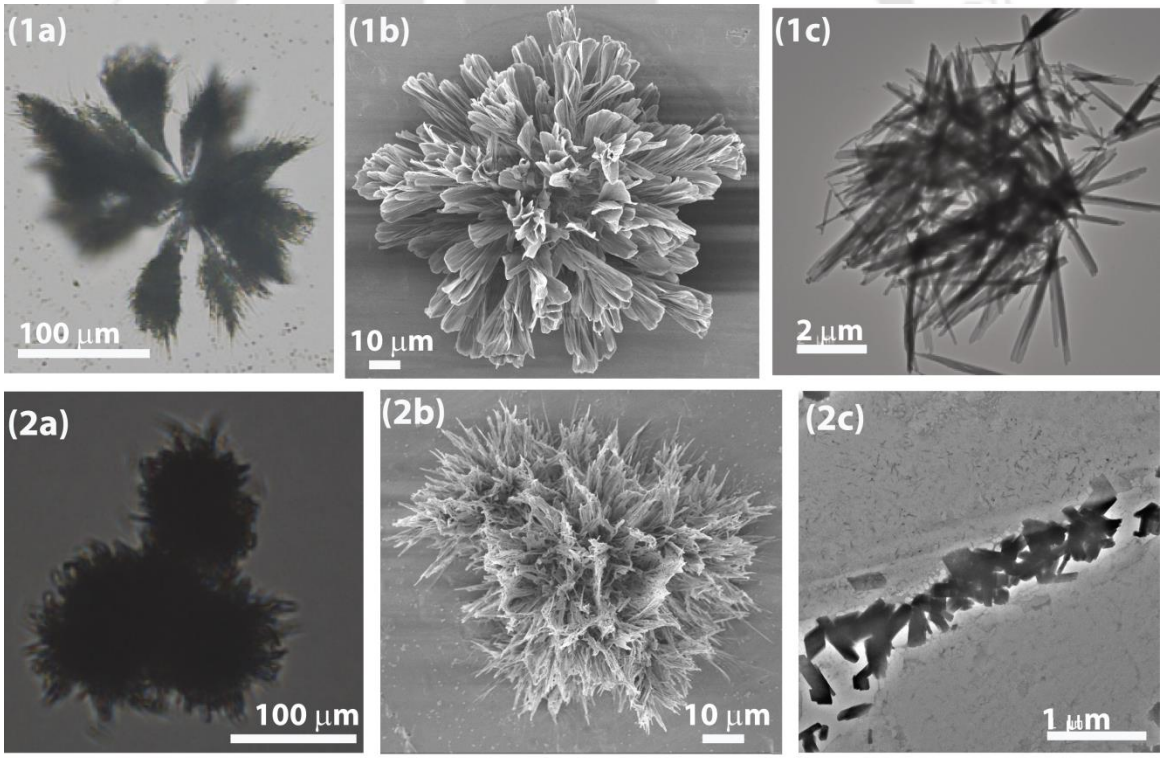

Figure 4.10. *Optical microscopic, FE-SEM and TEM images of self-associated tripeptides (1a), (1b) and (1c) of* ***4A*** *and (2a), (2b) and (2c) of* ***4B****, respectively, in 30% acetonitrile-water medium using a concentration of 1.5 mM.*

For that, we prepared a 1.5 mM solution of each of them in 30% acetonitrile-water and incubated them at 37 ^{o}C for seven days. These solutions were drop-cast on a microscopic

slide for analysis using an optical microscope and over Al-foil for the FE-SEM study. The obtained optical images indicated that both of these peptides self-associated to form two different flower-like structures (Figure 4.10, 1a and 2a). Similarly, the obtained FE-SEM images of **4A** and **4B** indicated that they self-associate to form highly organized two different flower-like structures (Figure 4.10, 1b, and 2b).

Next, to get a detailed morphological insight into these self-associated peptides, TEM experiments were performed. While **4A** exhibited a needle-like structure under TEM, **4B** organized in block-shaped structures (Figure 4.10, 1c, and 2c). These needle and block-shaped flakes observed under TEM self-assembled to form a different flower-like morphology viewed under FE-SEM.

4.11. Conclusion

In conclusion, we demonstrated the unique crystallographic signatures of the self-assembled supramolecular helical architectures of Boc-Gly-Phe-Phe-OMe (**4A**) and Boc-Gly-Phg-Phe-OMe (**4B**). SC-XRD revealed that **4A** formed a distorted type II β-turn conformation, called the open turn, which further self-assembled to form a herringbone helical architecture along the crystallographic *c*-axis. Such open turn formation is unusual for a standard amino acid containing the designed tripeptide without a kink forming elements like proline or Aib. On the other hand, **4B** exhibited a β-sheet structure, which further self-assembled to form a helical architecture along the *c*-axis in the crystalline state. Further, they self-associate to form two different flower-like architectures in a 30% acetonitrile-water medium. The differences in molecular and supramolecular level structural arrangements of these two peptides are due to the presence of the methylene group at the side chain of only one amino acid (Phe), which is the only difference in their chemical structures. This work may open up an avenue for the design of open turn structures without using any pre-organized kink inducing moieties. Furthermore, as **4A** contains C-terminal phenylalanylphenylalanine (–Phe-Phe–) residues, identical with the core hydrophobic self-recognizing unit of the amyloid-β peptide, such structural insight may be useful for amyloid research.

4.12. Experimental section

4.12.1. Materials and instrumentations

As described in chapter 8

4.12.2. General procedure for the synthesis of tripeptides

Boc protected amino acid (1 equiv), coupling reagent, *o*-NosylOXY (1 equiv), Hünig's base DIPEA (1 equiv) in DCM were taken in a 50 mL R.B.and the reaction mixture was kept 5 min for preactivation.[9] In another beaker methyl ester of the next amino acid (1.2 equiv) with DIPEA (1.2 equiv) in DCM was taken for neutralization. Then, this solution was added dropwise to the above reaction vessel and kept stirring for 4-5 h at room temperature. After completion of the reaction, the reaction mixture was diluted with DCM and washed with a 10% citric acid solution followed by the saturated $NaHCO_3$ solution 3 times in each case. Then, the organic layer was dried over anhydrous Na_2SO_4, and the decanted solvent was evaporated to get solid both *N*- and *C*- protected dipeptide. Next, this dipeptide was taken in a 50 mL RB and TFA:DCM (90:10) was added onto it. After 3 h reaction, the TFA was evaporated by passing N_2 over it and again neutralized it by adding DIPEA. Then this Boc deprotected dipeptide was coupled with next Boc-N-amino acid, using the procedure as mentioned earlier to get the tripeptide. The desired product was purified by silica gel column chromatography using ethyl acetate-hexane solvent system.

4.12.3. Sample preparation

2.07 mM peptide **4A** and 2.13 mM peptide **4B** solutions were prepared in two different Eppendorf vials (2 mL) by adding 1 mL 30% CH_3CN-H_2O solution. Then, we prepared a 1 mL (1.5 mM) solution (stock solution) from the above solutions for each peptide. These stock solutions were incubated for 7 days at 37 ^oC.

4.13. Characterization data

Boc-Gly-Phe-Phe-OMe 4A.

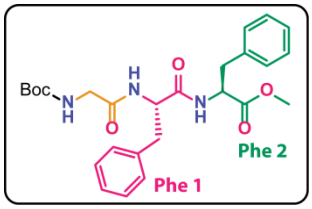

White solid, mp 158-160 ^{o}C, ^{1}H NMR ($CDCl_3$; 600 MHz) δ 1.44 (9H, s); 3.08-2.95 (4H, m); 3.67 (3H, s); 3.77-3.69 (2H, m); 4.68-4.65 (1H, q, *J* = 7.2 Hz, *J* = 7.2 Hz); 4.77-4.74 (1H, q, *J* = 6.6 Hz, *J* = 7.2 Hz); 5.13 (1H, brs); 6.48 (1H, brs); 6.74-6.73 (1H, d, *J* = 7.8 Hz), 7.01-7.00 (2H, d, *J* = 6.6 Hz); 7.16-7.15 (2H, d, *J* = 6.6 Hz), 7.26-7.20 (6H, m). ^{13}C NMR ($CDCl_3$; 150 MHz) δ 28.4, 37.9, 44.3, 52.5, 53.5, 54.2, 80.5, 127.2, 127.3, 128.7, 128.8, 129.3, 135.8, 136.3, 156.1, 169.5, 170.4, 171.5. HRMS (ESI): calculated $[M+H]^+$ 484.2369, found m/z . 484.2529. HPLC: retention time (t_R) = 8.90 min. Isolated pure product 663 mg (yield: 73% w.r.t. starting meterial Boc-Phe).

Boc-Gly-Phg-Phe-OMe 4B.

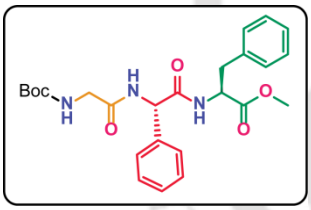

White solid, mp 157-159 ^{o}C, ^{1}H NMR ($CDCl_3$; 600 MHz) δ 1.43 (9H, s); 3.07-3.03 (1H, dd, *J* = 6 Hz); 3.17-3.13 (1H, dd, *J* = 5.4 Hz); 3.64 (3H, s); 3.86-3.76 (2H, m); 4.81-4.78 (1H, q, *J* = 6 Hz, *J* = 7.8 Hz); 5.21 (1H, brs); 5.47-5.46 (1H, d, *J* =6.6 Hz); 6.47 (1H, brs), 7.07-7.06 (2H, d, *J* = 7.2 Hz); 7.29-7.23 (8H, m). ^{13}C NMR ($CDCl_3$; 150 MHz) δ 28.4, 37.8, 44.3, 52.5, 53.7, 57.2, 80.4, 127.4, 127.5, 128.7, 128.8, 129.2, 129.4, 135.7, 137.0, 156.2, 169.1, 169.5, 171.5. HRMS (ESI): calculated $[M+H]^+$ 470.2213, found m/z . 470.2298. HPLC: retention time (t_R) = 8.74 min. Isolated pure product 668 mg (yield: 71% w.r.t. starting meterial Boc-Phg).

4.14. References

1. Sali, D.; Bycroft, M.; Fersht, A. R. Stabilization of protein structure by interaction of alpha-helix dipole with a charged side chain. *Nature* **1988**, *335*, 740–743.
2. Eichhorn, C. D.; Al-Hashimi, H. M. Structural dynamics of a single-stranded RNA-helix junction using NMR. *RNA* **2014**, *20*, 782–791.
3. Wittung, P.; Nielsen, P. E.; Buchardt, O.; Egholm, M.; Nordén, B. DNA-like double helix formed by peptide nucleic acid. *Nature* **1994**, *368*, 561–563.
4. Eyre, D. R. Collagen: molecular diversity in the body's protein scaffold. *Science* **1980**, *207*, 1315–1322.
5. Venkatachalam, C. M. Stereochemical criteria for polypeptides and proteins. V. Conformation of a system of three linked peptide units. *Biopolymers* **1968**, *6*, 1425-1436.
6. Dutt, A.; Frohlich, R.; Pramanik, A. β-Turn mimic in tripeptide with Phe(1)-Aib(2) as corner residues and β-strand structure in an isomeric tripeptide: an X-ray diffraction study. *Org. Biomol. Chem.* **2005**, *3*, 661-665.
7. Crisma, M.; Valle, G.; Toniolo, C.; Prasad, S.; Balaji Rao, R.; Balaram, P. β-Turn conformations in crystal structures of model peptides containing α,α-Di-*n*-propylglycine and α,α-Di-*n*-butylglycine. *Biopolymers* **1995**, *35*, 1-9.
8. Dutt, A.; Drew; M. G. B.; Pramanik, A. m-Aminobenzoic acid inserted β-turn in acyclic tripeptides: a peptidomimetic design. *Tetrahedron* **2005**, *61*, 11163–11167.
9. Dev, D.; Palakurthy, N. B.; Thalluri, K.; Chandra, J.; Mandal, B. Ethyl 2-cyano-2-(2-nitrobenzene sulfonyloxyimino)acetate (*o*-NosylOXY): A recyclable coupling reagent for racemization free synthesis of peptide, amide, hydroxamate and ester. *J. Org. Chem*. **2014**, *79*, 5420-5431.

4.15. Selected spectra

4.15.1. Spectra of peptide 4A

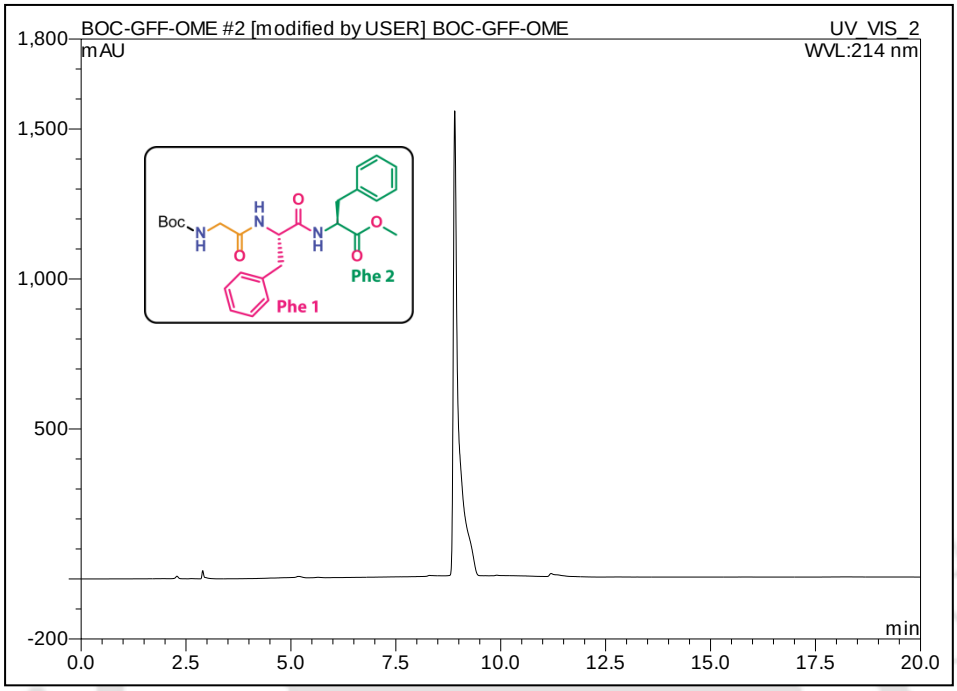

Figure 4.11. *HPLC profile picture of purified peptide* ***4A*** *(A linear gradient was used from 5 to 100% CH_3CN till 8 min, and a total run time of 20 min, flow rate 1mLmin^{-1})*

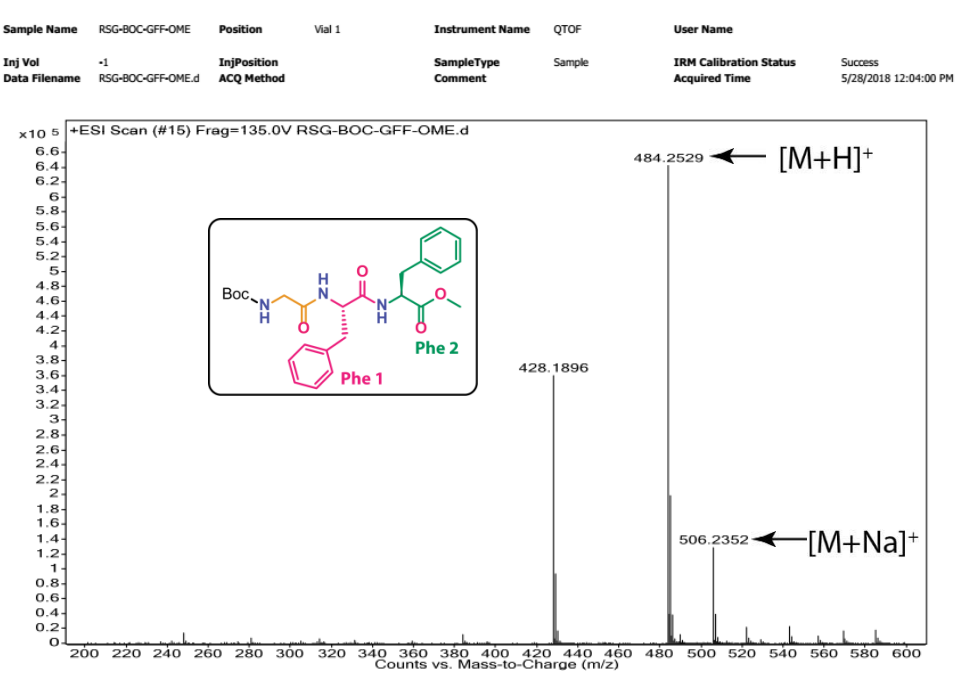

Figure 4.12. *MS spectra of peptide* ***4A***

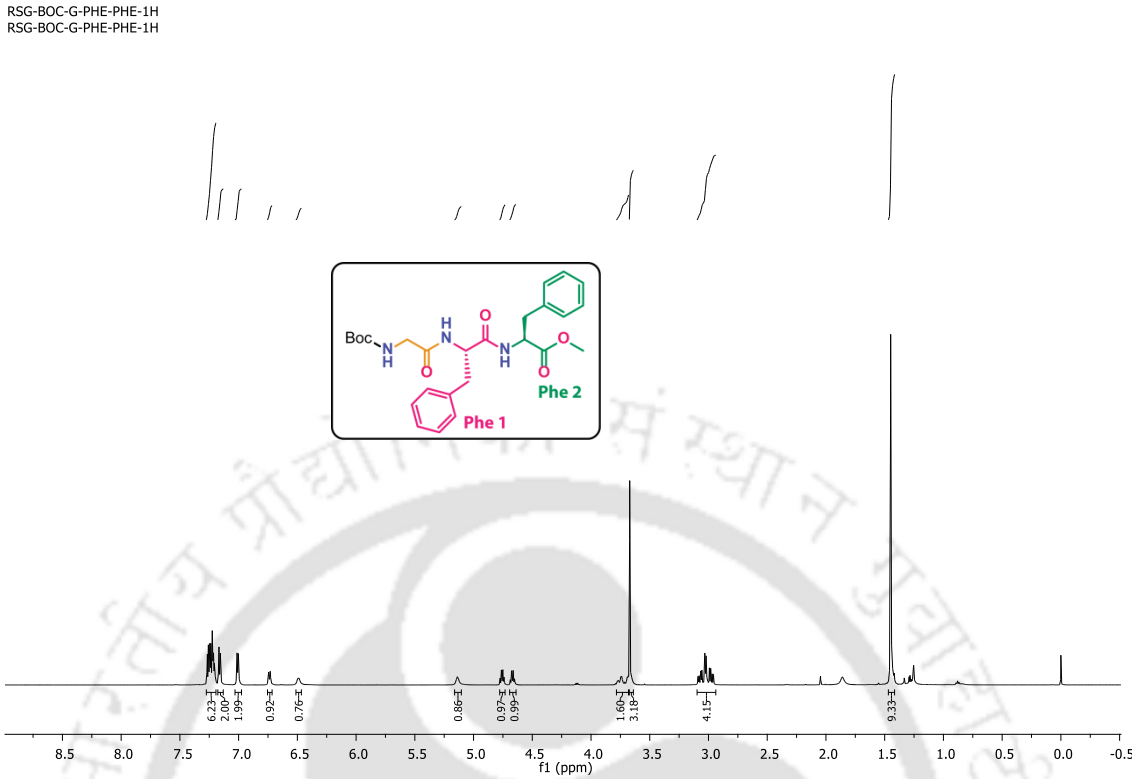

Figure 4.13. *^{1}H NMR spectra of peptide* ***4A***

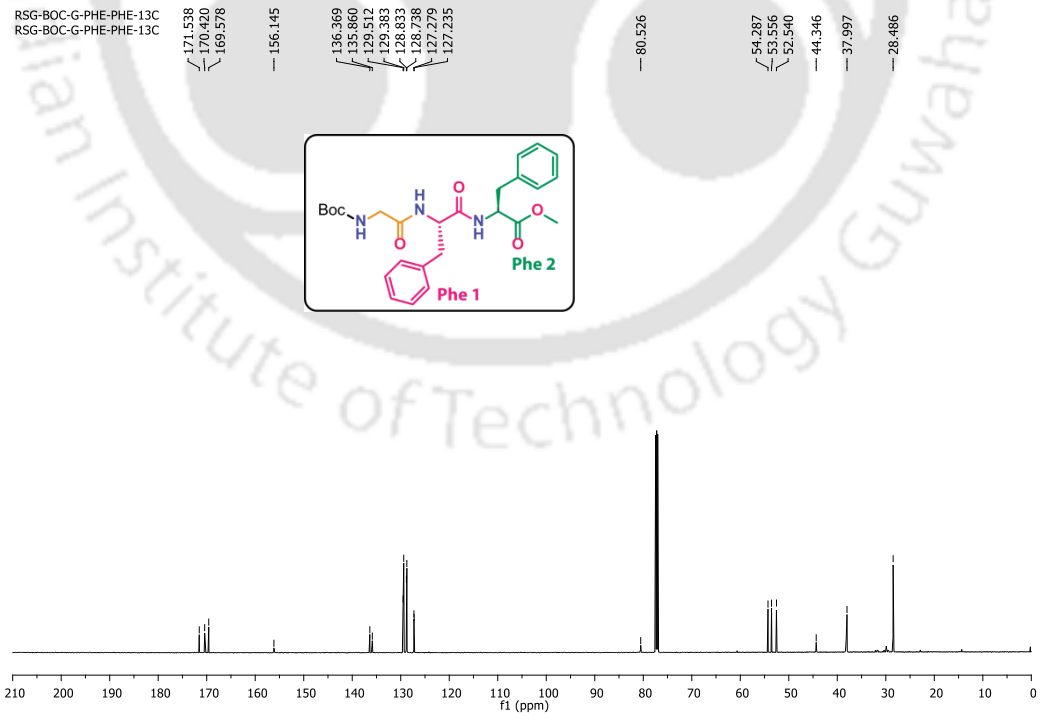

Figure 4.14. *^{13}C NMR spectra of peptide* ***4A***

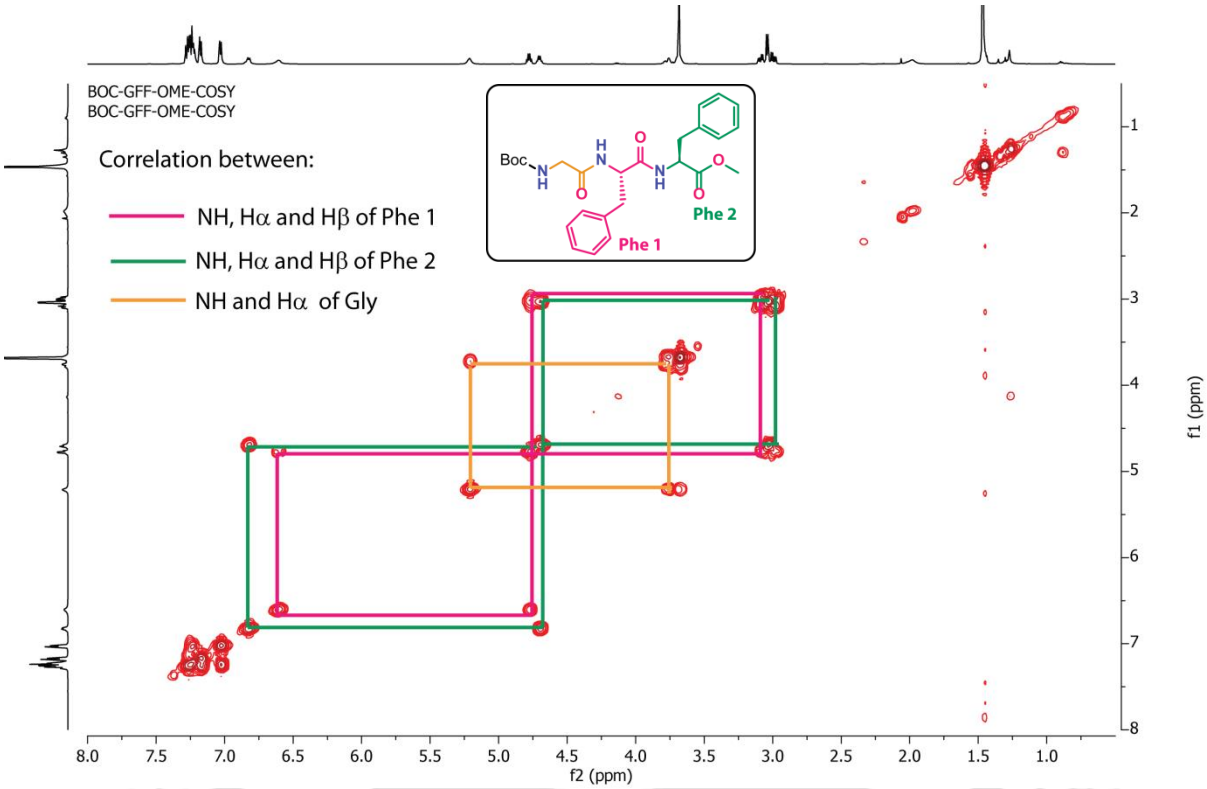

Figure 4.15. *COSY spectra of peptide* ***4A***

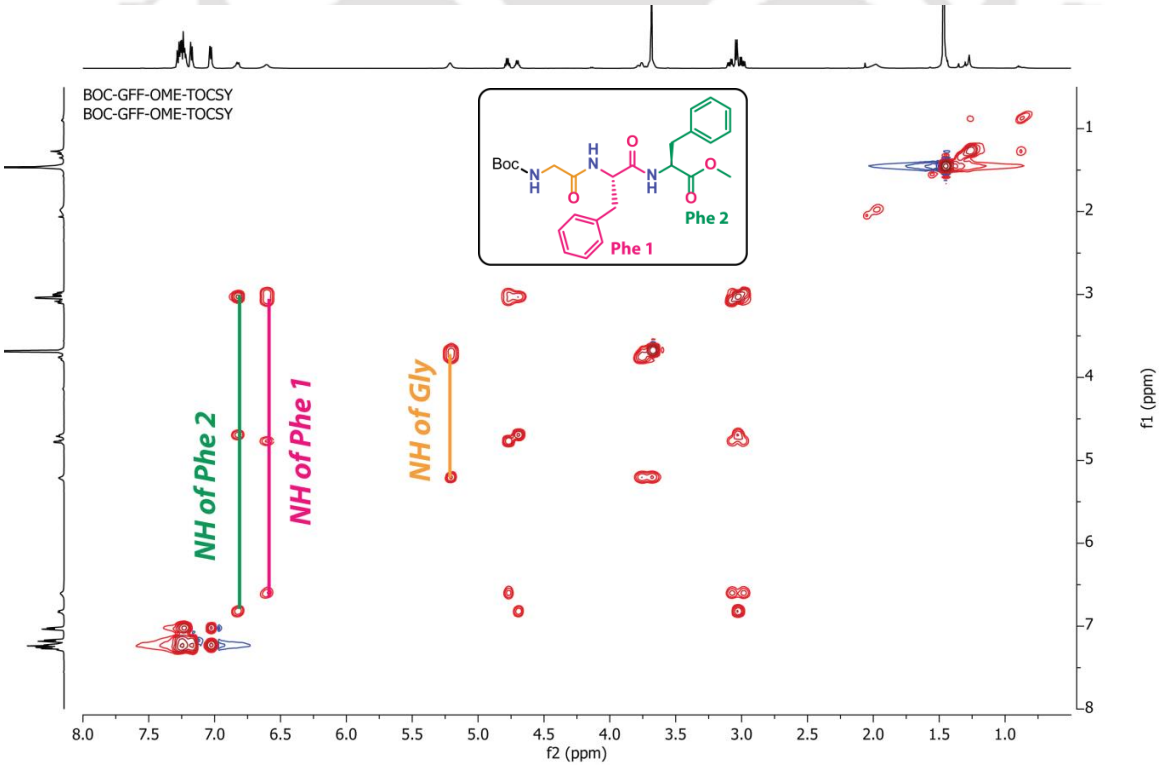

Figure 4.16. *TOCSY spectra of peptide* ***4A***

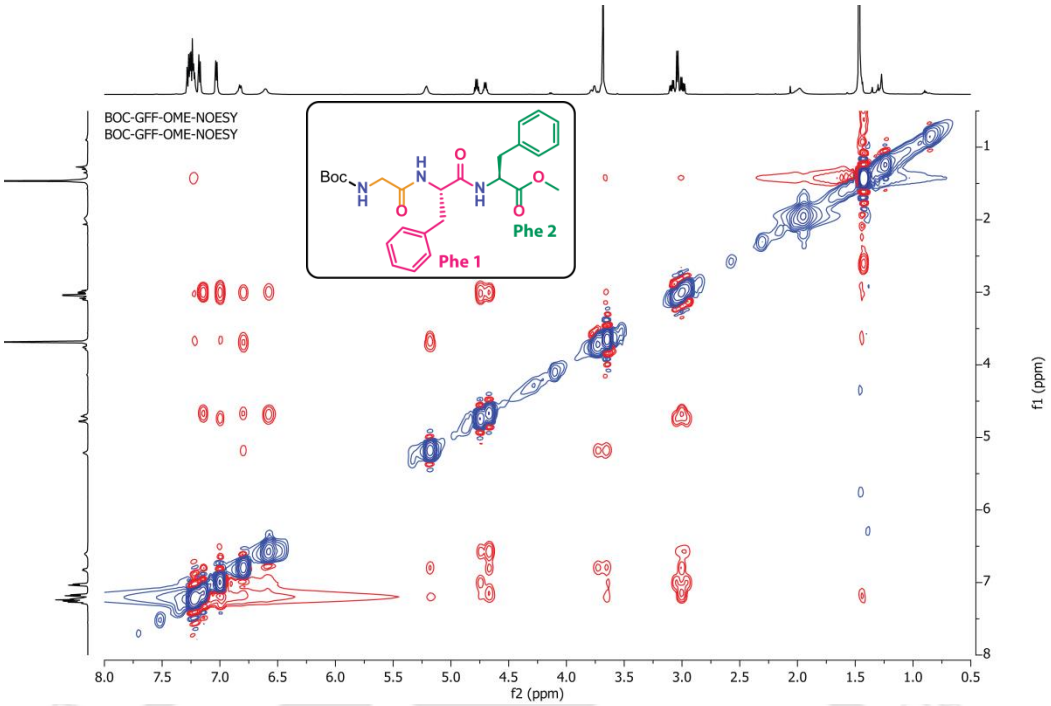

Figure 4.17. *NOESY spectra of peptide* ***4A***

4.15.2. Spectra of peptide 4B

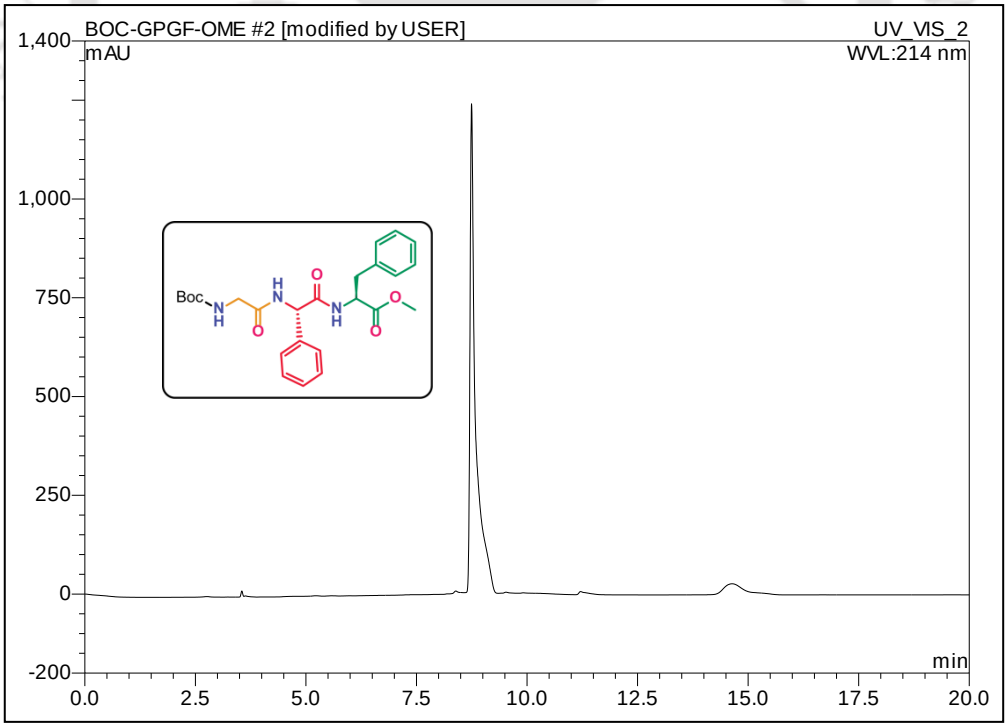

Figure 4.18. *HPLC profile picture of purified peptide* ***4B****(A linear gradient was used from 5 to 100% CH_3CN till 8 min, and a total run time of 20 min, flow rate 1mLmin^{-1})*

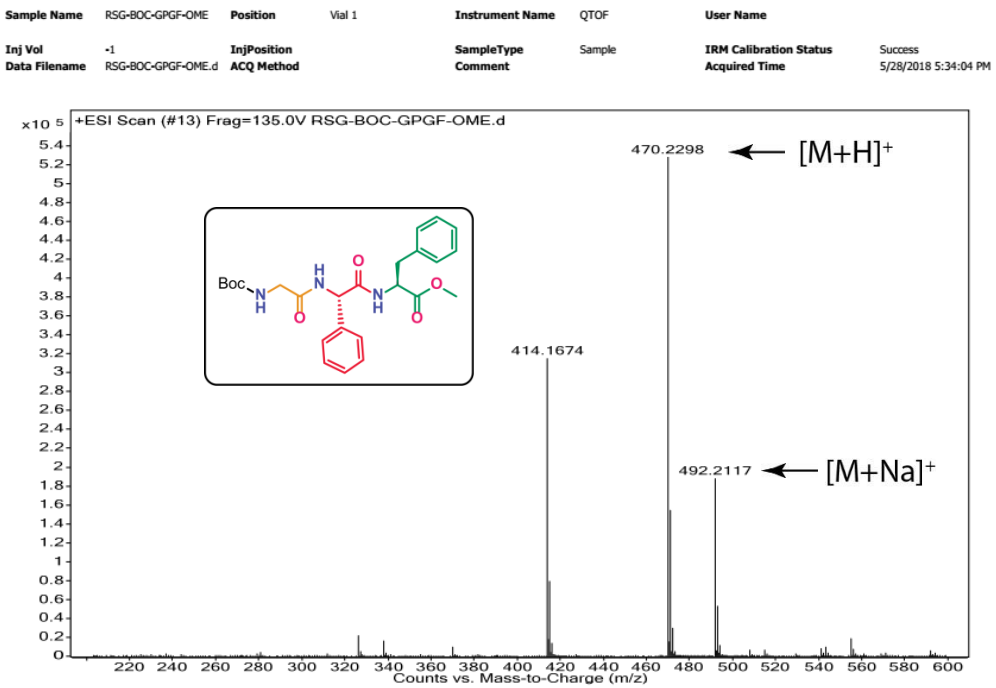

Figure 4.19. *MS spectra of peptide* ***4B***

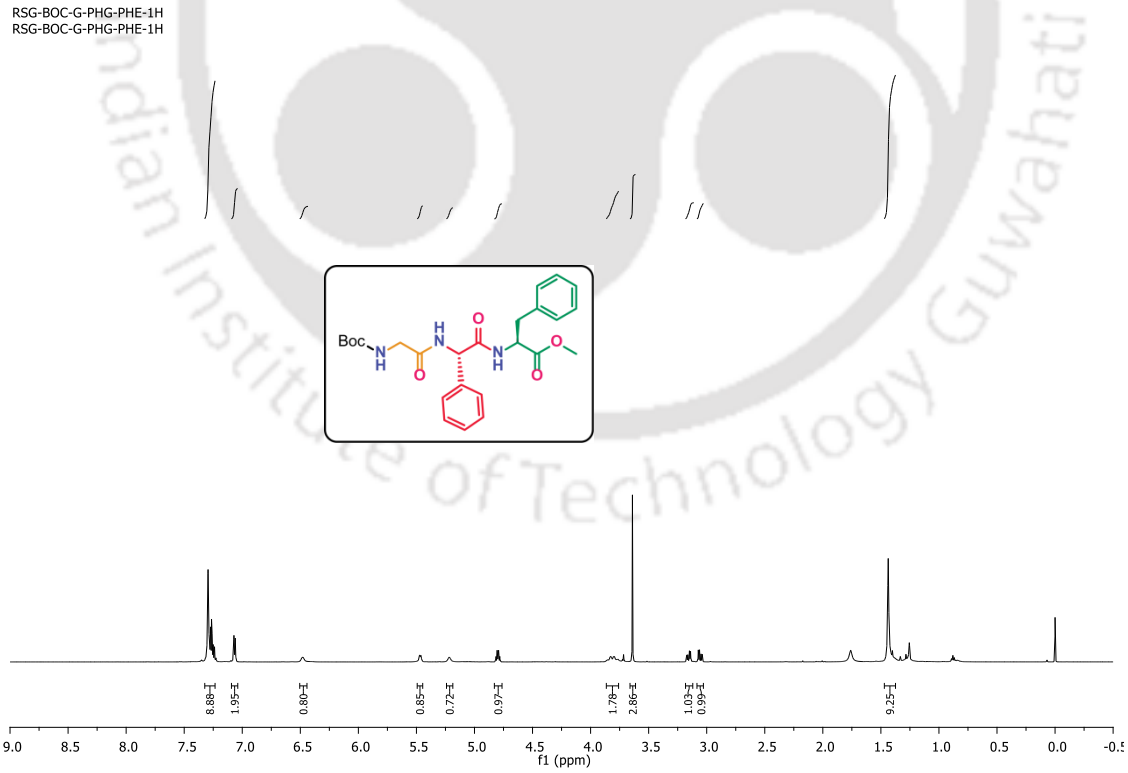

Figure 4.20. *^{1}H NMR spectra of peptide* ***4B***

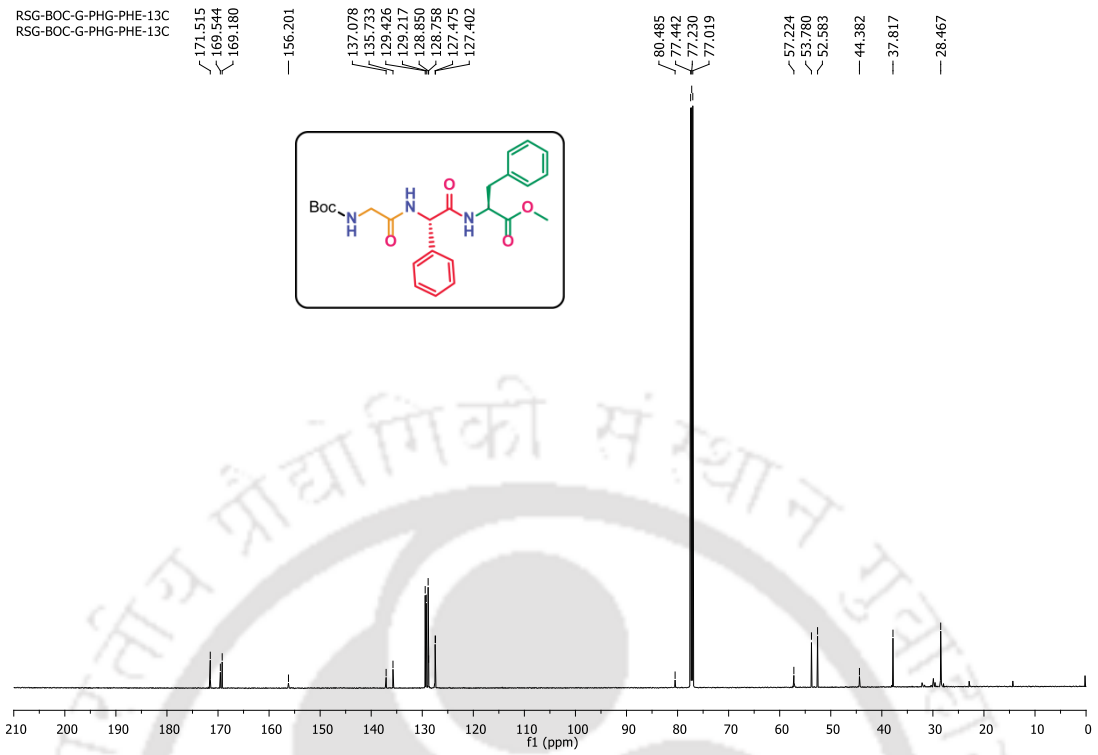

Figure 4.21. *^{13}C NMR spectra of peptide* ***4B***

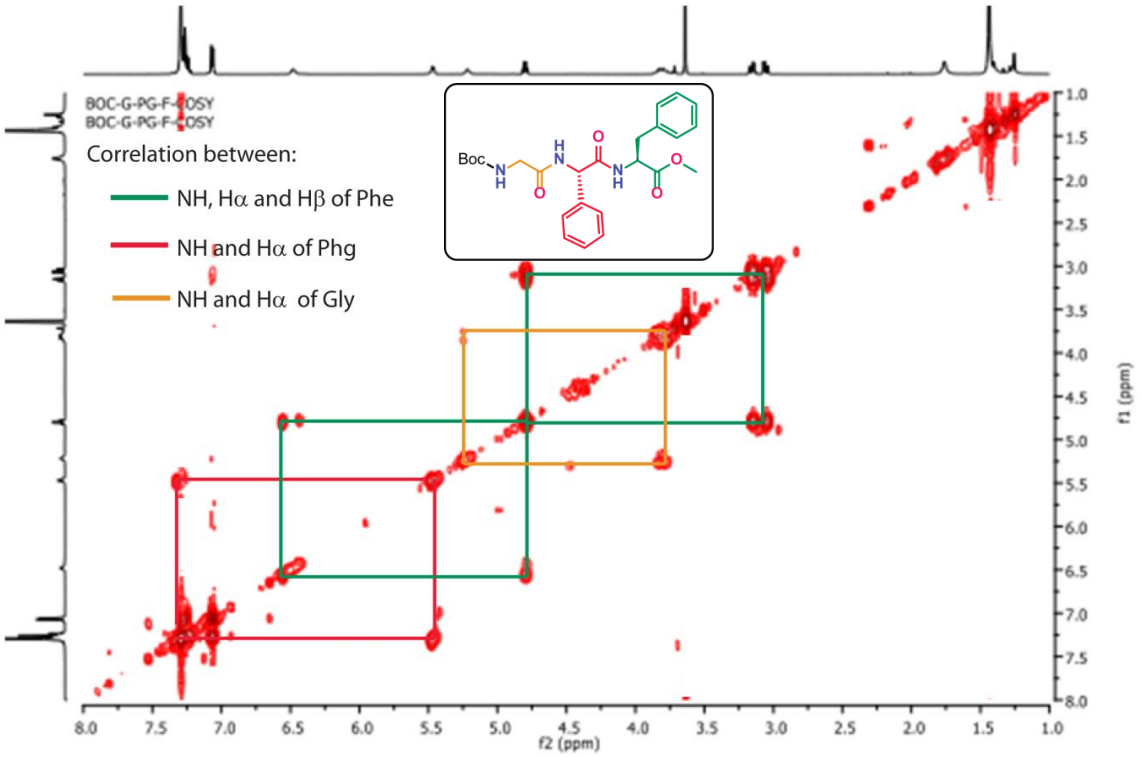

Figure 4.22. *COSY spectra of peptide* ***4B***

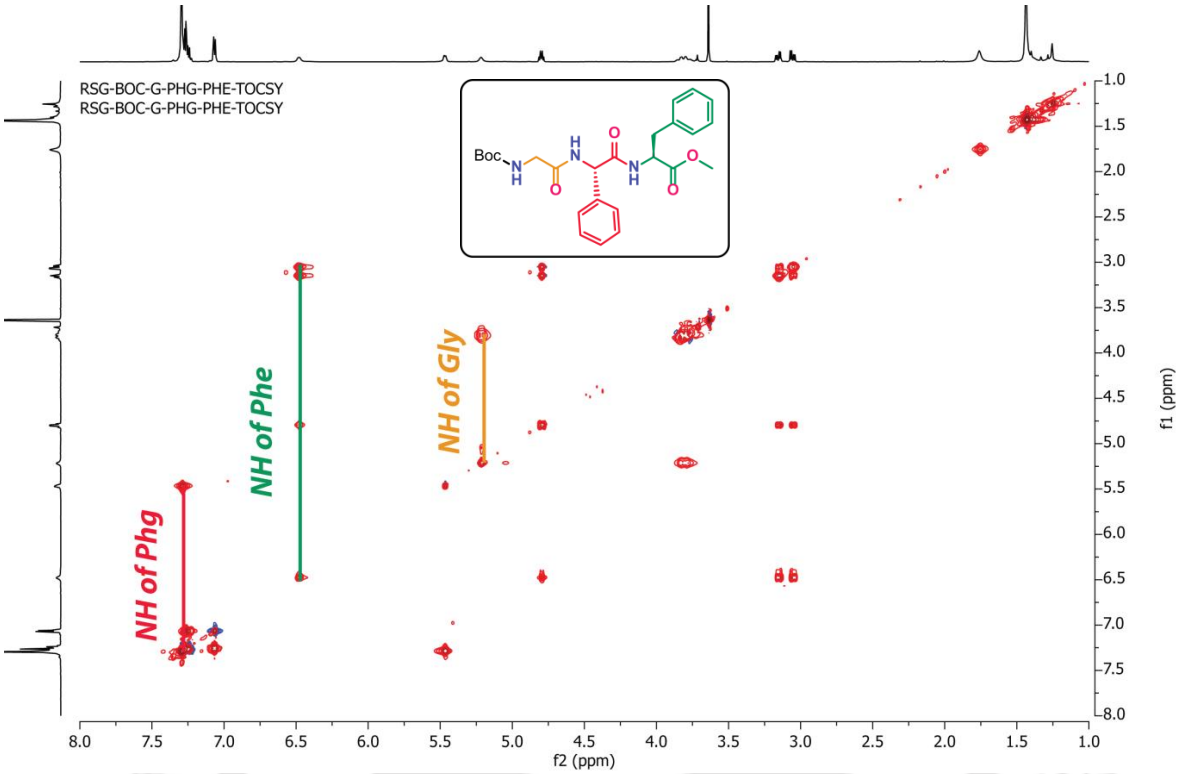

Figure 4.23. *TOCSY spectra of peptide* ***4B***

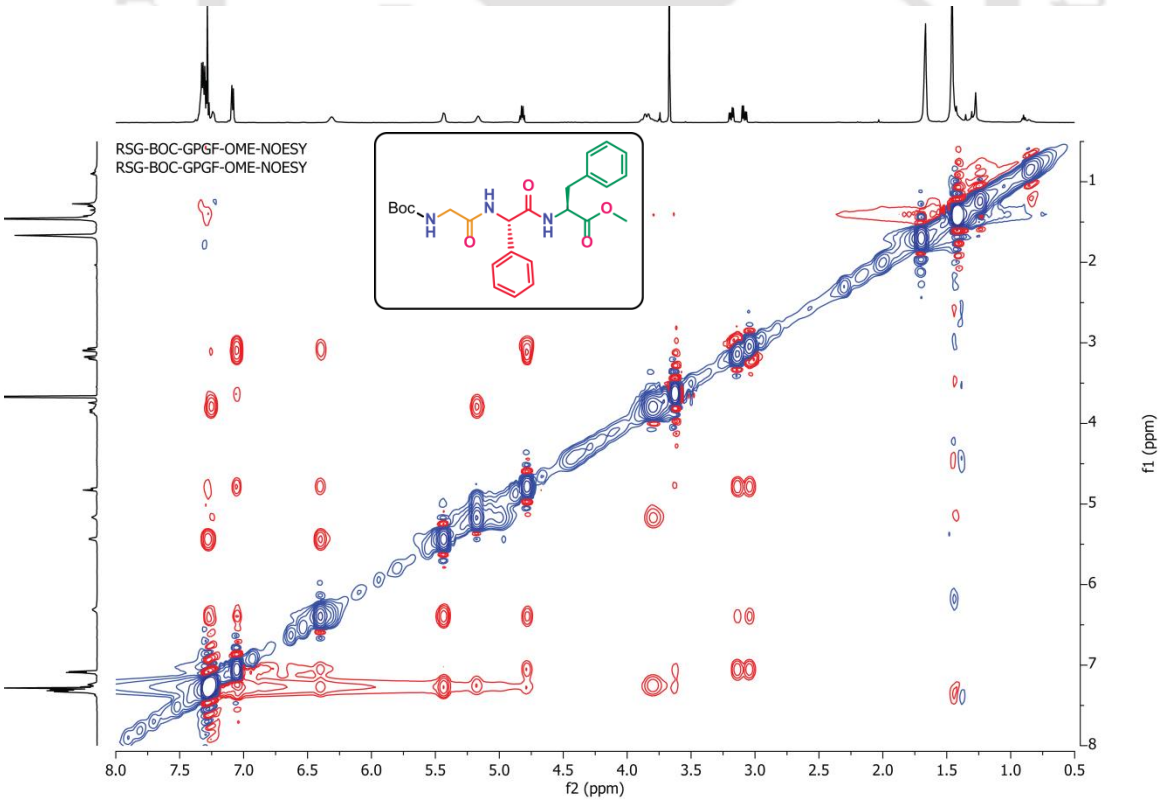

Figure 4.24. *NOESY spectra of peptide* ***4B***

4.16. Crystallographic data

Table 4.6. Hydrogen bonding distances (Å) and Bond angles (deg) of peptide **4A** and **4B**

Molecule	***D−H···A***	***d(D···H) /Å***	***d(H···A)/Å***	***d(D···A)/Å***	***<D−H··· A/°***
Boc-Gly-Phe-Phe-OMe (**4A**)	N1-H1···O3	0.86	2.03	2.8867(4)	171
	N2-H2···O4	0.86	1.96	2.8074(4)	170
	C6-H6A···O1	0.97	2.58	3.5507(5)	174
	C26-H26B···O5	0.96	2.35	3.2862(4)	166
Boc-Gly-Phg-Phe-OMe (**4B**)	N1-H1···O2	0.86	2.12	2.9784(1)	174
	N2-H2N···O3	0.86	2.17	3.0203(1)	170
	N3-H3···O4	0.86	2.32	3.1459(1)	160
	C6-H6A···O3	0.97	2.59	3.4705(1)	151
	C8-H8···O4	0.98	2.37	3.2979(1)	158
	C16-H16···O5	0.98	2.29	3.1517(1)	146

Table 4.7. Crystal parameters and refinement data of **4A** and **4B**

Parameters	***Boc-Gly-Phe-Phe-OMe (4A)***	***Boc-Gly-Phg-Phe-OMe (4B)***
Formula	C_{26} H_{33} N_3 O_6	C_{25} H_{31} N_3 O_6
Fw	483.55	469.53
Crystal system	Monoclinic	Monoclinic
Space group	P 21	P 21
a/Å	15.407(2)	4.96731(12)
b/Å	5.8843(6)	19.4022(5)
c/Å	15.664(2)	12.4703(3)
α/^{o}	90.00	90.00
β/^{o}	114.753(18)	92.486(3)
γ/^{o}	90.00	90.00
V/Å^3	1289.6(3)	1200.72(5)
Z	2	2
D_c/g cm^{-3}	1.245	1.299
μ Mo K_α/mm^{-1}	0.089	0.093
F000	516.0	500.0
T/K	293(2)	149.99(10)
θ max.	28.746	24.996
Total no. of reflections	6575	3488
Independent reflections	4934	2716
Observed reflections	3405	2545
Parameters refined	321	311
R_1, I > 2σ(I)	0.0721	0.0346
wR_2, I > 2σ(I)	0.1949	0.0996
GOF (F^2)	1.029	0.608
CCDC No.	1851441	1851442

Chapter 5

Formation of Supramolecular Single Helical and Double Helical Architectures from Alternating D/L Amino Acid Containing Designed Tripeptides

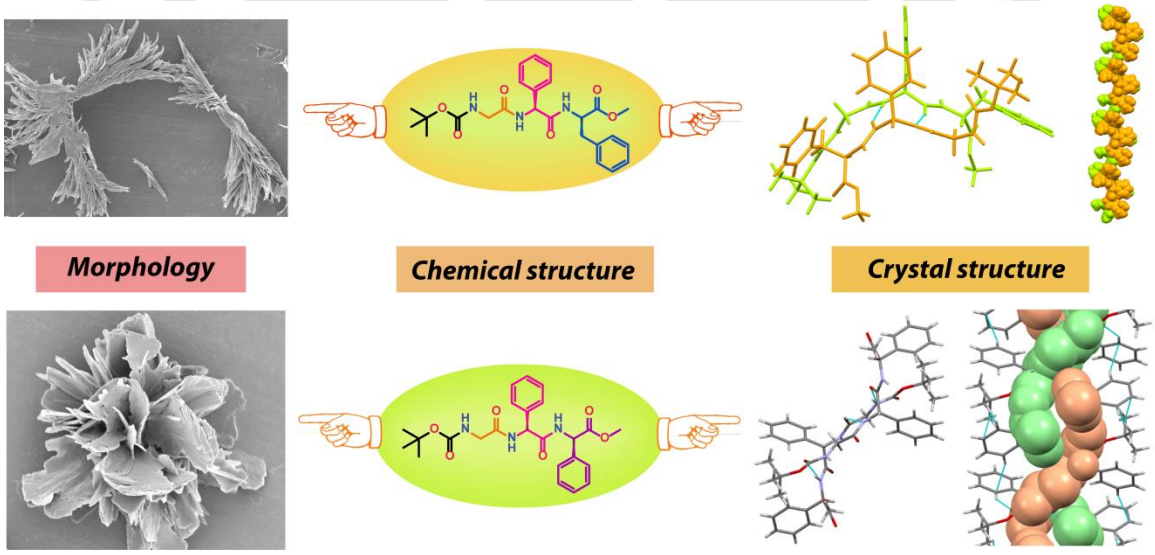

5.1. Background

In chapter 4, we have discussed the two tripeptides, which are very similar to each other but only differ by one methylene group of the side chain of Phe/Phg, located at the center of the sequence. They exhibited two different helical-like assemblies in the crystalline state. In nature, the double-stranded helix is rare, and only DNA contains a double-stranded helix. It plays an essential role in the biological system, e.g., information storage and transcription.[1,2] Scientists are trying to develop the peptide-based double-stranded helix artificially. Few double helices of small peptides are reported, which are discussed in Chapter 1, section 1.7. But most of the reported double-helical structures are generated from the installation of preorganized kink moieties in the peptide sequence. Herein, we have designed peptide-based helical and double helical structures by using D/L amino acids alternatingly.

5.2. Design of peptides

In chapter 4, we have seen the tripeptides, Boc-Gly-Phe-Phe-OMe (**4A**) and Boc-Gly-Phg-Phe-OMe (**4B**) adopted a rare novel open turn and parallel β-sheet structures, respectively in the crystalline state. The structural differences observed between the above two peptides were probably due to the presence of the non-proteinogenic amino acid L-phenylglycine. Keeping in mind the advantages and structural features of Phg and importance of alternating D/L amino acids in a sequence,[3-7] in this work, we kept the *N*-terminal dipeptide glycylphenylglycine (-Gly-L-Phg-) unaltered but changed the next *C*-terminal amino acid to D-Phe (**5A**) and D-Phg (**5A,** Figure 5.1), respectively, and wanted to observe the effect of the reversion of chirality.

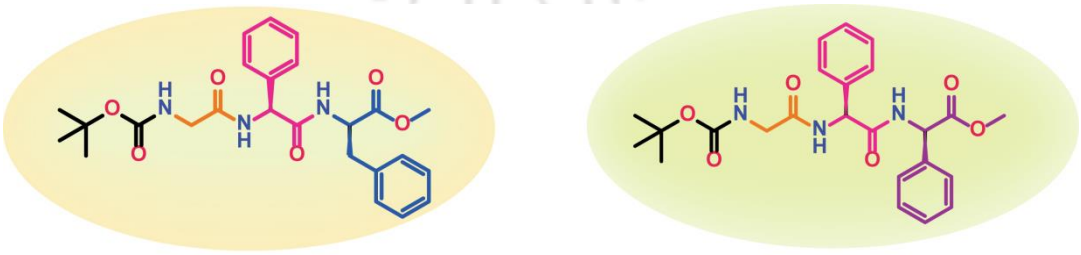

Boc-Gly-L-Phg-D-Phe-OMe (5A) Boc-Gly-L-Phg-D-Phg-OMe (5B)

Figure 5.1. *The chemical structures of tripeptides* ***5A*** *and* ***5B***

5.3. Synthesis and characterization of the designed peptides

At first, we have synthesized these both *N*- and *C*-protected alternating D/L amino acid containing designed peptides by using standard conventional coupling method in solution.[8] The detailed synthetic procedure is described in Chapter 4 in section 4.12.2. The synthetic scheme is displayed in scheme 5.1. The synthesized peptides were purified by silica gel column chromatography and purity was checked by analytical HPLC. The purified peptides were characterized by mass spectrometry and 1D [^{1}H] and 2D [^{1}H, ^{1}H] NMR spectroscopy. The characterization data and spectra for the synthesized peptides are shown in section 5.13 and 5.15, respectively.

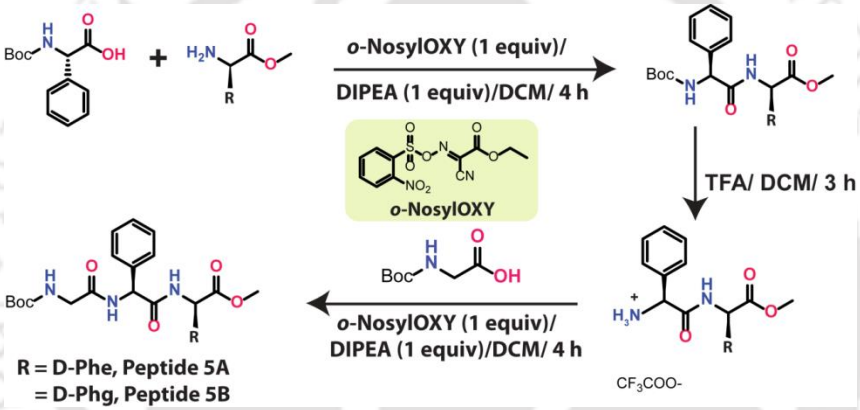

Scheme 5.1. *Schematic representation of peptide synthesis in solution.*

5.4. Investigation of self-assembly process by SC-XRD

To investigate the self-assembly of these peptides, we performed the SC-XRD experiment in the crystalline state. Colorless block-shaped crystals (Figure 5.2) of peptide **5A** and **5B**, suitable for X-ray diffraction were grown from the acetonitrile-water medium by slow evaporation at room temperature. The obtained triclinic crystal of **5A** and monoclinic crystal of **5B** contained space group *P1* and *C2*, respectively. Peptide **5A** exhibited two molecules (**A** in orange and **B** in green color, Figure 5.3a) in the asymmetric unit. The measured backbone torsion angles (Table 5.1) of **5A** and **5B** showed that they had extended backbone conformation. Molecule **A** and **B** of peptide **5A** were interconnected through intermolecular H-bond to form an antiparallel β-sheet arrangement along *a* direction (Figure 5.3b).

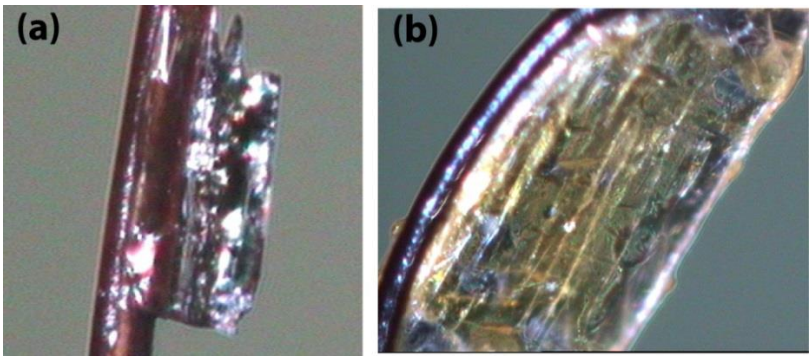

Figure 5.2. *The crystal structures of tripeptides (a)* ***5A*** *and (b)* ***5B****.*

Table 5.1. The measured backbone torsion angles (deg) of **5A** and **5B**

Torsion angles	Boc-Gly-L-Phg-D-Phe-OMe (**5A**)		Boc-Gly-L-Phg-D-Phg-OMe (**5B**)
	Molecule **A**	Molecule **B**	
ϕ1	C5-N1-C6-C7= -59.8(4)	C30-N4-C31-C32= 155.7(3)	C5-N1-C6-C7= 172.9(3)
ϕ2	C7-N2-C8-C15= -141.4(3)	C32-N5-C33-C40= -128.7(3)	C7-N2-C8-C15= -138.0(3)
ϕ3	C15-N3-C16-C24= 141.1(3)	C40-N6-C41-C49= 133.6(3)	C15-N3-C16-C23= 142.3(3)
ψ1	N1-C6-C7-N2= 150.1(3)	N4-C31-C32-N5= -143.2(3)	N1-C6-C7-N2= -175.1(3)
ψ2	N2-C8-C15-N3= 112.7(3)	N5-C33-C40-N6= 140.9(3)	N2-C8-C15-N3= 141.3(3)
ψ3	N3-C16-C24-O6= 8.0(5)	N6-C41-C49-O12= -109.7(3)	N3-C16-C23-O25= 18.1(4)
ω1	O1-C5-N1-C6= 165.2(3)	O7-C30-N4-C31= 175(3)	O1-C5-N1-C6= -166.4(3)
ω2	C6-C7-N2-C8= -179.9(3)	C31-C32-N5-C33= -174.4(3)	C6-C7-N2-C8= 179.4(3)
ω3	C8-C15-N3-C16= -175.4(3)	C33-C40-N6-C41= 172(3)	C8-C15-N3-C16= -175.3(3)

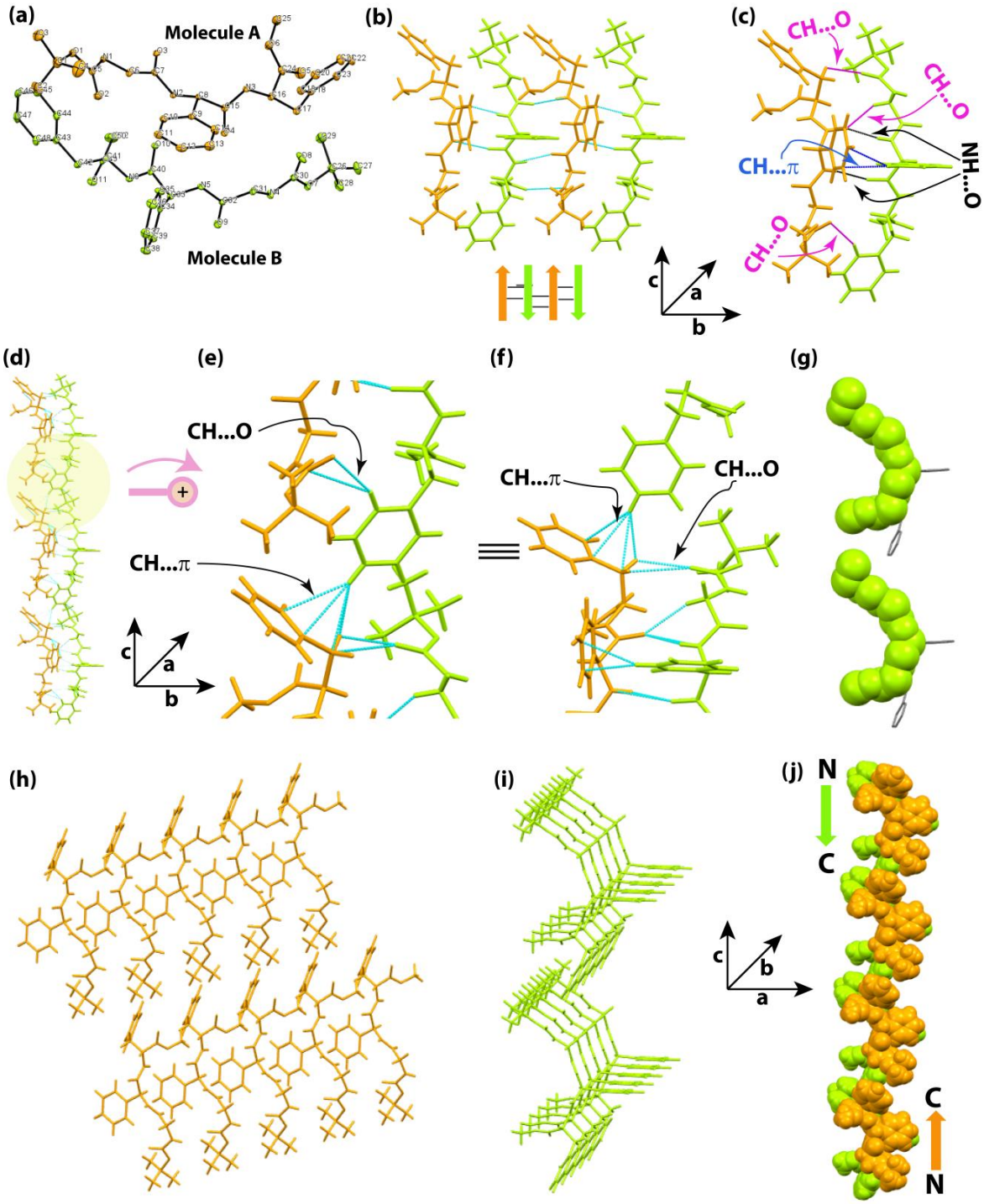

Figure 5.3. *(a) The ORTEP diagram with an ellipsoid of 30% probability, (b) antiparallel β-sheet along a axis, (c) non-covalent interactions, (d) higher-order assembly along a axis, (e) two* ***A*** *molecules are held by one* ***B*** *molecule, (f) two* ***B*** *molecules are held by one* ***A*** *molecule, (g) a partial spacefill representation of helical species of* ***B*** *molecules,(h) the individual capped sticks representation of self-assembled molecule* ***A****, (i) the individual capped sticks representation of self-assembled helical species of molecule* ***B****, and (j) the spacefill representation of helix-like structure in molecular packing along b axis, of peptide* ***5A.***

Each subunit of **5A** was further stabilized by two C-H…π (2.83 and 2.75 Å between aromatic H of L-Phg of molecule **B** and sp^2 C of L-Phg of molecule **A**) and three C-H…O (2.57 Å between βH of D-Phe of molecule **A** and urethane carbonyl oxygen of molecule **B**; 2.70 Å between aromatic H of D-Phe of molecule **B** and urethane carbonyl oxygen of molecule **A**; 2.43 Å between αH of Gly of molecule **B** and amide oxygen of L-Phg of molecule **A**) interactions (Figure 5.3c). It was further self-assembled in higher-order packing along crystallographic *a*-direction (Figure 5.3d). The structure was formed through the interaction of C-H…π (average CH-π distance 2.83 Å, the aromatic C-H of D-Phe of one particular **B** molecule and aromatic π of D-Phe of **A** molecule, Figure 5.3e) and C-H…O (average CH…O distance 2.70 Å, the aromatic C-H of D-Phe of that particular **B** molecule and the C=O of Boc of another **A** molecule). Similarly, two **B** molecules were stabilized by similar interactions with a nearby **A** molecule (Figure 5.3f). The backbone orientation of two consecutive **B** molecules of **5A** along the *b* axis appeared as a helix-like stretch (Figure 5.3g). The individual representation of self-assembled molecule **A** and **B** also displayed in Figure 5.3h and Figure 5.3i, respectively. The molecular packing along *b* direction also exhibited a helix-like structure (Figure 5.3j).

On the other hand, peptide **5B** exhibited one molecule in the asymmetric unit, and they were interconnected to form antiparallel β-sheet through intermolecular H-bonding along the *a* axis (Figure 5.4b). Each subunit of **5B** was further stabilized by two C-H…π (2.76 and 2.73 Å) and two C-H…O (2.61 and 2.45 Å) interactions (Figure 5.4c). Interestingly, it self-assembled to form supramolecular double helix-like architecture with a helical pitch of 18.53 Å in higher-order packing along the *b* axis (Figure 5.4 d and 5.4 g). This double helix was further stabilized through C-H…π interaction with average distance (CH-π) 2.79 Å and C-H…O (2.40 Å) interactions. Two subunits formed a dimer connected by two-fold rotational symmetry. No water molecule or solvent was observed inside the double helix. To the best of our knowledge, this is the first crystallographic report where alternating D/L unnatural amino acid containing small tripeptide exhibited double helix-like architecture. All crystallographic data are listed in section 5.16.

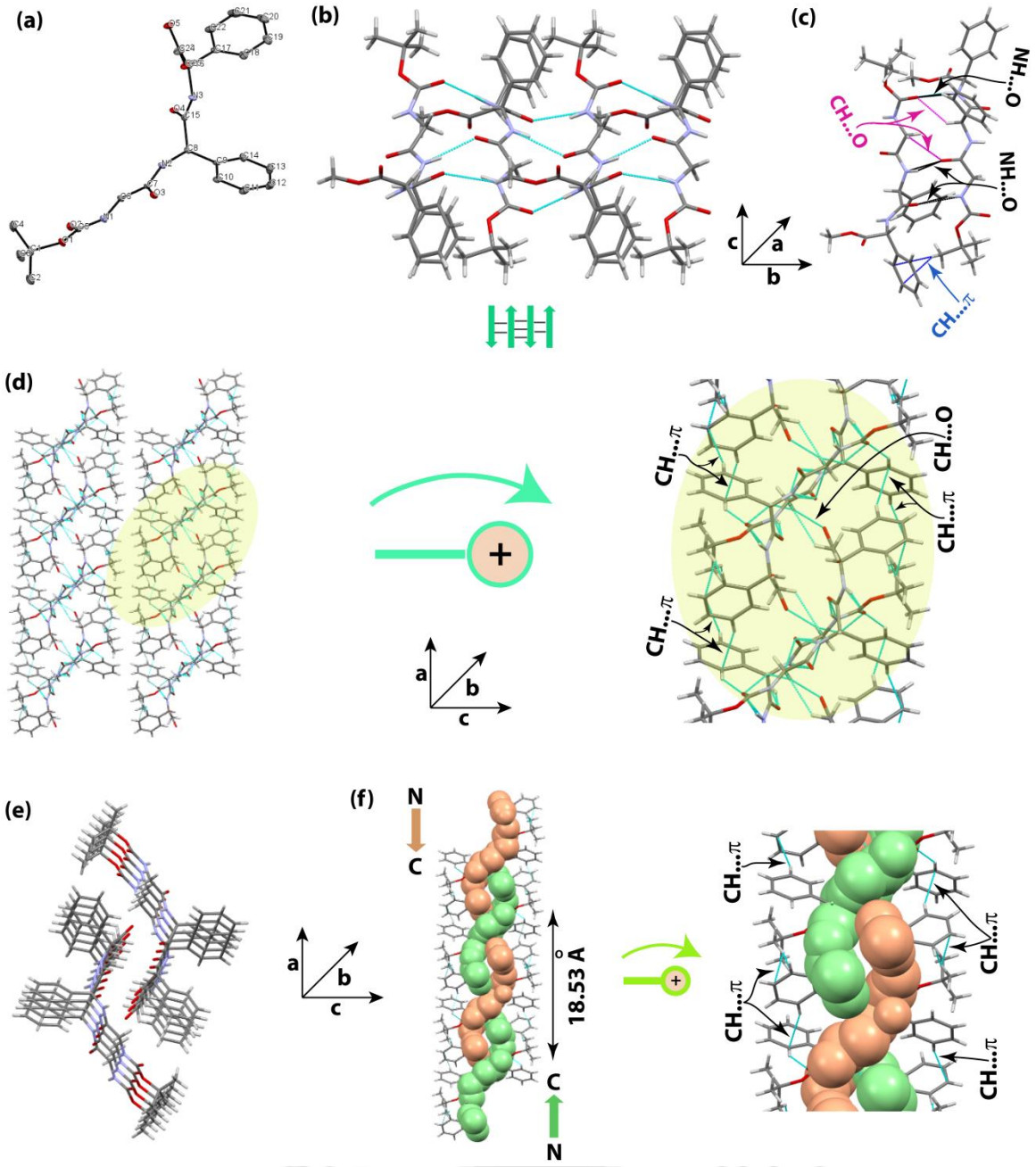

Figure 5.5. *The ORTEP diagram with an ellipsoid of 30% probability, (b) antiparallel β-sheet along a axis, (c) non-covalent interactions, (d) double helix-like structure in higher-order along the b axis, (e) The individual capped sticks representation of self-assembled double strands, and (f) spacefill representation of double helix-like structure along the b axis, of peptide* ***5B***

5.5. Comparison of the molecular structure of peptide 5A and 5B

Next, we compared the molecular structures of alternating L/L amino acid-containing peptides, **4A,** and **4B** (chapter 4) and newly designed alternating D/L amino acid-

containing peptides, **5A** and **5B**. The peptide **4A** contained L-Phe amino acid residue at the center of the sequence, and its side chain phenyl ring was connected with the backbone Cα through a methylene group. Therefore, no significant steric crowding was observed between ring hydrogens and Cα proton. As a result, the Cα became flexible and backbone oriented to form an open turn (Figure 5.6a) structure. On the other hand, a significant steric repulsion observed between *ortho* protons of the phenyl ring and Cα proton in peptide **4B** as it contained L-Phg at the central position of the sequence and its side chain phenyl ring was directly attached to the backbone Cα, therefore, the backbone was extended, and it adopted parallel β-sheet (Figure 5.6b) structure.

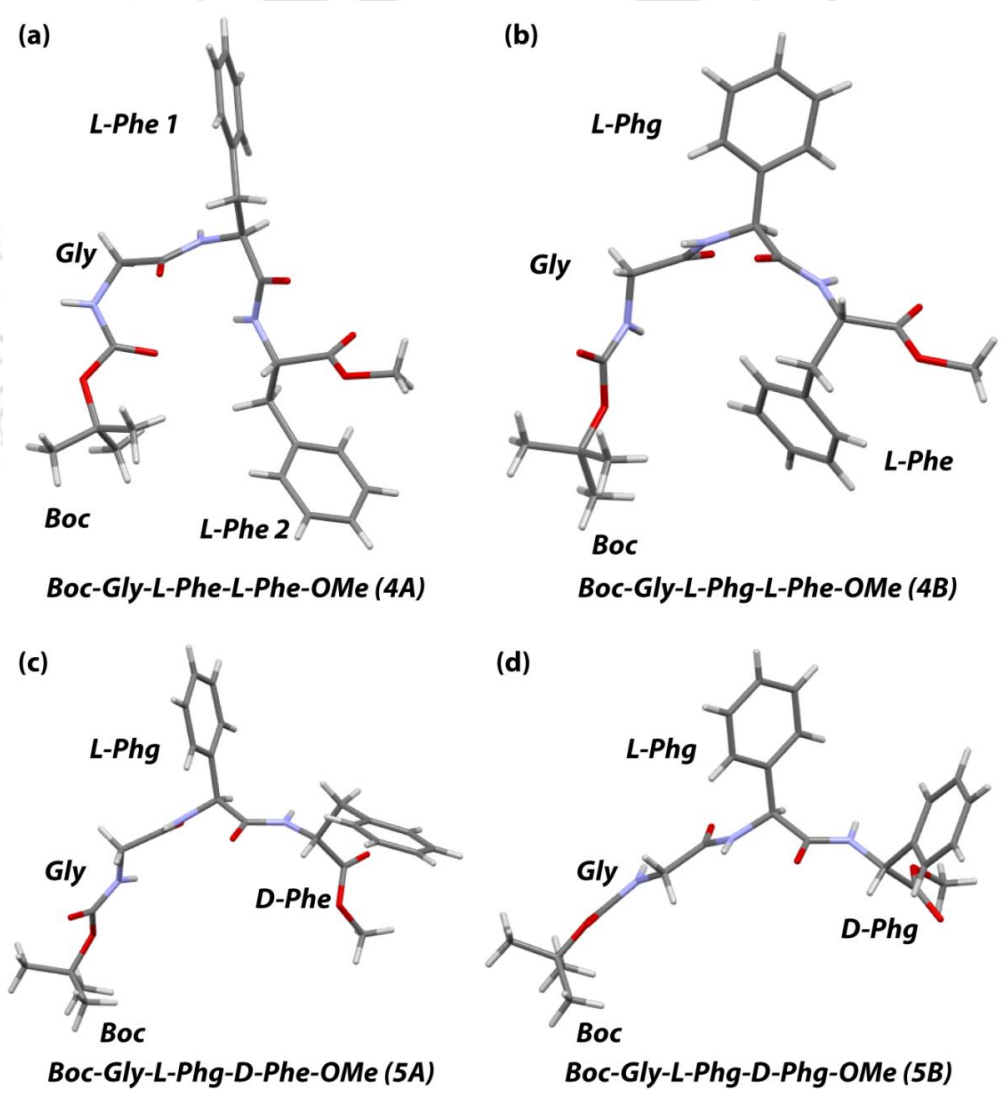

Figure 5.6. *Comparison of the molecular structures of* ***4A, 4B, 5A,*** *and* ***5B.***

The newly designed alternating D/L amino acid-containing peptides, **5A** and **5B,** also contained L-Phg at the central position of their sequence like **4B**. Therefore, a similar steric repulsion is present between Cα and *ortho* hydrogens of L-Phg, and it causes backbone extension. Moreover, in the C-terminus, both **5A** and **5B** contained D-Phe and D-Phg, respectively. The consecutive existence of L and D amino acid forces their side chains to flank in the same direction, which caused more backbone elongation than the L/L amino acid-containing peptides. The backbone elongation is more in **5B** for the presence of C-terminal D-Phg (the aromatic ring is directly attached to Cα) than **5A** (Figure 5.6c and 5.6d).

5.6. Investigation of intra- or intermolecular H-bond in solution

Next, to investigate the existence of intra- or inter-molecular H-bonds in these peptides, we performed a solvent titration NMR experiment. For that, the d_6-DMSO solvent was gradually added to the $CDCl_3$ solution of these peptides in the NMR tube and recorded NMR spectra. As d_6-DMSO acts as a hydrogen bond accepting solvent; therefore, by increasing its concentration, the peptide NHs are shifted to the downfield region.

The obtained solvent titration curve indicated that increasing the percentage of d_6-DMSO in $CDCl_3$ solution (v/v) from 0 to 20 % for **5A** and 0 to 12% for **5B**, a monotonic downfield chemical shift of NHs was observed. The net change of chemical shifts ($\Delta\delta$(NH)) were 0.43 (Gly NH), 0.48 (L-Phg NH), and 0.23 ppm (D-Phe NH) for **5A** (Figure 5.7 and Table 5.2), and 0.38 (Gly NH), 0.35 (L-Phg NH), and 0.57 ppm (D-Phg NH) for **5B**, respectively (Figure 5.7 and Table 5.3), indicating all NHs were involved in intermolecular H-bonding interactions, which was also supported by the SC-XRD experiment.

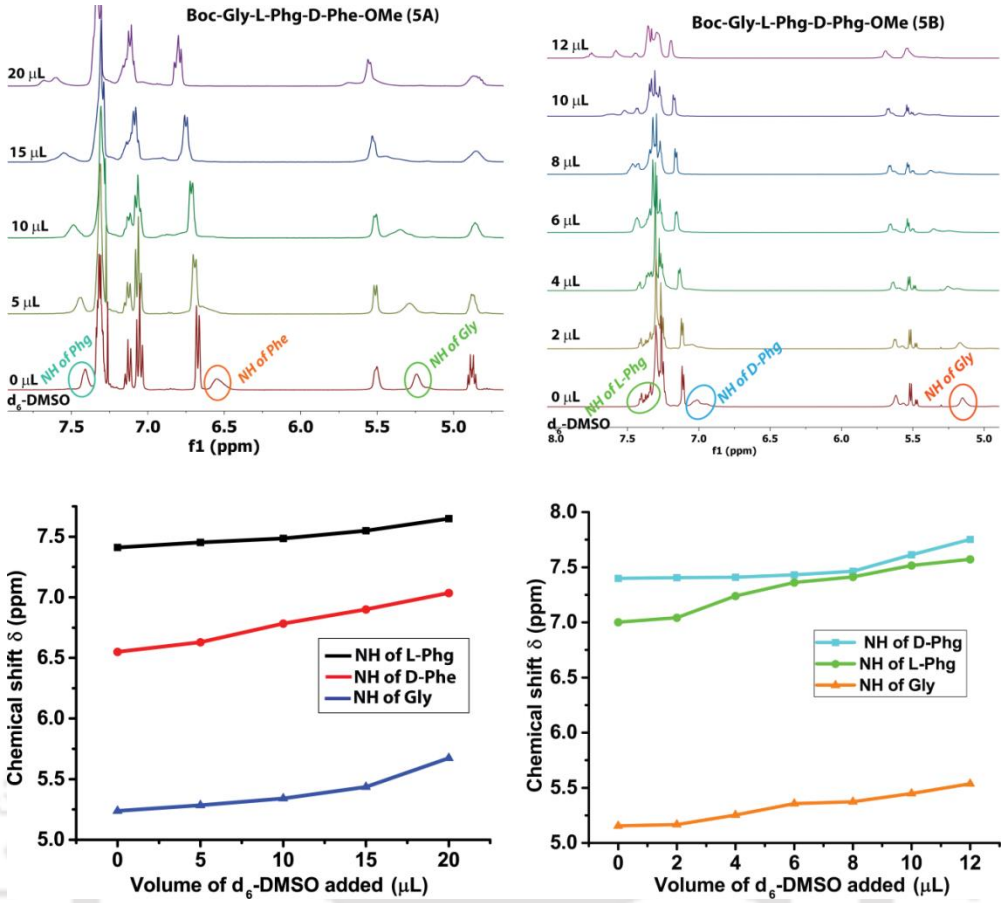

Figure 5.7. *NMR solvent titration spectra of the NH proton of* ***5A*** *and* ***5B.***

Table 5.2. NMR solvent titration data of peptide **5A** in $CDCl_3$ with d_6-DMSO

Sl. No.	***The volume of d_6-DMSO added (µL)***	***Chemical shifts δ (ppm)***					
		NH of L-Phg	***Δδ(NH) of L-Phg***	***NH of D-Phe***	***Δδ(NH) of D-Phe***	***NH of Gly***	***Δδ(NH) of Gly***
1	0	7.410		6.550		5.238	
2	5	7.452		6.630		5.285	
3	10	7.485		6.783		5.341	
4	15	7.549		6.900		5.435	
5	20	7.649	0.239	7.036	0.486	5.674	0.436

Table 5.3. NMR solvent titration data of peptide **5B** in $CDCl_3$ with d_6-DMSO

Sl. No.	*The volume of d_6-DMSO added (μL)*	*Chemical shifts δ (ppm)*					
		NH of D-Phg	*Δδ(NH) of D-Phg*	*NH of L-Phg*	*Δδ(NH) of L-Phg*	*NH of Gly*	*Δδ(NH) of Gly*
1	0	7.002		7.399		5.154	
2	2	7.0042		7.406		5.167	
3	4	7.239		7.409		5.253	
4	6	7.361		7.432		5.357	
5	8	7.412		7.463		5.374	
6	10	7.516		7.613		5.449	
7	12	7.573	0.571	7.752	0.353	5.536	0.382

5.7. Characterization of conformation of 5A and 5B by NOE interactions in solution

Next, to understand the conformation of these peptides in solution, we performed 2D [^{1}H, ^{1}H] NOESY experiment in $CDCl_3$ medium. In peptide **5A**, we observed two crucial inter-residual interactions, namely NH Phg ↔ H_α Gly and NH Phe ↔ H_α Phg and others NOEs, e.g. H_α Phg ↔ aromatic protons of Phg, NH Phe ↔ *meta* aromatic protons of Phe, NH Phe ↔ aromatic protons of Phg (Figure 5.8). This result indicated that peptide **5A** probably adopted a turn-like structure in solution, which also further supported by the CD experiment (*vide infra*). However, we could not observe any effective intra- or inter-residual NOE interactions for peptide **5B**.

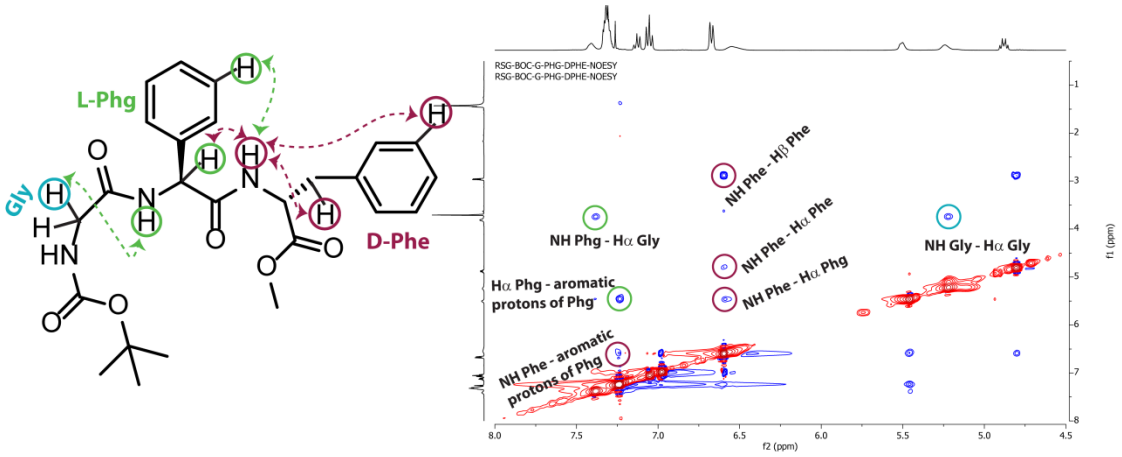

Figure 5.8. *NOE interactions of peptide* ***5A****, obtained from 2D NOESY NMR experiment in* $CDCl_3$

5.8. Conformation analysis by CD experiment in solution

To investigate the conformation of these peptides, we performed the CD experiment in solution. For that, we prepared 1.5 mM each peptide solution in 30% acetonitrile-water medium and incubated them at 37 ^{o}C for seven days.

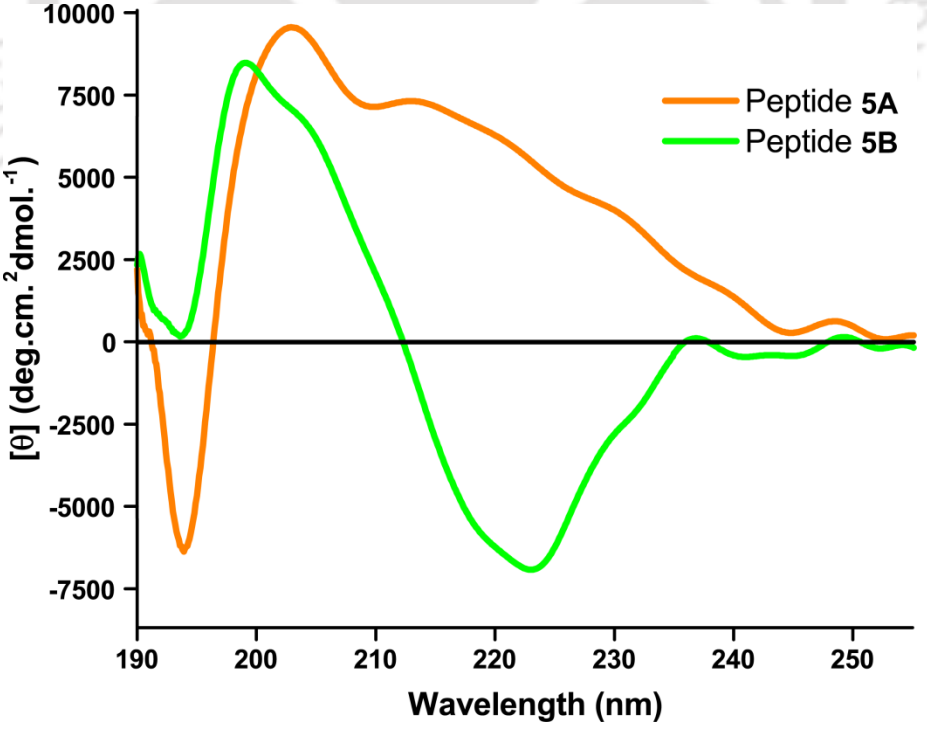

Figure 5.9. *CD profile of peptide* ***5A*** *(magenta curve) and* ***5B*** *(cyan curve)in 30% acetonitrile-water medium using a concentration of 300*μ*M.*

Then, the solutions (1.5 mM) were diluted to 300 µM (to avoid high voltage in CD), and from them, 400 µL of each were taken separately in a quartz cuvette, and CD was measured spanning the wavelength range between 190-260 nm (1 mm path length and 1 nm bandwidth). The obtained curve of peptide **5A** (Figure 5.9, orange curve) showed the positive Cotton effect at 202 nm and negative Cotton effect at 194 nm, which indicated that it adopted a turn-like structure in solution. Whereas peptide **5B** showed a negative Cotton effect at 223 nm and a positive Cotton effect at 198 nm, indicating the presence of a β-sheet conformation in solution.

5.9. Monitoring the self-association of 5A and 5B in solution by various microscopic experiment

Then we checked the morphology of these peptides to understand their self-association behavior. The morphologies of these self-associated tripeptides were analyzed under an optical microscope, a FE-SEM, and a TEM. For that, we prepared a 1.5 mM solution of each of them in 30% acetonitrile-water and incubated them at 37 ^{o}C for seven days.

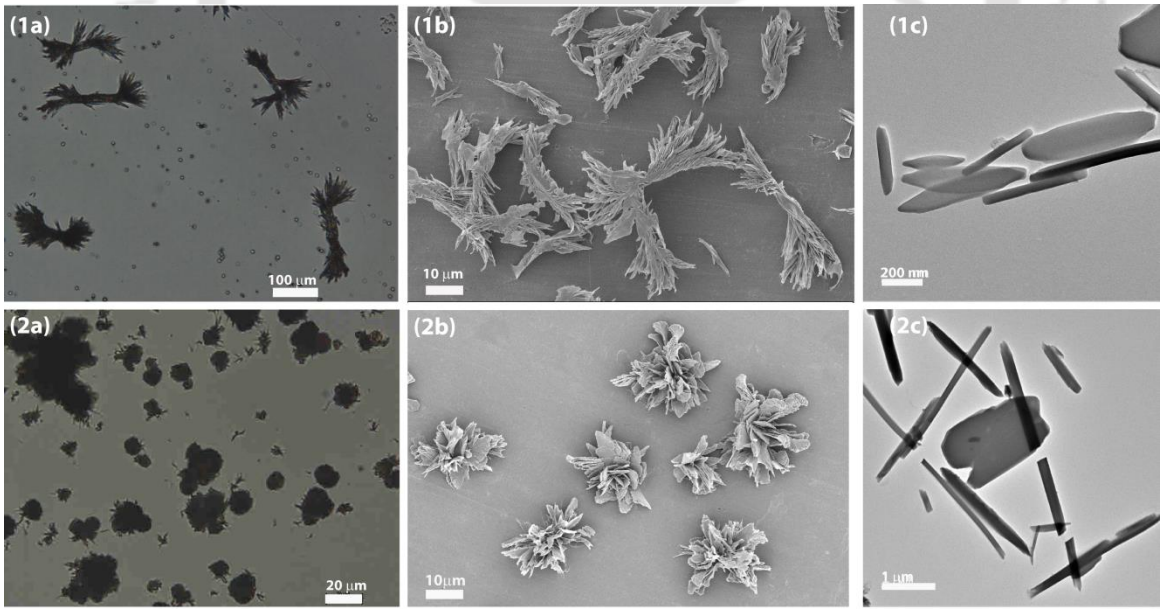

Figure 5.10. *Optical microscopic, FESEM and TEM images of self-associated tripeptides (1a), (1b) and (1c) of* ***5A*** *and (2a), (2b) and (2c) of* ***5B****, respectively, in 30% acetonitrile-water.*

These solutions were drop-cast on a microscopic slide for analysis using an optical microscope and over Al-foil for the FE-SEM study. The obtained optical microscope and

FE-SEM images both indicated that **5A** and **5B** self-associated in solution to form highly organized a bunch of flower-petals-like (Figure 5.10) and a flower-like (Figure 5.10) architecture, respectively. Next, to get more detail information about the morphology of these self-associated peptides, TEM experiments were performed. Both peptide **5A** and **5B** exhibited rod-like microcrystals of various sizes under TEM (Figure 5.10).

5.10. Conclusion

In conclusion, we demonstrated the unique crystallographic signatures of both N- and C-protected alternating D/L amino acids containing small tripeptides, Boc-Gly-L-Phg-D-Phe-OMe (**5A**) and Boc-Gly-L-Phg-D-Phg-OMe (**5B**). The SC-XRD experiment revealed that they adopted anti-parallel β-sheet structures, but **5A** further self-assembled to form single helix-like architecture through CH-π and C-H…O interactions in higher-order along the crystallographic *b* axis whereas **5B** self-associated through CH-π and C-H…O interactions to form double-helix like architecture along the crystallographic *b* axis. They also self-associated to form flower-petals-like and flower-like architectures in 30% acetonitrile-water medium, respectively. The differences in molecular arrangements among these peptides are due to the presence of the methylene group (D-Phe) or absence of methylene group (D-Phg) at the side chain. The obtained results may be helpful for the design of a supramolecular single or double helix-like structure using alternating D/L amino acids.

5.11. Experimental section

5.11.1. Materials and instrumentations

As described in chapter 8

5.11.2. General procedure for the synthesis of tripeptides

As described in chapter 4 section 4.12.2

5.11.3. Sample preparation

2.13 mM peptide **5A** and 2.19 mM peptide **5B** solutions were prepared in two different Eppendorf vials (2 mL) by adding 1 mL 30% CH_3CN-H_2O solution. Then, we prepared a 1 mL (1.5 mM) solution (stock solution) from the above solutions for each peptide. These stock solutions were incubated for 7 days at 37 ^oC.

5.12. Characterization data

Boc-Gly-L-Phg-D-Phe-OMe 5A.

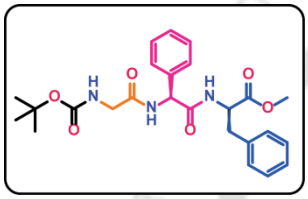

White solid; mp 171-173 ^oC. ^1H NMR ($CDCl_3$; 400 MHz) δ 1.43 (9H, s); 2.97-2.95 (2H, d, *J* = 6 Hz); 3.70 (3H, s); 3.81 (2H, s); 4.90-4.85 (1H, q, *J* = 6 Hz, *J* = 8 Hz); 5.24 (1H, brs); 5.50 (1H, brs); 6.55 (1H, brs); 6.68-6.66 (2H, d, *J* = 7.2 Hz), 7.07-7.03 (2H, t, *J* = 7.2 Hz); 7.14-7.11 (1H, t, *J* = 7.2 Hz); 7.33-7.29 (5H, m); 7.41 (1H, brs). ^{13}C NMR ($CDCl_3$; 100 MHz) δ 28.4, 37.8, 44.3, 52.6, 53.3, 57.1, 80.3, 127.1, 127.4, 128.6, 129.2, 129.3, 129.4, 135.4, 137.6, 156.2, 169.2, 169.4, 171.7. HRMS (ESI): calculated $[M+H]^+$ 470.2213, found m/z . 470.4121. HPLC: retention time (t_R) = 11.9 min. Isolated pure product 689 mg (yield: 74% w.r.t. starting meterial Boc-L-Phg).

Boc-Gly-L-Phg-D-Phg-OMe 5B.

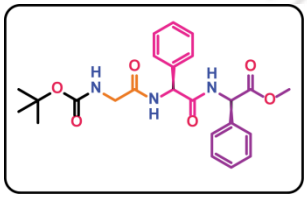

White solid; mp 168-172 ^oC. ^1H NMR ($CDCl_3$; 600 MHz) δ 1.41 (9H, s); 3.70 (3H, s); 3.82 (2H, s); 5.20 (1H, br); 5.52-5.51 (1H, d, *J* = 7.2 Hz); 5.66 (1H, brs); 7.12-7.11 (2H, d, *J* = 6.6 Hz), 7.29-7.23 (10H, m). ^{13}C NMR ($CDCl_3$; 150 MHz) δ 28.4, 44.4, 53.2, 56.8, 80.4, 127.1, 127.6, 128.7, 129.2, 135.8, 137.4, 156.1, 169.1, 171.0. HRMS (ESI): calculated $[M+H]^+$ 456.2136, found m/z . 456.2362. HPLC: retention time (t_R) = 11.8 min. Isolated pure product 650 mg (yield: 71% w.r.t. starting meterial Boc-L-Phg).

5.13. References

1. Watson, J. D.; Crick, F. C. H. Molecular structure of nucleic acids; a structure for deoxyribose nucleic acid. *Nature* **1953**, *171*, 737-738.
2. Nelson, D. L; Cox, M. M. *Lehninger's Principles of Biochemistry*, 7th ed.*;* W. H. Freeman and Company: New York, 2017.
3. Al Toma, R. S.; Brieke, C.; Cryle, M. J.; Süssmuth, R. D. Structural aspects of phenylglycines, their biosynthesis and occurrence in peptide natural products. *Nat. Prod. Rep.* **2015**, *32*, 1207-1235.
4. Mast, Y.; Wohlleben, W. Streptogramins - two are better than one! *Int. J. Med. Microbiol*. **2014**, *304*, 44-50.
5. Wallace, B. A.; Ravikumar, K. The gramicidin pore: crystal structure of a cesium complex. *Science* **1988**, *241*, 182-187.
6. Bunkóczi, G.; Vértesy, L.; Sheldrick, G. M. The antiviral antibiotic feglymycin: first direct-methods solution of a 1000+ equal-atom structure. *Angew. Chem. Int. Ed*. **2005**, *44*, 1340-1342.
7. Hamburger, J. B.; Hoertz, A. J.; Lee, A.; Senturia, R. J.; McCafferty, D. G.; Loll, P. J. A crystal structure of a dimer of the antibiotic ramoplanin illustrates membrane positioning and a potential Lipid II docking interface. *Proc. Natl. Acad. Sci. U. S. A.* **2009**, *106*, 13759-13764.
8. Dev, D.; Palakurthy, N. B.; Thalluri, K.; Chandra, J.; Mandal, B. Ethyl 2-cyano-2-(2-nitrobenzene sulfonyloxyimino)acetate (*o*-NosylOXY): A recyclable coupling reagent for racemization free synthesis of peptide, amide, hydroxamate and ester. *J. Org. Chem*. **2014**, *79*, 5420-5431.

5.14. Selected spectra

5.14.1. Spectra of peptide 5A

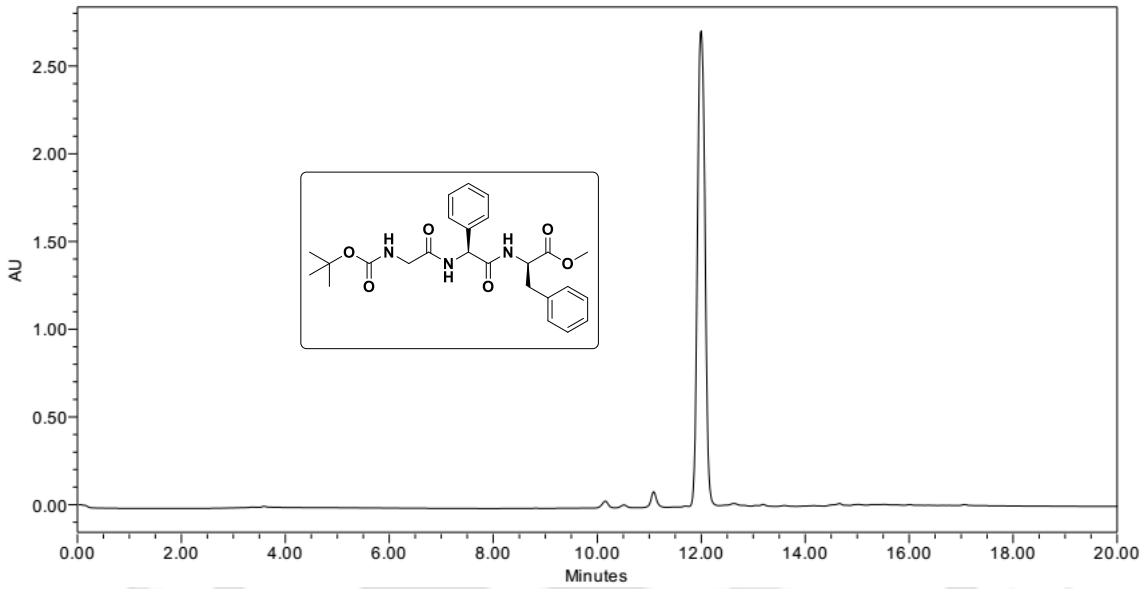

Figure 5.11. *HPLC profile picture of purified peptide* ***5A*** *(A linear gradient was used from 5 to 100% CH_3CN till 8 min, and a total run time of 20 min, flow rate 1mLmin^{-1})*

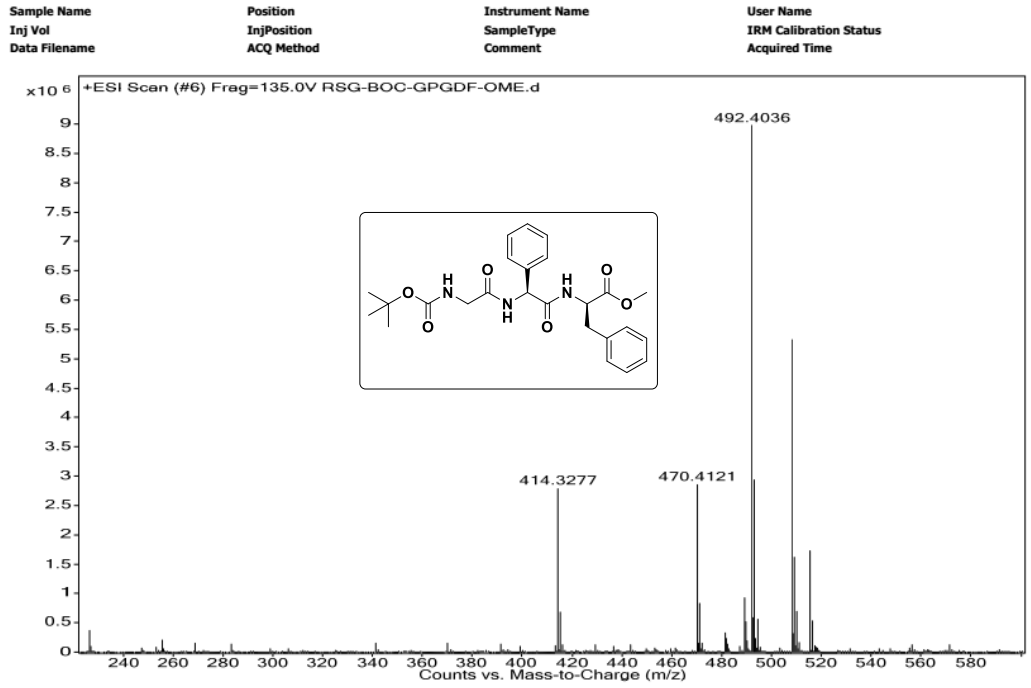

Figure 5.12. *MS spectra of peptide* ***5A***

RSG-GPGDF-0-1H
RSG-GPGDF-0-1H

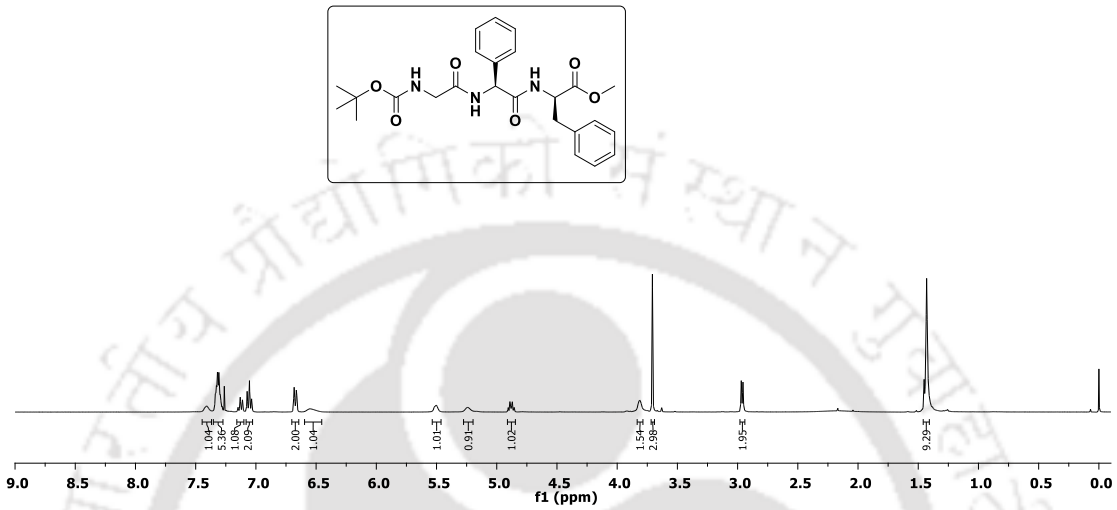

Figure 5.13. *^{1}H NMR spectra of peptide* ***5A***

RSG-GPGDF-13C
RSG-GPGDF-13C

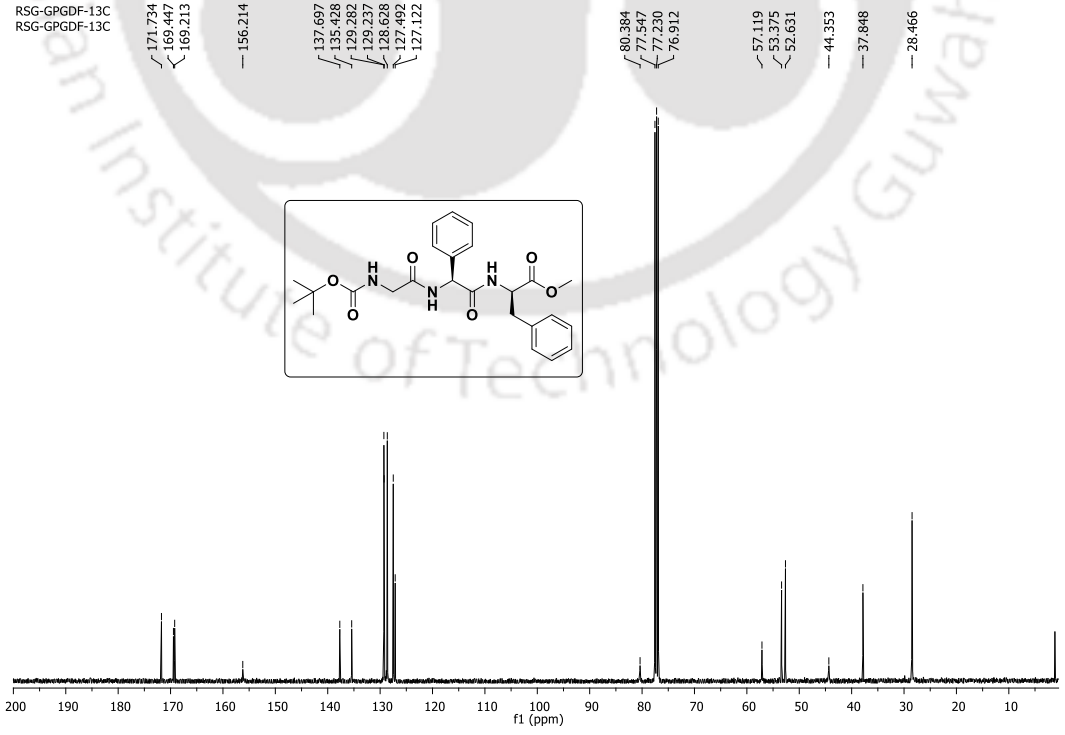

Figure 5.14. *^{13}C NMR spectra of peptide* ***5A***

5.14.2. Spectra of peptide 5B

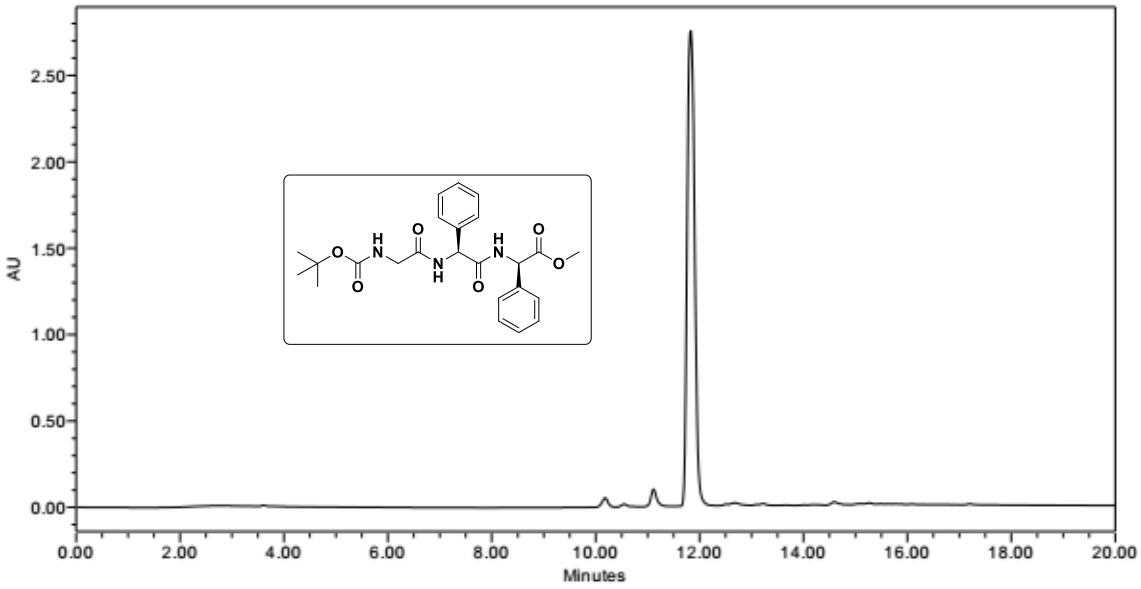

Figure 5.15. *HPLC profile picture of purified peptide* ***5B*** *(A linear gradient was used from 5 to 100% CH_3CN till 8 min, and a total run time of 20 min, flow rate 1mLmin^{-1})*

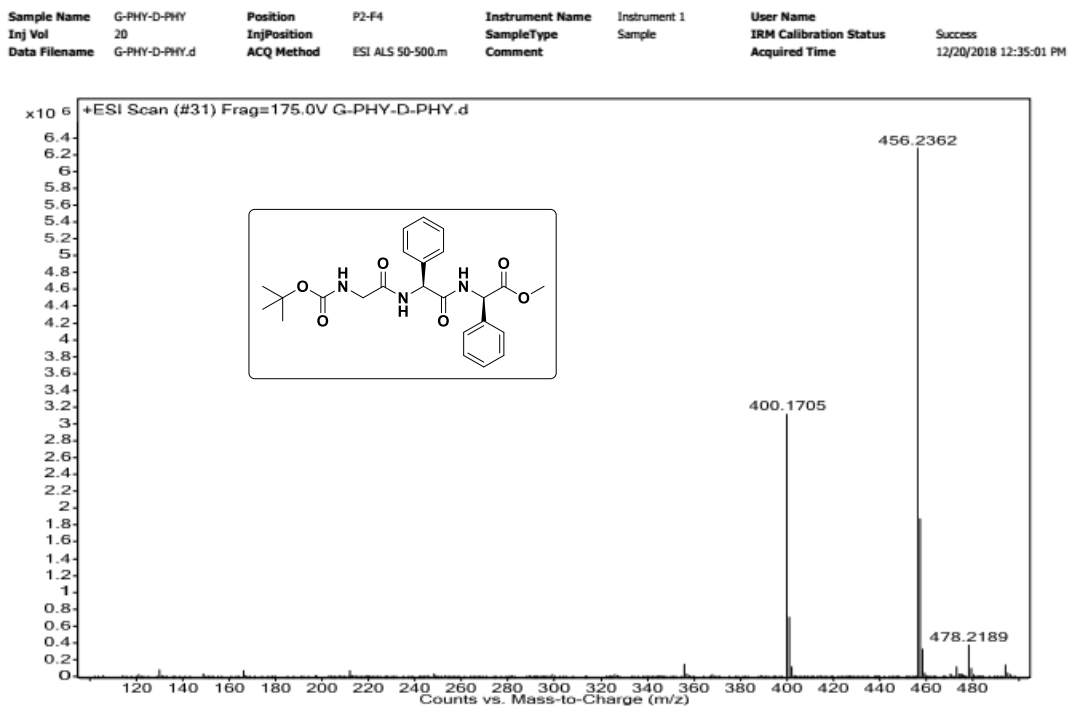

Figure 5.16. *MS spectra of peptide* ***5B***

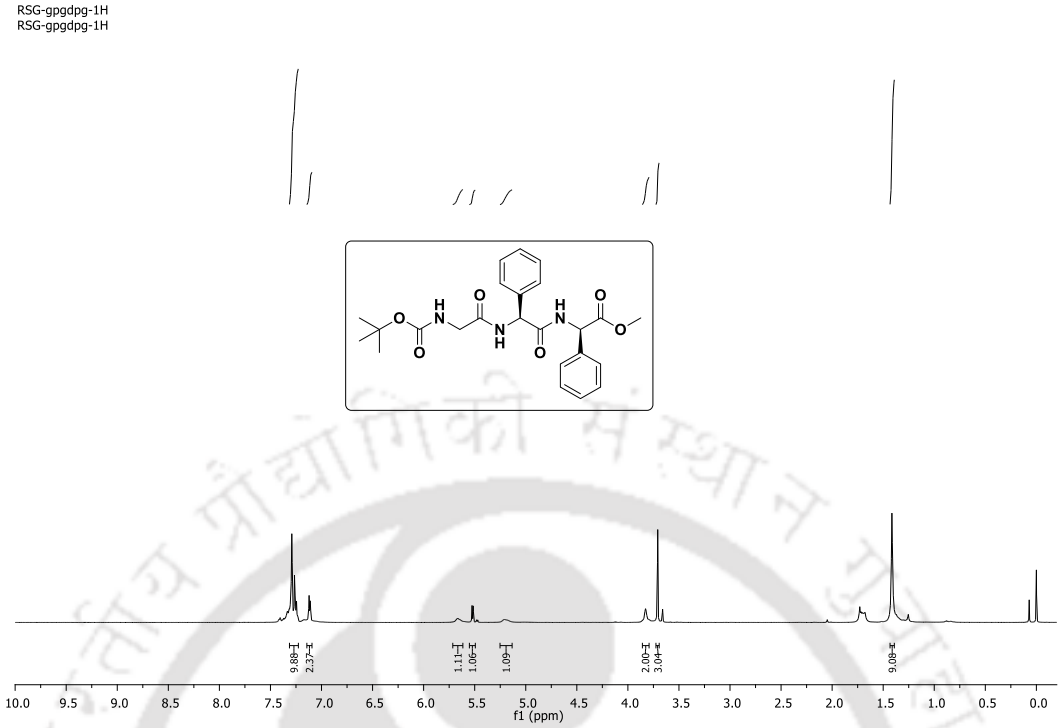

Figure 5.17. *^{1}H NMR spectra of peptide* ***5B***

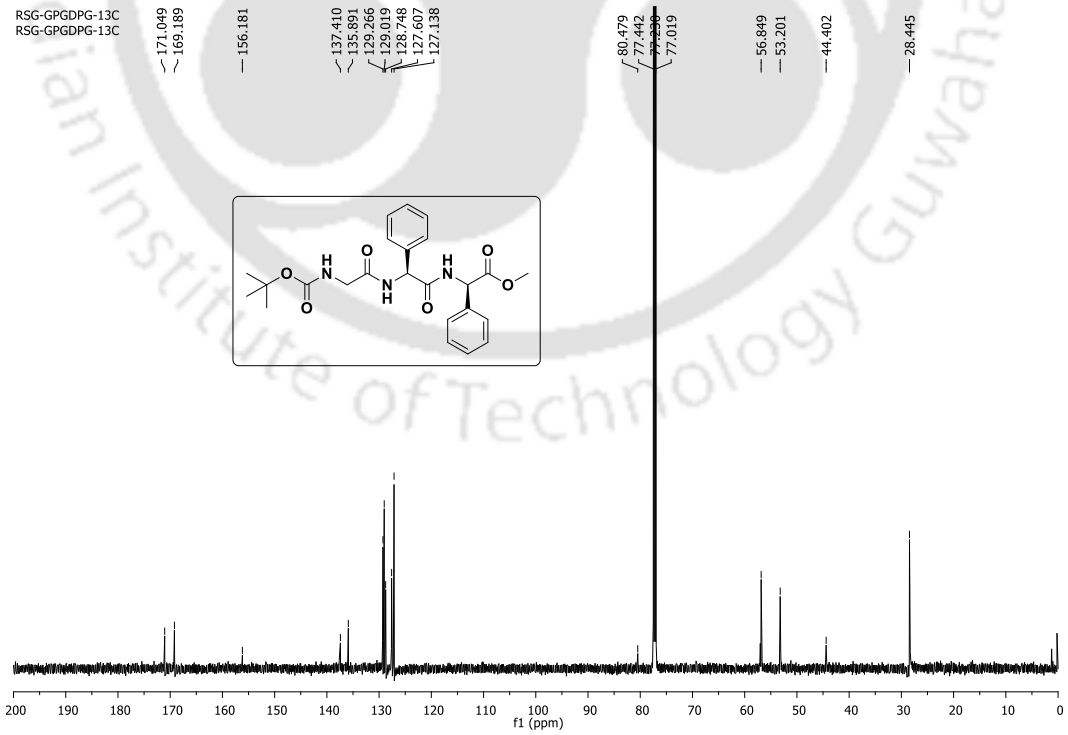

Figure 5.18. *^{13}C NMR spectra of peptide* ***5B***

5.15. Crystallographic data

Table 5.4. Hydrogen bonding distances (Å) and Bond angles (deg) of peptide **5A** and **5B**

molecule	***D−H···A***	***d(D···H)/ Å***	***d(H···A) /Å***	***d(D···A)/Å***	***<D−H··· A/°***	***symmetry operation***
Peptide **5A**	N1-H1···O11	0.86	2.39	3.009(2)	130	x,-1+y,z
	N2-H2···O10	0.86	2.09	2.906(2)	158	
	N3-H3···O9	0.86	2.05	2.899(2)	168	x,-1+y,z
	N4-H4···O6	0.86	2.56	3.390(2)	163	x,1+y,z
	N5-H5···O4	0.86	2.03	2.870(2)	164	
	N6-H6···O3	0.86	2.01	2.850(2)	166	x,1+y,z
	C8-H8···O9	0.98	2.53	3.400(2)	149	x,-1+y,z
	C17-H17B···O8	0.97	2.57	3.179(2)	121	
	C20-H20···O5	0.93	2.58	3.336(2)	139	-1+x,y,z
	C31-H31A···O4	0.97	2.43	3.278(2)	145	
	C33-H33···O3	0.98	2.39	3.213(2)	142	x,1+y,z
	C37-H37···O3	0.93	2.59	3.432(3)	152	-1+x,1+y,z
	C50-H50B···O2	0.96	2.51	3.367(2)	148	1+x,y,z
Peptide **5B**	N1-H1···O4	0.86	2.18	3.021(1)	164	1/2-x,-1/2+y,1-z
	N2-H2···O3	0.86	2.09	2.927(1)	164	1/2-x,1/2+y,1-z
	N3-H3···O2	0.86	2.12	2.968(1)	167	1/2-x,-1/2+y,1-z
	C6-H6B···O5	0.97	2.41	3.308(1)	155	1/2+x,1/2+y,z
	C14-H14···O2	0.93	2.45	3.296(1)	151	1/2-x,-1/2+y,1-z

Table 5.5. Crystal parameters and refinement data of **5A** and **5B**

Parameters	***Peptide (5A)***	***Peptide (5B)***
Formula	$C_{25}\ H_{31}\ N_3\ O_6$	$C_{24}\ H_{29}\ N_3\ O_6$
Fw	469.53	455.50
Crystal system	Triclinic	monoclinic
Space group	*P 1*	*C 2*
a/Å	8.3294(6)	18.5349(8)
b/Å	9.6074(7)	8.8497(3)
c/Å	16.4130(11)	14.3748(5)
α/°	86.861(5)	90
β/°	84.758(5)	91.092(4)
γ/°	74.072(6)	90
V/Å^3	1257.12(16)	2357.45(15)
Z	2	4
D_c/g cm^{-3}	1.240	1.283
μ Mo K_α/mm^{-1}	0.089	0.093
F000	500.0	968.0
T/K	100.00(10)	100.00(10)
θ max.	28.823	28.815
Total no. of reflections	9785	5011
Independent reflections	6889	4110
Observed reflections	6025	3677
Parameters refined	621	302
R_1, I > 2σ(I)	0.0544	0.0546
wR_2, I > 2σ(I)	0.1523	0.1562
GOF (F^2)	0.787	0.817
CCDC No.	1874425	1896847

Chapter 6

On-resin Side Chain Modification of AsparticAcid- and Glutamic acid-Containing Peptides

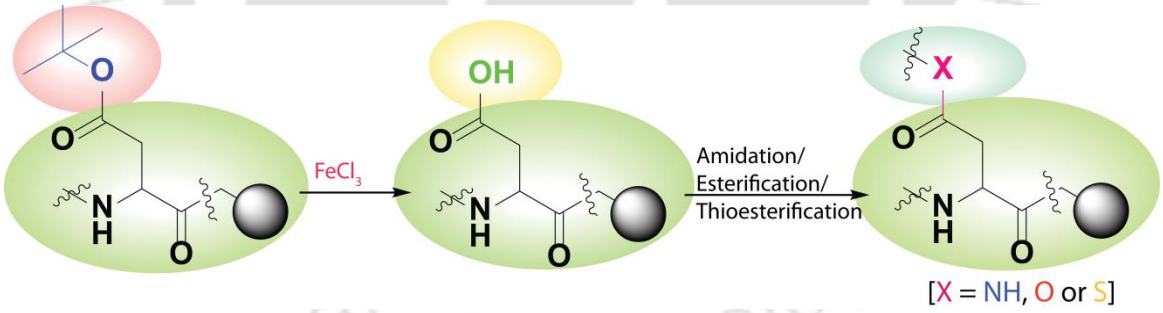

6.1. Background

We have discussed the post-translational modifications and the reported methods for modifications of peptides in Chapter 1 (section 1.8). In this chapter, we wanted to show the side-chain modification of aspartic acid and glutamic acid-containing peptide on a solid support. Normally, the tert-butyl ester protected side-chain of Fmoc-Asp/Glu are used to synthesis of peptides in SPPS. But, Allyl, Dmab, and Dmb protected side-chain of Asp/Glu are also commercially available. The Allyl, Dmab, and Dmb groups are removed by using excess phenyl silane and catalytic amount of tetrakis(triphenylphosphine)palladium(0) [$Pd(PPh_3)_4$] under an inert atmosphere; hydrazine and 20% DIPEA in 9:1 (v/v) DMF/H_2O; and 1% TFA, respectively.[1-6] But these methods suffer from some problems, e.g., the formation of side products, longer reaction time, and limited to less-acid sensitive resin.[1-6]

6.2. The existing method for removal of tert-butyl group

Moreover, tert-butyl ester is removed by various protic acids, e.g., HCl,[7] H_2SO_4,[8] HNO_3,[9] TFA,[10] and Lewis acids, such as $TiCl_4$,[11] silyl triflates,[12] $ZnBr_2$ in DCM[13] and $CeCl_3 \cdot 7H_2O$−NaI in acetonitrile.[14] But the reported methods for tert-butyl ester cleavage suffer from some problems such as high acidic conditions, corrosive, handling problems, *etc*. To the best of our knowledge, the above methods were used on tert-butyl ester cleavage in solution only. Therefore, a mild, efficient, convenient, and environmentally friendly method is needed for tert-butyl ester cleavage of the side-chain of Asp/Glu containing peptide on-resin.

6.3. Our approach

For that, we developed a Lewis acid, $FeCl_3$-based method for removal of tert-butyl group from the side-chain of Asp/Glu during SPPS. This protocol is mild, cost-effective, and Fmoc chemistry compatible and allows on-resin incorporation of amides, esters, and thioesters with good yield.

Scheme 6.1. *Overview of the reaction*

6.4. Optimization of the tert-butyl cleavage condition

At first, we optimized the tert-butyl cleavage condition. For that, we have chosen Fmoc-Asp(OtBu)-OMe (**I**) as a model substrate along with various Lewis acids and solvents, and the results are outlined in Table 6.1. The isolated yield of the deprotected product increased, and the reaction time decreased gradually with an increment of the amount of $FeCl_3$ used (entry 1-6, Table 6.1). We were delighted to get that the reaction performed well in DCM using $FeCl_3$ (1.5 equiv) at room temperature and provided a maximum yield (80%, isolated by column chromatography) within 1 h. This condition was accepted as optimum for reactions in solution.

The reaction worked well in acetonitrile also, but 5 equiv $FeCl_3$ and 6h time were required. Whereas, in DMF, THF, and methanol solvent we could not get tert-butyl deprotected product till 72h, starting material was recovered back. During optimization, we have observed that $ZnBr_2$ and $ZnCl_2$ also provided a comparative yield as $FeCl_3$ but at longer reaction time (24h and 72h, respectively). We did not get any trace of tert-butyl deprotection in the presence of $CuCl_2$, till 72h. The reaction was monitored by TLC, and the product was purified by column chromatography, which was later characterized by ^1H NMR, ^{13}C NMR, and Mass Spectrometry.

Table 6.1. Optimization of the reaction conditions[a]

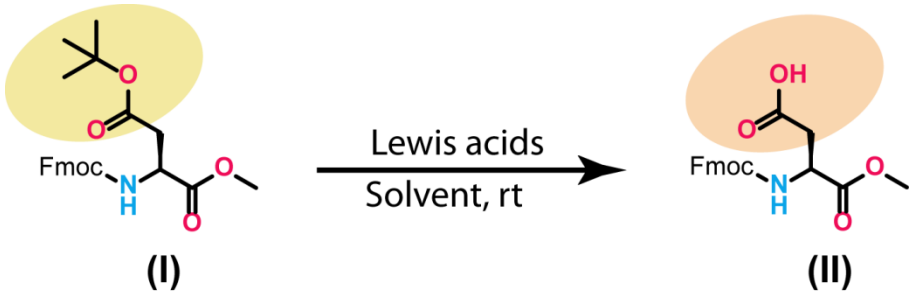

(I) (II)

Entry	Lewis acids (equiv)	Solvent	Time	Isolated yield (%)
1	$FeCl_3$ (0.1)	DCM	24h	20
2	$FeCl_3$ (0.5)	DCM	24h	45
3	$FeCl_3$ (1)	DCM	2h	70
4	$FeCl_3$ (1.5)	DCM	1h	80
5	$FeCl_3$ (2)	DCM	30 min	80
6	$FeCl_3$ (5)	DCM	15 min	80
7	$FeCl_3$ (5)	MeCN	6h	78
8	$FeCl_3$ (5)	DMF	72h	n.d.[b]
9	$FeCl_3$ (5)	THF	72h	n.d.[b]
10	$FeCl_3$ (5)	MeOH	72h	n.d.[b]
11	$ZnCl_2$ (5)	DCM	72h	73
12	$ZnBr_2$ (5)	DCM	24h	76
13	$CuCl_2$ (5)	DCM	72h	n.d.[b]

[a]Reaction condition: **I** (1 mmol), $FeCl_3$, solvent (2 mL), rt. [b]Product spot could not be observed in TLC.

6.5. Compatibility with some frequently used protecting groups in solution

Next, we wanted to check the selectivity of this protocol. For that, we performed time-dependent HPLC of the various protecting group containing substrates. At first, we applied the optimized condition (1.5 equiv of $FeCl_3$) on the compound (**I**), and we observed that $FeCl_3$ selectively removed tBu from **I** without affecting the methyl group (Table 6.2). An overlay of the HPLC profiles (Figure 6.1) revealed a gradual conversion of the tert-butyl ester (**I**) (t_R = 8.6 min) to its free carboxylic acid analog (**II**) (t_R = 6.8 min). At 6 min, both (**I**) and (**II**) existed in 50:50 ratio, and at 20 min, in 95:5 ratio. After 1 h, we observed a 98% conversion from (**I**) to (**II**). The detailed procedure is discussed in section 6.14.3.

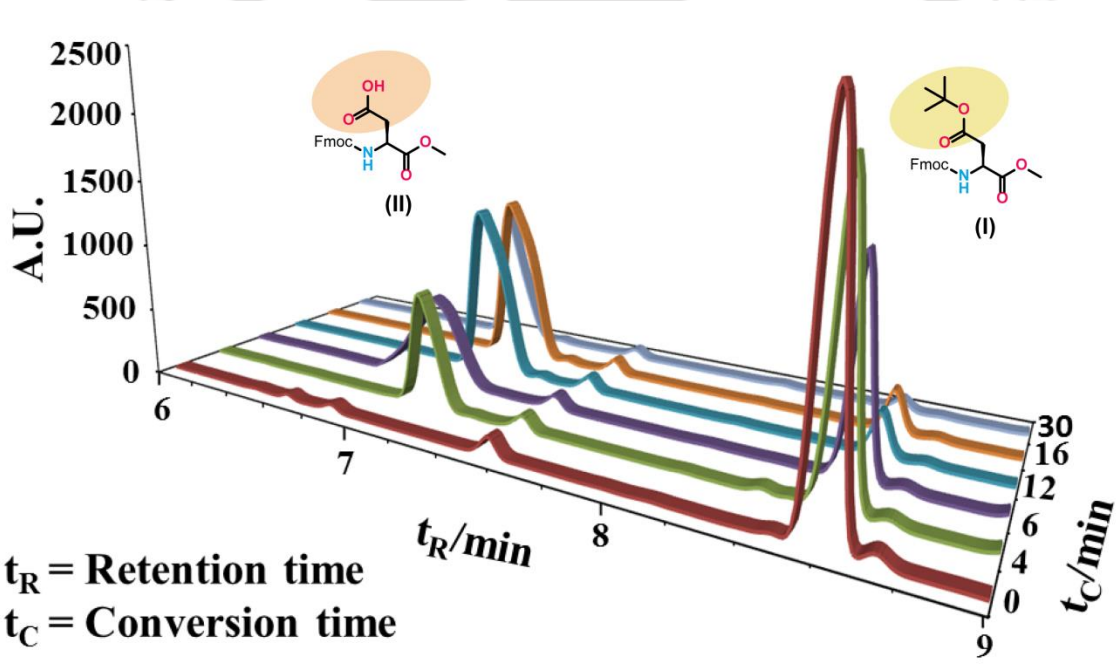

Figure 6.1. *A time-dependant HPLC profile of conversion of (**I**) to (**II**)*

Similarly, we applied this optimized condition on the benzyl ester derivative of **I** (Fmoc-Asp(OBzl)-OMe), the allyl ester of benzoic acid (Allyl benzoate) and the ethyl ester of benzoic acid (Ethyl benzoate). We found that these groups were unaltered till 12 h.

We also monitored the stability of some acid-sensitive protecting groups, e.g., Trt and Pbf, by HPLC and observed that the Trt group got cleaved while the Pbf was intact. Such HPLC analyses revealed that some protecting groups, such as Bzl, Cbz, All, Alloc, Pbf, *o*-NBS, Fmoc, Me, and Et are orthogonal to tBu group for $FeCl_3$ based cleavage condition. These groups can be used as a side chain protecting group for suitable amino acids while applying the $FeCl_3$ based cleavage condition during SPPS. However, acid-sensitive groups like Boc or Trt or tert-butyl ether do not resist the reaction conditions under which a tert-butyl ester is cleaved. The compatibility of the few commonly used protecting groups under the $FeCl_3$ condition is listed in Table 6.2.

Table 6.2. Compatibility of some of the frequently used protecting groups to $FeCl_3$ condition

Entry	***Protecting group***	***Tolerance***	***Removal method***	***References***
1	Trt	Not stable	1% TFA-DCM	15
2	Pbf	Stable	90% TFA/TIS/H_2O	16
3	Bzl	Stable	Hydrogenation	17
4	All/ Alloc	Stable	$Pd(PPh_3)_4$/ $PhSiH_3$	1
5	*o*-NBS	Stable	β-mercaptoethanol/ DBU/ DMF	18
6	Fmoc	Stable	20% piperidine/ DMF	19
7	Et	Stable	LiOH	20
8	Me	Stable	LiOH	20

6.6. Racemization study

Next, to examine the racemization probability of our protocol, we synthesized L-Fmoc-Asp (OtBu)-OMe and DL-Fmoc-Asp (OtBu)-OMe. Then applied this method on them and checked the HPLC profile of the products. DL-Fmoc-Asp (OH)-OMe exhibited two distinct peaks at retention time 17.45 min, and 20.57 min in HPLC (chiral column, an isocratic gradient of 15% 2-propanol in hexane up to 40 min) indicated that two enantiomers were present. Whereas L-Fmoc-Asp(OH)-OMe showed a single peak at 20.83 min, indicating the presence of a single enantiomer (Figure 6.2 and Figure 6.3 and 6.4). Therefore, a comparison of these HPLC profiles indicated no detectable racemization caused by this method for enantiomerically pure substrates.

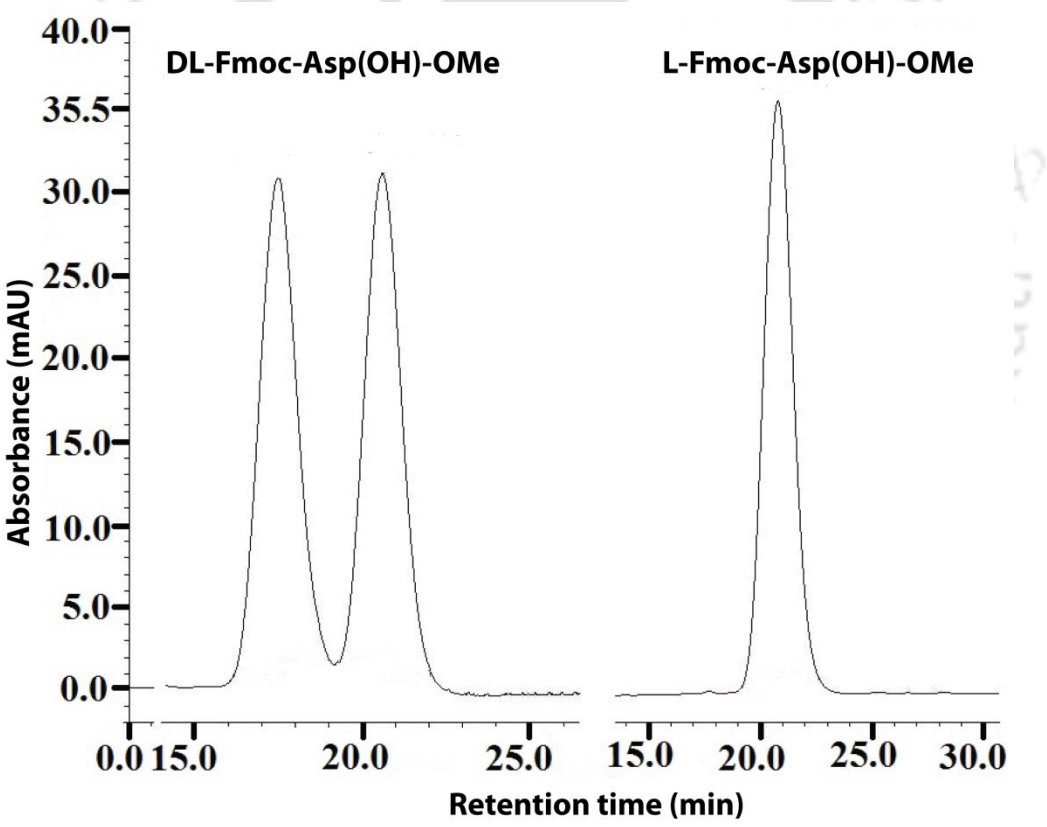

Figure 6.2. *HPLC profile picture of DL-Fmoc-Asp (OH)-OMe (left) and L-Fmoc-Asp (OH)-OMe (right).*

6.7. Formation of C-N/C-O/C-S bond after removal of tBu in SPPS

Next, we synthesized a broad range of model peptides containing various amino acid residues, including side-chain tert-butyl ester protected aspartic acid (Table 6.3). The

synthesis of these peptides was carried out by the conventional coupling method using BOP as the coupling reagent and DIPEA as the base. The standard Fmoc/tBu orthogonal protection/deprotection strategy[19] was applied on Rink amide AM resin (loading 0.7 mmol/g) to synthesis a whole peptide sequence. Then, the *N*-terminus of the peptides were acetylated using acetic anhydride and *N*-methyl morpholine (NMI). After that, the tert-butyl ester group of the side chain of aspartic acid was removed by using $FeCl_3$ (5 equiv, excess reagent was used to facilitate SPPS) in dichloromethane on-resin for 1.5 h. Next, the esterification, thioesterification, or amidation was performed in the presence of BOP (2.5 equiv), DIPEA (5 equiv) and the corresponding alcohol, thiol, or amine (3 equiv) (scheme 6.2), respectively, on-resin.

Table 6.3. A list of various side-chain modified peptides

Entry	Peptides (id)	Spectroscopic yield (%)	Isolated yield (%)
1	Ac-D(X_1)PFFA-NH_2 (**6A**)	94	40
2	Ac-LFD(X_2)PG-NH_2 (**6B**)	92	37
3	Ac-LFD(X_3)PG-NH_2 (**6C**)	93	38
4	Ac-LFD(X_4)PG-NH_2 (**6D**)	87	35
5	Ac-AFLGD(X_5)-NH_2 (**6E**)	86	32
6	Ac-AFLGD(X_6)-NH_2 (**6F**)	81	28

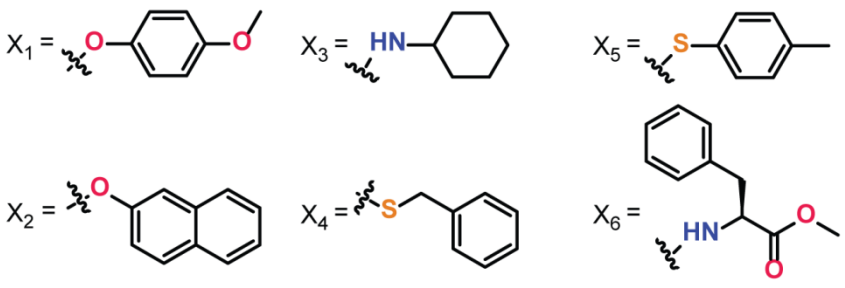

After synthesizing those peptides, they were allowed for cleave from the resin using the cleavage-cocktail TFA: DCM: H_2O (95:5:5), precipitated from the cold ether and dried. Then, the dried crude peptides were solubilized by acetonitrile-water solution and were subjected to HPLC analysis. The integration of the peak corresponding to the desired

peptide represents its relative abundance for the associated impurities (displayed in Table 6.3 as spectroscopic yield). This is very important in peptide chemistry as it is related to the ease of chromatographic purification and the efficiency of synthesis. After purification of those crude peptides by semi-preparative HPLC were allowed to freeze-dry and were calculated the isolated yields of purified products from them (listed in Table 6.3 as isolated yield). The overall synthetic procedure was described in section 6.14.4.

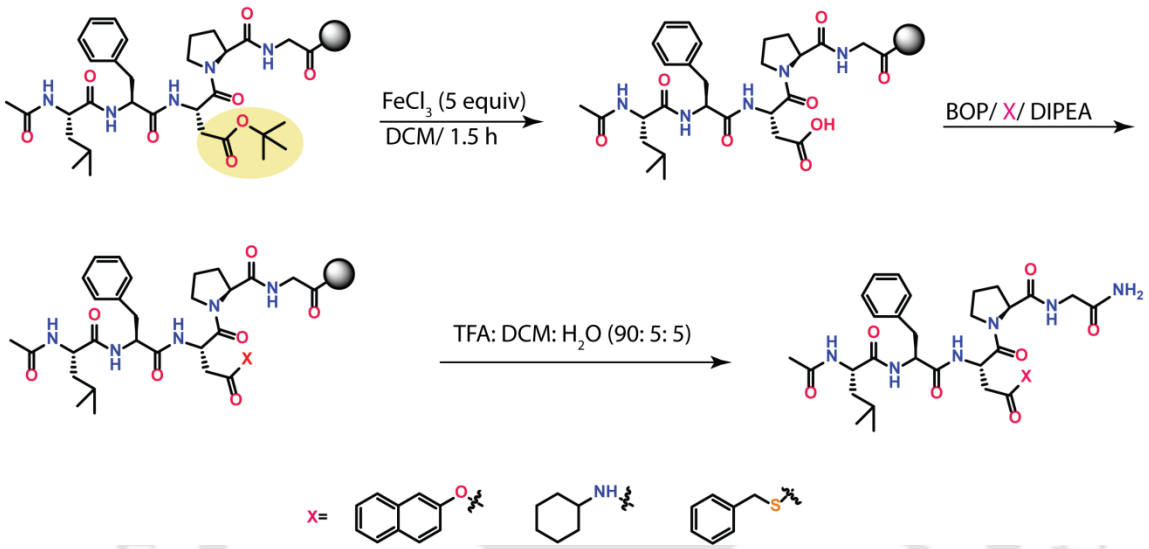

Scheme 6.2. *Tert-butyl ester cleavage and the side-chain modification on peptide anchored resin during SPPS.*

6.8. Sustainability of the Rink amide resin during $FeCl_3$ treatment

To understand the stability of the acid sensitive Rink amide resin during $FeCl_3$ treatment, we synthesized a peptide, Ac-LFD(OBzl)PG-NH_2 (**6G**), which contains the same amino acid sequence to that of peptide **6C**. The peptide **6G** considered as a reference, as Fmoc-Asp(OBzl)-OH was incorporated directly, not from Asp(OtBu)-OH, in the peptide on-going sequence. On the other hand, cyclohexylamine group was inserted after tert-butyl ester cleavage from pre-inserted Asp(OtBu)-OH in peptide **6C**. After final cleavage, the yields (both spectroscopic and isolated) of **6C** (spectroscopic yield = 83% and isolated yield = 38%) and **6G** (spectroscopic yield = 96% and isolated yield = 45%) were found comparable. That indicates no considerable loss of peptide occurred due to $FeCl_3$ treatment and subsequent modification. Furthermore, we analyzed the washing mixture

after $FeCl_3$ treatment, but could not find any trace of the cleaved peptide in it. Therefore, we concluded that the Rink amide resin was not cleaved by $FeCl_3$ treatment.

6.9. Compatibility with some frequently used protecting groups in solid phase

Next, we wanted to check the compatibility to various side-chain protecting groups (Table 6.2) that are frequently used in Fmoc based SPPS. For that, we synthesized a model peptide (**6H**), which contains some of those protecting groups and applied our protocol for removal of tert-butyl group from the side chain of Asp, followed by incorporation of an important cyclopropylamine moiety onto it on the solid support (scheme 6.3).

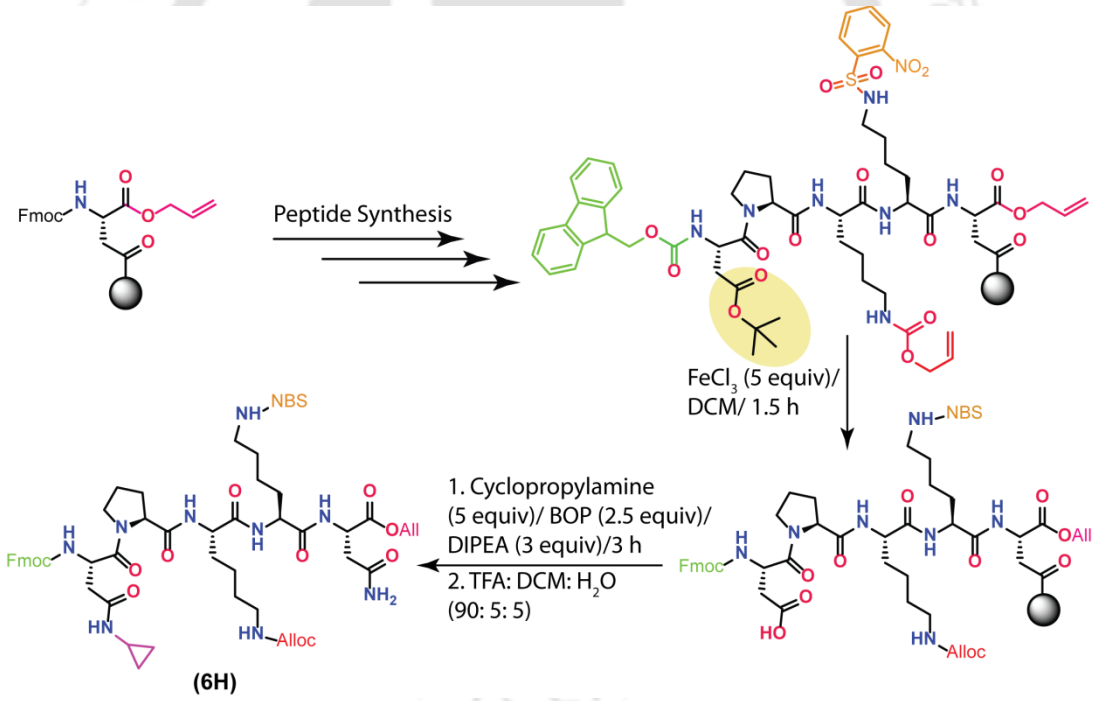

Scheme 6.3. *A model peptide containing various protecting groups during SPPS*

After that, the mass spectrometry and NMR spectroscopy-based analyses suggested that the other protecting groups, e.g., All, Alloc, *o*-NBs, and Fmoc remained unchanged. The attachment of the side chain carboxylic acid group of the first Asp to the Rink amide resin to selectively address each of the Asp residues present in it after cleavage from the resin.

6.10. Multi-functionalization of the side-chain of Asp/Glu on solid-support

Next, we performed the multi-functionalization of the side-chain of Asp/Glu on peptide anchored resin. For that, we choose a partial peptide sequence of the α-synuclein peptide (110-115). The α-synuclein peptide is known as the main culprit for Parkinson's disease.[21] At first, we incorporated benzyl alcohol as a benzyl ester on the side chain of C-terminal Asp, then incorporated the benzyl amine as benzyl amide on the side chain of next Glu and then elongated the peptide sequence (scheme 6.4).

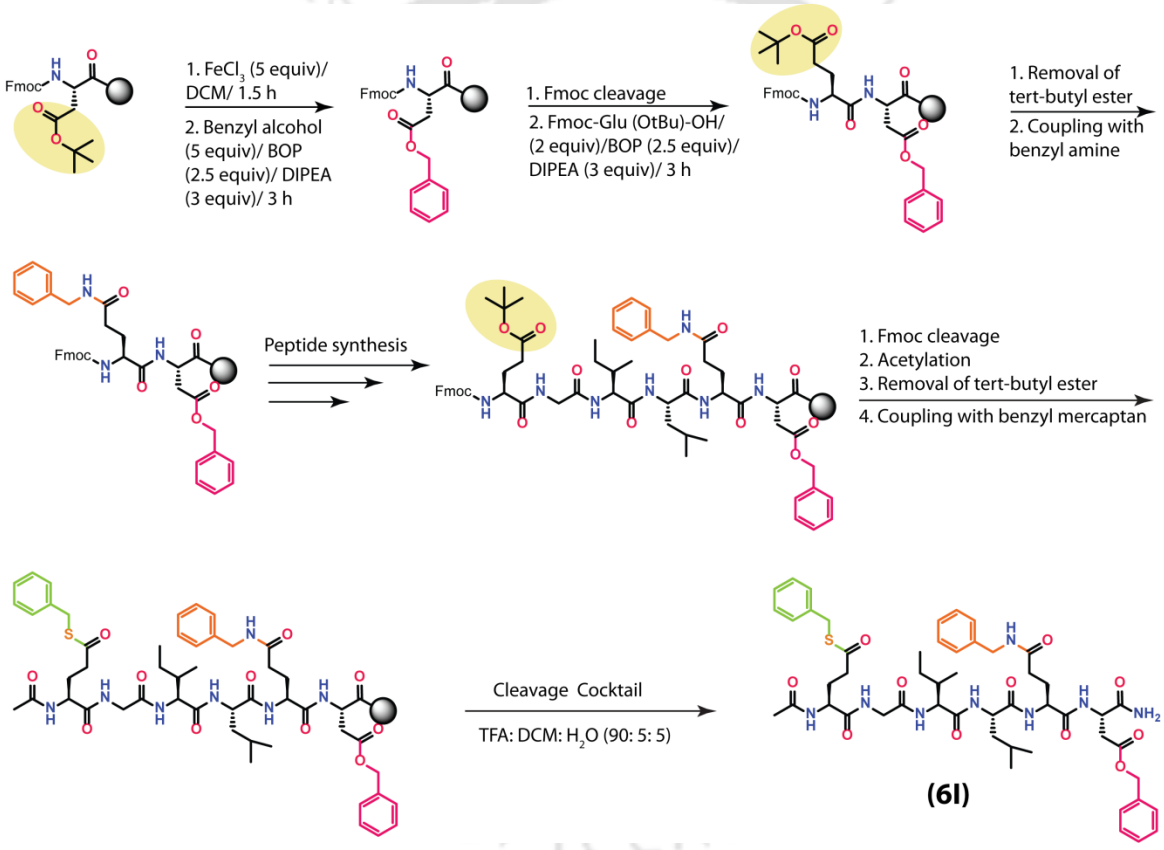

Scheme 6.4. *Esterification/Thioesterification and Amidation Reaction Performed on α-Synuclein (110-115)*

At last, benzyl mercaptan was introduced as a thioester modification on the side chain of the *N*-terminal Glu (scheme 6.4). The synthesis of such type of side-chain modified peptide is difficult as there is a chance to form aspartimide or glutamide in each step of Fmoc cleavage and also coupling steps of the side chain of Asp/Glu. To reduce the formation of aspartimide or glutamide, we used 20% piperidine/DMF with 5% formic acid[22] for Fmoc cleavage and added a base (DIPEA) carefully, not to exceed the required

amount at the side-chain coupling step. With all of these precautions, we were delighted to obtain 32% as the spectroscopic yield and 7% as the isolated of (**6I)**.

6.11. Fluorophore attachment

Next, we incorporated a fluorophore at the side-chain of Asp during SPPS. After synthesis of a whole peptide sequence, the tert-butyl group of the side-chain of Asp was cleaved by our protocol, and the obtained free carboxylic acid was coupled with the one side of the diethylamine, and the other side was dansylated with the dansyl chloride (Scheme 6.5). The fluorophore, dansyl chloride is important as it is widely used in protein conformational studies.[23] In this way, we synthesized the model peptide **6J** with 72% spectroscopic and 21% isolated yield, respectively.

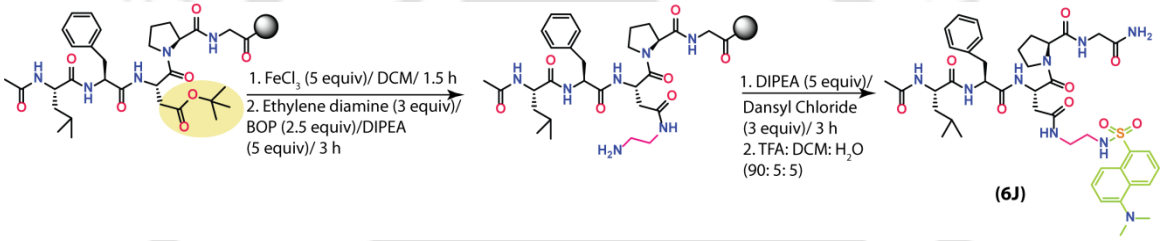

Scheme 6.5. *Fluorophore attachment on peptide* ***6J***

6.12. Plausible mechanism

A plausible mechanistic pathway of the deprotection of tert-butyl ester is drawn based on the existing literature (scheme 6.6).[24,25] $FeCl_3$ is a Lewis acid, so Fe(III) co-ordinated with the oxygen atom of tert-butyl ester group. As a result, the electron density on oxygen was shifted towards Fe, and therefore, the C-O bond becomes week and breaks down to form isobutene and the desired deprotected carboxylic acid.

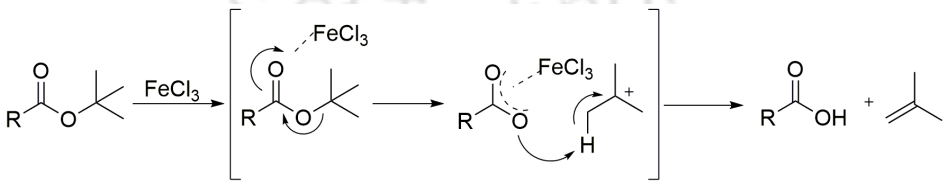

Scheme 6.6. *A plausible mechanism of deprotection of tert-butyl ester group*

6.13. Conclusion

An efficient, convenient, Lewis acid-based deprotection strategy for modification of tert-butyl ester containing a side chain of aspartic acid and glutamic acid during solid-phase peptide synthesis has been discussed in this chapter. By this method, various nucleophiles (both electron-donating and withdrawing groups) and fluorophores can be incorporated in the side-chain of Asp/Glu during SPPS with good yields. The advantage of this method is, it eliminates the effort, cost, time, and waste generation for modification of the amino acids separately when such amino acid derivatives are not commercially available. Therefore, the method is cost-effective and environmentally friendly.

6.14. Experimental section

6.14.1. Materials and instrumentation

As described in chapter 8

6.14.2. General procedure for the removal of tert-butyl ester

A stirred solution of tert-butyl ester (1 mmol) in 2 mL of DCM was treated with 1.5 equiv of $FeCl_3$ at room temperature and stirred for 1 h. After completion of the reaction (monitored by TLC), the reaction mixture was diluted with water and extracted with DCM. The organic layer was concentrated under reduced pressure and purified by silica gel column chromatography using an ethyl acetate-hexane mixture as eluent.

6.14.3. Monitoring of removal of tert-butyl ester (I) by HPLC

To monitor the tert-butyl ester cleavage, we performed HPLC studies at a fixed time interval. At first, we took Fmoc-Asp(OtBu)-OMe (1 mmol, **I**) and $FeCl_3$ (1.5 equiv) in the DCM medium. Then 10 μL of the reaction mixture was taken in an Eppendorf vial at 2 min interval. Next, 5 μL of DIPEA was added to it for quenching the reaction. After that, the solvent was evaporated by passing N_2 gas into it, and the reaction mixture was diluted by adding HPLC-grade acetonitrile (500 μL) and filtered via 0.22 μm filter paper. The

sample (20 μL) from that Eppendorf vial was injected in the HPLC system, and the HPLC profile was checked.

6.14.4. General procedure for peptide syntheses in SPPS

Swelling of Resin, Rink amide AM

Rink amide AM resin (100 mg, 0.7 mmol/g) was taken into a 2 mL frit-fitted plastic syringe and was swollen in DCM (1.5 mL) for 2h followed by DMF (1.5 mL) for 1h on a Stuart blood tube rotator (30 rpm).

Fmoc deprotection/ coupling

Next, 1.5 mL of 20% piperidine/DMF (v/v) was taken inside the syringe and rotated it for 7 min, then removed it from the syringe. This step was repeated three times (7 min x 3 times) and washed the resin with DMF for ten times. The coupling reaction was carried out by taking Fmoc protected amino acid (2 equiv), coupling reagent (BOP, 2.5 equiv), and base (DIPEA, 5 equiv) for 10 h to 12 h, depending on amino acids. After coupling, the peptide anchored resin was washed with DMF (1 mL x 5 times) followed by DCM.

Capping

Next, acetic anhydride (2 equiv) and NMI (2.5 equiv) in DCM were taken in that syringe and stirred 1 h. Then removed it from the syringe and washed within DCM.

Elongation of the peptide sequence

Next, the Fmoc group from *N*-terminal amino acid was cleaved by 20% piperidine in DMF. Then the peptide anchored resin was washed several times by DMF, and the coupling process was continued using Fmoc protected amino acid (2 equiv), BOP (2.5 equiv), and DIPEA (5 equiv) in DMF for 3 h to 5 h, depending on amino acids.

Acetylation

After elongation of the peptide sequence, the *N*-terminal amino was acetylated by acetic anhydride and NMI.

Tert-butyl ester cleavage from the side chain of Asp/Glu

Next, 5 equiv of $FeCl_3$ and DCM (1 mL) were taken in that syringe and kept stirring for 1.5 h for removal of tert-butyl group. Then peptide anchored resin was washed with DCM (3 x 1 min) and DMF (10 x 1 min).

Attachment of various nucleophiles on the side chain of Asp/Glu

Nest, the coupling of the free carboxylic acid of the side-chain of Asp/Glu was carried out by using nucleophile (3 equiv), BOP (2.5 equiv), and DIPEA (5 equiv) for 3 h. Then, the peptide-anchored resin was washed with DMF (1 x 5 times) followed by DCM (1 x 3 times).

Final cleavage from the resin

The final desired peptide was cleaved from the resin using a cleavage cocktail, TFA:DCM:H_2O (90: 5: 5) for 3 h. Then, the crude peptide was precipitated by cold ether followed by centrifugation to obtain crude solid peptide.

6.15. Characterization data

Fmoc-Asp-OMe (II).

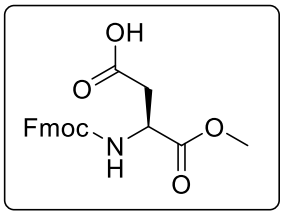

^{1}H NMR (DMSO-d_6, 300 MHz) δ 2.78-2.55 (2H, m); 3.61 (3H, s); 4.32-4.19 (3H, m); 4.44-4.37 (1H, m); 7.35-7.30 (2H, t, *J* = 7.5 Hz); 7.44-7.39 (2H, t, *J* = 7.5 Hz); 7.71-7.68 (2H, d, *J* = 7.2); 7.84 (1H, br); 7.90-7.87 (2H, d, *J* = 7.8 Hz). ^{13}C NMR (DMSO-d_6; 150 MHz) δ 35.8, 46.6, 50.4, 52.2, 65.7, 120.1, 125.2, 127.1, 127.6, 140.7, 143.7, 143.8, 155.8, 171.4, 171.7. HRMS (ESI) m/z: calculated $[M+H]^+$ 370.1212, found 370.1223.

Peptide 6A.

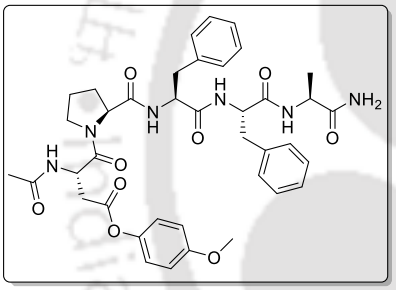

^{1}H NMR (DMSO-d_6, 600 MHz) δ 1.20 (3H, s); 1.73-1.33 (4H, m); 1.84 (3H, s), 2.76-2.59 (2H, m); 3.09-2.85 (4H, m); 3.60-3.56 (2H, m); 3.71 (3H, s); 4.20-4.19 (1H, m); 4.25 (1H, br); 4.53 (1H, br); 4.43 (1H, br); 5.01 (1H, br); 6.90 (2H, br); 7.26-7.01 (14H, m); 7.99 (1H, br s); 8.00 (1H, br s); 8.47 (1H, br s). ^{13}C NMR (DMSO-d_6; 150 MHz) δ 18.2, 22.2, 23.8, 28.8, 36.4, 36.9, 37.3, 46.8, 47.3, 48.1, 53.5, 53.8, 55.4, 59.9, 114.3, 122.6, 126.3, 127.9, 128.1, 129.1, 129.2, 137.6, 143.7, 156.9, 169.0, 169.2, 170.0, 170.3, 170.4, 170.9, 173.9. ESI-MS: calculated $[M+H]^+$ 743.3326, found m/z 743.3404. HPLC: retention time (t_R) = 11.90 min. Isolated pure product 21 mg (yield: 40 % w.r.t. resin loading).

Peptide 6B.

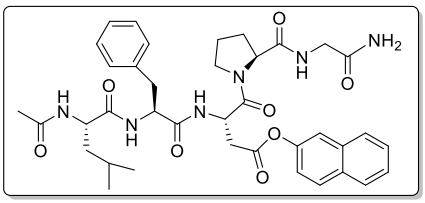

^{1}H NMR (DMSO-d_6, 600 MHz) δ 0.81-0.77 (6H, m); 1.34-1.32 (2H, m); 1.50-1.48 (1H, m); 1.78 (1H, br); 1.81 (3H, s); 2.02-1.86 (3H, m); 2.87-2.84 (1H, m), 3.04-2.95 (2H, m); 3.26-3.22 (1H, m); 3.6 (2H); 4.28-4.22 (2H, m); 5.11-5.09 (1H, m); 7.11 (2H, br s); 7.31-7.20 (6H, m); 7.55-7.51 (3H, m);

7.85-7.84 (1H, d, *J* = 7.8 Hz), 7.93-7.91 (2H, t, *J* = 7.8 Hz); 7.98-7.97 (2H, br); 8.15 (1H, br); 8.69 (1H, br).^{13}C NMR (DMSO-d_6; 150 MHz) δ 21.6, 22.4, 22.9, 24.3, 24.1, 29.1, 36.1, 37.3, 40.4, 41.9, 46.9, 47.9, 51.0, 53.5, 60.3, 118.5, 121.4, 125.7,125.9, 126.3,126.4, 126.5, 126.6, 127.8, 128.0, 129.2, 134.0, 137.3, 146.3, 168.6, 169.2, 169.3, 170.6, 171.0, 171.5, 171.9. HPLC: retention time (t_R) = 12.08 min. ESI-MS: calculated $[M+H]^+$ 715.3377, found m/z 715.3649. Isolated pure product 18 mg (yield: 37 %, w.r.t. resin loading).

Peptide 6C.

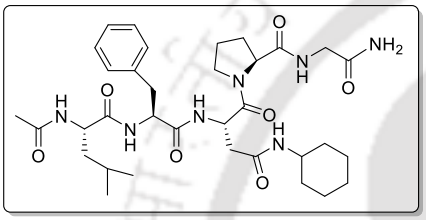

^{1}H NMR (DMSO-d_6, 600 MHz) δ 0.84-0.78 (6H, m); 1.11-1.08 (4H, m); 1.22-1.21 (3H, m); 1.36-1.32 (2H, t, *J* = 7.2 Hz); 1.52-1.49 (2H, m); 1.71-1.53 (5H, m); 1.81 (3H, s); 1.92-1.87 (2H, m); 2.08-2.04 (1H, m); 2.44-2.41 (2H, m); 2.71-2.67 (1H, m); 2.80-2.77 (1H, m); 2.95-2.92 (1H, m); 3.48-3.42 (2H, m); 3.65 (2H, br); 4.23-4.20 (2H, m); 4.51-4.48 (1H, m); 4.80-4.76 (1H, m); 6.91 (1H, br s); 7.22-7.12 (6H, m); 7.75-7.74 (1H, d, *J* = 7.8 Hz); 7.97-7.96 (1H, d, *J* = 7.8 Hz); 8.03-8.01 (1H, d, *J* = 7.8 Hz); 8.11 (1H, br); 8.41-8.40 (1H, d, *J* = 7.8 Hz). ^{13}C NMR (DMSO-d_6; 150 MHz) δ 21.5, 22.4, 22.9, 24.1, 24.5, 25.1, 29.1, 32.1, 32.3, 37.3, 37.5, 40.4, 42.1, 47.0, 47.3, 47.7, 51.0, 53.1, 60.3, 126.3, 127.9, 129.2, 137.2, 168.8, 169.3, 170.2, 170.4, 171.0, 171.4, 171.7. HPLC: retention time (t_R) = 10.45 min. ESI-MS: calculated $[M+H]^+$ 670.3850, found m/z 670.4146. Isolated pure product 18 mg (yield: 38 % w.r.t. resin loading).

Peptide 6D.

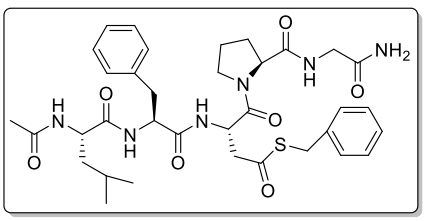

^{1}H NMR (DMSO-d_6, 600 MHz) δ 0.84-0.78 (6H, m); 1.34-1.33 (2H, m); 1.50-1.48 (1H, m); 1.81 (3H, s); 1.91-1.77 (2H, m); 2.0-1.91 (2H, m); 2.78-2.85 (2H, m); 2.95-3.11 (2H, m); 3.60-3.54 (4H, m); 4.13 (2H, s); 4.21 (2H, br); 4.47 (1H, br); 4.94 (1H, br); 7.01 (1H, br); 7.09 (1H, br); 7.28-7.15 (10H, m); 7.85 (1H, br); 7.98 (1H, br); 8.05 (1H, br); 8.48 (1H, br); ^{13}C NMR (DMSO-d_6;

150 MHz) δ 21.6, 22.4, 22.9, 24.3, 24.1, 29.0, 32.4, 37.3, 40.4, 41.9, 44.4, 46.8, 47.6, 51.0, 53.4, 60.4, 126.3, 127.1, 128.0, 128.5, 128.7, 129.2, 137.3, 137.4, 168.6, 169.4, 170.5, 171.1, 171.5, 171.9, 195.5. ESI-MS: calculated $[M+H]^+$ 695.3149, found m/z 695.3088. HPLC: retention time (t_R) = 11.90 min. Isolated pure product 18 mg (yield: 35 % w.r.t. resin loading).

Peptide 6E.

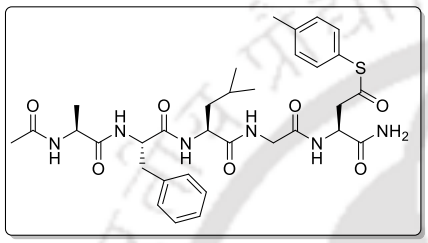

^{1}H NMR (DMSO-d_6, 600 MHz) δ 0.85-0.78 (6H, m); 1.07-1.06 (3H, d, J = 7.2 Hz); 1.50-1.44 (2H, m); 1.56-1.53 (1H, m); 1.79 (3H, s); 2.84-2.78 (1H, m); 2.97-2.91 (1H, m); 3.13-3.02 (2H, m); 3.76-3.66 (1H, m); 4.17-4.12 (1H, q, *J* = 7.2 Hz); 4.24-4.19 (1H, m); 4.49-4.43 (1H, m); 4.63-4.57 (1H, m); 7.28-7.16 (10H, m); 7.34 (1H, br); 7.99 (2H, br); 8.14-8.04 (3H, m). ^{13}C NMR (DMSO-d_6; 100 MHz) δ 17.6, 20.7, 21.3, 22.3, 22.9, 23.8, 36.6, 40.3, 42.0, 44.5, 48.4, 49.2, 51.3, 53.6, 123.5, 126.2, 127.9, 129.1, 129.9, 134.3, 137.5, 139.3, 168.6, 169.6, 171.0, 171.7, 172.4, 172.5. ESI-MS: calculated $[M+H]^+$ 669.2992, found m/z 669.3103. HPLC: retention time (t_R) = 11.36 min. Isolated pure product 15 mg (yield: 32% w.r.t. resin loading).

Peptide 6F.

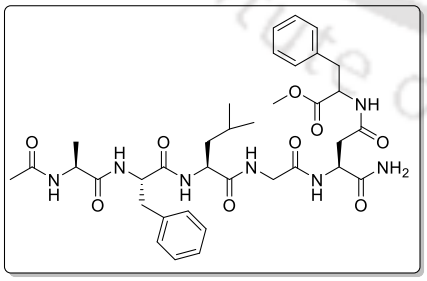

^{1}H NMR (DMSO-d_6, 400 MHz) δ 0.87-0.80 (6H, m); 1.08-1.07 (3H, d, *J* = 7.2 Hz); 1.49-1.45 (2H, m); 1.57-1.56 (1H, m); 1.79 (3H, s); 2.48-2.42 (1H, m); 2.60-2.55 (1H, m); 3.06-2.77 (4H, m); 3.55 (3H, s); 3.72-3.62 (2H, m); 7.18-4.14 (1H, m); 4.28-4.23 (1H, m); 4.49-4.39 (3H, m); 7.13 (1H, br); 7.12 (1H, br); 7.28-7.14 (10H, m); 8.06-7.99 (5H, m); 8.41-8.40 (1H, d, *J* = 7.6 Hz). ^{13}C NMR (DMSO-d_6; 100 MHz) δ 17.9, 21.5, 22.5, 23.1, 24.0, 36.9, 40.6, 42.2, 48.4, 49.5, 51.3, 51.9, 53.8, 53.9, 126.3, 126.7, 128.1, 128.4, 129.1, 129.3, 137.1, 137.8, 168.5, 169.5, 169.8, 171.0, 172.0, 172.5, 172.6, 172.9. ESI-

MS: calculated $[M+H]^+$ 724.3592, found m/z 724.3728. HPLC: retention time (t_R) = 6.79 min. Isolated pure product 14 mg (yield: 28 % w.r.t. resin loading).

Peptide 6G.

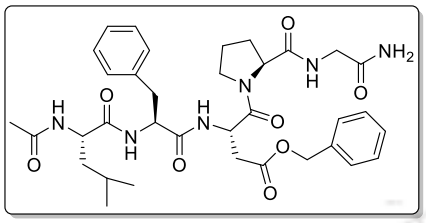

^{1}H NMR (DMSO-d_6; 600MHz) δ 0.83-0.77 (6H, m); 1.34-1.31 (2H, t, *J* = 7.2 Hz); 1.50-1.46 (1H, m); 1.78-1.74 (2H, m); 1.80 (3H, s); 2.0-1.87 (2H, m); 2.60-2.56 (1H, m); 2.81-2.78 (1H, m); 2.87-2.83 (1H, m); 2.98-2.96 (1H, m); 3.45-3.41(1H, m); 3.55-3.52 (1H, m); 3.62-3.57 (2H, m); 4.23-4.20 (2H, m); 4.50-4.46 (1H, m); 4.91-4.88 (1H, m); 5.09-5.04 (2H, m); 7.00 (1H, br); 7.10 (1H, br); 7.18-7.15 (3H, m); 7.23-7.21 (2H, m); 7.38-7.31 (5H, m); 7.86-7.84 (1H, d, *J* = 7.8 Hz); 7.97-7.96 (1H, d, *J* = 7.8); 8.06 (1H, br); 8.47-8.46 (1H, d, *J* = 7.8 Hz); ^{13}C NMR (DMSO-d_6; 150 MHz) δ 21.6, 22.4, 22.9, 24.1, 24.3, 29.1, 35.8, 37.3, 40.5, 42.0, 46.8, 47.5, 51.1, 53.4, 65.9, 60.3, 126.3, 128.0, 128.1, 128.2, 128.4, 129.3, 135.9, 137.3, 168.9, 169.4, 170.2, 170.4, 171.1, 171.5, 171.9. ESI-MS: calculated $[M+H]^+$ 679.3377 , found m/z 679.3343. HPLC: retention time (t_R) = 11.37 min. spectroscopic yield = 96 %. Isolated pure product 21 mg (yield: 45 % w.r.t. resin loading).

Peptide 6H.

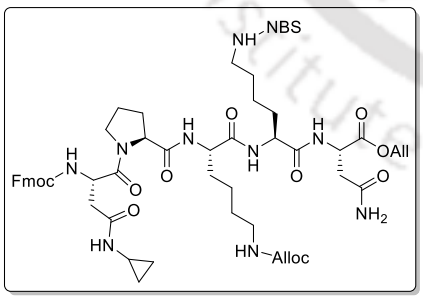

^{1}H NMR (DMSO-d_6; 600MHz) δ 0.56-0.32 (4H, m); 1.40-1.17 (9H, m); 1.86-1.62 (7H, m); 2.38-2.36 (2H, m); 2.62-2.54 (2H, m); 2.94-2.81 (4H, m); 3.73-3.63 (2H, m); 4.30-4.06 (5H, m); 4.43-4.42 (2H, d, *J* = 4.8 Hz); 4.51-4.50 (2H, d, *J* = 4.8 Hz); 4.62-4.56 (2H, m); 5.15-5.13 (2H, d, *J* = 10.2 Hz); 5.28-5.23 (2H, m); 5.90-5.80 (2H, m); 6.93 (1H, br); 7.17 (1H, br); 7.44-7.30 (5H, m); 7.75-7.68 (3H, m); 7.89-7.84 (4H, m); 8.06-8.05 (2H, m); 8.13 (1H, br); 8.18 (1H, br) ESI-MS: calculated $[M+H]^+$ 1171.4692 , found m/z 1171.4759. HPLC: retention time (t_R) = 8.70 min. spectroscopic yield = 71%. Isolated pure product 20 mg (yield: 24 % w.r.t. resin loading).

Peptide 6I.

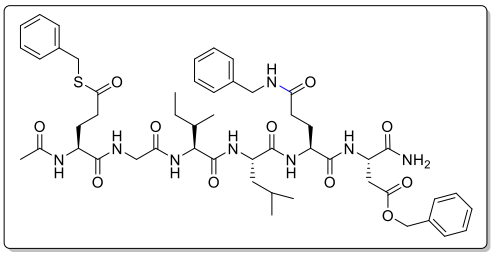

^{1}H NMR (DMSO-d_6; 400MHz) δ 0.80-0.73 (8H, m); 0.85-0.84 (3H, d, *J* = 6 Hz); 1.06-1.00 (1H, m); 1.22 (3H, s); 1.34 (1H, br); 1.48- 1.43 (2H, m); 1.57 (1H, br); 1.69 (1H, br); 1.82 (4H, br); 1.94-1.89 (2H, m); 2.05 (3H, s); 2.20-2.17 (2H, t, *J* = 7.2 Hz); 2.66-2.60 (2H, m); 2.83-2.77 (1H, m); 3.45 (1H, s); 3.76-3.63 (2H, m); 4.09 (2H, s); 4.25-4.17 (4H, m); 4.56-4.50 (1H, q, *J* = 7.6 Hz, 6.4 Hz); 5.05 (2H, s); 7.33-7.21 (14H, m); 7.79-7.77 (1H, d, *J* = 8.4 Hz); 7.97-7.96 (1H, d, *J* = 6.8 Hz); 8.08-8.02 (2H, m); 8.15-8.14 (1H, d, *J* = 7.2 Hz). ^{13}C NMR (DMSO-d_6; 150 MHz) δ 11.0, 15.3, 21.4, 22.5, 23.0, 24.1, 27.3, 27.8, 29.0, 32.1, 32.2, 35.9, 36.6, 42.1, 49.3, 51.4, 52.0, 52.7, 57.1, 65.7, 118.1, 126.7, 127.2, 127.9, 128.0, 128.3, 128.4, 128.6, 128.7, 135.9, 137.8, 139.1, 168.9, 169.8, 169.9, 170.0, 171.1, 171.3, 171.6, 171.8, 172.1, 172.3, 197.6. ESI-MS: calculated $[M+H]^+$ 1001.4728 , found m/z 1001.4726. HPLC: retention time (t_R) = 8.29 min. spectroscopic yield = 32 %. Isolated purify product yield 7 %.w.r.t. resin loading.

Peptide 6J.

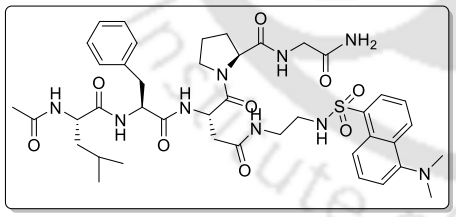

^{1}H NMR (DMSO-d_6; 600 MHz) δ 0.83-0.78 (6H, m); 1.32 (2H, br s), 1.49 (1H, br); 1.80 (3H, s); 1.85 (2H, br); 2.08 (1H, br); 2.33 (1H, br); 2.63 (1H, br); 2.81-2.77 (2H, m); 2.85 (6H, s); 3.07-2.92 (3H, m); 3.45-3.43 (1H, m); 4.19 (4H, br); 4.47 (1H, br); 4.74 (1H, br); 6.91 (1H, br); 7.07 (1H, br); 7.31-7.12 (6H, m); 7.62 (2H, br); 7.76 (1H, br); 8.12-7.96 (5H, m); 8.29 (1H, br); 8.35 (1H, br); 8.46 (1H, br). ^{13}C NMR (DMSO-d_6; 150 MHz) δ 21.5, 22.4, 22.9, 24.1, 29.1, 37.3, 37.4, 40.4, 41.6, 42.1, 42.1, 45.2, 47.0, 47.3, 51.1, 53.2, 60.3, 115.5, 119.5, 123.1, 126.3, 127.9, 128.3, 129.0, 129.3, 136.5, 137.2, 158.2, 169.4, 170.0, 170.2, 170.3, 171.1, 171.5, 171.8. ESI-MS: calculated $[M+H]^+$ 864.4000, found m/z 864.4067. HPLC: retention time (t_R) = 10.68 min. spectroscopic yield = 72 %. Isolated pure product 13 mg (yield: 21 % w.r.t. resin loading).

6.16. References

1. Grieco, P.; Gitu, P. M.; Hruby, V. J. Preparation of 'side-chain-to side-chain' cyclic peptides by Allyl and Alloc strategy: potential for library synthesis. *J. Pept. Res.* **2001**, *57*, 250-256.
2. Grieco, P.; Han, G.; Weinberg, D.; MacNeil, T.; Van der Ploeg, L. H. T.; Hruby, V. J. Design and synthesis of highly potent and selective melanotropin analogues of SHU9119 modified at position 6. *Biochem. Biophys. Res. Commun*. **2002**, *292*, 1075-1080
3. Guo, H.; Gallazzi, F.; Miao, Y. Gallium-67-labeled lactam bridge-cyclized alpha-MSH peptides with enhanced melanoma uptake and reduced renal uptake. *Bioconjug. Chem.* **2012**; *23*, 1341-1348.
4. Chan, W. C.; Bycroft, B. W.; Evans, D. J.; White, P. D. A novel 4-aminobenzyl ester-based carboxy-protecting group for synthesis of a typical peptides by Fmoc-Bu^t solid-phase chemistry. *J. Chem. Soc., Chem. Commun.* **1995,** 2209-2210.
5. Conroy, T.; Jolliffe, K. A.; Payne, R. J. Efficient use of the Dmab protecting group: applications for the solid-phase synthesis of N-linked glycopeptides. *Org. Biomol. Chem*. **2009**, *7*, 2255-2258.
6. McMurray, J. S. Solid phase synthesis of a cyclic peptide using Fmoc chemistry. *Tetrahedron Lett.* **1991**, *32*, 7679-7682.
7. Gibson, F. S.; Bergmeier, S. C.; Rapoport, H. Selective removal of an N-BOC protecting group in the presence of a tert-butyl ester and other acid-sensitive groups. *J. Org. Chem.* **1994**, *59*, 3216-3218.
8. Strazzolini, P.; Misuri, N.; Polese, P. Efficient cleavage of carboxylic tert-butyl and 1-adamantyl esters, and N-Boc-amines using H_2SO_4 in CH_2Cl_2. *Tetrahedron Lett.* **2005**, *46*, 2075-2078.
9. Strazzolini, P.; Dall'Arche, M. G.; Giumanini, A. G. Nitrolysis of carboxylic t-butyl and 1-adamantyl esters. *Tetrahedron Lett.* **1998**, *39*, 9255-9258.
10. Srinivasan, N.; George, A. Y.; Ganesan, A. Rapid deprotection of N-Boc amines by TFA combined with freebase generation using basic ion-exchange resins. *Molec. Divers*. **2005**, *9*, 291-293.
11. Valecic, M.; van der Does, T.; Vroom, E. de Titanium tetraehloride promoted hydrolysis of cephalosporin tert-butyl esters. *Tetrahedron Lett.* **1998**, *39*, 1625-1628.
12. Jones, A. B.; Villalobos, A.; Linde II, R. G.; Danishefsky, S. J. A formal synthesis of FK-506. exploration of some alternatives to macrolactamization. *J. Org. Chem*. **1990**, *55*, 2786-2797.
13. Kaul, R.; Brouillette, Y.; Sajjadi, Z.; Hansford, K. A.; Lubell, W. D. Selective tert-butyl ester deprotection in the presence of acid labile protecting groups with use of $ZnBr_2$. *J. Org. Chem.* **2004**, *69*, 6131-6133.
14. Marcantoni, E.; Massaccesi, M.; Torregiani, E. Selective deprotection of N-Boc-protected tert-butyl ester amino acids by the $CeCl_3,7H_2O$-NaI system in acetonitrile. *J. Org. Chem.* **2001**, *66*, 4430-4432.
15. Barlos, K.; Mamos, P.; Papaioannou, D.; Patrianakou, S.; Sanida, C.; Schaefer, W. Einsatz von trt- und Fmoc-gruppen zum schutz polyfunktioneller α-aminosauren. *Liebigs Ann. Chem.* **1987**, *12*, 1025-1030.
16. Carpino, L. A.; Shroff, H.; Triolo. S. A.; Mansour, El Sayed M. E.; Wenschuh, H.; Albericio, F. The 2,2,4,6,7-pentamethyldihydrobenzofuran-5-sulfonyl Group (Pbf) as arginine side chain protectant. *Tetrahedron Lett.* **1993**, *34*, 7829-7832.

17. Bajwa, J. S. Chemoselective deprotection of benzyl esters in the presence of benzyl ethers, benzyloxymethyl ethers and N-benzyl groups by catalytic transfer hydrogenation. *Tetrahedron Lett.* **1992**, *33*, 2299-2302.
18. Poreddy, A. R.; Schall, O. F.; Marshall, G. R.; Ratledge, C.; Slomczynska, U. Solid-phase synthesis of methyl carboxymycobactin T 7 and analogues as potential antimycobacterial agents. *Bioorg. Med. Chem. Lett.* **2003**, *13*, 2553-2556.
19. Coin, I.; Beyerman, M.; Bienert, M. Solid-phase peptide synthesis: from standard procedures to the synthesis of difficult sequences. *Nat. Protoc*. **2007**, *2*, 3247-3256.
20. Dayal, B.; Salen, G.; Toome, B.; Tint, G. S.; Shefer, S.; Padia, J. Lithium hydroxide/aqueous methanol: mild reagent for the hydrolysis of bile acid methyl esters. *Steroids* **1990**, *55*, 233-237.
21. Goedert, M. Alpha-synuclein and neurodegenerative diseases. *Nat. Rev. Neurosci.* **2001**, *2*, 492-501.
22. Michels, T.; Dolling, R.; Haberkorn, U.; Mier, W. Acid-mediated prevention of aspartimide formation in solid phase peptide synthesis. *Org. Lett*. **2012,** *14*, 5218-5221.
23. Weber, G. Polarization of the fluorescence of macromolecules. *Biochem. J.*, **1952**, *51*, 155-167.
24. Navath, R. S.; Pabbisetty, K. B.; Hu, L. Chemoselective deprotection of N-Boc group in amino acids and peptides by bismuth(III) trichloride. *Tetrahedron Lett.* **2006**, *47*, 389-393.
25. Lopez-Soria, J. M.; Perez, S. J.; Hernandez, J. N.; Ramirez, M. A.; Martin, V. S.; Padron, J. I. A practical, catalytic and selective deprotection of a Boc group in N,N′-diprotected amines using iron(III)-catalysis. *RSC Adv.* **2015**, *5*, 6647-6651.

6.17. Selected spectra

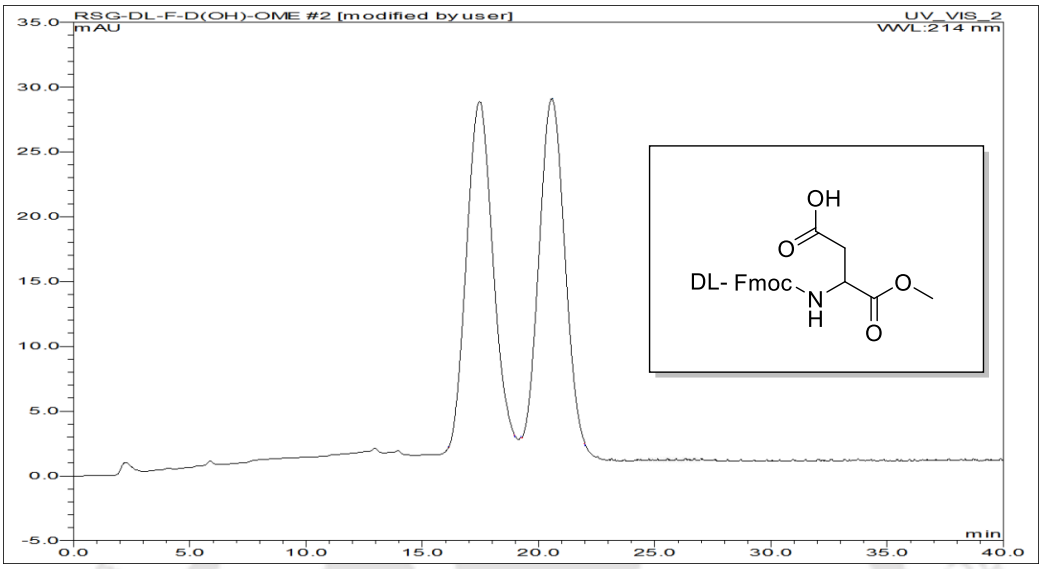

Figure 6.3. *HPLC profile picture of compound DL-Fmoc-Asp (OH)-OMe. (Chiral column, Diacel Chiralpak-ASH), the isocratic gradient of 15% 2-propanol in hexane up to 40 min)*

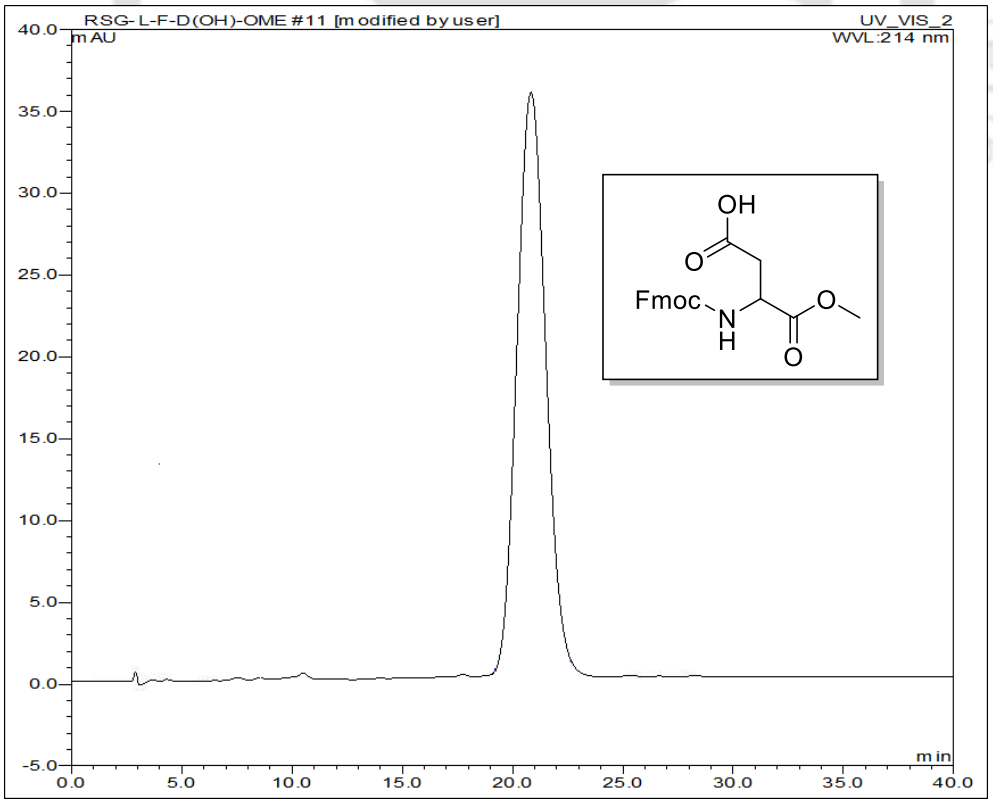

Figure 6.4. *HPLC profile picture of compound L-Fmoc-Asp (OH)-OMe. (Chiral column, Diacel Chiralpak-ASH), the isocratic gradient of 15% 2-propanol in hexane up to 40 min)*

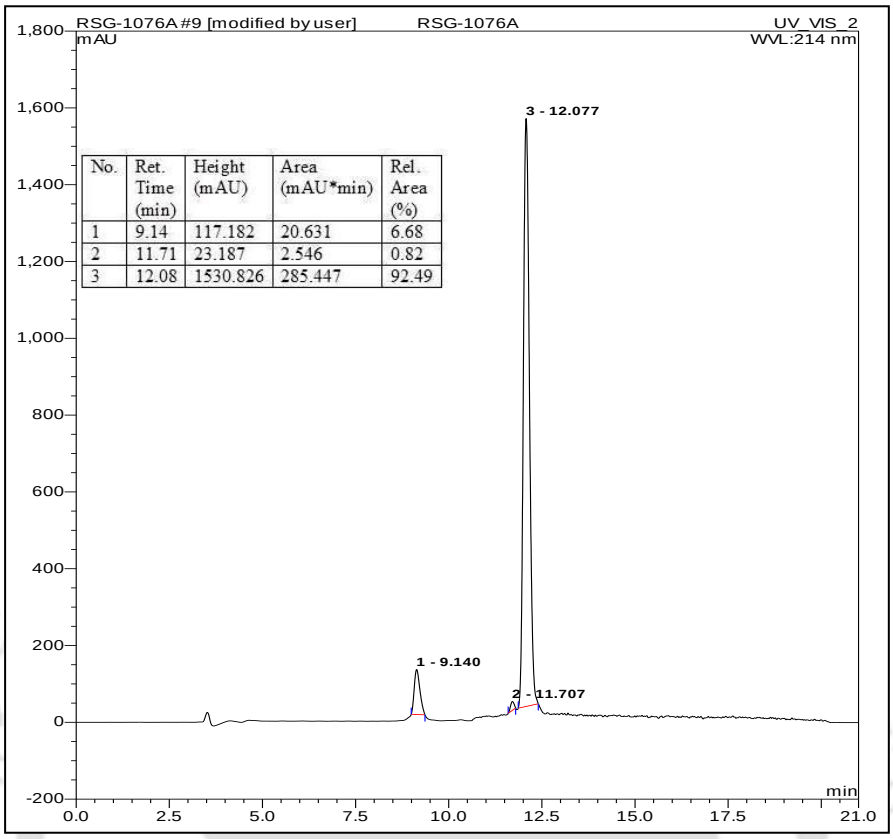

No.	Ret. Time (min)	Height (mAU)	Area (mAU*min)	Rel. Area (%)
1	9.14	117.182	20.631	6.68
2	11.71	23.187	2.546	0.82
3	12.08	1530.826	285.447	92.49

Figure 6.5. *HPLC profile picture of crude peptide* ***6B*** *(A linear gradient from 5 to 100% CH_3CN till 18 min, and a total run time of 20 min)*

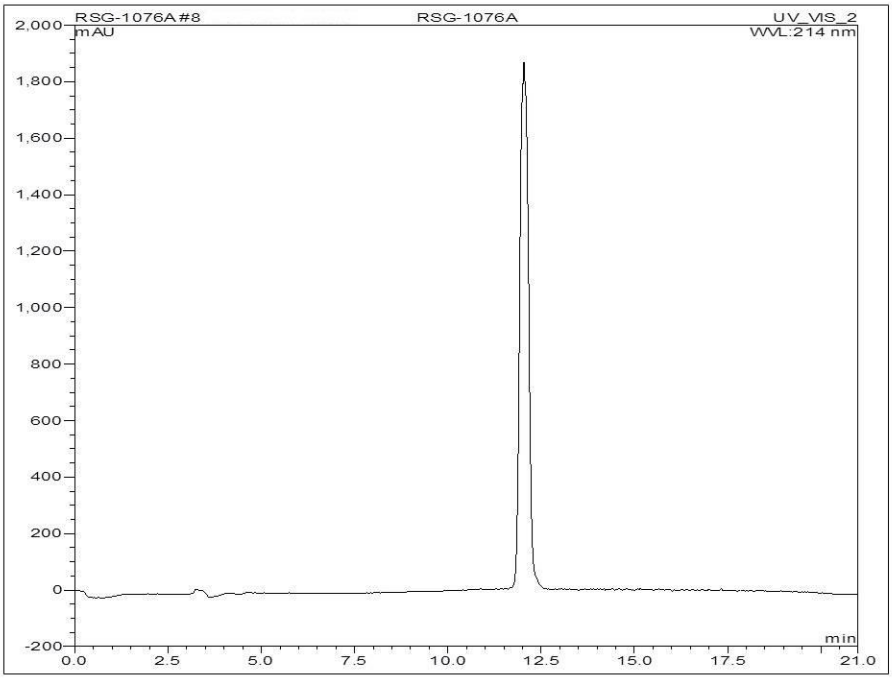

Figure 6.6. *HPLC profile picture of purified peptide* ***6B***

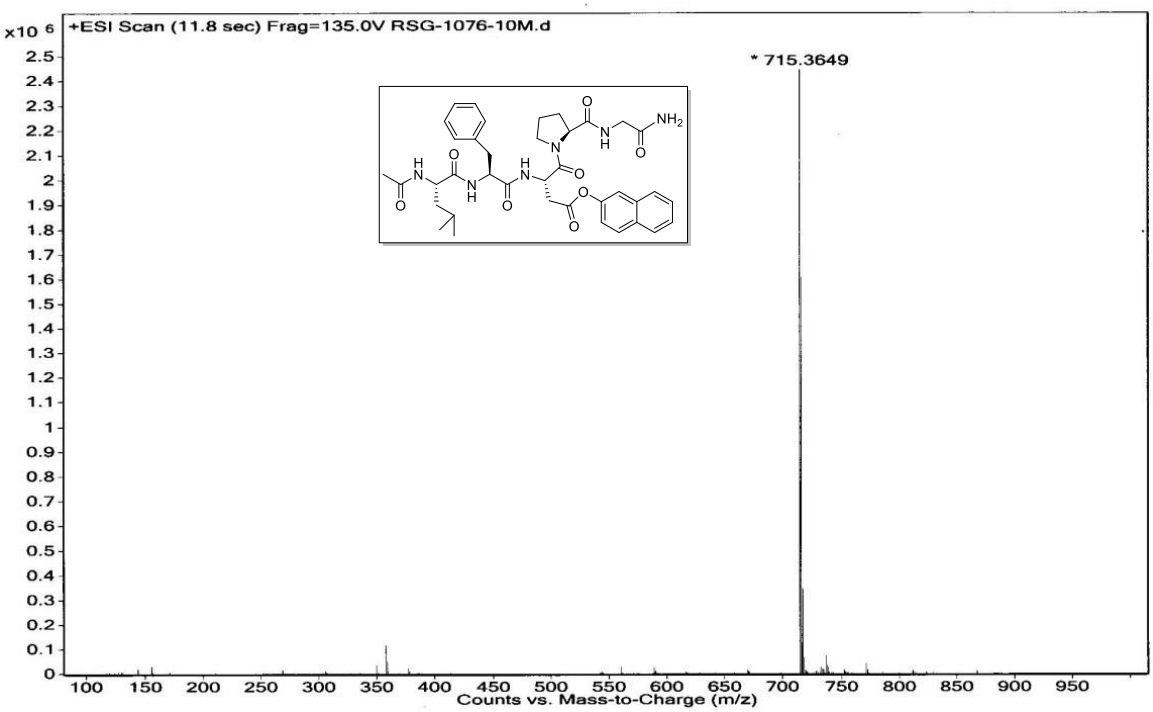

Figure 6.7. *MS spectra of peptide* ***6B***

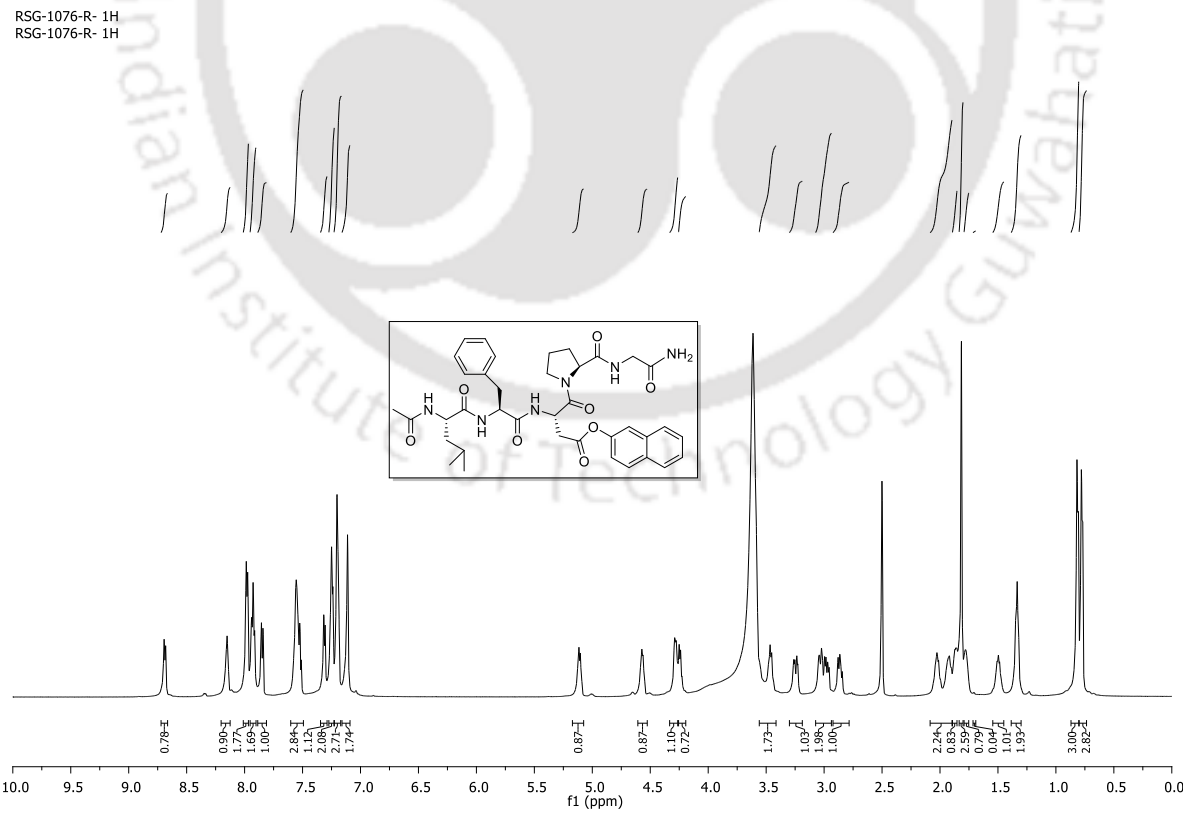

Figure 6.8. *^{1}H NMR spectra of peptide* ***6B***

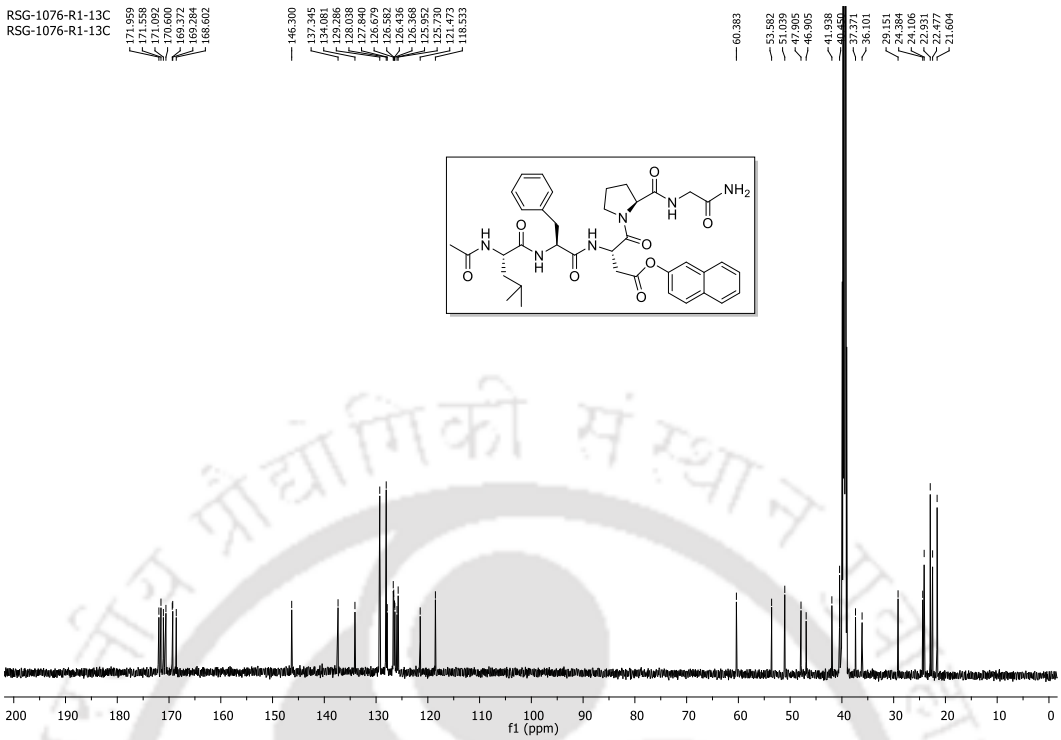

Figure 6.9. *^{13}C NMR spectra of peptide* ***6B***

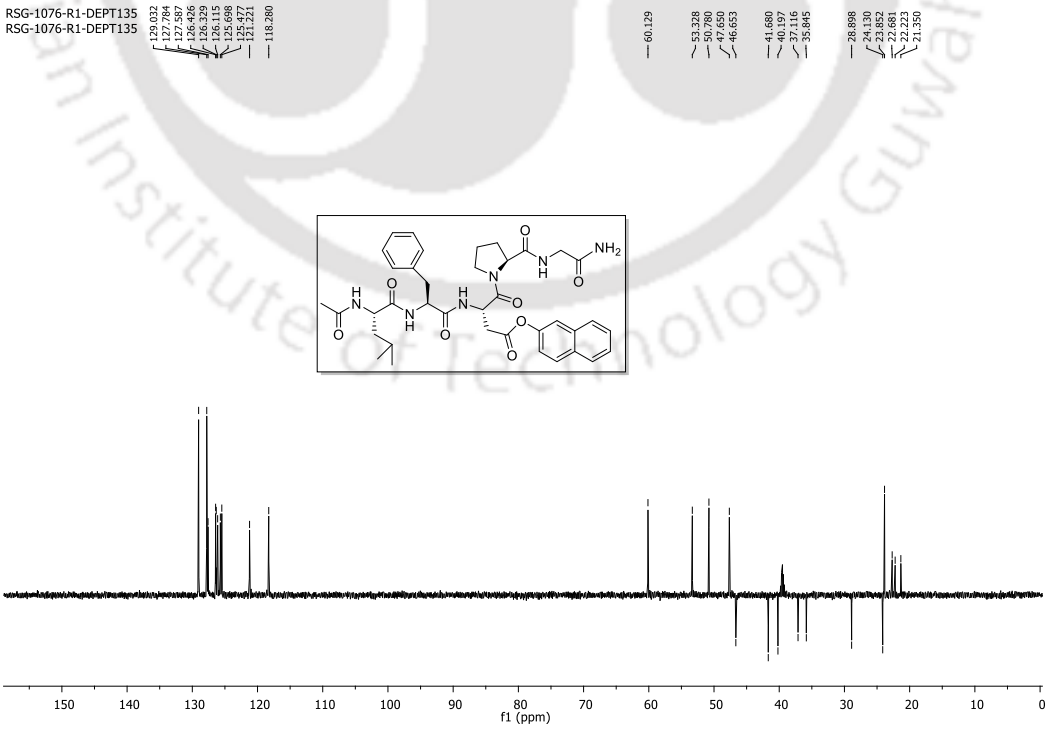

Figure 6.10. *DEPT 135 spectra of peptide* ***6B***

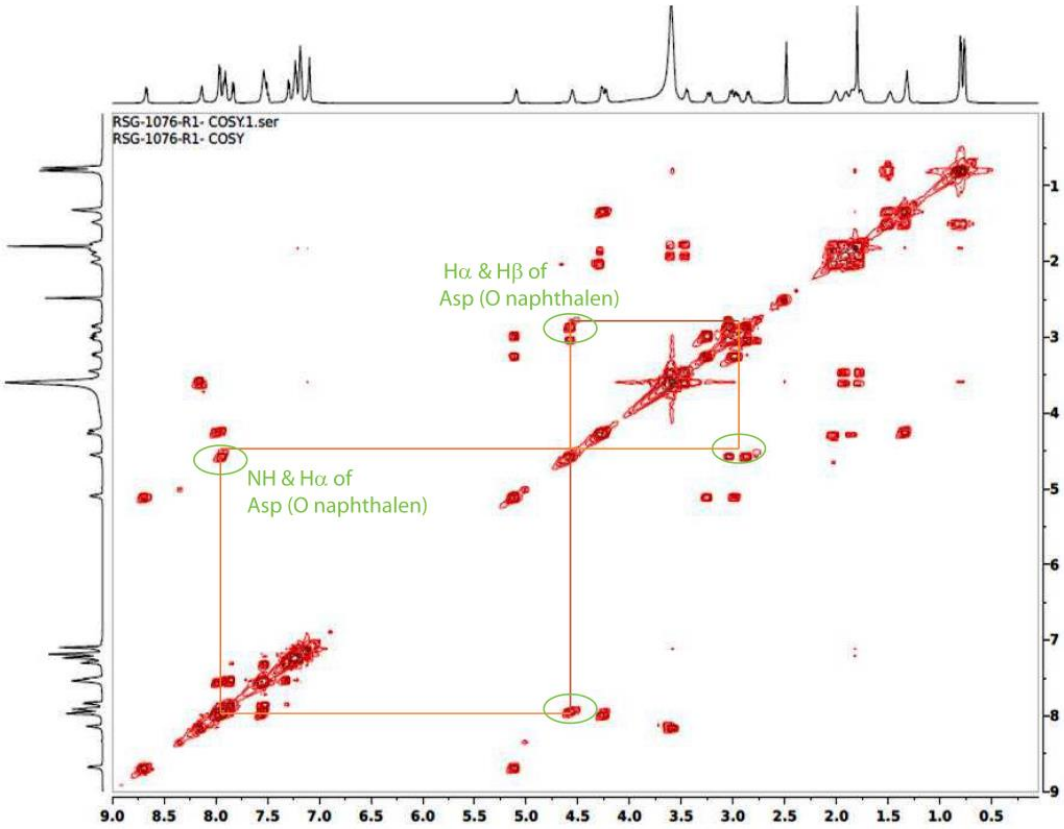

Figure 6.11. *COSY spectra of peptide* ***6B***

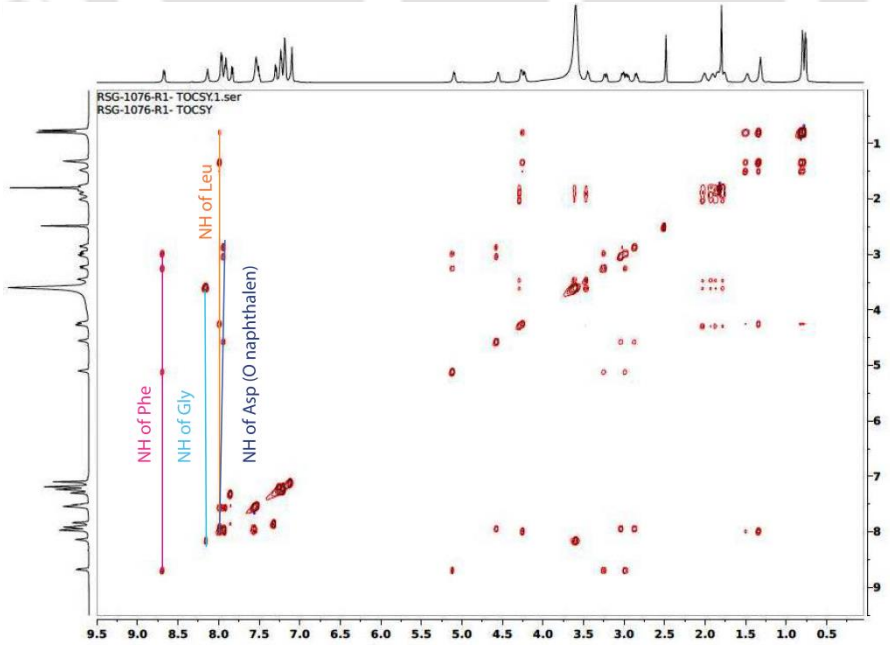

Figure 6.12. *TOCSY spectra of peptide* ***6B***

Chapter 7

$FeCl_3$-Mediated Boc Deprotection and Peptide Synthesis in Solution and SPPS

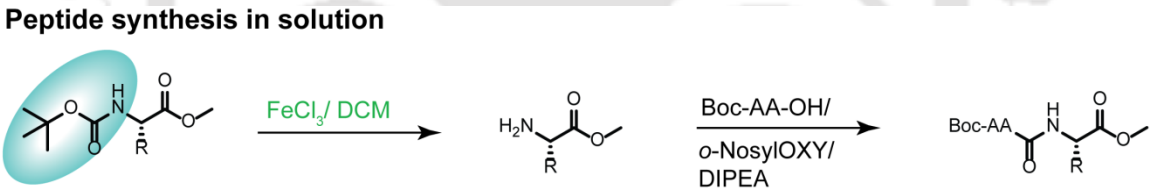

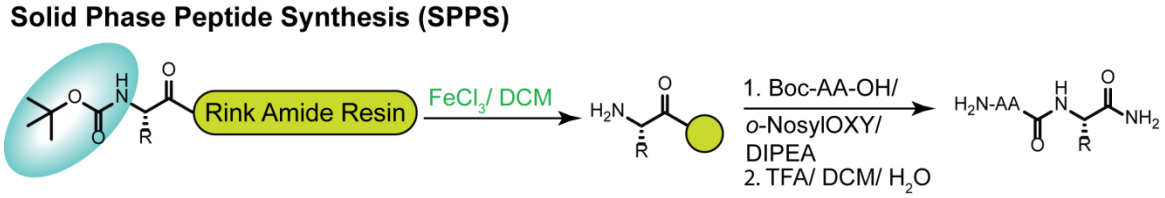

7.1. Background

We have discussed the peptide synthesis both in solution and SPPS in Chapter 1 (section 1.9). We also discussed the $FeCl_3$-mediated tert-butyl ester cleavage of the side chain of Asp/Glu containing peptide on-resin in the previous chapter. Normally, peptides are synthesized by standard coupling method in solution. In this method, Boc protected amino acids are frequently used as the protecting group is easily removed by TFA. On the other hand, peptides are synthesized by the Boc/Bzl strategy in SPPS, and here also, each step of Boc deprotection of *N*-terminal amino acid is carried out by TFA.[1] But, the TFA is not environmentally friendly, cost-effective, and corrosive. Moreover, the Boc/Bzl strategy is used on Merrifield resin, PAM-resin, and BHA-resin, which are cleaved by strong acid HF. This acid is highly corrosive and destructive; therefore, a particular experimental set-up is required.

7.2. Existing method for removal of Boc group

Boc group is also removed by strong acids, e.g., HCl,[2] H_2SO_4,[3] and HNO_3,[4] or by neutral condition, e.g., Zn, In,[5] Bu_4NF,[6] and water/reflux,[7] or by Lewis acids, e.g., $Sn(OTf)_2$[8] and $BiCl_3$.[9] Recently, Padron *et al.* disclosed the removal of the Boc group from dimethyl ester of *N*, *N*-Boc, Ts-amino acid using Lewis acid, $FeCl_3$.[10] To the best of our knowledge, the Lewis acid-based methods mentioned above were applied for Boc deprotection of only amine or amino acids but were not explored further for peptide synthesis.

7.3. Our approach

We demonstrated a mild, effective, and environmentally friendly $FeCl_3$ based method for deprotection of the Boc group from the *N*-terminus of amino acid containing peptide and peptide sequence could be elongated by using coupling reagent and base both in solution and SPPS. Interestingly, this method can be applied for peptide synthesis by using Boc protected amino acid on the acid-sensitive Rink amide resin, which is usually used for Fmoc chemistry.

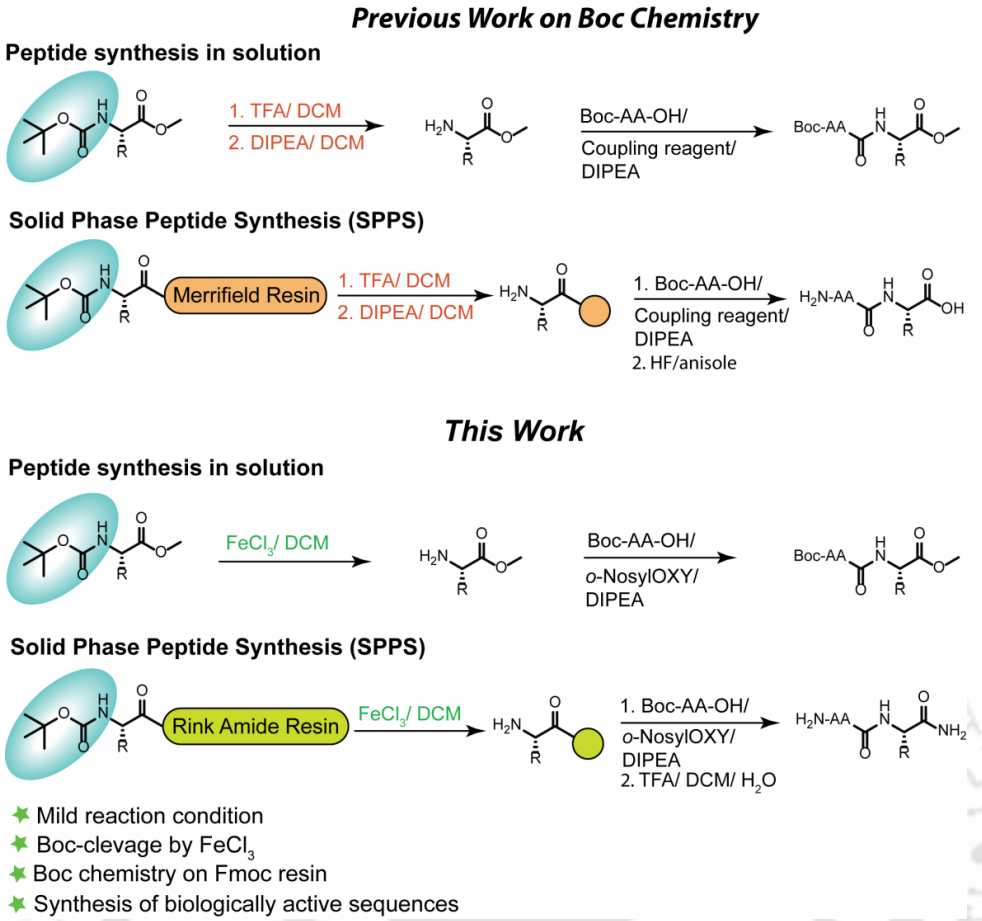

Scheme 7.1. *Overview of the work*

7.4. A time-dependent HPLC study to monitor the Boc cleavage

To monitor the Boc cleavage, we performed a time-dependent HPLC experiment. For that, we took Boc-Phe-OMe (***A***, 1 mmol) as a model substrate and $FeCl_3$ (1.5 equiv) in DCM. The obtained HPLC profiles suggested that within 1 h, 95% of Boc deprotected product (***B***) was produced, and 5% of starting material (***A***) remained unchanged (Figure 7.10 in section 7.19.1). Next, we performed a similar experiment with 2 equiv of $FeCl_3$. The stacked diagram of time-dependent HPLC indicated that the time of conversion of half of the substrate to be ~2-3 min, and the reaction was completed within 30 min (Figure7.1). Therefore, the two equiv of $FeCl_3$ was considered as the optimized condition for the deprotection of the Boc group from the methyl ester of Boc protected amino acids. The detailed procedure is described in the experimental section (section 7.16.2 and 7.16.3).

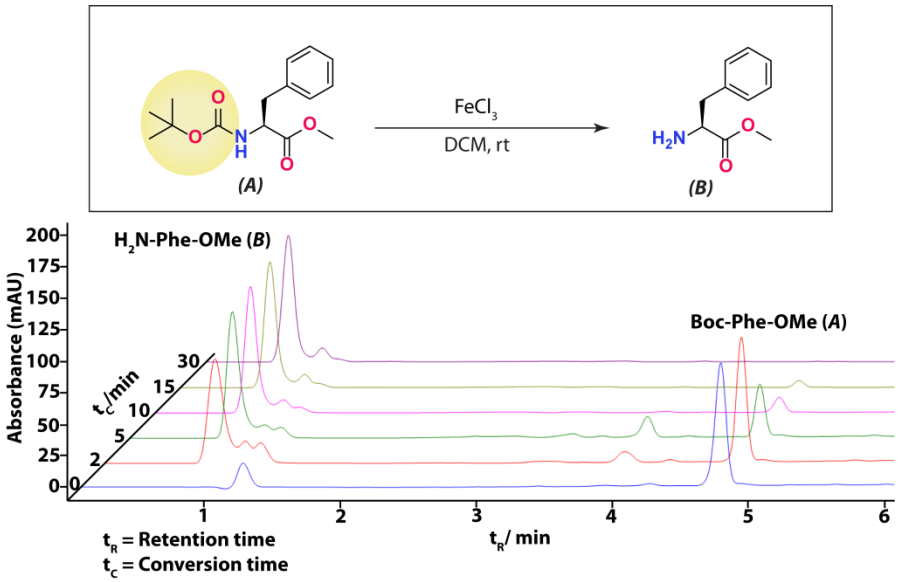

Figure 7.1. *A time-dependent stacked HPLC profiles of conversion of* ***A*** *(t_R = 4.9 min) to* ***B*** *(t_R = 0.9 min).*

7.5. Isolation of Boc-deprotected product

The isolation of Boc cleaved product (***B***) by work-up or column chromatography was difficult as in water-based work-up a large amount of product (***B***) went to the water with iron (iron is water-soluble). On the other hand, when we performed column chromatography without workup, the isolation of the product was difficult as the product might be chelated with iron and silica gel. Therefore, to overcome this problem, we added a few drops of 1% (v/v) phosphoric acid (H_3PO_4) to the reaction mixture. After adding this, the reaction mixture became colorless from brown color, indicating the formation of a complex with iron and phosphoric acid. The generated complex may be $Fe(H_2PO_4)^{2+}$ as reported.[11]

7.6. Substrates scope for the synthesis of peptides in solution

Next, we applied this protocol for peptide synthesis in solution. For that, we added base, DIPEA dropwise to the above reaction mixture to neutralize it and at the same time Boc protected amino acid, e.g. Boc-Phg-OH (1 equiv), coupling reagent, *o*-NosylOXY (1 equiv) and base, DIPEA (1 equiv) were taken in a 50 mL R.B. with DCM and stirred for 5 min for preactivation. Then, the above-neutralized reaction mixture was added to that preactivated solution and was kept the reaction for completion (Scheme 7.2).

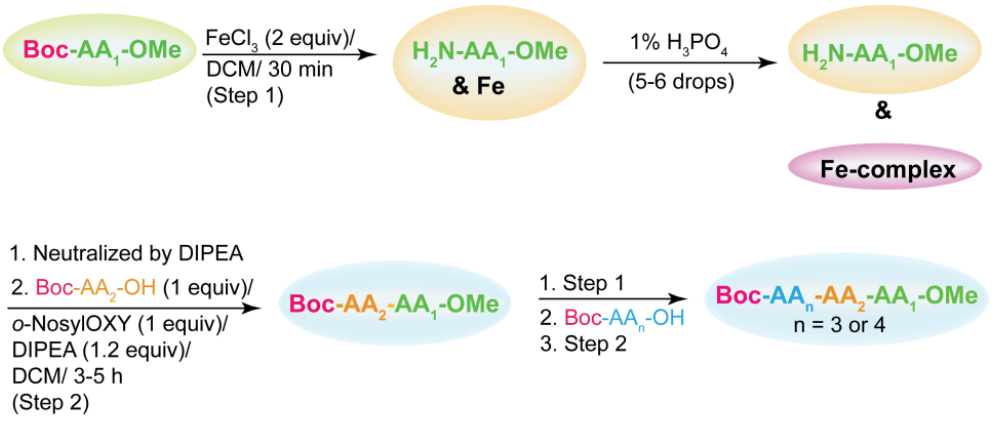

Scheme 7.2. *A schematic representation of peptide synthesis in solution*

In this way, we first synthesized a dipeptide, Boc-Phg-Phe-OMe (**7a**, Table 7.1, entry 1) with a 73% isolated yield. Next, we synthesized a library of dipeptides and tripeptides using this protocol. Interestingly, the reaction worked well with the carboxylic acid of Boc protected aromatic or aliphatic amino acid and the amine of aromatic or aliphatic methyl ester. The reaction also worked well for some sterically hindered natural amino acid (Val, Ile, and Leu); unnatural amino acid L-Phg, D-Phg, D-Phe, Aib, β-Ala, and m-ABA; secondary natural amino acid, pro; and various side-chain protecting groups containing amino acids, e.g., OBzl, Bzl, Alloc and Tos (Table 7.1). The isolated yields were found to be moderate to good for each dipeptide or tripeptide (Table 7.1). We were also able to synthesize a hydrophobic tetrapeptide, Boc-Leu-Gly-Phe-Phe-OMe, using this protocol with a 46% yield (7q, Table 7.1, entry 17). All the synthesized peptides were purified by silica gel column chromatography, and the purity was checked by analytical HPLC. They also further characterized by mass spectrometry and 1D (^{1}H and ^{13}C) and 2D (COSY and TOCSY) spectroscopy. The detailed procedure for di-, tri- and tetra-peptide synthesis in solution is described in section 7.16.4 and 7.16.5.

Table 7.1. The wide scope of di-,tri-, and terta-peptide synthesis using this protocol

entry	peptides (id)	structures	isolated yield (%)
1	Boc-Phg-Phe-OMe (**7a**)	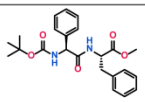	73
2	Boc-Val-Val-OMe **(7b)**	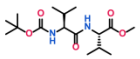	71
3	Boc-Ile-Ala-OMe (**7c**)	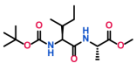	76
4	Boc-Glu(OBzl)-Pro-OMe (**7d**)	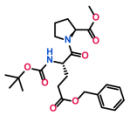	67
5	Boc-L-Ile-D-Phe-OMe (**7e**)	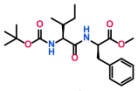	72
6	Boc-m-ABA-Aib-OMe (**7f**)	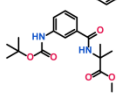	69
7	Boc-β-Ala-m-ABA-OMe (**7g**)	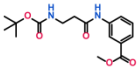	67
8	Boc-Gly-DL-Phg-OMe (**7h**)	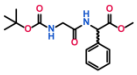	70
9	Boc-Gly-L-Phg-OMe (**7i**)	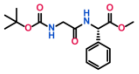	71
10	Boc-Phe-Lys(Alloc)-OMe (**7j**)	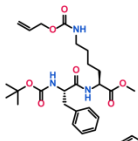	68
11	Boc-Phe-Tyr(Bzl)-OMe (**7k**)	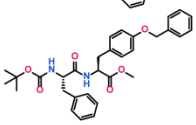	70
12	Boc-Ala-His(Tos)-OMe (**7l**)	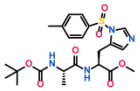	67
13	Boc-Gly-Phe-Phe-OMe (**7m**)	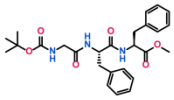	63
14	Boc-Val-Val-Ile-OMe (**7n**)	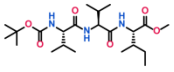	60
15	Boc-L-Val-L-Phe-D-Phe-OMe (**7o**)	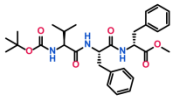	61
16	Boc-Gly-L-Phg-D-Phg-OMe (**7p**)	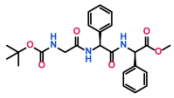	62
17	Boc-Leu-Gly-Phe-Phe-OMe (**7q**)	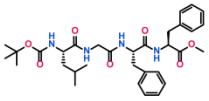	46

7.7. Crystallographic evidence of the formation of the dipeptides

The chemical structure of two dipeptides, Boc-m-ABA-Aib-OMe (**7f**, Table 7.1, entry 6) and Boc-β-Ala-m-ABA-OMe (**7g**, Table 7.1, entry 7) were confirmed by the SC-XRD experiment. The crystallographic data are listed in section 7.20 (Table 7.3).

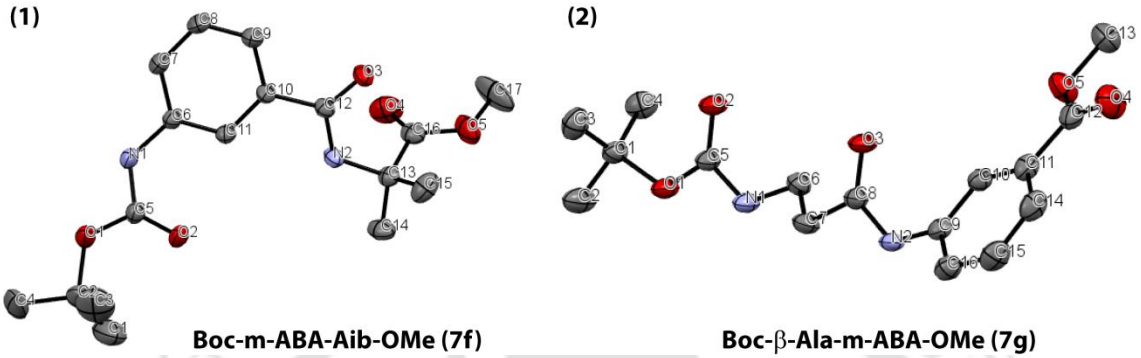

Figure 7.2. *The ORTEP diagram of peptides (1)* ***7f****, and (2)* ***7g*** *with an ellipsoid of 30% probability*

7.8. Racemization study

Next, to investigate the racemization probability of this protocol, we synthesized two dipeptides, Boc-Gly-DL-Phg-OMe (**7h**, Table 7.1, entry 8) and Boc-Gly-L-Phg-OMe (**7i**, Table 7.1, entry 9). We kept the unnatural amino acid, Phg at the *C*-terminus in the peptide sequence, as it is known as racemization prone amino acid and then performed the HPLC studies.

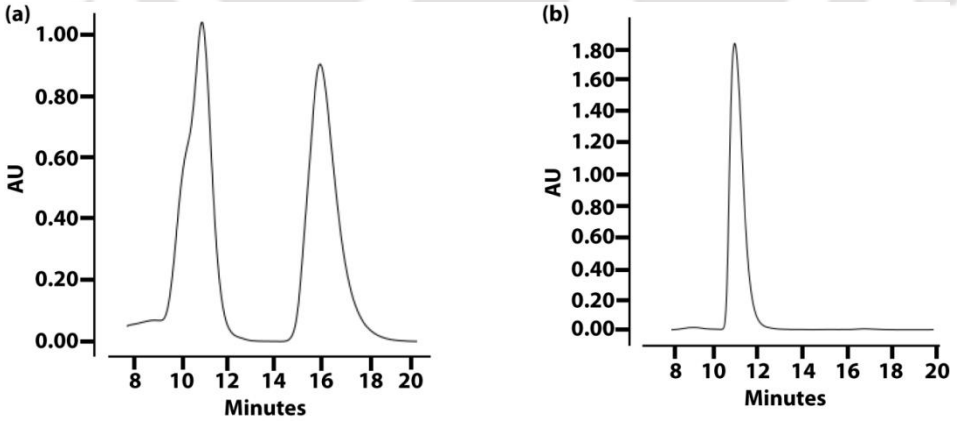

Figure 7.3. *A partial HPLC profile of (a) DL- and (b) L- isomer of a dipeptide, Boc-Gly-Phg-OMe. (CHIRALPAK® AS-H column, 5 µm, 4.6×250 mm, an isocratic gradient of 20% isopropanol in hexane)*

The obtained HPLC profile of **7h** showed two distinct peaks with retention times 10.84 min and 15.92 min (CHIRALPAK® AS-H column, 5 µm, 4.6mm × 250 mm, isocratic gradient of 20% isopropanol in hexane till 30 min), indicating the presence of two

enantiomers (Figure 7.3 and Figure 7.15 in section 7.19.3). However, the HPLC profile of **7i** displayed a single peak at 10.79 min (in similar isocratic gradient), indicating the presence of single enantiomer (Figure 7.3 and Figure 7.16 in section 7.19.3). Thus, these obtained results imply that no detectable racemization was observed during peptide synthesis using this protocol.

7.9. Wide scope for SPPS on acid-sensitive Rink amide resin

Next, we applied our protocol on solid phase peptide synthesis. For that, we have chosen Fmoc-Rink amide AM resin as solid support. In Chapter 7, section 6.5, we discussed the sustainability of this resin for $FeCl_3$ treatment.

At first, Fmoc-Rink amide AM resin (100 mg, loading 0.7 mmol/g) was taken into a 2 mL frit-fitted plastic syringe and was swollen with DCM followed by DMF and was converted to free amine, using 20% piperidine in DMF, and then washed properly with DMF. Next, the first Boc protected amino acid was loaded onto that Fmoc deprotected resin using coupling reagent, *o*-NosylOXY (2.5 equiv) and base, DIPEA (5 equiv) in DMF medium.

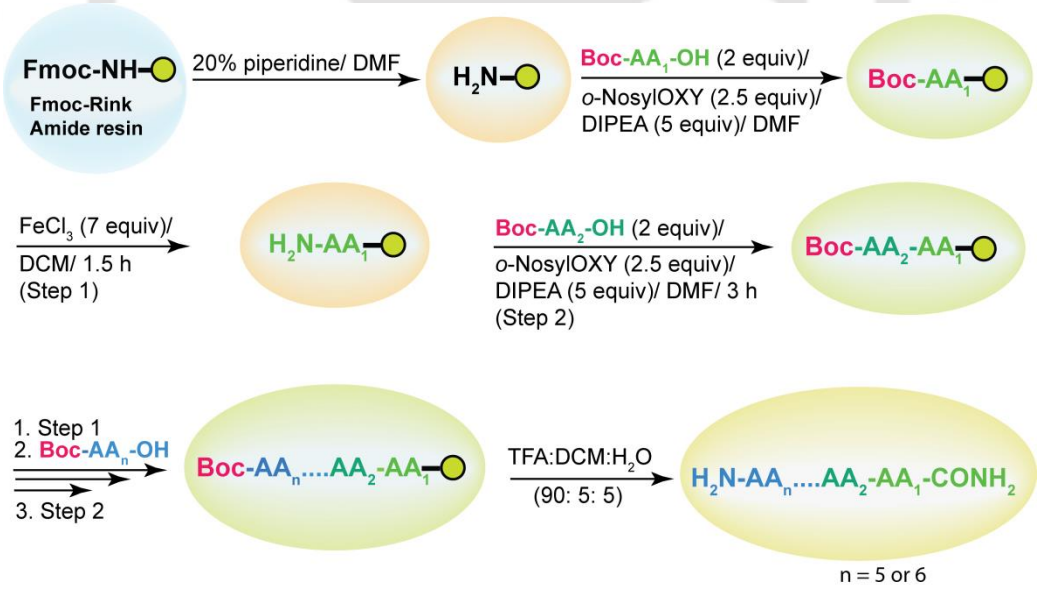

Scheme 7.3. *A schematic representation of peptide synthesis using Boc protected amino acid on Fmoc-Rink amide resin during SPPS*

After the coupling of the first amino acid, the possible unreacted free amine of that resin was capped using acetic anhydride and NMI in DCM. After proper washing, 7 equiv of $FeCl_3$ and DCM (1 mL) were taken for removal of Boc group from the *N*-terminal amino

acid of peptide anchored resin within 1.5 h. Then, peptide anchored resin was washed several times with DMF for removing excess $FeCl_3$. After that we performed coupling reaction of that deprotected amine of first amino acid residue attached with resin, and next Boc protected amino acid using above coupling reagent and base during SPPS (Scheme 7.3).

7.10. Monitoring of peptide synthesis by HPLC

After completion of the coupling reaction, a small portion of the peptide anchored resin was taken for test cleavage using the cleavage cocktail, TFA: DCM: H_2O (90: 5: 5). We got a hundred less mass from the desired mass, indicating Boc cleavage from *N*-terminal amino acid residue. In this way, we monitored several Boc cleavage and coupling steps of peptide **8a** (FA-NH_2, FFA-NH_2, VFFA-NH_2, and LVFFA-NH_2) by a reverse-phase analytical HPLC and Mass spectrometry. The obtained results indicated that the coupling and deprotection proceeded smoothly in each step. The HPLC and mass spectra are displayed in section 7.19 (Figure 7.17-7.24).

7.11. Synthesis of some biologically important peptides

By using this protocol we synthesized four biologically active small peptides e.g. LVFFA-NH_2 (17-21) of $A\beta_{1\text{-}42}$, which is responsible for Alzheimer's disease (AD);[12] NFGAIL-NH_2 (22-27) of Amylin (1-37), which is main culprit of type II diabetes (T2D);[13] YGGFL-NH_2 of Leu-enkephalin, which is an endogenous opioid neurotransmitter;[14] and YaGFM-NH_2 of [D-Ala^2, Met^5]-enkephalinamide, which is a peptidase inhibitor[15] (Table 7.2) using our protocol.

Table 7.2. Synthesis of some biologically important peptides in SPPS

Entry	***Peptides (id)***	***Spectroscopic Yield (%)***	***Isolated Yield (%)***
1	LVFFA-NH_2 (**8a**)	90	14
2	NFGAIL-NH_2 (**8b**)	91	09
3	YGGFL-NH_2 (**8c**)	100	13
4	YaGFM-NH_2 (**8d**)	83	10

After synthesis, the peptide anchored resin was cleaved by cleavage cocktail TFA: DCM: H_2O (90: 5: 5) and precipitated from the cold ether and dried. Then these crude peptides were analyzed by HPLC. The relative abundance of the peptide with associated impurities was calculated by integrating the peak in HPLC (Table 7.2, reported as a spectroscopic yield). Next, the crude peptides were purified by reverse phase semi-preparative HPLC and the obtained purified products were freeze-dried, and the isolated yields were calculated (Table 7.2, reported as an isolated yield). The purity of those peptides was checked by reverse phase analytical HPLC and characterized by mass spectrometry and 1D (^{1}H and ^{13}C) and 2D (COSY and TOCSY) NMR spectroscopy.

7.12. Peptide synthesis by both Fmoc and Boc chemistry on Rink amide resin

To explore the scope of this protocol, we performed both Fomc chemistry and Boc chemistry on the same resin (Rink amide). In this way, we synthesized a model *N*-terminally branched peptide (**8e**) and a model side-chain to side-chain cyclic peptide (**8f**).

7.12.1. Application of the protocol for peptide branching

At first, we synthesized the peptide sequence, Fmoc-Lys(Boc)-Phe-Leu-Gly-resin by standard Fmoc-SPPS on Rink amide resin. Then the *N*-terminal Fmoc of Lys was removed by 20% piperidine/DMF and acetylated it by using acetic anhydride and NMI on-resin. Next, Boc protected side chain of the *N*-terminal Ac-Lys- was cleaved by $FeCl_3$, and the deprotected amine was coupled with the next amino acid, Boc-Ala-OH, to form an amide bond, on the resin. Similarly, the next amino acid, Boc-Val-OH was also coupled, and finally, the resin was cleaved by the cleavage cocktail TFA: DCM: H_2O (90: 5: 5) and the peptide was precipitated out in cold diethyl ether (Scheme 7.4). The obtained spectroscopic and isolated yields of **8e** were 83% and 19%, respectively. Here we used both standard Fmoc/tBu and newly reported Boc-strategy on the same resin during SPPS. This is the beauty of our protocol.

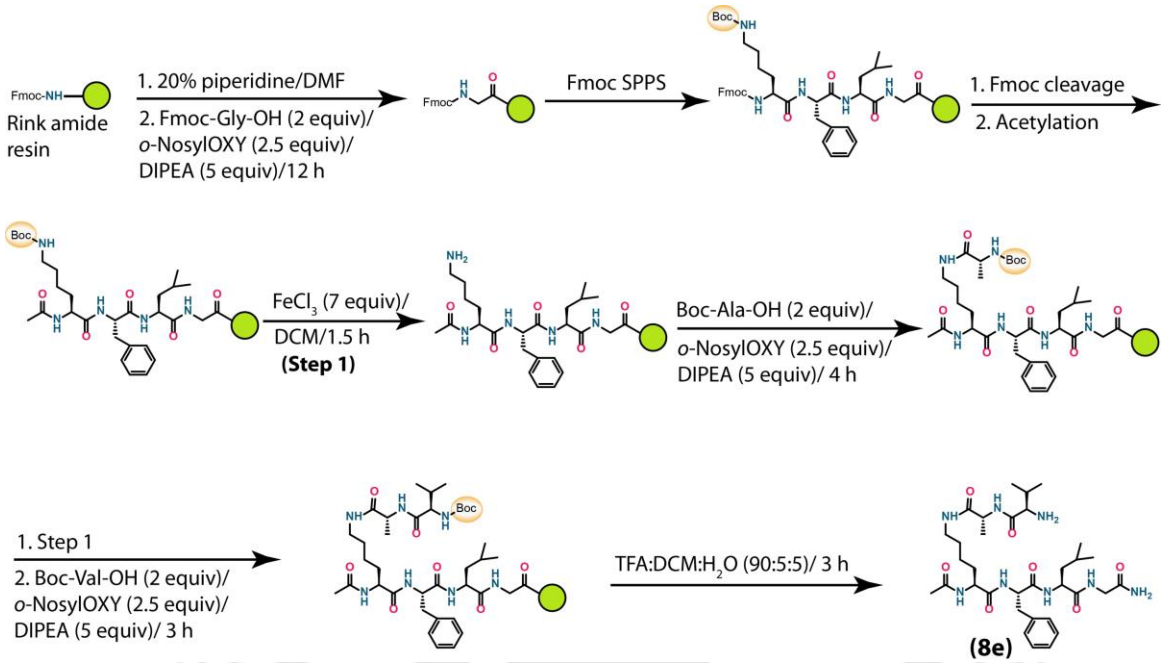

Scheme 7.4.. *Synthetic scheme of a model branched peptide*

7.12.2. Application of the protocol for cyclic peptide synthesis

Next, we synthesized a model side-chain to side-chain cyclic peptide, H_2N-cyclo[Glu-Pro-Phe-Phe-Lys]-NH_2 (**8f**, Scheme 7.5) by using both standard Fmoc/tBu and our newly reported protocol.

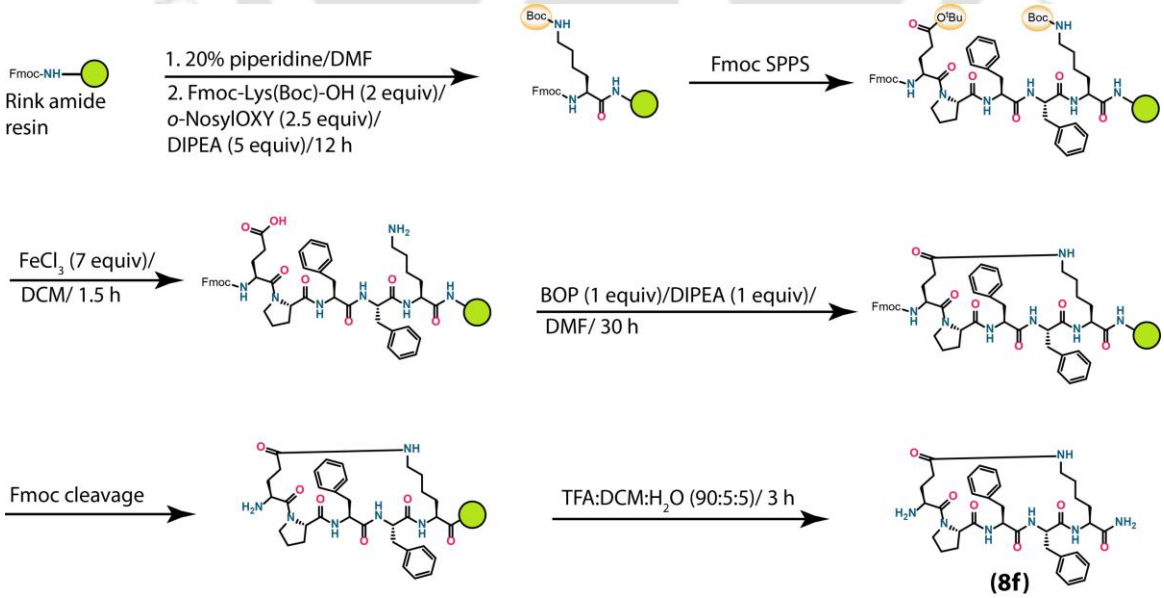

Scheme 7.5. *Side-chain to side-chain cyclization*

At first, Fmoc-Glu(OtBu)-Pro-Phe-Phe-Lys(Boc)-resin was synthesized by using the standard Fmoc/tBu method, and then tBu/Boc of the side chain of Glu/Lys was removed by using our protocol. Finally, the cyclization of side-chain to side-chain was carried out in presence of coupling reagent (BOP, 1 equiv) and base (DIPEA, 1 equiv) for 30 h. We obtained 76% spectroscopic and 9 % isolated yield of **8f**.

7.13. Drawbacks and advantages of this protocol

Although we have synthesized the peptides in SPPS using the present protocol, it has a few drawbacks. The isolated yield of the long-chain peptides was relatively less probably due to the cleavage of some of the peptides in each step of Boc cleavage. Nevertheless, the spectroscopic yields were excellent in each case. Moreover, acid-sensitive side-chain protecting groups (Boc, *t*Bu, and Trt) are not compatible with this protocol.

The present protocol offers several excellent features, e.g., peptides could be synthesized by using Boc/Bzl orthogonal protection/deprotection technique on acid-sensitive Fmoc-compatible resin, Rink amide AM, without using TFA for each step of Boc-cleavage. The final step for peptide cleavage from the resin could be carried out using TFA. This feature is vital as the Boc-protected amino acids are less expensive than the Fmoc protected amino acids. Moreover, this protocol can be used for Boc-chemistry on Boc-chemistry compatible resins, e.g., Merrifield resin, PAM-resin, and BHA resin, as well. However, HF should be used to cleave the peptide from the resin at the final stage in that case.

7.14. Plausible mechanism

A plausible mechanism of the deprotection of Boc is drawn based on the existing literature (Scheme 7.6).[9,10] At first, Fe(III) coordinates with the oxygen atom of urethane (C=O) and forms a complex. At this stage, iron pulls electron density towards itself; therefore, the C-O bond becomes week and breaks down to form Boc deprotected amine, carbon dioxide, and isobutene.

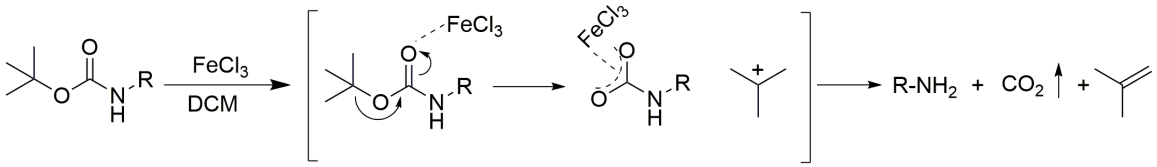

Scheme 7.6. *A plausible mechanistic pathway for deprotection of Boc*

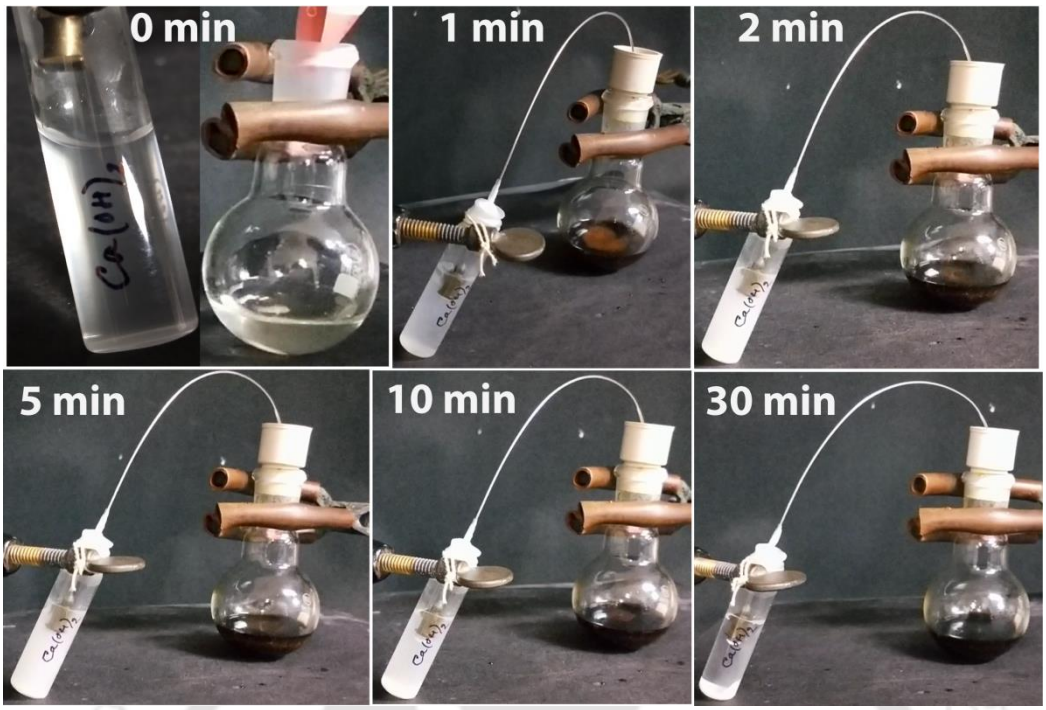

Figure 7.4. *Monitoring the evolution of CO_2 from the reaction*

To prove the evolution of carbon dioxide from the reaction mixture, we took benzylamide of Boc-Ala-OH (2.69 mmol), $FeCl_3$ (2 equiv) in DCM, which result in the evolution of CO_2. The evolution of CO_2 was monitored by changing the colorless solution of $Ca(OH)_2$ to white suspense, i.e., the formation of $CaCO_3$ in the presence of CO_2 (Figure 7.4).

7.15. Conclusion

In conclusion, we have developed a mild and efficient method for Boc deprotection from amino acids and used it in peptide synthesis both in solution and SPPS. The greener $FeCl_3$ is used to deprotect the Boc group from *N*-terminal amino acid instead of TFA, which is non-environment friendly and corrosive. We have synthesized various natural or unnatural amino acids containing small peptides in solution and SPPS with moderate to good yield by using this protocol. This new method allows practicing Boc-chemistry on a Fmoc-compatible resin, increasing the flexibility of the SPPS design as well as increasing the environment-friendly nature of Boc chemistry. Also, it allows practicing both Boc chemistry and Fmoc chemistry depending on the need for a single peptide chain synthesis on Solid support. Thus, the inherent orthogonality of Boc-and Fmoc-chemistry allows branched and cyclized peptides easier.

7.16. Experimental section

7.16.1. Materials and instrumentation

As described in chapter 8

7.16.2. General procedure for Boc-deprotection in solution

Both *N*- and *C*- protected (Boc-AA-OMe, AA = amino acid) amino acid (1 equiv) was dissolved in 2 mL DCM. Then 2 equiv of $FeCl_3$ was added to it and kept stirring. The reaction was monitored by TLC as well as analytical HPLC.

7.16.3. Monitoring of Boc-cleavage by HPLC

For monitoring the Boc cleavage, we performed HPLC studies with time. We took 0.107 mmol Boc-Phe-OMe (***A***) and 2 equiv of $FeCl_3$ in 2 mL DCM medium. Then, 50 μL of the reaction mixture was taken in five different Eppendorf vial at 2, 5, 10, 15 and 30 min. Next, to quench the reaction, 5 μL of DIPEA was added to that Eppendorf vials, and then the solvent was evaporated by passing N_2 gas. The dried reaction mixture was dissolved by adding HPLC-grade acetonitrile (1mL) and then filtered through 0.22 μm filter paper and injected 20 μL of each solution in reverse phase analytical HPLC.

7.16.4. General procedure for dipeptide synthesis in solution

At first, both *N*-and *C*-protected amino acid (1 equiv) was taken in a 50 mL R.B. and was dissolved with DCM. Then 2 equiv of $FeCl_3$ was added to it. The reaction was monitored by TLC. After completion of the reaction, 1% H_3PO_4 was added dropwise to it until the brown color became colorless or slightly yellowish. Then DIPEA was added slowly to it for maintaining the neutral pH. At the same time, next Boc protected amino acid (1 equiv), *o*-NosylOXY (1 equiv), and DIPEA (1 equiv) were taken in another 50 mL R.B. with DCM and stirred for 5 min for preactivation. Then the above Boc deprotected amino acid methyl ester was added dropwise to the activated ester solution and kept stirring for 4-5 h at room temperature. After completion of the reaction, monitored by TLC, was diluted with DCM, and the organic layer was washed with 10% citric acid, followed by a saturated $NaHCO_3$ solution three times in each case. Then the organic layer was collected in a conical flask and was dried over Na_2SO_4 followed by evaporated this organic mixture for getting a solid product of both *N*- and *C*- protected dipeptide.

7.16.5. General procedure for tri-/tetra-peptide synthesis in solution

At first, both *N*- and *C*- protected dipeptide was synthesized by the above method. Then this dipeptide was dissolved with DCM in a 50 mL R.B. and was added $FeCl_3$ (2 equiv). After 1h, a few drops of 1% H_3PO_4 was added to it until the color was masked. Then this solution was neutralized by adding DIPEA. At the same time, next Boc protected amino acid (1 equiv), *o*-NosylOXY (1 equiv), and DIPEA (1 equiv) were taken in another 50 mL R.B. with DCM and stirred for 5 min for preactivation. Then the Boc deprotected dipeptide methyl ester was added dropwise to that vessel, contain activated ester solution. After completion of the reaction, the organic layer was washed followed by evaporated for getting solid tripeptide, described above. Tetrapeptide was also synthesized by this protocol. All desired di-/tri-/tetra-peptides were purified by silica gel Column chromatography using an ethyl acetate-hexane system.

7.16.6. General procedure for peptide synthesis in the solid phase (SPPS)

Swelling of Resin, Rink amide AM

Rink amide AM resin (100 mg, 0.7 mmol/g) was taken into a 2 mL frit-fitted plastic syringe and was swollen in DCM (1.5 mL) for 2h followed by DMF (1.5 mL) for 1h on a Stuart blood tube rotator (30 rpm).

Fmoc deprotection/ coupling

Next, 1.5 mL of 20% piperidine/DMF (v/v) was taken inside the syringe and rotated it for 7 min, then removed it from the syringe. This step was repeated three times (7 min x 3 times) and washed the resin with DMF for ten times. The coupling reaction was carried out by taking two equiv of Boc protected amino acid (2 x 0.07 = 0.14 mmol), 2.5 equiv (2.5 x 0.07 = 0.175 mmol) of a coupling reagent (*o*-NosylOXY), and five equiv (5 x 0.07 = 0.35 mmol) of a base (DIPEA) for 10 h to 12 h, depending on amino acids. After coupling, the peptide anchored resin was washed with DMF (1 mL x 5 times) followed by DCM.

Capping

Next, 2 equiv. (2 x 0.07 = 0.14 mmol) of acetic anhydride and 2.5 equiv. (2.5 x .07 = 0.175 mmol) of NMI in DCM were taken in that syringe and stirred 1 h. Then removed it from the syringe and washed within DCM. This capping step is important as the resin is bulky, therefore if any unreacted amine-free resin was left, it should be capped by

acetylation. Otherwise, another undesired truncated peptide fragment would start with the main fragment.

Boc deprotection

Next, 7 equiv (7 x 0.07 = 0.49 mmol) of $FeCl_3$ and DCM (1 mL) were taken in that syringe and kept stirring for 1.5 h for removal of Boc group. Then peptide anchored resin was washed with DCM (3 x 1 min) and DMF (10 x 1 min).

Coupling

Next, the coupling process was continued using Boc protected amino acid (2 equiv), *o*-NosylOXY (2.5 equiv), and DIPEA (5 equiv) in DMF for 3 h to 5 h, depending on amino acids.

Final cleavage from the resin

The final desired peptide was cleaved from the resin using a cleavage cocktail, TFA:DCM:H_2O (90: 5: 5) for 3 h. Then, the crude peptide was precipitated by cold ether, followed by centrifugation to obtain crude solid peptide.

Table 7.2. The tabular form of Solid-phase peptide synthesis by using the newly reported method

Description	***Reagents***	***time***
Boc removal	$FeCl_3$ (7 equiv)/ DCM	1.5 h x 1 time
Washing	DCM	1 mL x 3 min x 3 times
	DMF	1 mL x 10 min x 10 times
Coupling	Boc-AA-OH (2 equiv)/ *o*-NosylOXY (2.5 equiv)/ DIPEA (5 equiv)/ DMF	3 h x 1 time
Washing	DMF	1 mL x 5 min x 5 times
	DCM	1 mL x 3 min x 3 times
Cleavage cocktail	TFA:DCM:H_2O (90: 5: 5)	3 h x 1 times

7.17. Characterization data

Boc-Phg-Phe-OMe (7a).

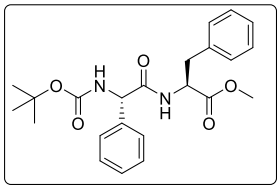

^{1}H NMR ($CDCl_3$; 600 MHz) δ 1.42 (9H, s); 3.08-3.06 (1H, q, *J* = 6 Hz, *J* = 8.4 Hz); 3.18-3.14 (1H, q, *J* = 6 Hz, *J* = 7.8 Hz); 3.65 (3H, s); 4.82-4.79 (1H, q, *J* = 6 Hz, *J* = 7.8 Hz); 5.10 (1H, br); 5.66 (1H, br); 6.20 (1H, br); 7.05-7.04 (2H, d, *J* = 6.6 Hz); 7.33-7.25 (8H, m). ^{13}C NMR ($CDCl_3$; 150 MHz) δ 28.4, 37.8, 52.4, 53.6, 58.8, 80.2, 127.2, 127.3, 128.7, 129.0, 129.3, 135.7, 137.8, 155.2, 169.9, 171.5. HRMS (ESI): calculated $[M+H]^+$ 413.1998, found m/z . 413.2054. HPLC: retention time (t_R) = 9.50 min. Isolated pure product 302 mg (yield: 73%).

Boc-Val-Val-OMe (7b).

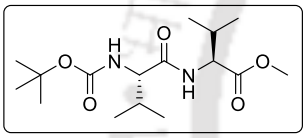

^{1}H NMR ($CDCl_3$; 600 MHz) δ 0.97-0.90 (12H, m); 1.44 (9H, s); 2.20-2.12 (2H, m); 3.73 (3H, s); 3.92-3.90 (1H, m); 4.56-4.53 (1H, m); 5.04 (1H, br); 6.36 (1H, br). ^{13}C NMR ($CDCl_3$; 150 MHz) δ 17.9, 18.1, 19.1, 19.4, 28.4, 30.8, 31.4, 52.3, 57.3, 60.4, 80.2, 156.1, 172.3, 174.3. HRMS (ESI): calculated $[M+H]^+$ 331.2155, found m/z 331.2265. HPLC: retention time (t_R) = 8.97 min. Isolated pure product 234 mg (yield: 71%).

Boc-Ile-Ala-OMe (7c).

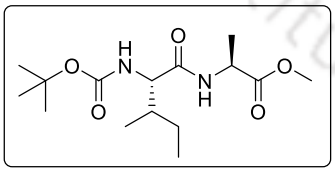

^{1}H NMR ($CDCl_3$; 600 MHz) δ 0.95-0.90 (6H, m); 1.42-1.40 (3H, d, *J* = 7.2 Hz); 1.44 (9H, s); 1.17-1.12 (1H, m); 1.72-1.71 (1H, br); 1.87 (1H, br); 3.75 (3H, s); 3.97-3.95 (1H, m); 4.61-4.56 (1H, m); 5.07 (1H, br); 6.45 (1H, br). ^{13}C NMR ($CDCl_3$; 150 MHz) δ 11.5, 15.5, 18.3, 24.3, 28.4, 37.5, 48.1, 52.5, 59.2, 80.0, 115.9, 171.4, 173.3. HRMS (ESI): calculated $[M+H]^+$ 317.1998, found m/z 317.2110. HPLC: retention time (t_R) = 8.57 min. Isolated pure product 240 mg (yield: 76%).

Boc-Glu(OBzl)-Pro-OMe (7d).

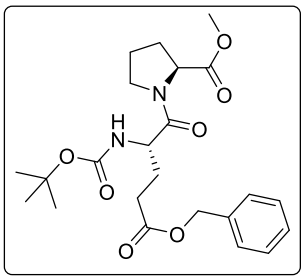

^{1}H NMR ($CDCl_3$; 600 MHz) δ 1.41 (9H, s); 1.82-1.77 (1H, m); 2.00-1.95 (3H, m); 2.21-2.15 (2H, m); 2.50-2.45 (1H, m); 2.58-2.53 (1H, m); 3.69 (3H, s); 4.52-4.51 (1H, m); 4.57-4.55 (1H, m); 5.14 (2H, s); 5.39-5.37 (1H, d, *J* = 8.4 Hz); 7.36-7.31 (5H, m). ^{13}C NMR ($CDCl_3$; 150 MHz) δ 25.1, 28.0, 28.4, 29.1, 29.6, 47.1, 51.0, 52.4, 58.9, 66.5, 79.9, 128.3, 128.4, 128.7, 136.0, 155.8, 170.9, 172.4, 173.0. HRMS (ESI): calculated $[M+H]^+$ 449.2210, found m/z 449.2305. HPLC: retention time (t_R) = 9.35 min. Isolated pure product 300 mg (yield: 67%).

Boc-L-Ile-D-Phe-OMe (7e).

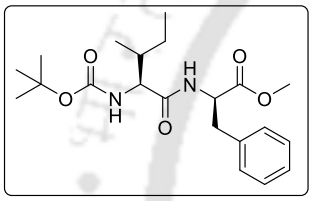

^{1}H NMR ($CDCl_3$; 600 MHz) δ 0.86-0.83 (6H, m); 0.99 (1H, brs); 1.43 (9H, s); 1.77 (1H, brs); 1.86 (1H, brs); 3.15-3.06 (2H, m); 3.71 (3H, s); 4.01 (1H, brs); 4.90-4.87 (1H, q, *J* = 6.6 Hz, *J* = 6 Hz); 4.96 (1H, br); 6.43 (1H, br); 7.11-7.10 (2H, d, *J* = 7.2 Hz); 7.29-7.23 (3H, m). ^{13}C NMR ($CDCl_3$; 150 MHz) δ 11.7, 15.6, 24.4, 28.4, 37.3, 38.1, 59.4, 80.1, 127.3, 128.8, 129.3, 135.9, 155.9, 171.4, 172.0. HRMS (ESI): calculated $[M+H]^+$ 393.2391, found m/z 393.2465. HPLC: retention time (t_R) = 12.77 min. Isolated pure product 282 mg (yield: 72%).

Boc-mABA-Aib-OMe (7f).

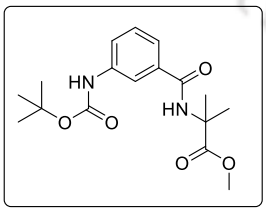

^{1}H NMR ($CDCl_3$; 600 MHz) δ 1.52 (9H, s); 1.66 (6H, s); 3.77 (3H, s); 6.72 (1H, s); 6.85 (1H, s), 7.35-7.32 (1H, t, *J* = 7.8 Hz), 7.43-7.42 (1H, d, *J* = 7.2 Hz), 7.57 (1H, br); 7.73 (1H, s). ^{13}C NMR ($CDCl_3$; 150 MHz) δ 24.9, 28.4, 52.9, 56.9,. 80.9, 117.2, 121.6, 121.7, 129.3, 135.1, 138.9, 152.9, 166.7, 175.4. HRMS (ESI): calculated $[M+H]^+$ 337.1765, found m/z 337.1939, HPLC: retention time (t_R) = 12.88 min. Isolated pure product 232 mg (yield: 69%).

Boc-β-Ala-mABA-OMe (7g).

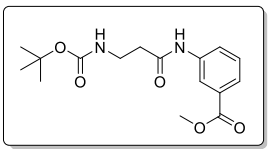

^{1}H NMR ($CDCl_3$; 600 MHz) δ 1.43 (9H, s); 2.65-2.63 (2H, t, *J* = 5.4 Hz); 3.52-3.49 (2H, q, *J* = 6 Hz, *J* = 5.4 Hz); 3.90 (3H, s); 5.35 (1H, brs); 7.40-7.37 (1H, t, *J* = 7.8Hz); 7.77-7.76 (1H, d, *J* = 7.2 Hz); 7.92-7.90 (1H, d, *J* = 7.8 Hz); 8.14 (1H, s); 8.66 (1H, br). ^{13}C NMR ($CDCl_3$; 150 MHz) δ 28.5, 36.5, 37.6, 52.4, 79.8, 120.8, 124.5, 125.3, 129.2, 130.8, 138.5, 156.6, 167.0, 170.3. HRMS (ESI): calculated $[M+Na]^+$ 345.1427, found m/z 345.1491. HPLC: retention time (t_R) = 11.23 min. Isolated pure product 216 mg (yield: 67%).

Boc-Gly-DL-Phg-OMe (7h).

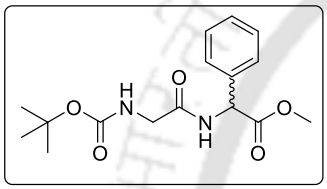

^{1}H NMR ($CDCl_3$; 600 MHz) δ 1.44 (9H, s); 3.72 (3H, s); 3.84 (2H, brs); 5.18 (1H, brs); 5.58-5.57 (1H, d, *J* = 5.4 Hz); 7.16 (1H, brs); 7.35-7.32 (5H, m). ^{13}C NMR ($CDCl_3$; 150 MHz) δ 28.4, 44.4, 53.0, 56.4, 80.5, 127.4, 128.8, 129.1, 136.3, 156.3, 169.1, 171.3. HRMS (ESI): calculated $[M+H]^+$ 323.1609, found m/z 323.1623. Isolated pure product 227 mg (yield: 70%).

Boc-Gly-L-Phg-OMe (7i).

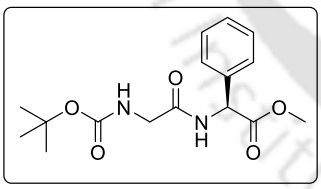

^{1}H NMR ($CDCl_3$; 600 MHz) δ 1.44 (9H, s); 3.73 (3H, s); 3.84 (2H, brs); 5.15 (1H, brs); 5.58-5.57 (1H, d, *J* = 6 Hz); 7.13 (1H, brs); 7.36-7.32 (5H, m). ^{13}C NMR ($CDCl_3$; 150 MHz) δ 28.4, 44.3, 53.0, 56.4, 80.4, 127.3, 128.7, 129.1, 136.3, 156.3, 169.2, 171.2. HRMS (ESI): calculated $[M+H]^+$ 323.1609, found m/z 323.1621. Isolated pure product 230 mg (yield: 71%).

Boc-Phe-Lys(Alloc)-OMe (7j).

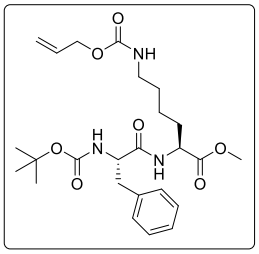

^{1}H NMR ($CDCl_3$; 600 MHz) δ 1.39 (9H, s); 1.52-1.46 (2H, m); 1.68-1.62 (1H, m); 1.81-1.76 (1H, m); 3.02-2.98 (1H, q, *J* = 7.8 Hz, *J* = 6 Hz); 3.18-3.10 (3H, m); 3.70 (3H, s); 4.46 (1H, brs); 4.59-4.53

(3H, m); 5.32-5.20 (3H, dd, *J* = 17.4 Hz, *J* = 10.2 Hz); 5.95-5.89 (1H, m); 6.79 (1H, br); 7.29-7.19 (5H, m). ^{13}C NMR ($CDCl_3$; 150 MHz) δ 22.3, 28.4, 29.3, 32.0, 38.4, 40.5, 52.5, 55.8, 65.6, 80.4, 117.8, 127.0, 128.7, 129.4, 133.1, 136.7, 155.7, 156.5, 171.7, 172.4. MALDI-TOF: calculated $[M+H]^+$ 492.2712, found $[M+Na]^+$ 514.214. HPLC: retention time (t_R) = 6.87 min. Isolated pure product 324 mg (yield: 68%).

Boc-Phe-Tyr(Bzl)-OMe (7k).

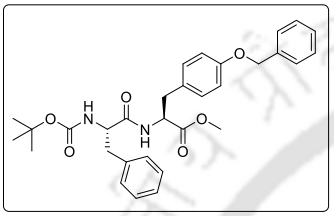

^{1}H NMR ($CDCl_3$; 600 MHz) δ 1.40 (9H, s); 3.03-2.94 (4H, m); 3.66 (3H, s); 4.34 (1H, br); 4.73 (1H, br); 5.01 (2H, s); 6.33 (1H, br); 6.84-6.83 (2H, d, *J* = 9 Hz); 6.89-6.87 (2H, *J* = 8.4 Hz); 7.42-7.18 (10H, m). ^{13}C NMR ($CDCl_3$; 150 MHz) δ 28.2, 37.0, 38.2, 52.2, 53.3, 55.6, 69.9, 80.1, 114.8, 127.4, 127.9, 128.5, 128.6, 129.3, 130.2, 136.8, 157.8, 170.7, 171.4. MALDI-TOF: calculated $[M+H]^+$ 533.2653, found $[M+Na]^+$ 555.216. HPLC: retention time (t_R) = 8.32 min. Isolated pure product 374 mg (yield: 70%).

Boc-Ala-His(Tos)-OMe (7l).

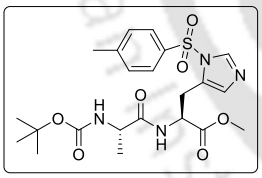

^{1}H NMR ($CDCl_3$; 600 MHz) δ 1.31-1.30 (3H, d, *J* = 6.6 Hz); 1.44 (9H, s); 2.44 (3H, s); 4.16 (1H, br); 4.80-4.77 (1H, q, *J* = 5.4 Hz, *J* = 7.2 Hz); 5.14 (1H, br); 7.11 (1H, s); 7.18 (1H, br); 7.37-7.36 (2H, d, *J* = 7.8 Hz); 7.81-7.80 (2H, d, *J* = 8.4 Hz); 7.91 (1H, s). ^{13}C NMR ($CDCl_3$; 150 MHz) δ 18.7, 21.9, 28.4, 29.8, 50.2, 51.8, 52.6, 80.1, 115.1, 127.5, 130.6, 134.9, 136.5, 140.0, 146.5, 155.4, 171.1, 172.7. MALDI-TOF: calculated $[M+H]^+$ 495.1915, found m/z 495.107. HPLC: retention time (t_R) = 6.39 min. Isolated pure product 330 mg (yield: 67%).

Boc-Gly-Phe-Phe-OMe (7m).

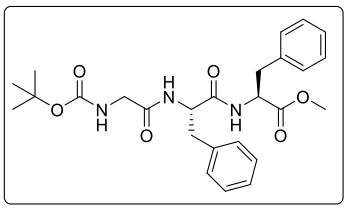

^{1}H NMR ($CDCl_3$; 600 MHz) δ 1.44 (9H, s); 3.09-2.95 (4H, m); 3.67 (3H, s); 3.77-3.68 (2H, m); 4.68-4.64 (1H, q, *J* = 6.6 Hz, *J* = 7.8 Hz); 4.77-4.73 (1H, q, *J* = 6.6 Hz, *J* = 7.2

Hz); 5.11 (1H, br); 6.46-6.45 (1H, d, *J* = 6 Hz); 6.72-6.70 (1H, d, *J* = 7.8 Hz); 7.01-7.00 (2H, d, *J* = 7.2 Hz); 7.16-7.15 (2H, d, *J* = 7.2 Hz); 7.27-7.20 (6H, m). ^{13}C NMR ($CDCl_3$; 150 MHz) δ 28.4, 38.0, 38.1, 44.3, 52.5, 53.5, 54.2, 80.5, 127.2, 127.3, 128.7, 128.8, 129.3, 129.5, 135.8, 136.3, 156.1, 169.5, 170.4, 171.5. HRMS (ESI): calculated $[M+H]^+$ 448.2449, found m/z 448.2459. HPLC: retention time (t_R) = 12.16 min. Isolated pure product 281 mg (yield: 63%, w.r.t. starting meterial Boc-Phe).

Boc-Val-Val-Ile-OMe (7n).

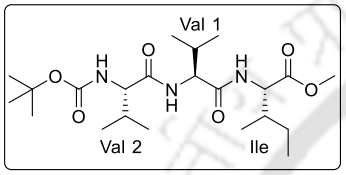

^{1}H NMR ($CDCl_3$; 600 MHz) δ 0.89-0.85 (6H, m); 0.93-0.89 (13H, m); 1.17-1.11 (1H, m); 1.41 (9H, s); 1.89-1.84 (1H, m); 2.09-2.08 (2H, br); 3.71 (3H, s); 3.94-3.91 (1H, t, *J* = 7.2 Hz); 4.34-4.32 (1H, t, *J* = 7.2 Hz); 4.57-4.55 (1H, q, *J* = 4.8 Hz, *J* = 3.6 Hz); 5.31-5.30 (1H, d, *J* = 7.8 Hz); 6.75-6.73 (1H, d, *J* = 9 Hz); 6.85-6.84 (1H, d, *J* = 7.8 Hz). ^{13}C NMR ($CDCl_3$; 150 MHz) δ 11.6, 15.6, 18.1, 18.4, 19.3, 19.4, 25.2, 28.4, 30.8, 31.0, 37.8, 52.2, 56.0, 58.8, 60.4, 79.9, 156.1, 171.2, 172.1, 172.3. HRMS (ESI): calculated $[M+H]^+$ 444.3075, found m/z 444.3091. HPLC: retention time (t_R) = 12.44 min. Isolated pure product 266 mg (yield: 60%, w.r.t. starting meterial Boc-Val).

Boc-L-Val-L-Phe-D-Phe-OMe (7o).

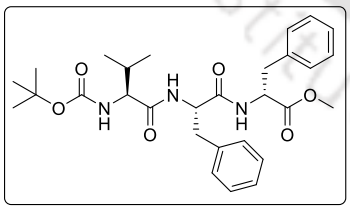

^{1}H NMR ($CDCl_3$; 600 MHz) δ 0.77-0.76 (3H, d, *J* = 6.6 Hz); 0.87-0.86 (3H, d, *J* = 6.6 Hz); 1.42 (9H, s); 2.11-2.06 (1H, m); 3.04-3.03 (2H, d, *J* = 6.6 Hz); 3.01-2.96 (2H, m); 3.04-3.03 (2H, d, *J* = 6.6 Hz); 3.63 (3H, s); 3.90-3.88 (1H, t, *J* = 6 Hz); 4.70-4.67 (1H, q, *J* = 6.6 Hz, *J* = 7.8 Hz); 4.76-4.73 (1H, q, *J* = 6 Hz, *J* = 6.6 Hz); 4.95-4.94 (1H, d, *J* = 6.6 Hz); 6.57 (1H,br); 6.63 (1H, br); 6.96-6.95 (1H, d, *J* = 6 Hz); 7.14-7.13 (1H, d, *J* = 7.2 Hz); 7.23-7.21 (4H, m); 7.29-7.26 (2H, t, *J* = 7.2 Hz). ^{13}C NMR ($CDCl_3$; 150 MHz) δ 17.5, 19.4, 28.4, 30.6, 37.8, 38.1, 52.4, 53.7, 54.1, 60.3, 80.4, 127.2, 128.7, 128.8, 129.3, 129.5, 135.5, 136.5, 156.2, 170.5, 171.5, 171.6. HRMS (ESI): calculated $[M+H]^+$ 526.2919, found m/z 526.2938. HPLC: retention time (t_R) = 12.85 min. Isolated pure product 320 mg (yield: 61%, w.r.t. starting meterial Boc-L-Phe).

Boc-Gly-L-Phg-D-Phg-OMe (7p).

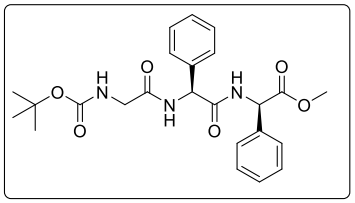

^{1}H NMR ($CDCl_3$; 600 MHz) δ 1.40 (9H, s); 3.69 (3H, s); 3.83 (2H, brs); 5.35 (1H, br); 5.53-5.52 (1H, d, *J* = 7.2 Hz); 5.79-5.78 (1H, d, *J* = 6.6 Hz); 7.12-7.11 (2H, d, *J* = 6.6 Hz); 7.30-7.22 (8H, m); 7.48-7.40 (2H, br). ^{13}C NMR ($CDCl_3$; 150 MHz) δ 28.4, 44.3, 53.1, 56.7, 88.3, 127.1, 127.4, 128.5, 128.6, 128.9, 129.0, 135.9, 137.4, 156.1, 169.3, 169.4, 171.1. HRMS (ESI): calculated $[M+H]^+$ 456.2136, found m/z 456.2132. HPLC: retention time (t_R) = 11.83 min. Isolated pure product 283 mg (yield: 62%, w.r.t. starting meterial Boc-L-Phg).

Boc-Leu-Gly-Phe-Phe-OMe (7q).

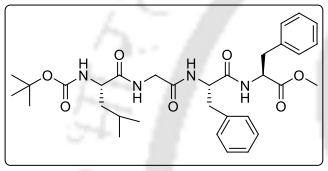

^{1}H NMR ($CDCl_3$; 600 MHz) δ 0.94-0.92 (6H, m); 1.42 (9H, s); 1.50-1.46 (1H, m); 1.67-1.60 (2H, m); 2.95-2.92 (1H, m); 3.01-2.98 (1H, m); 3.08-3.04 (2H, m); 3.65 (3H, s); 3.80-3.77 (1H, br); 3.90-3.86 (1H, dd, *J* = 5.4 Hz); 4.19 (1H, brs); 4.81-4.80 (2H, d, *J* = 6 Hz); 5.39 (1H, br); 7.06-7.05 (3H, d, *J* = 6.6 Hz); 7.12-7.10 (2H, d, *J* = 7.2 Hz); 7.23-7.16 (8H, m). ^{13}C NMR ($CDCl_3$; 150 MHz) δ 22.1, 23.1, 24.8, 28.4, 38.3, 39.0, 42.0, 42.9, 52.3, 53.5, 54.3, 79.6, 126.8, 127.0, 128.4, 128.5, 129.3, 129.4, 136.0, 136.6, 155.8, 168.9, 171.0, 171.8, 173.6. HRMS (ESI): calculated $[M+H]^+$ 597.3290, found m/z 597.3306. HPLC: retention time (t_R) = 7.42 min. Isolated pure product 276 mg (yield: 46%, w.r.t. starting meterial Boc-Phe).

H_2N-LVFFA-$CONH_2$ (8a)

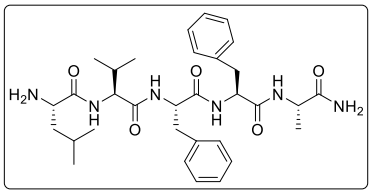

^{1}H NMR (DMSO-d_6; 600 MHz) δ 0.83-0.77 (12H, m); 1.20-1.19 (3H, d, *J* = 7.2 Hz); 1.38-1.34 (1H, m); 1.45-1.41 (1H, m); 1.53-1.49 (1H, m); 1.89-1.83 (1H, m); 2.73-2.69 (1H, m); 2.83-2.79 (1H, m); 2.96-2.93 (1H, m); 3.04-3.01 (1H, m); 3.83-3.81 (1H, t, *J* = 6.6 Hz); 4.21-4.16 (2H, m); 4.55-4.51 (2H, m); 7.03 (1H, s); 7.23-7.12 (9H, m); 8.04 (2H, br); 8.18-8.16 (2H, t, *J* = 7.8 Hz); 8.36 (1H, br). ^{13}C NMR (DMSO-d_6; 150 MHz) δ 18.3, 18.4, 19.2, 21.9, 22.8, 23.5, 31.0, 37.4, 37.5, 40.4, 48.1, 50.7, 53.5, 53.8, 57.7, 126.2, 126.3, 128.0, 128.1, 129.1, 129.2, 137.6, 137.7, 168.7,

170.2, 170.4, 171.0, 174.1. ESI-MS: calculated $[M+H]^+$ 595.3530, found m/z 595.3687. HPLC: retention time (t_R) = 9.18 min. Spectroscopic yield = 90%. Isolated pure product 6 mg (yield: 14% w.r.t. resin loading).

H_2N-NFGAIL-$CONH_2$ (8b):

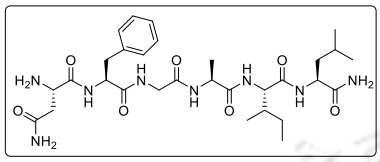

^{1}H NMR (DMSO-d_6; 600 MHz) δ 0.81-0.78 (9H, m); 0.86-0.85 (3H, d, *J* = 6.6 Hz); 1.07-1.02 (1H, m); 1.18-1.16 (3H, d, *J* = 6.6 Hz); 1.45-1.38 (3H, m); 1.56-1.53 (1H, m); 1.72 (1H, br); 2.56-2.53 (1H, m); 2.77-2.72 (2H, m); 3.08-3.05 (1H, m); 3.74-3.72 (1H, m); 3.99 (1H, br); 4.10-4.07 (1H, t, *J* =.8.4 Hz); 4.24-4.20 (1H, m); 4.36-4.34 (1H, t, *J* = 7.2 Hz); 4.53 (1H, br); 6.99 (1H, s); 7.30-7.20 (8H, m); 7.71 (1H, br); 7.82 (1H, br); 7.99 (3H, br); 8.46 (1H, br); 8.69 (1H, br). ^{13}C NMR (DMSO-d_6; 150 MHz) δ 11.0, 15.4, 18.3, 21.5, 23.1, 24.2, 35.6, 36.3, 37.3, 41.0, 41.9, 48.1, 49.0, 50.8, 54.6, 57.2, 126.5, 128.3, 129.2, 137.6, 168.2, 168.5, 170.7, 170.9, 171.0, 172.3, 174.1. ESI-MS: calculated $[M+H]^+$ 633.3646, found m/z 633.3786. HPLC: retention time (t_R) = 9.90 min. Spectroscopic yield = 91%. Isolated pure product 4 mg (yield: 9% w.r.t. resin loading).

H_2N-YGGFL-$CONH_2$ (8c).

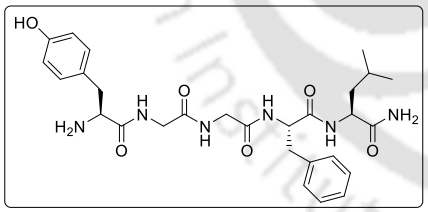

^{1}H NMR (DMSO-d_6; 600 MHz) δ 0.88-0.87 (3H, d, *J* = 6.6 Hz); 0.83-0.82 (3H, d, *J* = 6.6 Hz); 1.47-1.44 (2H, m); 1.57-1.54 (1H, m); 2.82-2.74 (2H, m); 3.04-2.97 (2H, m); 3.75-3.72 (3H, m); 3.85-3.81 (1H, m); 3.97 (1H, br); 4.21-4.18 (1H, m); 4.54-4.50 (1H, m); 6.70-6.69 (2H, d, *J* = 8.4 Hz); 6.99 (1H, br); 7.05-7.04 (2H, d, *J* = 8.4 Hz); 7.18-7.17 (2H, t, *J* = 4.2 Hz); 7.24-7.24 (4H, d, *J* = 4.2 Hz); 8.07 (3H, br); 8.12-8.11 (1H, d, *J* = 8.4 Hz); 8.16-8.14 (1H, m); 8.75 (1H, br). ^{13}C NMR (DMSO-d_6; 150 MHz) δ 21.6, 23.1, 24.3, 36.3, 37.5, 40.9, 41.8, 42.0, 51.1, 54.0, 115.5, 124.9, 126.4, 128.2, 129.3, 130.6, 137.8, 156.6, 168.5, 168.6, 168.7, 170.9, 174.1. ESI-MS: calculated $[M+H]^+$ 555.2853, found m/z 555.3030. HPLC: retention time (t_R) = 8.78 min. Spectroscopic yield = 100%. Isolated pure product 5 mg (yield: 13% w.r.t. resin loading).

H_2N-YaGFM-$CONH_2$ (8d).

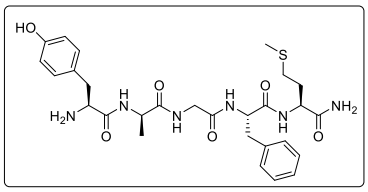

^{1}H NMR (DMSO-d_6; 600 MHz) δ 1.05-1.04 (3H, d, *J* = 6.6 Hz); 1.81-1.74 (1H, m); 1.96-1.90 (1H, m); 2.02 (3H, s); 2.38-2.35 (1H, m); 2.45-2.40 (1H, m); 2.80-2.76 (1H, m); 2.92-2.83 (2H, m); 3.04-3.01 (1H, m); 3.72-3.68 (1H, m); 3.98-3.96 (1H, m); 4.32-4.27 (1H, m); 4.25-4.21 (1H, m); 4.52-4.49 (1H, m); 6.70-6.69 (2H, d, *J* = 8.4Hz); 7.02-7.01 (2H, d, *J* = 8.4Hz); 7.07 (1H, br); 7.13 (1H, br); 7.19-7.17 (1H, m); 7.26-7.23 (4H, m); 8.05-8.03 (1H, d, *J* = 8.4Hz); 8.10 (2H, br); 8.18-8.17 (1H, d, *J* = 8.4 Hz); 8.23-8.21 (1H, t, *J* = 6 Hz); 8.59-8.54 (1H, d, *J* = 7.2 Hz). ^{13}C NMR (DMSO-d_6; 150 MHz) δ 14.6, 18.3, 29.6, 31.7, 36.3, 37.4, 41.6, 48.2, 51.9, 53.6, 54.0, 115.3, 124.8, 126.4, 128.1, 129.1, 129.2, 130.5, 137.6, 156.5, 167.7, 168.5, 171.1, 171.8, 172.9. ESI-MS: calculated $[M+H]^+$ 587.2574, found m/z 587.2713. HPLC: retention time (t_R) = 8.36 min. Spectroscopic yield = 83%. Isolated pure product 4 mg (yield: 10% w.r.t. resin loading).

Ac-K(AV)FLG-$CONH_2$ (8e).

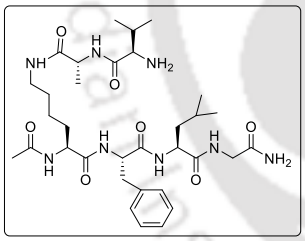

^{1}H NMR (DMSO-d_6; 600 MHz) δ 0.81-0.80 (3H, d, *J* = 6.6 Hz); 0.86-0.85 (3H, d, *J* = 6.6 Hz); 0.92-0.90 (6H, dd, *J* = 2.4 Hz); 1.16-1.10 (2H, m); 1.22-1.21 (3H, d, *J* = 6.6 Hz); 1.38-1.27 (3H, m); 1.48-1.45 (3H, m); 1.56-1.52 (1H, m); 1.80 (3H, s); 2.06-2.00 (1H, m); 2.82-2.78 (1H, q, *J* = 9.6 Hz, *J* = 4.2 Hz); 2.97-2.91 (1H, m); 3.05-2.98 (2H, m); 3.41 (1H, s); 3.66-3.52 (1H, m); 4.10-4.07 (1H, m); 4.24-4.20 (1H, q, *J* = 7.8 Hz, *J* = 6.6 Hz); 4.31-4.29 (1H, t, *J* = 7.2 Hz); 4.50-4.46 (1H, q, *J* = 8.4 Hz, *J* = 4.8 Hz); 7.09 (1H, s); 7.18-7.15 (2H, m); 7.24-7.20 (4H, m); 7.93-7.91 (1H, t, *J* = 5.4 Hz); 8.01-7.98 (2H, m); 8.05-8.02 (2H, m); 8.10-8.07 (2H, br); 8.57-8.55 (1H, t, *J* = 7.2 Hz). ^{13}C NMR (DMSO-d_6; 150 MHz) δ 17.6, 18.2, 18.4, 21.4, 22.4, 22.6, 23.1, 24.0, 28.7, 29.8, 31.4, 36.8, 38.4, 40.4, 41.9, 48.3, 51.3, 52.8, 53.7, 57.3, 126.2, 128.0, 129.2, 137.7, 167.3, 169.6, 170.8, 171.1, 171.4, 171.8, 172.0. ESI-MS: calculated $[M+H]^+$ 675.4195, found m/z 675.4142. HPLC: retention time (t_R) = 4.8 min. Spectroscopic yield = 83%. Isolated pure product 9 mg (yield: 19% w.r.t. resin loading).

H_2N-cyclo[EPFFK]-$CONH_2$ (8f).

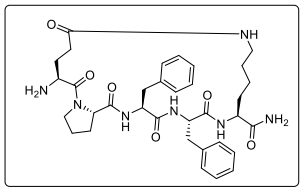

^{1}H NMR (DMSO-d_6; 600 MHz) δ 1.32-1.30 (4H, m); 1.42-1.39 (1H, m); 1.50-1.48 (2H, m); 1.73-1.65 (4H, m); 1.91-1.85 (1H, m); 2.17-1.99 (4H, m); 2.84-2.77 (2H, m); 3.04-2.98 (3H, m); 3.80-3.14 (1H, m); 4.14-4.11 (1H, q, *J* = 5.4 Hz, *J* = 3.6 Hz); 4.30-4.26 (2H, m); 4.44-4.40 (1H, m); 4.74-4.70 (1H, m); 6.99 (2H, s); 7.08 (1H, s); 7.19-7.16 (1H, m); 7.23-7.20 (5H, m); 7.27-7.25 (1H, m); 7.32-7.29 (2H, t, *J* = 7.2 Hz); 7.38-7.37 (2H, d, *J* = 7.8 Hz); 8.12 (2H, br); 8.20-8.18 (1H, d, *J* = 9 Hz); 8.57-8.56(1H, d, *J* = 6 Hz). ^{13}C NMR (DMSO-d_6; 150 MHz) δ 22.4, 24.2, 25.2, 27.4, 28.7, 29.0, 31.3, 36.8, 37.5, 38.1, 47.1, 50.3, 51.6, 52.0, 54.6, 61.2, 126.3, 126.5, 127.8, 128.2, 129.2, 129.3, 137.3, 137.9, 168.1, 169.9, 171.1, 171.2, 171.9, 173.8. ESI-MS: calculated $[M+H]^+$ 648.3511, found m/z 648.7143. HPLC: retention time (t_R) = 8.96 min. Spectroscopic yield = 76%. Isolated pure product 4 mg (yield: 9% w.r.t. resin loading).

7.18. References

1. Muttenthaler, M.; Albericio, F.; Dawson, P. E. Methods, setup and safe handling for anhydrous hydrogen fluoride cleavage in Boc solid-phase peptide synthesis *Nat. Protoc*. **2015**, *10*, 1067-1083.
2. Han, G.; Tamaki, M.; Hruby, V. J. Fast, efficient and selective deprotection of the tert-butoxycarbonyl (Boc) group using HCL/dioxane (4 M). *J. Peptide Res*. **2001**, *58*, 338-341.
3. Strazzolini, P.; Misuri, N.; Polese, P. Efficient cleavage of carboxylic tert-butyl and 1-adamantyl esters, and N-Boc-amines using H_2SO_4 in CH_2Cl_2. *Tetrahedron Lett.* **2005**, *46*, 2075-2078.
4. Strazzolini, P.; Melloni, T.; Glumanini, A. G. Selective nitrolytic deprotection of *N*-Boc-amines and *N*-Boc-amino acids derivatives. *Tetrahedron* **2001**, *57*, 9033–9043.
5. Yadav, J. S.; Reddy, B. V. S.; Reddy, K. S.; Reddy, K. B. Indium-meditated facile cleavage of the *t*-butoxycarbonyl group from di-*t*-butylimidodicarbonate. *Tetrahedron Lett.* **2002**, *43*, 1549–1551.
6. Routier, S.; Sauge, L.; Ayerbe, N.; Coudert, G.; Merour, J. Y. A mild and selective method for N-Boc deprotection. *Tetrahedron Lett.* **2002**, *43*, 589–591.
7. Wang, G.; Li, C.-J.; Li, J.; Jia, X.-S. Catalyst-free water-mediated *N*-Boc deprotection. *Tetrahedron Lett.*, **2009**, *50*, 1438-1440.
8. Bose, D. S.; Kumar, K. K.; Reddy, A. V. N. A New Protocol for Selective Deprotection of *N*- tert-Butoxycarbonyl Protective Group (*t*-Boc) with $Sn(OTf)_2$. *Synth. Commun.* **2003**, *33*, 445-450.
9. Navath, R. S.; Pabbisetty, K. B.; Hu, L. Chemoselective deprotection of N-Boc group in amino acids and peptides by bismuth(III) trichloride. *Tetrahedron Lett.* **2006**, *47*, 389-393.
10. Lopez-Soria, J. M.; Perez, S. J.; Hernandez, J. N.; Ramirez, M. A.; Martin, V. S.; Padron, J. I. A practical, catalytic and selective deprotection of a Boc group in N,N′-diprotected amines using iron(III)-catalysis. *RSC Adv.* **2015**, *5*, 6647-6651.
11. Filatova, L. N.; Vendilo, A. G.; Sandu, R. A. Chemical forms of iron(III) in solutions of orthophosphoric acid as probed by electronic absorption spectroscopy. *Russ. J. Inorg. Chem.*, **2012**, *57*, 1272-1275.
12. Saucede, L.; Santos, S. D.; Chandravarkar, A.; Mandal, B.; Mimna, R.; Murat, K.; Camus, M.-S.; Berard, J.; Grouzmann, E.; Adrian, M.; Dubochet, J.; Lopez, J.; Lashuel, H.; Tuchscherer, G.; Mutter, M. Switch-peptides: From conformational studies to Alzheimer's disease. *Chimia*, **2006**, *60*, 199–202.
13. Paul, A.; Kalita, S.; Kalita, S.; Sukumar, P.; Mandal, B. Disaggregation of amylin aggregate by novel conformationally restricted aminobenzoic acid containing α/β and α/γ hybrid peptidomimetics. *Sci. Rep*., **2017**, *7*, 1–13.
14. Bhargava, H. N. New *In Vivo* Evidence for narcotic agonistic property of Leucine-Enkephalin. *J. Pharm. Sci.*, **1977**, *67*, 136-137.
15. Fukunaga, Y.; Inoue, N.; Miyamoto, M.; Kishioka, S.; Yamamoto, H. Effects of peptidase inhibitors, [D-Ala^2, Met^5]-Enkephalinamide and antiserum to Methionine-Enkephalin microinjected into the caudal periaqueductal gray on morphine withdrawal in rats. *Jpn. J. Pharmacol*, **1998**, *78*, 455-461.

7.19. Selected spectra

7.19.1. HPLC profile of deprotection of Boc-Phe-OMe (*A*) to H_2N-Phe-OMe (*B*) using 1.5 equiv of $FeCl_3$ in DCM with time

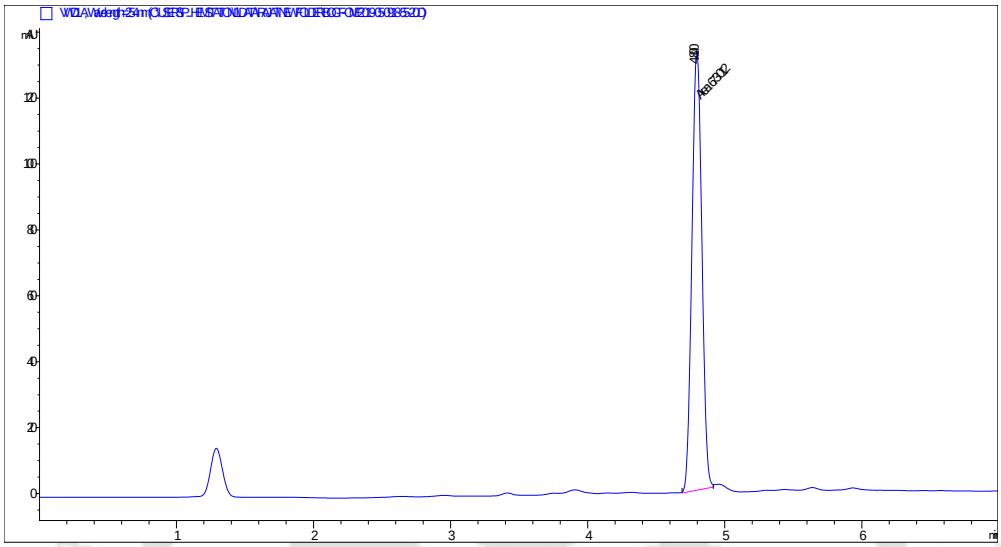

Figure 7.5. *HPLC profile picture of (**A**) at 0 min. (A linear gradient was used from 5 to 100% CH_3CN till 4 min, and a total run time of 7 min, flow rate 1mLmin^{-1}). This HPLC was done in the Agilent 1260 Infinity II system using a C18 Agilent (4 µm, 4.6x100mm) column (Figure 7.5-7.10).*

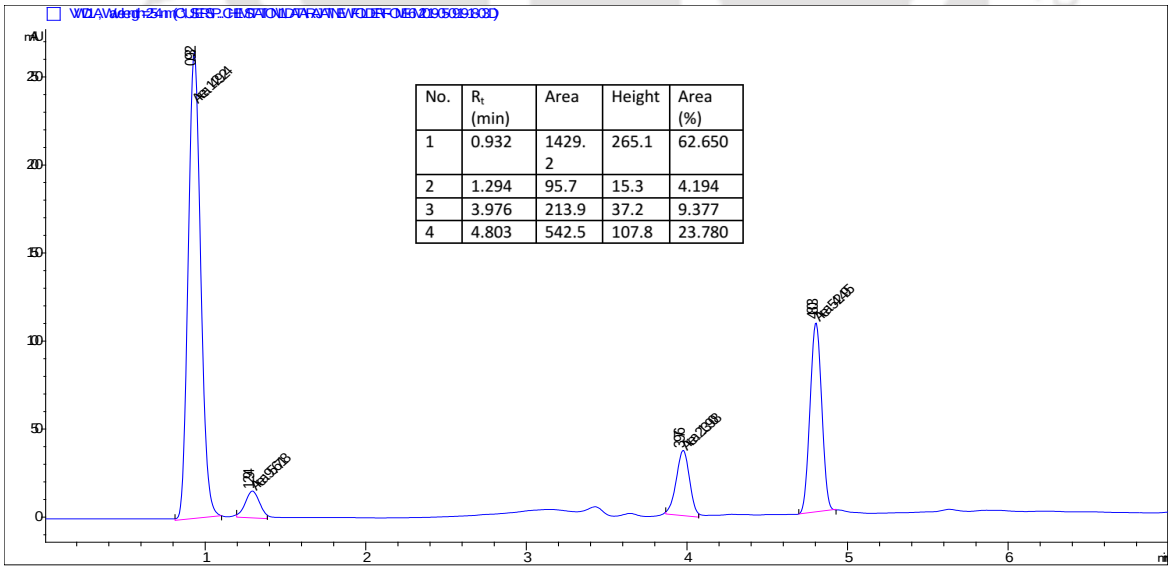

No.	R_t (min)	Area	Height	Area (%)
1	0.932	1429.2	265.1	62.650
2	1.294	95.7	15.3	4.194
3	3.976	213.9	37.2	9.377
4	4.803	542.5	107.8	23.780

Figure 7.6. *HPLC profile picture of conversion of (**A**) to (**B**) at 6 min.*

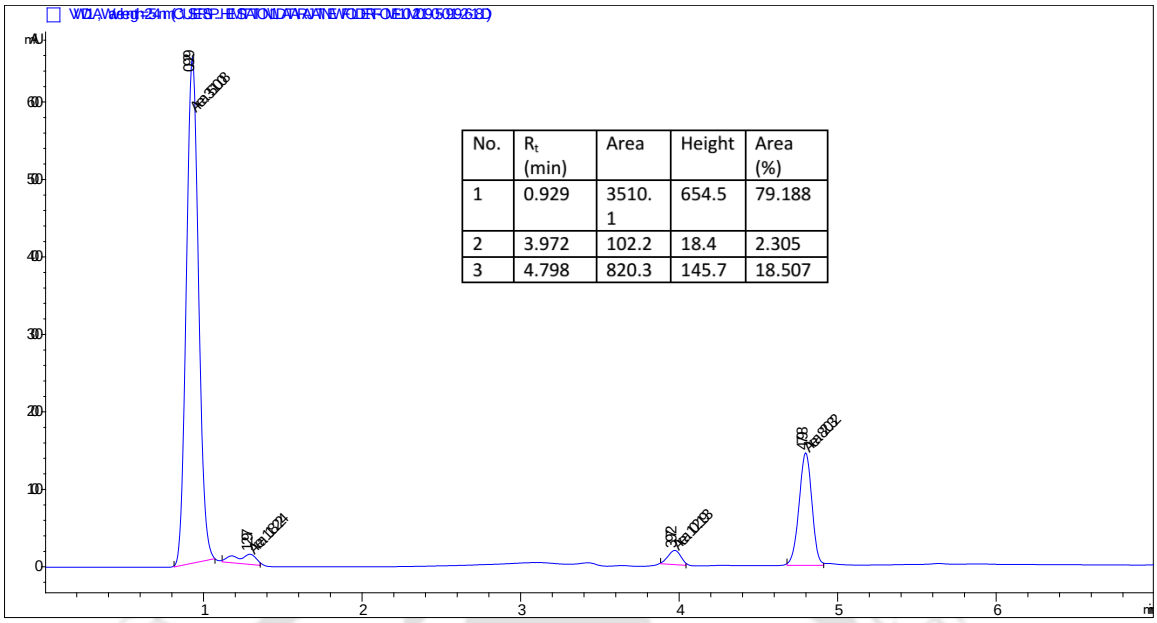

No.	R_t (min)	Area	Height	Area (%)
1	0.929	3510.1	654.5	79.188
2	3.972	102.2	18.4	2.305
3	4.798	820.3	145.7	18.507

Figure 7.7. *HPLC profile picture of conversion of (**A**) to (**B**) at 10 min.*

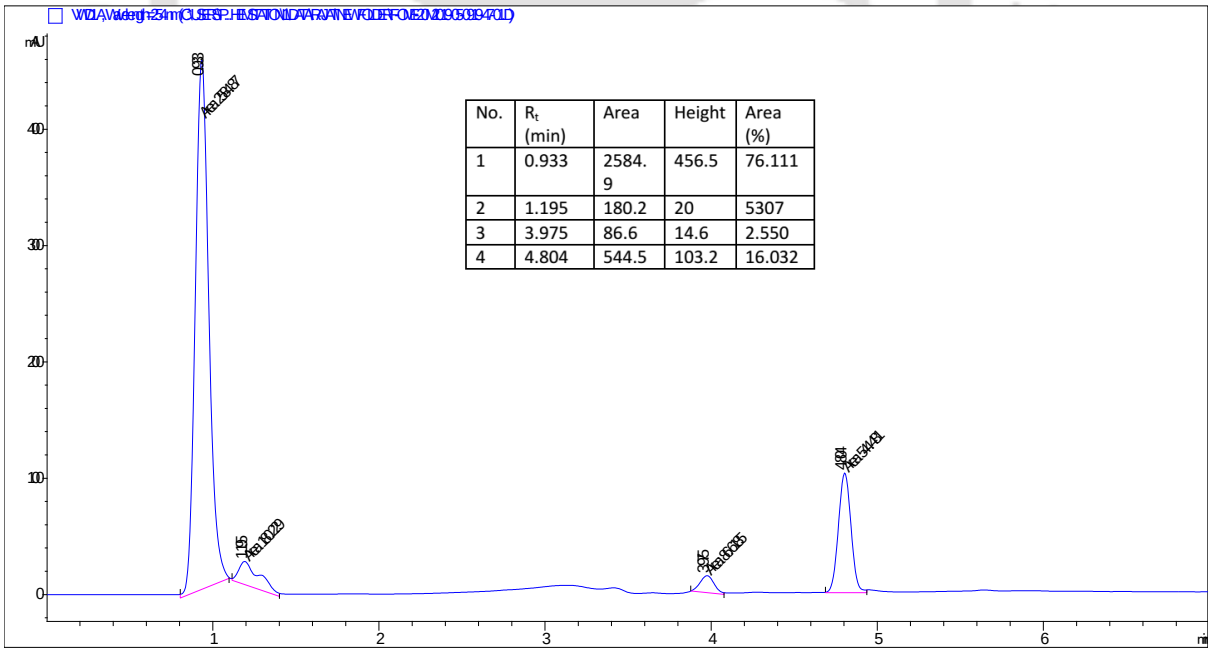

No.	R_t (min)	Area	Height	Area (%)
1	0.933	2584.9	456.5	76.111
2	1.195	180.2	20	5307
3	3.975	86.6	14.6	2.550
4	4.804	544.5	103.2	16.032

Figure 7.8. *HPLC profile picture of conversion of (**A**) to (**B**) at 20 min.*

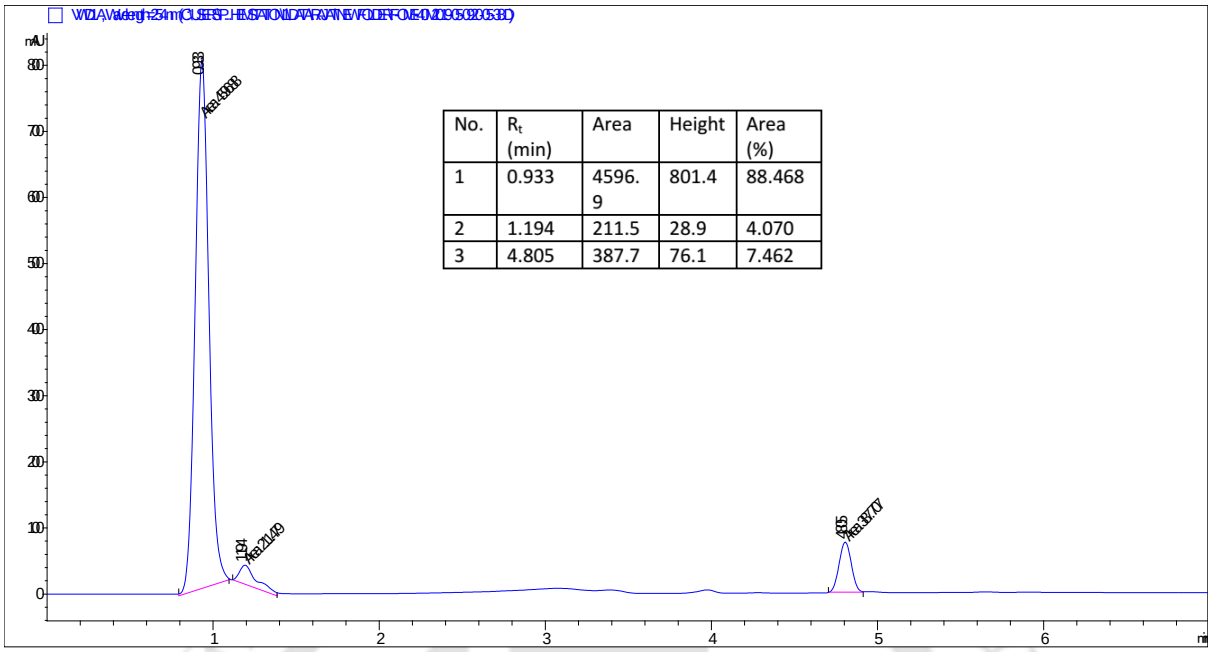

No.	R_t (min)	Area	Height	Area (%)
1	0.933	4596.9	801.4	88.468
2	1.194	211.5	28.9	4.070
3	4.805	387.7	76.1	7.462

Figure 7.9. *HPLC profile picture of conversion of (**A**) to (**B**) at 40 min.*

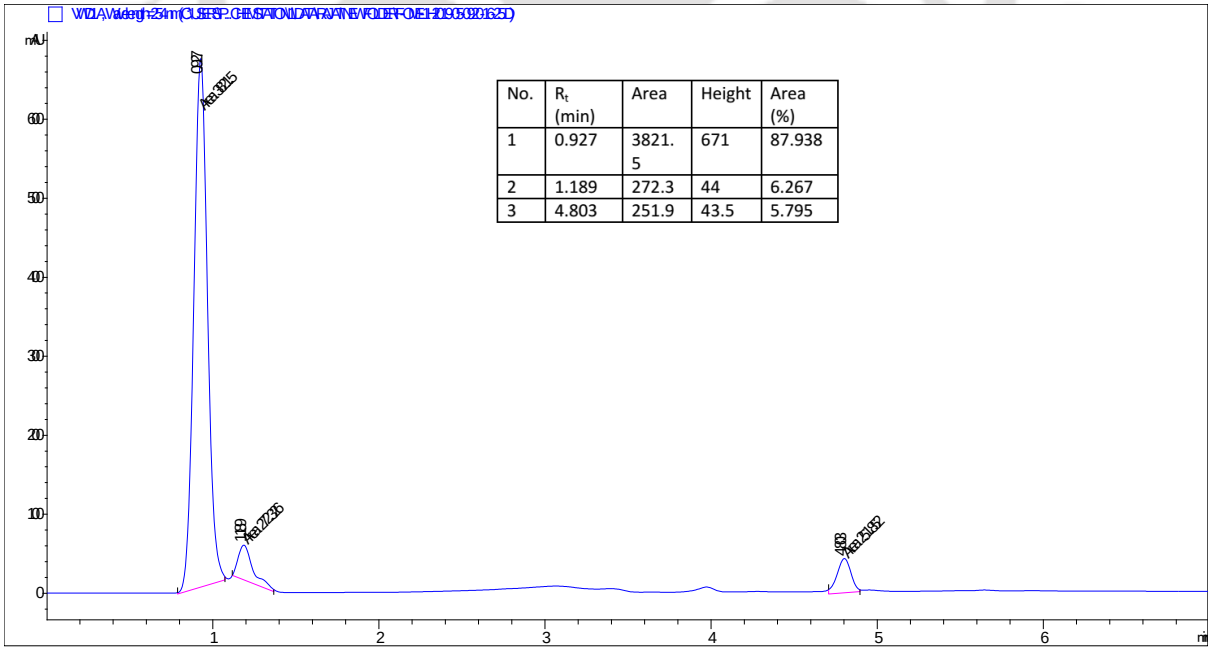

No.	R_t (min)	Area	Height	Area (%)
1	0.927	3821.5	671	87.938
2	1.189	272.3	44	6.267
3	4.803	251.9	43.5	5.795

Figure 7.10. *HPLC profile picture of conversion of (**A**) to (**B**) at 1 h.*

7.19.2. Spectra of synthesized peptides from solution

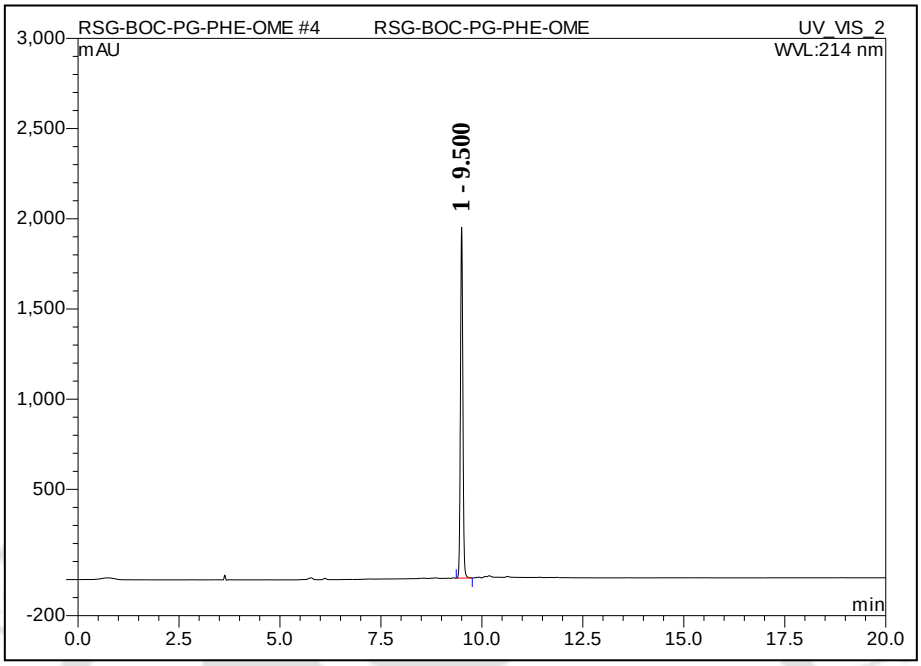

Figure 7.11. *HPLC profile picture of purified peptide* ***7a*** *(A linear gradient was used from 5 to 100% CH_3CN till 8 min, and a total run time of 20 min, flow rate 1mLmin^{-1}). This HPLC was done in Thermo Scientific Dionex UltiMate 3000 Rapid Separation LC (RSLC) system using a C18 Thermo scientific (Hypersil Gold, 5 µm, 250x4.6 mm) column.*

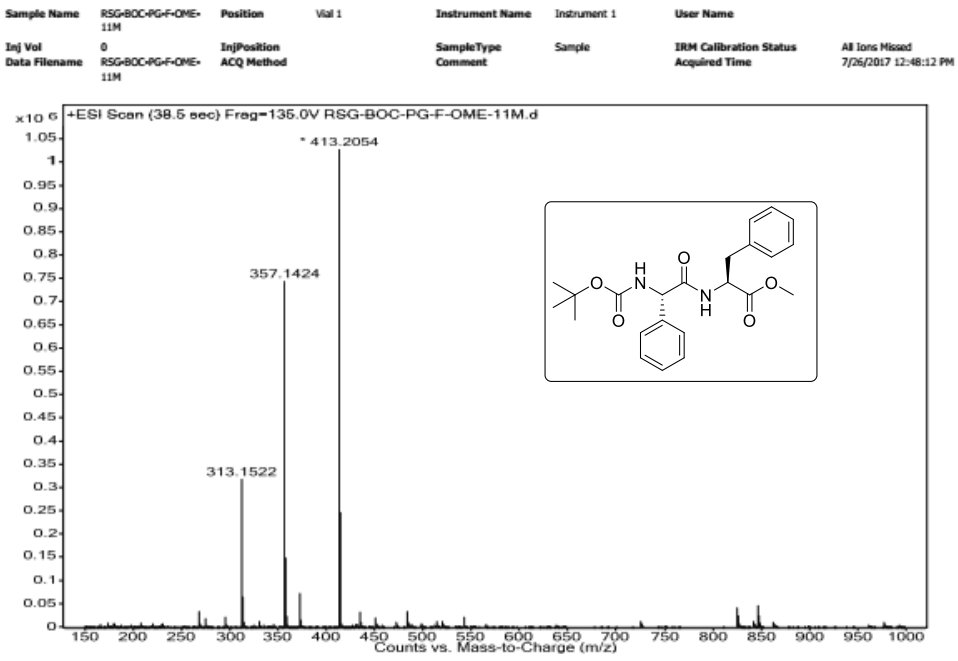

Figure 7.12. *MS spectra of peptide* ***7a***

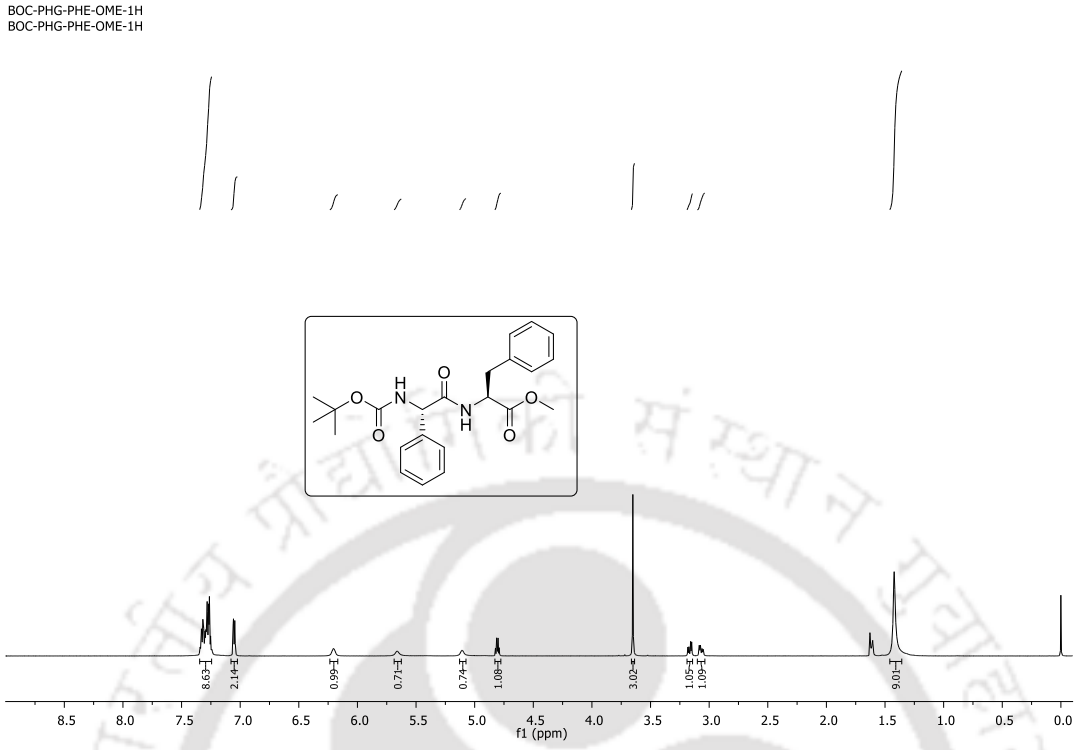

Figure 7.13. *^{1}H NMR spectra of peptide* ***7a***

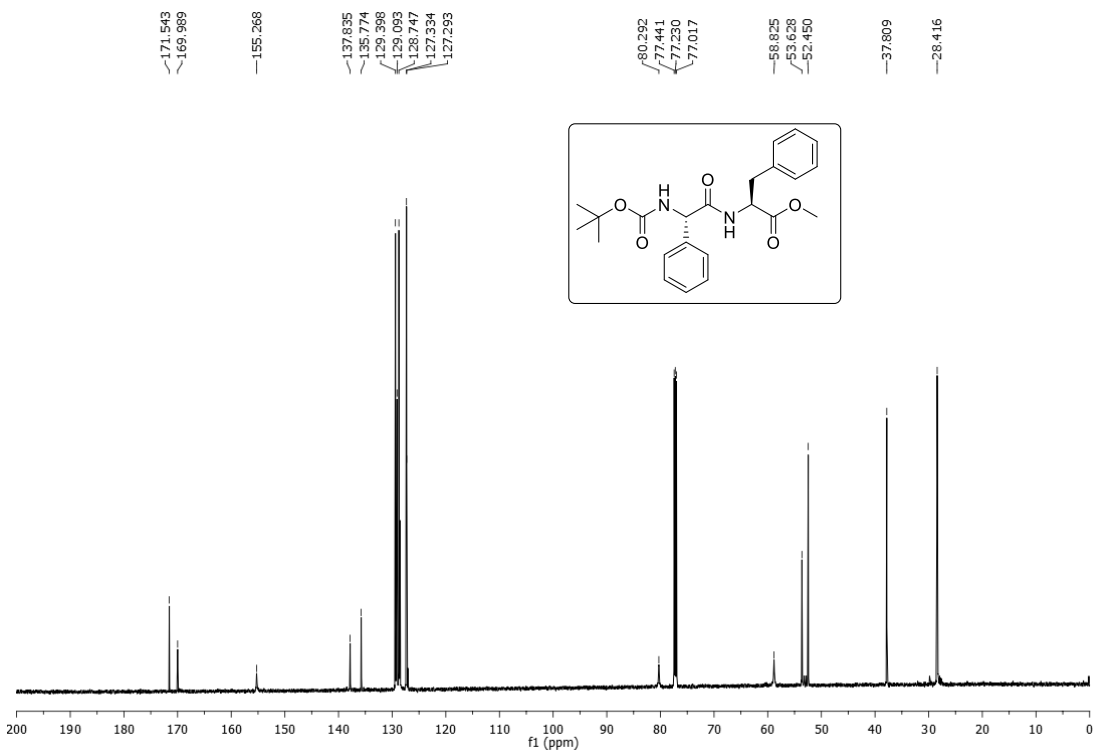

Figure 7.14. *^{13}C NMR spectra of peptide* ***7a***

7.19.3. Racemization study

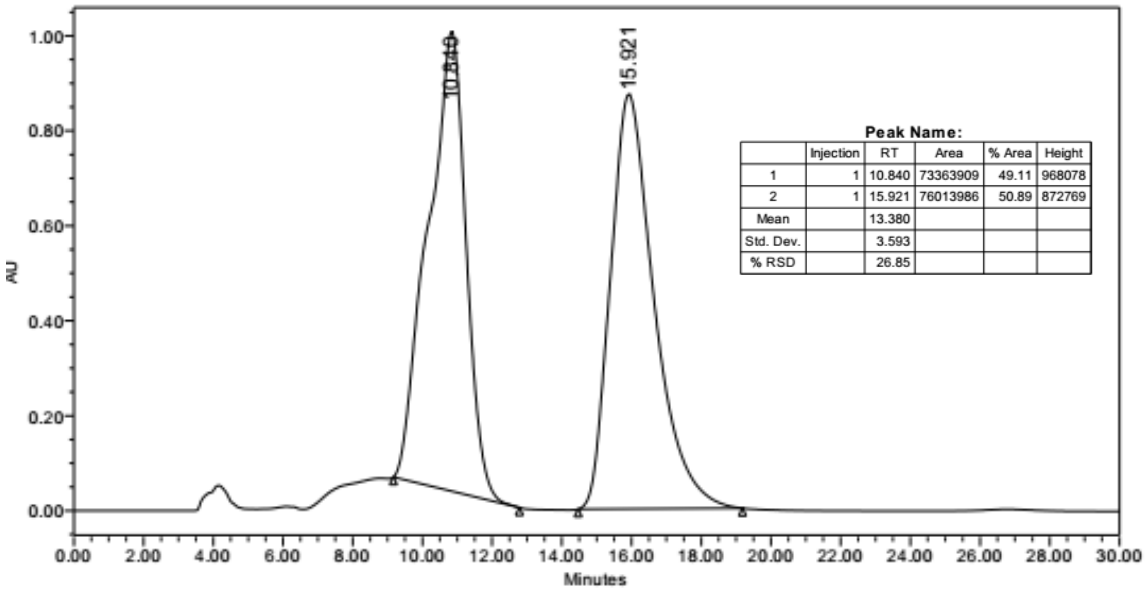

Figure 7.15. *HPLC profile of Boc-Gly-DL-Phg-OMe (**1h**) (CHIRALPAK® AS-H column, 5 µm, 4.6×250 mm, an isocratic gradient of 20% isopropanol in hexane, flow rate 1mLmin^{-1}) run up to 30 min.*

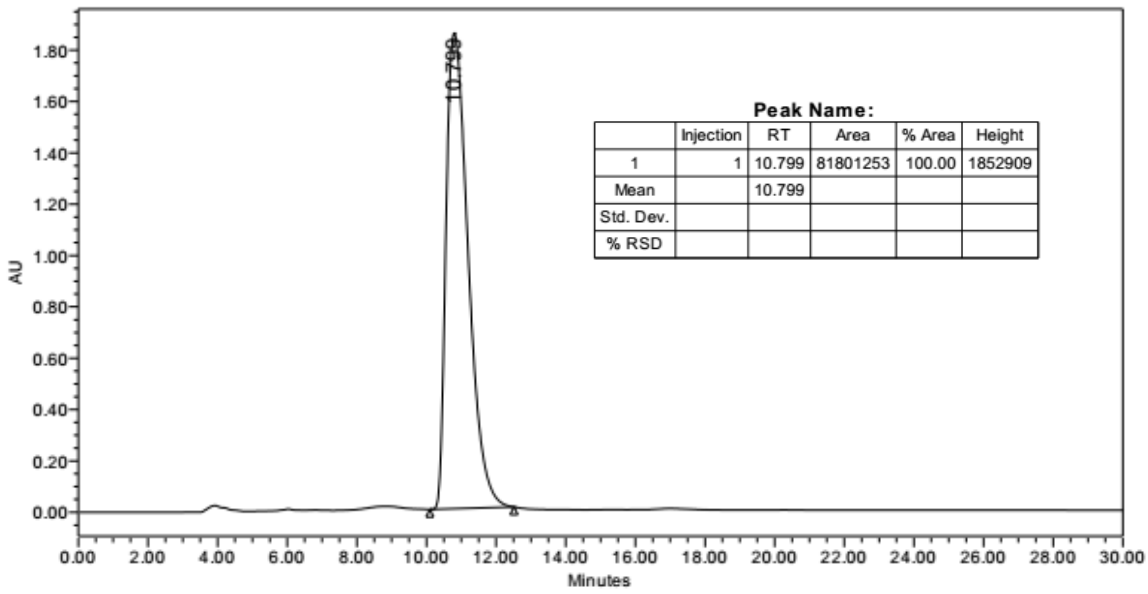

Figure 7.16. *HPLC profile of Boc-Gly-L-Phg-OMe (**1i**) (CHIRALPAK® AS-H column, 5 µm, 4.6×250 mm, an isocratic gradient of 20% isopropanol in hexane, flow rate 1mLmin^{-1}) run up to 30 min.*

7.19.4. Spectra of synthesized peptides from SPPS

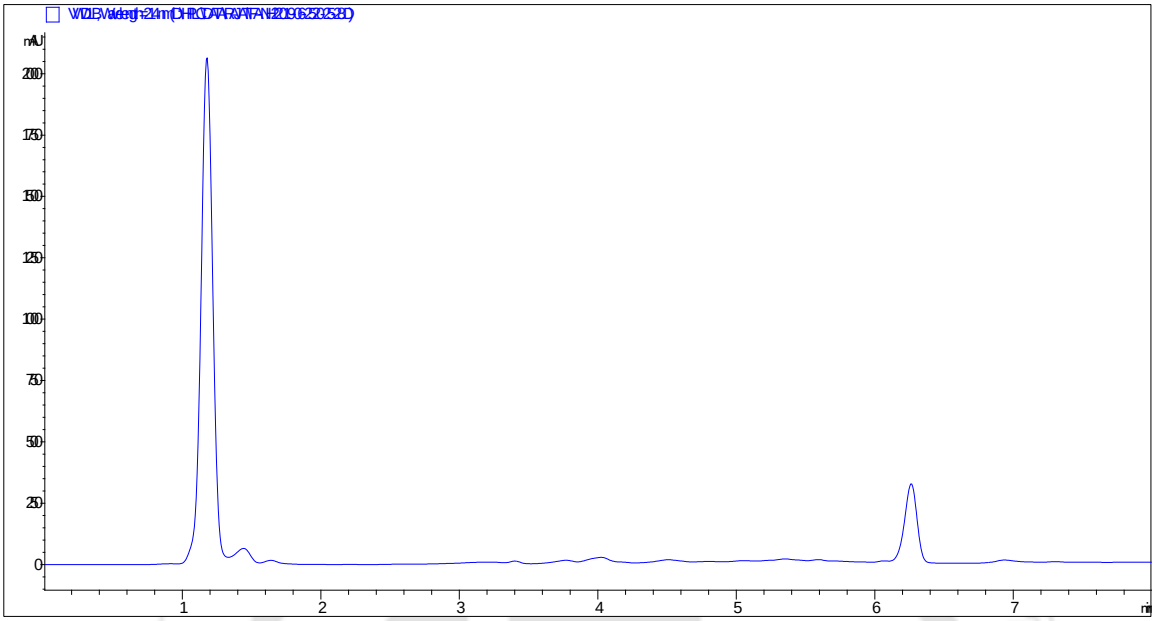

Figure 7.17. *HPLC profile picture of a crude peptide fragment, NH_2-FA-$CONH_2$ from* ***8a*** *(A linear gradient was used from 5 to 95% CH_3CN till 7 min, and a total run time of 8 min, flow rate 1mLmin^{-1}). This HPLC was done in the Agilent 1260 Infinity II system using a C18 Agilent (4 µm, 4.6x100mm) column (Figure 7.17,7.19,7.21, and 7.23).*

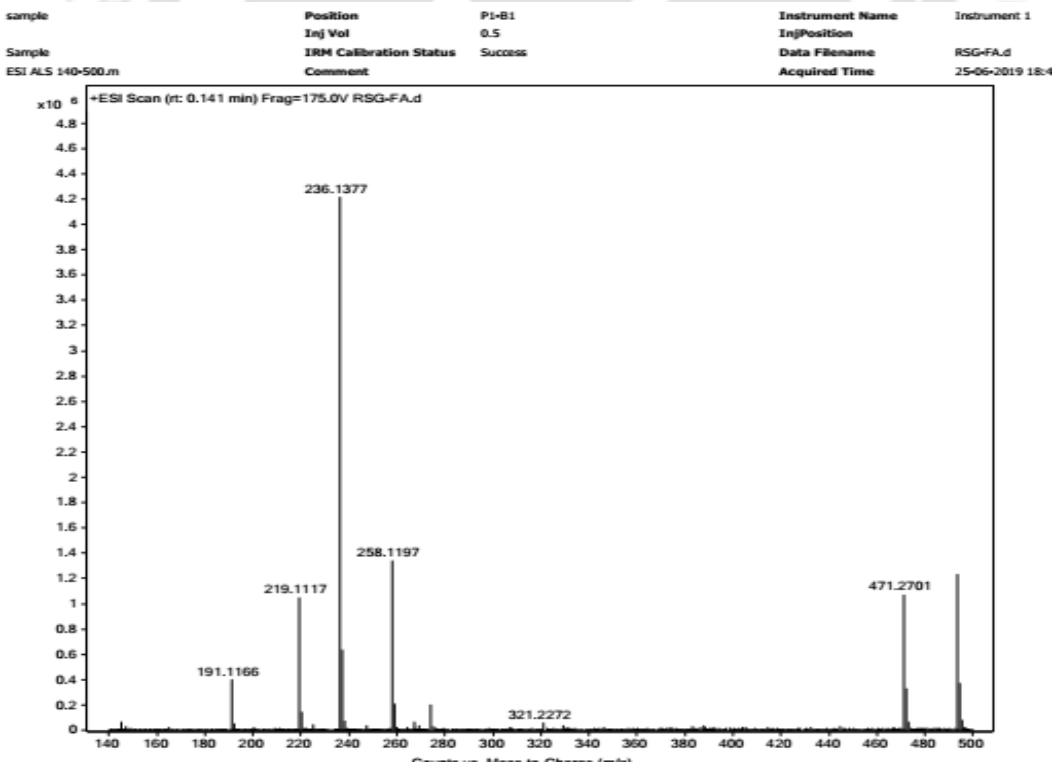

Figure 7.18*. MS spectra of a peptide fragment, NH_2-FA-$CONH_2$ from* ***8a***

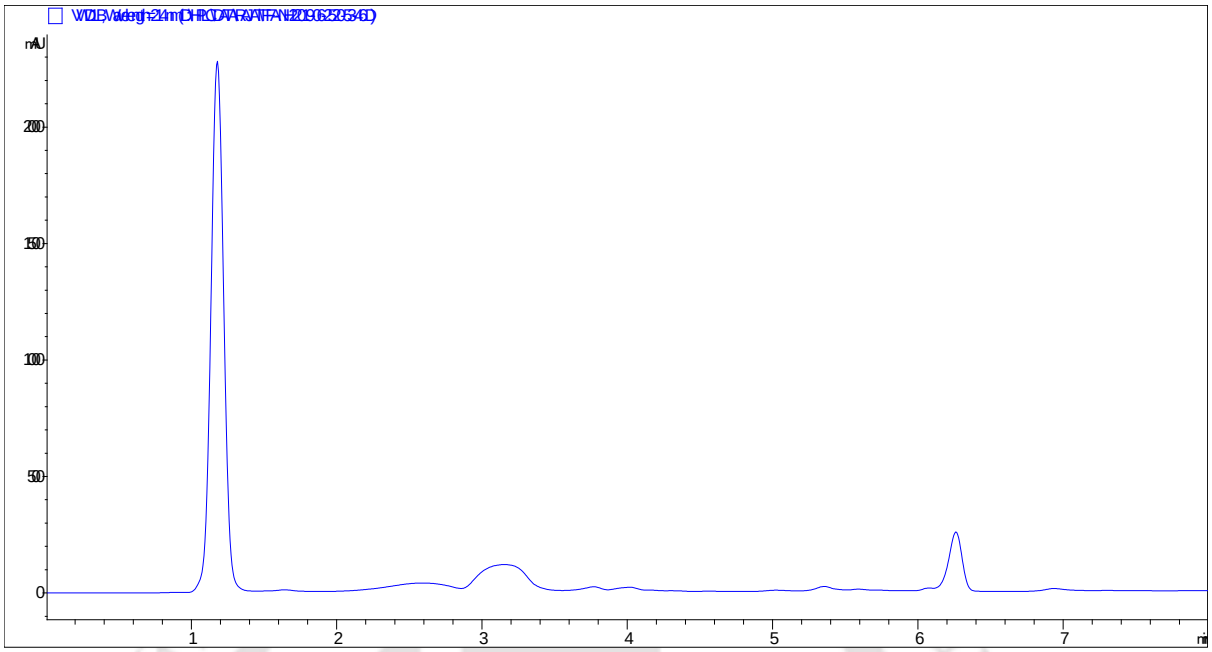

Figure 7.19. *HPLC profile picture of a crude peptide fragment, NH_2-FFA-$CONH_2$ from* ***8a***

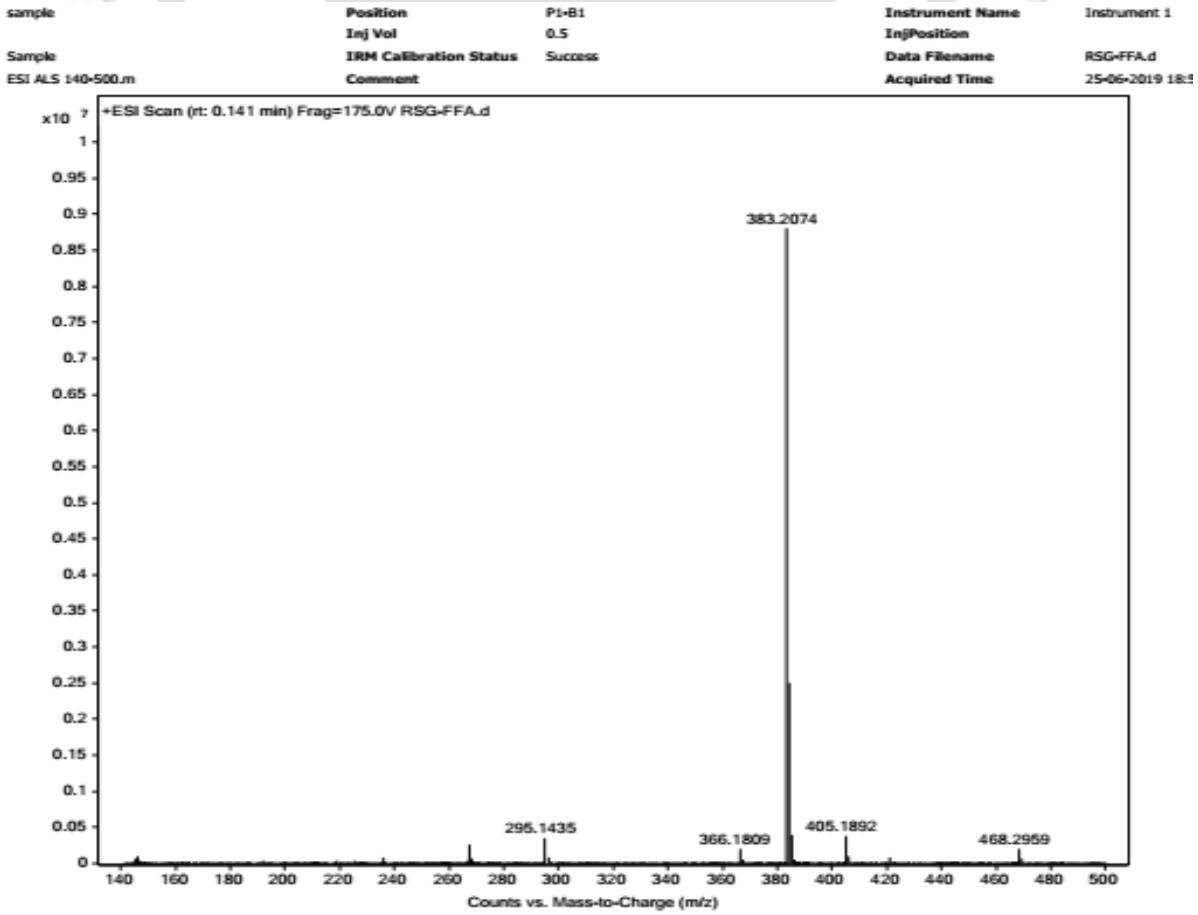

Figure 7.20. *MS spectra of a peptide fragment, NH_2-FFA-$CONH_2$ from* ***8a***

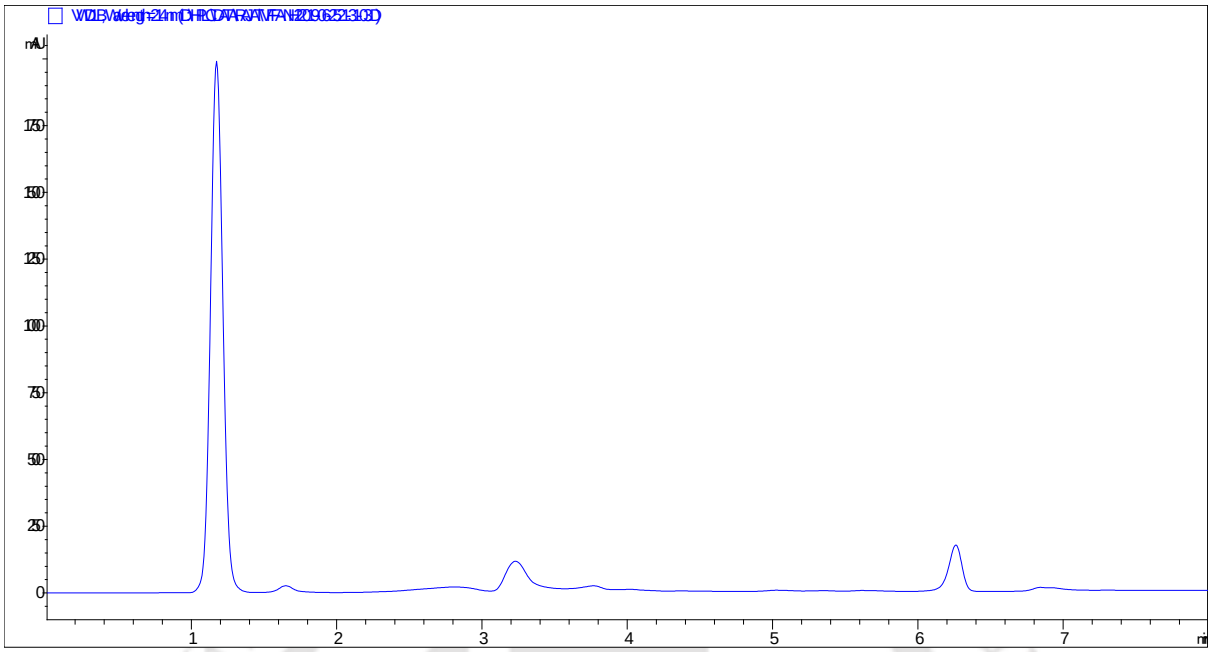

Figure 7.21. *HPLC profile picture of a crude peptide fragment, NH_2-VFFA-$CONH_2$ from* ***8a***

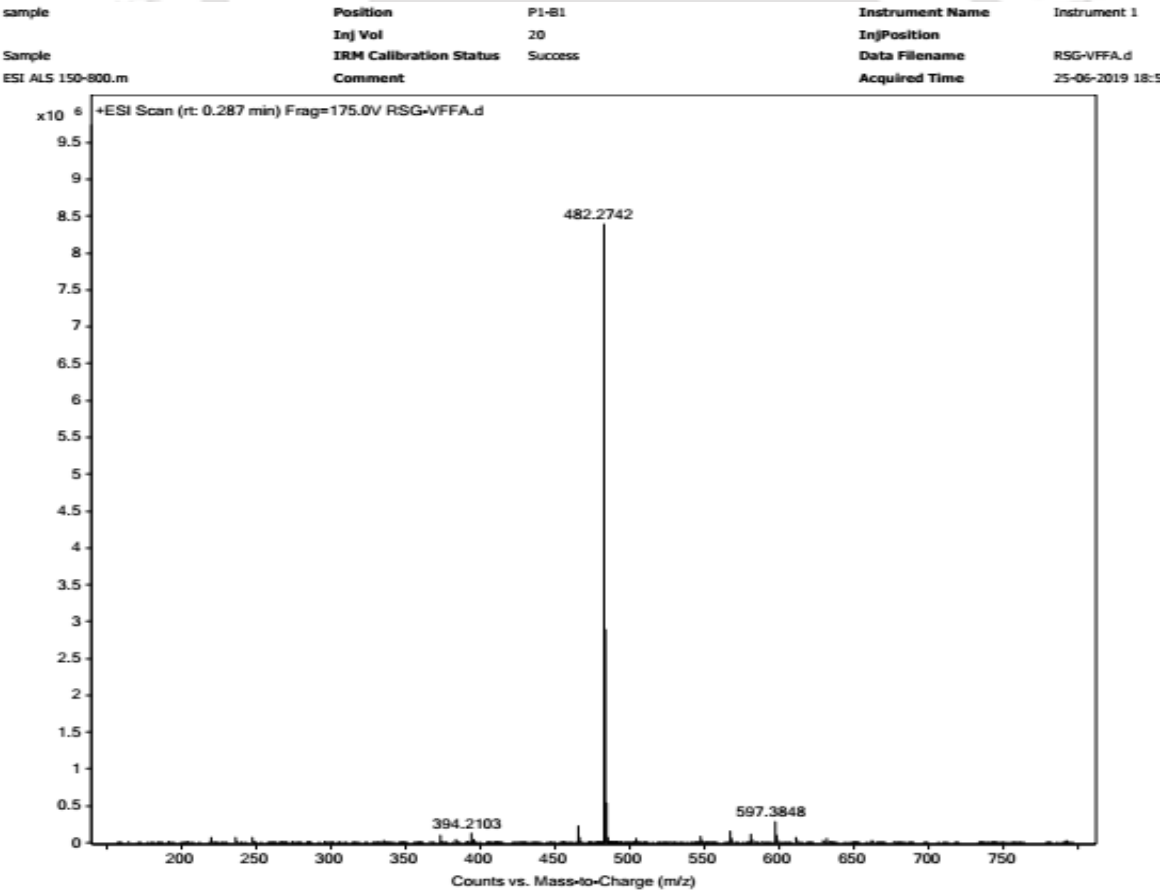

Figure 7.22. *MS spectra of a peptide fragment, NH_2-VFFA-$CONH_2$ from* ***8a***

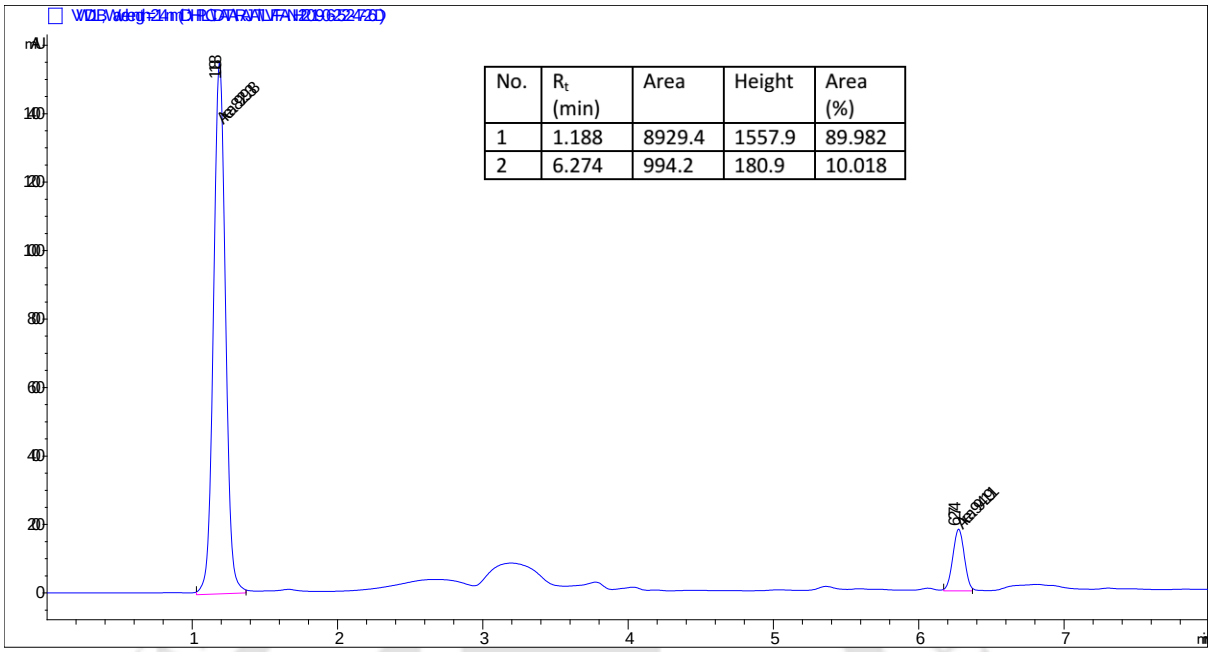

No.	R_t (min)	Area	Height	Area (%)
1	1.188	8929.4	1557.9	89.982
2	6.274	994.2	180.9	10.018

Figure 7.23. *HPLC profile picture of a crude peptide fragment, NH_2-LVFFA-$CONH_2$ from* ***8a***

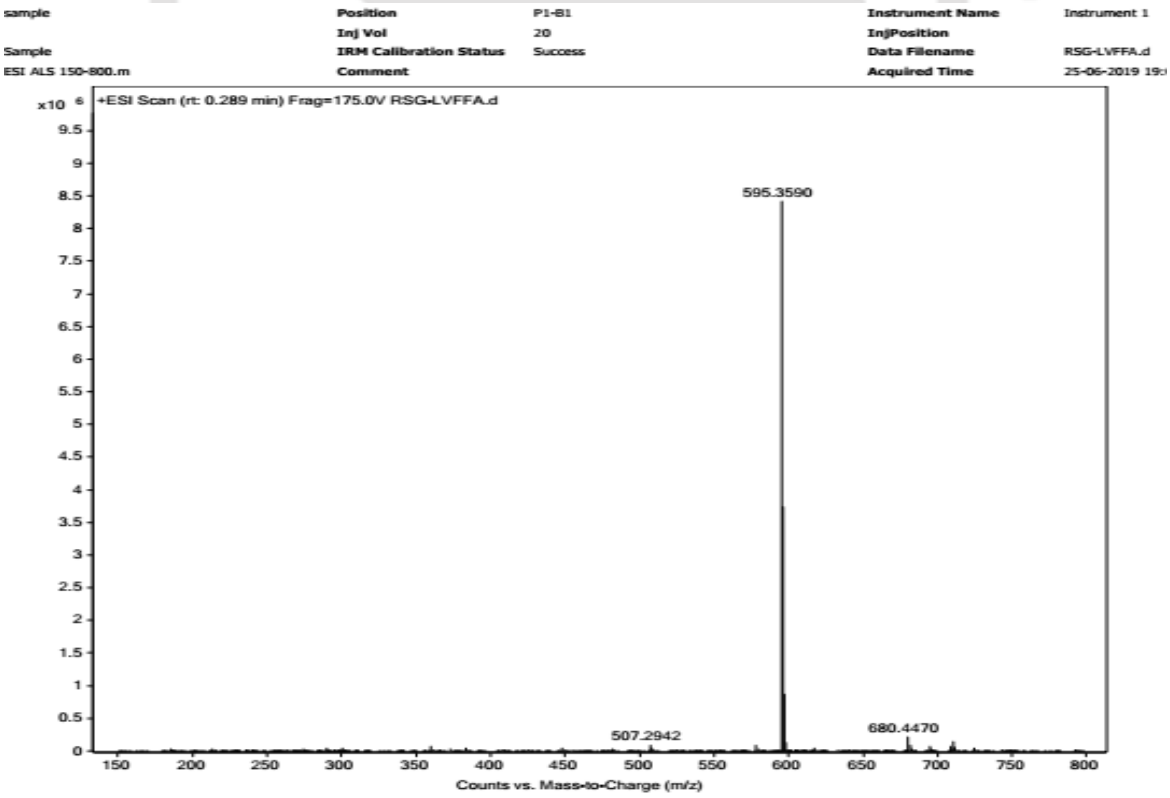

Figure 7.24. *MS spectra of a peptide fragment, NH_2-LVFFA-$CONH_2$ from* ***8a***

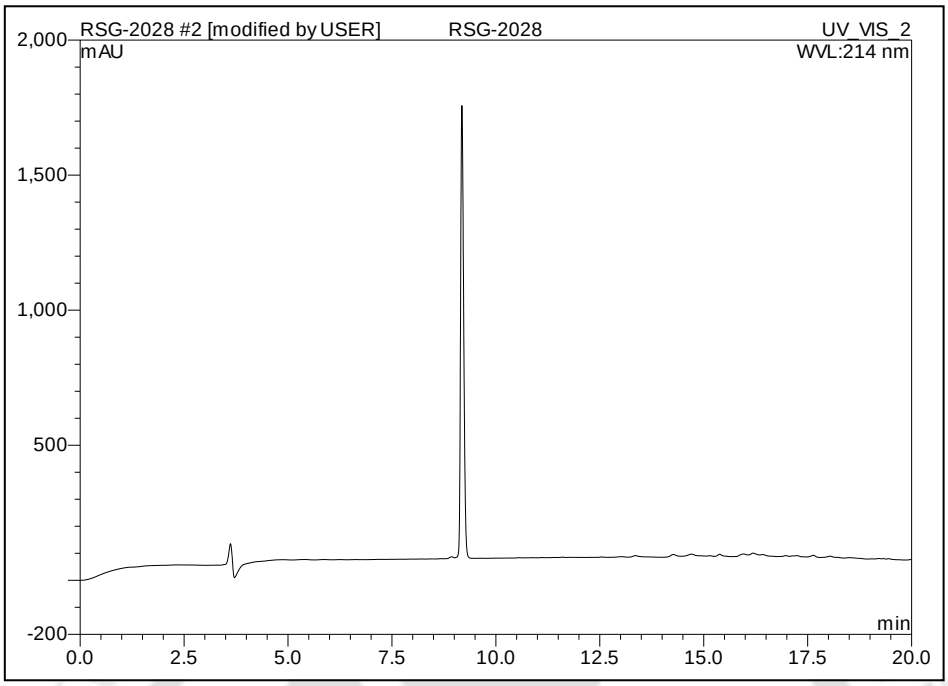

Figure 7.25. *HPLC profile picture of purified peptide* ***8a*** *(A linear gradient was used from 5 to 100% CH_3CN till 18 min, and a total run time of 20 min, flow rate 1mLmin^{-1}). This HPLC was done in Thermo Scientific Dionex Ulti Mate 3000 Rapid Separation LC (RSLC) system using a C18 Thermo scientific (Hypersil Gold, 5 µm, 250x4.6 mm) column*

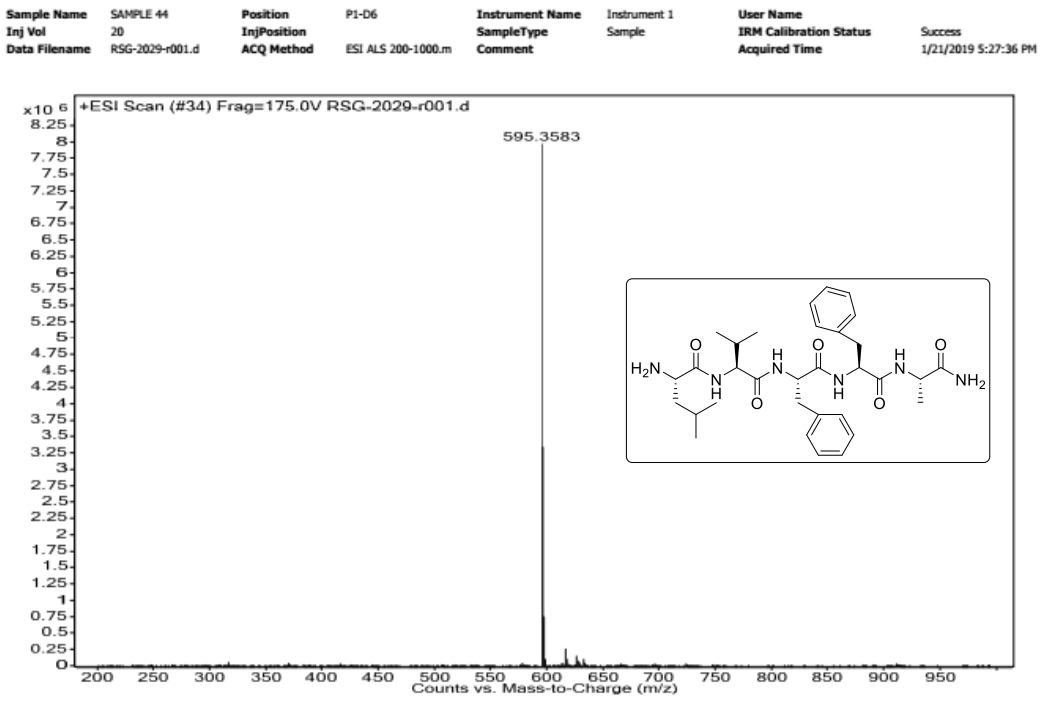

Figure 7.26. *MS spectra of peptide* ***8a***

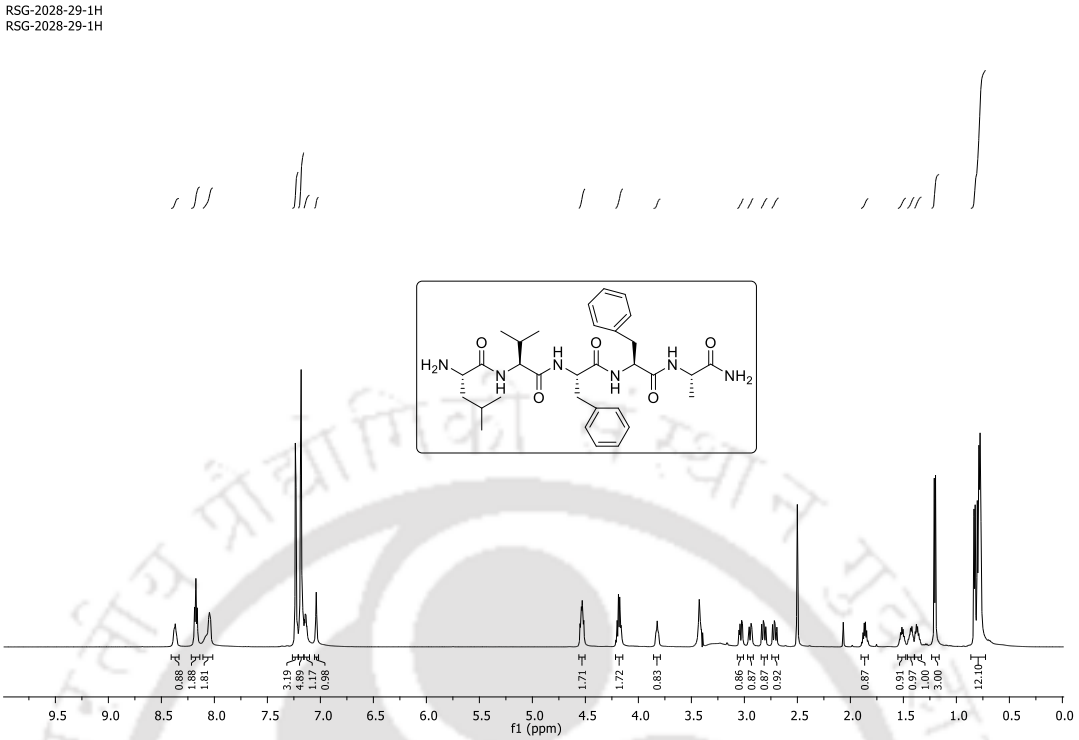

Figure 7.27. *^{1}H NMR spectra of peptide* ***8a***

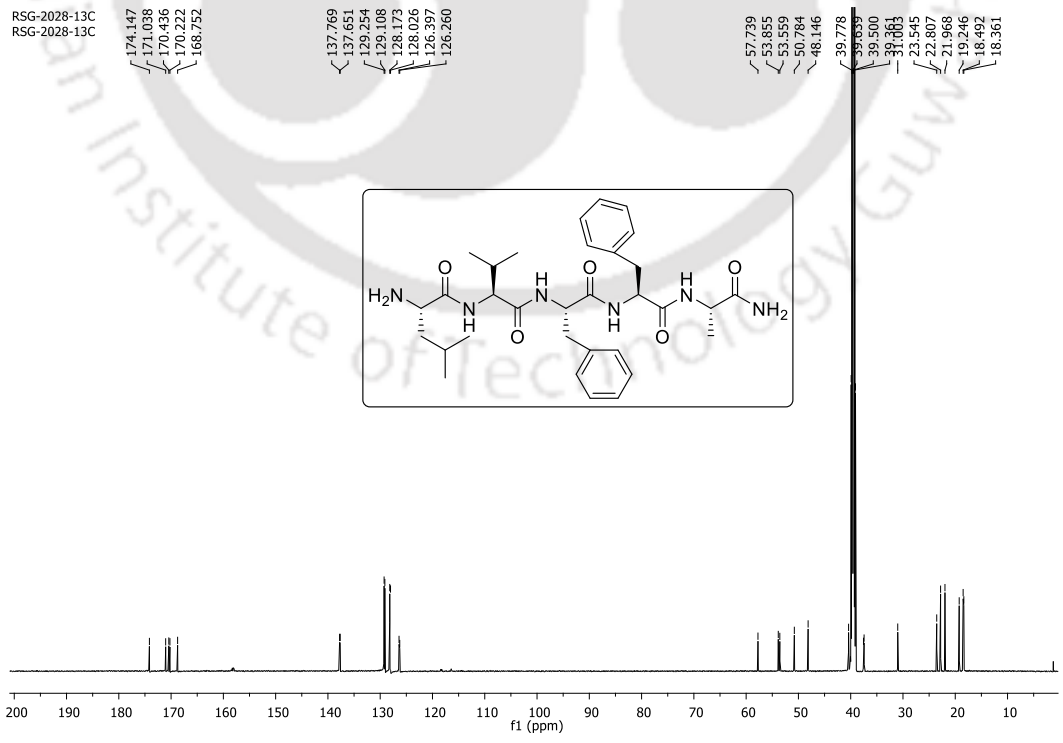

Figure 7.28. *^{13}C NMR spectra of peptide* ***8a***

7.20.Crystallographic data:

Table 7.3. Crystal parameters and refinement data of **7f** and **7g**

Parameters	***Boc-m-ABA-Aib-OMe (7f)***	***Boc-β-Ala-m-ABA-OMe (7g)***
Formula	C_{17} H_{24} N_2 O_5	$C1_6$ H_{22} N_2 O_5
Fw	336.38	322.36
Crystal system	Monoclinic	triclinic
Space group	*C 2/c*	*P 1*
a/Å	14.2735(7)	5.0931(6)
b/Å	13.3424(5)	5.6844(9)
c/Å	21.1718(11)	14.855(2)
α/°	90.00	79.497(13)
β/°	108.562(5)	81.119(10)
γ/°	90.00	89.699(11)
V/Å^3	3822.3(3)	417.68(10)
Z	8	1
D_c/g cm^{-3}	1.169	1.282
μ Mo $K_α$/mm^{-1}	0.086	0.096
F000	1440.0	172
T/K	293(2)	293(2)
θ max.	28.780	28.742
Total no. of reflections	8753	3269
Independent reflections	4392	2310
Observed reflections	2576	1820
Parameters refined	223	213
R_1, I > 2σ(I)	0.0611	0.0453
wR_2, I > 2σ(I)	0.1490	0.1315
GOF (F^2)	1.047	0.939
CCDC No.	1923207	1923208

Chapter 8

Materials and Instrumentations

8.1. Materials

All unprotected, Boc and Fmoc protected amino acids, Oxyma and 2-nitrobenzenesulfonyl chloride, BOP, and Rink amide AM resin (0.7 mmol/g) were purchased from GL Biochem (Shanghai). DIPEA, benzyl amine, benzyl alcohol, benzyl mercaptan, cyclohexylamine, cyclopropylamine, diethylamine, DCM (extra pure grade), and acetonitrile (HPLC grade) were obtained from Spectrochem (India). Acetic anhydride (synthesis grade), *N*-methyl imidazole (extra pure), TFA of extra pure grade were purchased from SRL (India). Ferric chloride, citric acid, $NaHCO_3$, DMSO-d_6, DMF (extra pure grade), hexane (reaction grade and HPLC grade), isopropanol (HPLC grade), MeOH (HPLC grade), THF (extra pure), and EtOAc (extra pure) were obtained from Merck (India). KBr, ThT, Congo red, and $CDCl_3$ were obtained from Sigma Aldrich. Dansyl chloride was purchased from Alfa Aesar.

8.2. Instrumentation

8.2.1. Chromatographic technique

Reactions were monitored by using thin-layer chromatography with silica gel G and silica gel GF254 using EtOAc/Hexane as a solvent system. Purification of the reaction products was carried out by column chromatography using silica gel (60-120 mesh) using eluent EtOAc/Hexane.

8.2.2. High-performance liquid chromatography (HPLC)

All crude peptides were purified by reverse phase semi-preparative HPLC (Thermo Scientific Dionex UltiMate 3000 Rapid Separation LC (RSLC) system) using a C18 Thermo Scientific column at a flow rate of 4 or 5 mL min^{-1}. The purity of peptides was checked by analytical HPLC, Thermo Scientific Dionex UltiMate 3000 or Waters 600E or Agilent 1260 Infinity II system with a C18 Thermo Scientific column (Hypersil Gold, 5 µm, 250x4.6 mm) or Agilent column (4.6 x 100 mm, 4mm) at a flow rate 1 $mLmin^{-1}$. A binary solvent, water (solvent A) and acetonitrile (solvent B) were used. A UV detector with dual-wavelength at 214 and 254 nm was used.

8.2.3. Solvent evaporation technique

Solvents were removed under reduced pressure using a Buchi rotary evaporator. Purified HPLC peptide samples were freeze-dried under lyophilizer (Labconco).

8.2.4. Mass spectrometry

Mass spectra of the peptide samples were recorded on an Agilent-Q-TOF 6500 instrument, in ESI positive mode, equipped with Mass hunter workstation software. The MALDI-TOF mass was obtained from the Bruker auto flex speed instrument.

8.2.5. Nuclear magnetic resonance (NMR) spectroscopy

All NMR spectra were recorded on a Bruker Ascend 600 MHz or 400 MHz instrument at 298 K using $CDCl_3$ or DMSO-d_6 solvent. 1D [^{1}H] spectra were recorded with NS = 16 scans. Chemical shifts were referenced to $CDCl_3$ at δ = 7.26 ppm and δ = 77.23 in ^{1}H NMR and ^{13}C NMR, respectively. Coupling constants (J) are reported in Hz singlet (s), doublet (d), triplet (t), quartet (q), doublet of doublet (dd), multiplet (m) or broad (br). 2D [^{1}H, ^{1}H] total correlation spectroscopy (TOCSY), 2D [^{1}H, ^{1}H] nuclear Overhauser enhancement spectroscopy (NOESY), and 2D [^{1}H, ^{1}H] correlated spectroscopy spectra (COSY) were recorded with NS = 32 scans, relaxation delay = 2 s, acquisition time = 0.1556 s, spectral width = 6578.9 Hz, and acquired size = 1024 × 217 in both dimensions (F1 and F2). The mixing times are 0.08 s (for TOCSY) and 0.6 s (for NOESY).

8.2.6. Single crystal X-ray diffraction (SC-XRD)

The single-crystal XRD data were collected with an Oxford SuperNova diffractometer (Agilent Technologies) using MoKα radiation. Computing data collection, cell refinement, and data reductions were performed by CrysAlisPro 1.171.38.46 (Rigaku OD, 2015). The structures were solved by direct methods implemented in SHELX-2014/7 software and refined by full-matrix least-squares methods. All non-hydrogen atoms were refined anisotropically.

8.2.7. Fourier-transform infrared (FT-IR) spectroscopy

FT-IR experiment was performed on a PerkinElmer Spectrum-One FT-IR spectrophotometer. The KBr pellet technique was applied to get solid-state FT-IR spectra over the range of 4000–400 cm^{-1}.

8.2.8. Melting point

Melting points were recorded on the Buchi melting point apparatus.

8.2.9. Circular dichroism (CD)

CD spectra were recorded from 190 nm to 260 nm wavelength with JASCO J-1500 instrument using 1 mm pathlength and 1 nm bandwidth. Three measurements were accumulated, and the average data were reported. The mean residue molar ellipticity was calculated using the following equation:

θ (deg. cm^2 .$dmol^{-1}$) = Ellipticity (mdeg). 10^6 / Pathlength (mm). [Protein] (μM). N

8.2.10. Powder X-ray diffraction (PXRD)

Powder XRD patterns were recorded on a Bruker D2 phaser X-ray diffractometer (30 kV, 10 mA) fitted with a Mythen detector, employing Cu-Kα1 (λ = 1.5406 Å) radiation or Rigaku SmartLab X-ray diffractometer (45 kV) fitted with a D/teX Ultra detector, employing Cu-Kα_1 (λ = 1.5406 Å) radiation.

8.2.11. Thermogravimetric analysis (TGA)

Thermal analysis was carried out using a NETZSCH STA 449F3 TGA thermal analyzer with a heating rate of 10 °C min^{-1} under an N_2 atmosphere.

8.2.12. Optical microscopic images

The obtained bright-field images (40X magnificence) were captured from the Nikon Digital Sight DS-U3 microscope.

8.2.13. Field emission scanning electron microscopy (FE-SEM)

The reported FE-SEM images were captured from FE-SEM SIGMA-300 (ZEISS) instrument. 10 µL of 7 or 10 days old peptide solutions were dropped cast on Al-foil and dried over $CaCl_2$ inside a desiccator overnight.

8.2.14. Transmission electron microscope (TEM)

10 µL of each sample solution (100 µM) was dropped cast on a carbon-coated copper grid and allowed to float 1 min. Then, 2% uranyl acetate solution (10 µL) was added to it and allowed to float for another 1 min. After removing the excess solution by tissue

paper, the samples were kept inside the desiccator. TEM images were recorded under the JEOL (Model: 2100F*)* instrument.

8.2.15. Atomic force microscopy (AFM)

The 7 days old 1.5 mM peptides solution was diluted to make concentration 30 µM, and from these solutions, 10 µL of each sample was dropped cast on a silicon wafer and dried inside the desiccator for overnight. AFM images were recorded on the Oxford Cypher instrument.

8.2.16. Congo red and ThT dye interacting image

5 µL of 7 or 10 days old peptides solution (1.5 mM) and 5µL of Congo red solution (saturated solution of ethanol) were mixed and dropped cast (10 µL) on a microscopic slide and dried it. Similarly, 5 µL of ThT (1 mM) in 50 µM PBS pH 7.4 and 5 µL of these peptides solution (1.5 mM) were mixed and dropped cast on a microscopic slide and kept for drying. Then, this Congo red and ThT strained peptides were applied under Olympus BX51 digital microscope for capturing the bright field and its corresponding fluorescence image (20X magnification). The filter with excitation of 510-560 nm and emission of 580 nm bands was passed onto Congo red-stained slide. And also, an excitation of 465-495 nm and emission of 512-558 nm were applied on the ThT strained slide.

Conclusions and Future Directions

Conclusions

The works presented in this thesis are mainly focused on the investigation of self-assembly, conformation, and morphology of small di- and tri-peptides and the development of new greener $FeCl_3$ based strategy for tert-butyl or Boc cleavage during peptide synthesis in solution as well as in SPPS. The overview of the thesis is depicted in Scheme 1.

In chapter 1, we described the secondary structures of peptide and their various supramolecular self-associations, peptide modifications, peptide synthesis, and drawbacks associated with the existing methods.

In chapter 2, we investigated the self-assembly, conformation, and morphology of two dipeptides bearing sequence homogeneity with the *C*-terminus of Alzheimer's $A\beta_{39-40}$ and $A\beta_{41-42}$, respectively.

In chapter 3, we demonstrated the formation of various nanostructures from alternating L/L and D/L amino acid-containing dipeptides.

In chapter 4, we described the formation of supramolecular helical structures from two tripeptides without using pre-organized kink moieties in the peptide sequence.

In chapter 5, we developed and demonstrated the supramolecular helical and double helical assemblies from alternating D/L amino acids containing tripeptides.

In chapter 6, we illustrated a mild, efficient, and environmentally friendly $FeCl_3$-based method for the removal of tert-butyl group from the side-chain of aspartic acid- and glutamic acid-containing peptide on-resin.

In chapter 7, we described the greener $FeCl_3$-mediated Boc chemistry in solution and solid-phase peptide synthesis.

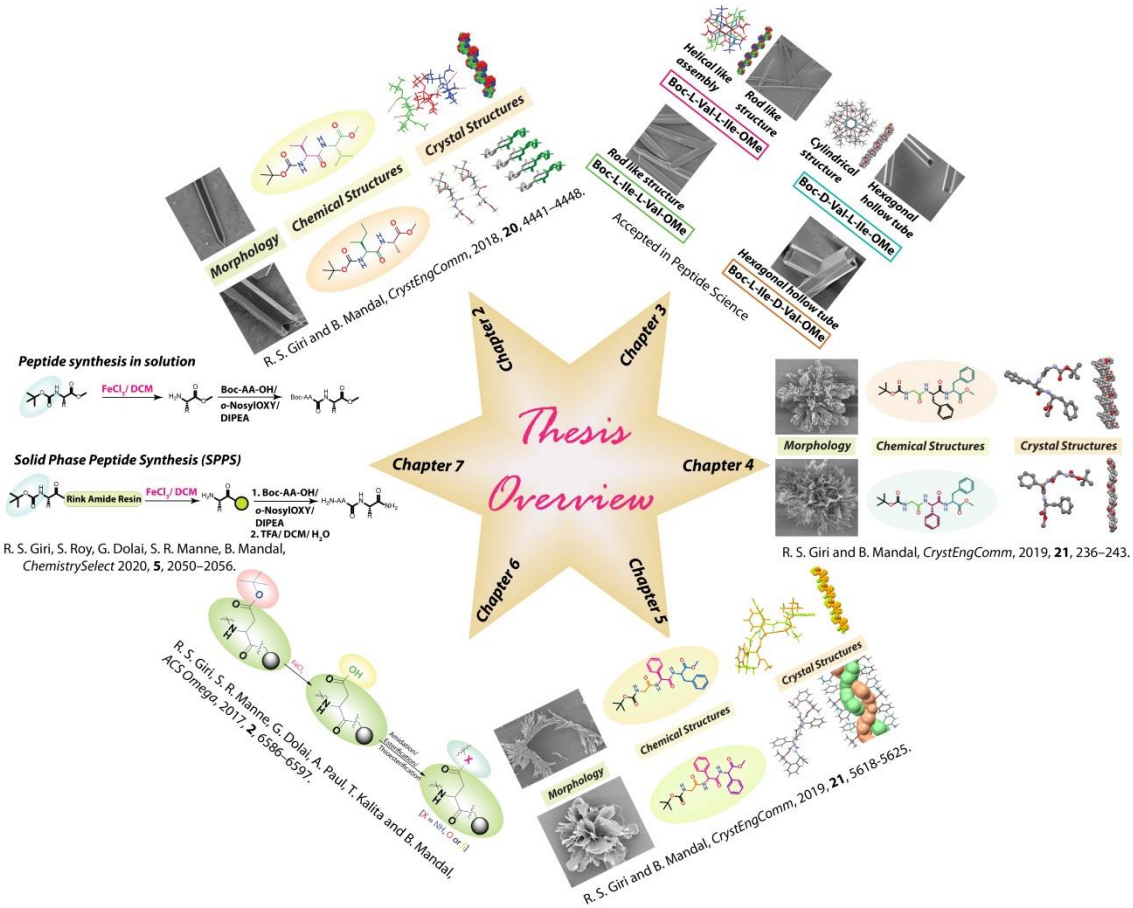

Scheme 1. *Thesis overview*

Future Directions

The investigation of supramolecular self-assembly, conformation, and morphology of some di- and tripeptides and the development of new methods for the modification of side-chain of Asp/Glu and peptide synthesis in solution as well as in SPPS were demonstrated in this thesis. We can further explore the various supramolecular structures from the various di-, tri- or tetra-peptides. We can also explore the side-chain modification of various polar amino acids, e.g., Ser, Lys, Trp, Tyr, Arg, *etc*. using our protocol.

Research Outcome

Publications:

1. **Giri, R. S.;**[a] Dolai, G.;[a] Roy, S.; Mandal, B. Investigation of supramolecular arrangements of heterochiral tripeptides. (a: These authors contributed equally, manuscript in preparation)
2. **Giri, R. S.;**[a] Roy, S.;[a] Dolai, G.; Mandal, B. Investigation of the role of side-chains for the formation of various supramolecular assemblies on a peptide. (a: These authors contributed equally, communicated)
3. **Giri, R. S.**; Roy, S.; Dolai, G.; Manne, S. R.; Pal, S.; Paul, S.; Mandal, B. Nanostructures from protected L/L and D/L amino acid containing dipeptides. (Accepted in Peptide Science)
4. **Giri, R. S.**; Roy, S.; Dolai, G.; Manne, S. R.; Mandal, B. $FeCl_3$-mediated Boc deprotection: mild facile Boc-chemistry in solution and on resin *ChemistrySelect* **2020**, *5*, 2050-2056.
5. **Giri, R. S.**; Mandal, B. Formation of supramolecular single and double helix-like structures from designed tripeptides. *CrystEngComm* **2019**, *21*, 5618-5625.
6. Kumar, S.; Srivastav, S.; Fatima, M.; **Giri, R. S.**; Mandal B.; Mondal, A. C. A synthetic pro-drug peptide reverses amyloid-β-induced toxicity in the rat model of Alzheimer's disease. *J Alzheimers Dis.* **2019**, *69*, 499-512.
7. **Giri, R. S.**; Mandal, B. Unique crystallographic signatures of Boc-Gly-Phe-Phe-OMe and Boc-Gly-Phg-Phe-OMe and their self-association. *CrystEngComm* **2019**, *21*, 236-243.
8. **Giri, R. S.**; Mandal, B. Boc-Val-Val-OMe ($A\beta_{39-40}$) and Boc-Ile-Ala-OMe ($A\beta_{41-42}$) crystallize in parallel β-sheet arrangement but generate different morphology. *CrystEngComm* **2018**, *20*, 4441-4448.
9. Manne, S. R.; Chandra, J.; **Giri, R. S.**; Kalita, T.; Mandal, B. Synthesis of β-amino alcohols using Ethyl 2-Cyano-2-(2-nitrobenzenesulfonyloxyimino)acetate (*o*-NosylOXY). *ChemistrySelect* **2018**, *3*, 992-996.

10. **Giri, R. S.**; Manne, S. R.; Dolai, G., Paul, A., Kalita, T., Mandal, B. $FeCl_3$-Mediated side chain modification of aspartic acid- and glutamic acid-containing peptides on a solid support. *ACS Omega***. 2017**, *2*, 6586-6597.
11. Manne, S. R.; Thalluri, K.; **Giri, R. S.**; Chandra, J.; Mandal, B. Ethyl 2-(tert-Butoxycarbonyloxyimino)-2-cyanoacetate (Boc-Oxyma): An efficient reagent for the racemization free synthesis of ureas, carbamates and thiocarbamates via lossen rearrangement. *Adv. Synth. Catal.* **2017**, *359*, 168-176.
12. Manne, S. R.; Thalluri, K.; **Giri, R. S.**; Paul, A.; Mandal, B. Racemization free longer *N*-terminal peptide hydroxamate synthesis on solid support using Ethyl 2-(*tert*-butoxycarbonyloxyimino)-2- cyanoacetate. *Tetrahedron Lett.* **2015**, *56*, 6108-6111.

Conferences:

Poster presentation:

1. **Giri, R. S.**; Mandal, B. "Self-assembly of Boc-Gly-Phe-Phe-OMe and Boc-Gly-Phg-Phe-OMe Exhibits Supramolecular Helical Architecture." **Frontiers in Chemical Sciences [FICS 2018]**, 6-8th December 2018, Department of Chemistry, Indian Institute of Technology Guwahati, Guwahati, India, Page 365 (P-213).
2. **Giri, R. S.**; Mandal, B. "*C*-terminal Dipeptides of Amyloid β Crystallize in Parallel β-Sheet Arrangement." **Research Conclave'18**, 8-11th March, 2018, Students' Academic Board (SAB), Indian Institute of Technology Guwahati, India.
3. **Giri, R. S.**; Mandal, B. "Solid Phase Peptide Synthesis by Boc-chemistry on a Resin Usually Used for Fmoc-chemistry." **International Conference on Chemistry for Human Development [ICCHD-2018]** 8-10th January 2018, Heritage Institute of Technology, Kolkata, India, Page 113 (P-076).
4. **Giri, R. S.**; Mandal, B. "NMR Studies of a Model Aβ (1-4) and α-synuclein (110-115) Peptide Fragment." **International Conference on Sophisticated Instrument in Modern Research [ICSIMR-20170]**, 30th June-1st July, Indian Institute of Technology Guwahati, India, Page 113 (PP-52).
5. **Giri, R. S.**; Mandal, B. "Lewis Acid based Side Chain Modification of Aspartic Acid and Glutamic Acid during Solid Phase Peptide Synthesis." **20th CRSI National**

Symposium in Chemistry [CRSI-NSC-20], Department of Chemistry, 3rd-5th February 2017, Gauhati University, India, Page 221 (PP-296).

6. **Giri, R. S.**; Mandal, B. "On resin Lewis Acid based Peptide Modification on Asp or Glu." **Frontiers in Chemical Sciences [FICS 2016],** 2016, 8-10th December 2016, Department of Chemistry, Indian Institute of Technology Guwahati, India, Page 97 (P-42).

Oral presentation:

Giri, R. S.; Mandal, B. "Supramolecular Self-association of two different tripeptides: Crystallographic Insights" **Regional Seminar on Science for Sustainable Development (SSD-2019)**, 9th January, 2019, Department of Chemistry, B. Borooah College, Guwahati, India, Page 50 (OP-36).

Workshops:

1. The silver jubilee **NMRS** workshop held during October 29-31, 2018 at Bose Institute, Darjeeling Campus, West Bengal, India.
2. Workshop on procedures and applications of **XRD, XRF and Single Crystal XRD**, 27th July to 1st August, 2018, organized by Sophisticated Analytical Instrument Facility (SAIF), Guwahati, sponsored by Dept, of Science and Technology (DST), govt. of India.
3. MHRD-Global Initiative on Academic Network (GAIN), workshop on **Protein Structure And Drug Discovery**, 27th August- 05th September, 2017, School of Life Sciences, University of Hyderabad, India.

Rajat Subhra Giri

Personal Information:

Date of Birth: 19th July 1991
Father's Name: Satyajit Giri
Nationality: Indian
Religion: Hindu
Gender: Male
Height 5'7"
EyeSight: 6/6
Tel no. +91-9954248386
Email: rsgiri001@gmail.com/ rajat.giri@iitg.ac.in

Present Address:

Senior Research Fellow, C/O: Dr. Bhubaneswar Mandal, Laboratory of Peptide & Amyloid Research, Department of Chemistry, IIT Guwahati, Guwahati, Assam, India-781039.

Permanent Address:

Gopiballavpur, Jhargram, West Bengal, India-721506.

Academic Qualifications

07/2014–Present

Ph.D. in Chemistry (CPI 8.25 out of 10)

Indian Institute of Technology Guwahati, Assam, India-781039

Thesis: **Investigation on Supramolecular Arrangement and On-Resin Modification of Small Peptides**

Thesis advisor: Dr. Bhubaneswar Mandal

07/2012–05/2014

M.Sc. in Chemistry (CPI 8.43 out of 10)

Indian Institute of Technology Guwahati, Assam, India-781039

Thesis: **Synthesis of 1H-Indazoles through Oxime-Phosphonium ion Intermediate**

Thesis advisor: Dr. Debasis Manna

07/2008–05/2012

B.Sc. in Chemistry Honours (First Class)

with Physics, Mathematics, and English

Midnapore College, Vidyasagar University, West Bengal, India-721101

Achievements and Awards

- Qualified "Joint Admission Test for M.Sc. (JAM 2012)" examination, India.
- Received National Eligibility Test (NET-CSIR) June-2014 (CSIR rank-71) in Chemical Science, India.
- Qualified Graduate Aptitude Test (GATE) held in February 2014 in Chemistry, organized by the Ministry of Human Resource Development, Government of India.
- Awarded best poster prize in the competition organized by the Department of Chemistry, Midnapore College, on 25th November 2011 in connection with the celebration of International Year of Chemistry-2011 (IYC 2011).

Research Experience

- I have worked on the investigation of molecular self-assembly and secondary structures of small peptides in the solid-state as well as solution and also the determination of their morphology in solution. I have also worked on the development of the new strategy for peptide synthesis in solution as well as solid phase peptide synthesis (SPPS) and development of a new method for side-chain modification of peptides on-resin during my Ph.D. program.
- I have expertise in various instrumental techniques e.g., HPLC, ESI-MS, NMR, CD, FT-IR, Optical-polarizable microscope, *etc*.
- In parallel, I have worked on coupling reagent-based (Boc-Oxyma) various organic transformations, e.g., biologically active peptide urea and hydroxamate synthesis. I have also worked on coupling reagent-based (*o*-NosylOXY) reduction of carboxylic acid to alcohol.

Academic and Professional skills

- **Laboratory and Instrumentation:** Familiar with Synthetic Organic Chemistry, peptide synthesis and their modification (solution phase and solid phase), crystallization of peptides, NMR Spectroscopy (1D, 2D), Single-Crystal X-Ray Diffraction (SC–XRD), Powder-XRD, HPLC, Mass Spectrometry (ESI, MALDI), FT-IR spectroscopy, FE-SEM, TEM, AFM, TGA-DSC, Circular Dichroism (CD), DLS, Optical Polarizable and fluorescence microscopy.
- **Software:** Gaussian, Origin, Adobe Illustrator, Adobe Photoshop, MS-Office, Chem Draw, and SHELXL, WINGX, Mercury, Mestrenova, Topspin.

- **Instrumental Experience**: Selected as an authorized operator for **Nuclear Magnetic Resonance (NMR, 600 MHz Bruker Ascend)** instrument at **'Central Instrument Facility (CIF), IIT Guwahati',** June 2015-May 2019.
- **Teaching Experience:** Worked as a Teaching Assistant (TA) in B.Tech Laboratory at IIT Guwahati, India.
- **Language:** Bengali, English, and Hindi.

Research interests

- Peptide chemistry
- Chemical biology
- Supramolecular chemistry
- Alzheimer's disease
- Synthetic organic chemistry